

2023

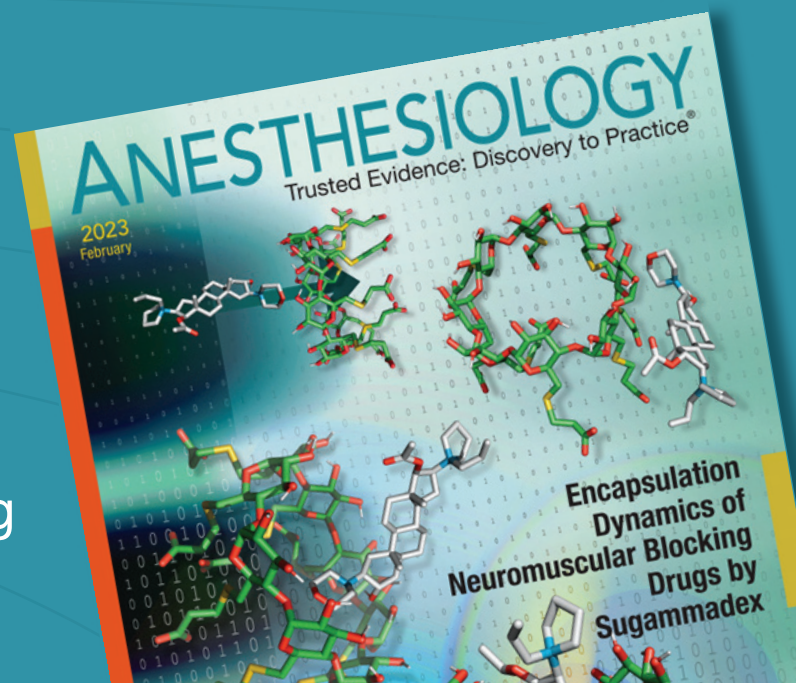
ASA Practice Guidelines for Preoperative Fasting



These practice guidelines are a modular update of the “Practice guidelines for preoperative fasting and the use of pharmacologic agents to reduce the risk of pulmonary aspiration: Application to healthy patients undergoing elective procedures.” The guidance focuses on topics not addressed in the previous guideline: ingestion of carbohydrate-containing clear liquids with or without protein, chewing gum, and pediatric fasting duration.



anesthesiology.org



Volume 138 No. 3 Pp. 235–344

ANESTHESIOLOGY®

MARCH 2023

ANESTHESIOLOGY

2023
March

Trusted Evidence: Discovery to Practice®



Noninvasive Maneuvers to Assess Lung Stress and Diaphragm Effort in Mechanically Ventilated Patients

Volume 138
Number 3
anesthesiology.org

The Official Journal of the American Society of Anesthesiologists

Downloaded from anesthesiology.org issue 138/3 by guest on 19 April 2024

Manage pressure and flow with intelligent decision support

Stay ahead of hemodynamic instability with predictive technology.



Acumen intelligent decision support suite is the hemodynamic monitoring solution that predicts hemodynamic instability and delivers comprehensive pressure and flow insights on a single monitor. Now, with smart alerts and trends, you will have a focused view of the potential targets for intervention such as preload, afterload and contractility – so you can prevent or treat hypotension.*

Discover the suite of solutions that enables you to detect hemodynamic instability, reduce hypotension,¹ and optimize fluid administration:

- Predict the likelihood of hypotension with Acumen Hypotension Prediction Index (HPI) software.
- Optimize fluid administration with Acumen Assisted Fluid Management (AFM) software.



Discover the power of predictive decision support at [Edwards.com/Acumen](https://www.edwards.com/Acumen)

*Any treatment decisions should be based on a full hemodynamic review of your patient
**Surgical patient use only, not compatible with Acumen AFM software

Reference:
1. U.S. Food and Drug Administration. 2021. K203224 510k Summary, Acumen Hypotension Prediction Index
CAUTION: Federal (United States) law restricts this device to sale by or on the order of a physician. See instructions for use for full prescribing information, including indications, contraindications, warnings, precautions, and adverse events.
Edwards, Edwards Lifesciences, the stylized E logo, Acumen, Acumen AFM, Acumen HPI, Acumen IQ, AFM, HemoSphere, HPI, and Hypotension Prediction Index are trademarks of Edwards Lifesciences Corporation or its affiliates. All other trademarks are the property of their respective owners.



Acumen IQ finger cuff**

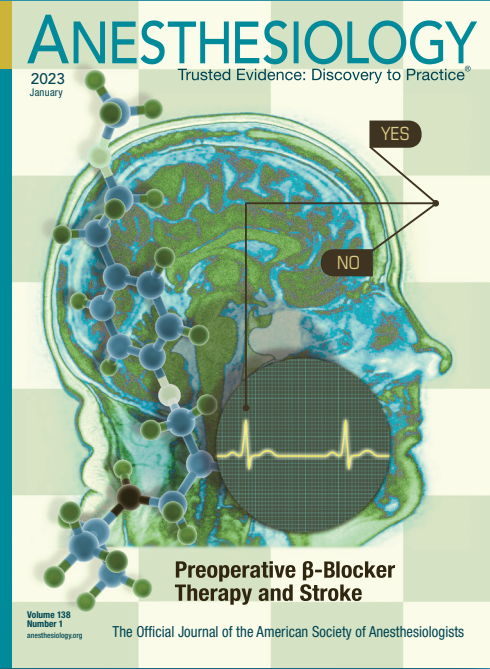


Acumen IQ arterial line sensor



2023

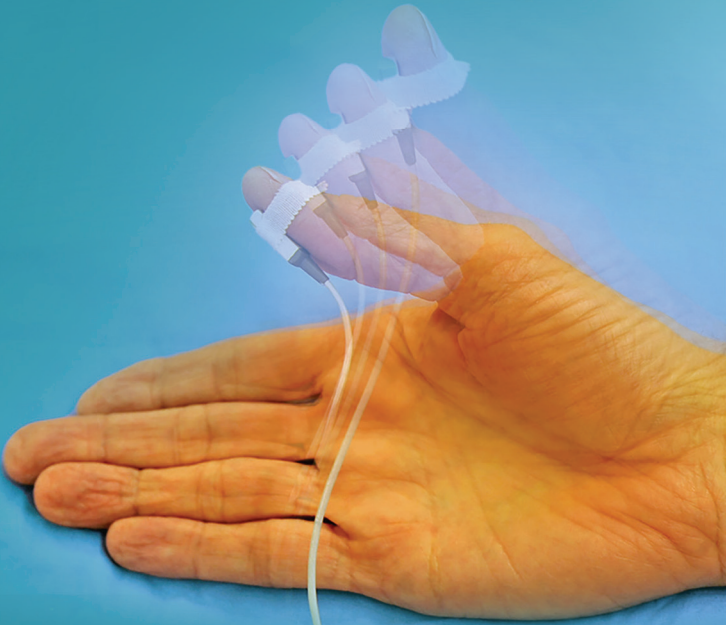
ASA Practice Guidelines for Monitoring and Antagonism of Neuromuscular Blockade

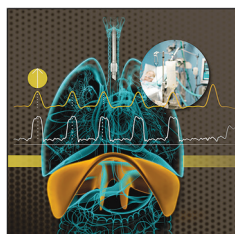


This practice guideline provides evidence-based recommendations on the management of neuromuscular monitoring and antagonism of neuromuscular blocking agents during and after general anesthesia. The guidance focuses primarily on type and site of monitoring and the process of antagonizing neuromuscular blockade to reduce residual neuromuscular blockade.



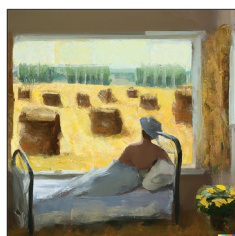
[anesthesiology.org](https://www.anesthesiology.org)





274 Performance of Noninvasive Airway Occlusion Maneuvers to Assess Lung Stress and Diaphragm Effort in Mechanically Ventilated Critically Ill Patients

Monitoring and controlling lung stress and diaphragm effort has been hypothesized to limit lung and diaphragm injury in mechanically ventilated critically ill patients. The reference methods to assess lung stress and diaphragm effort are esophageal and gastric manometry to calculate the transpulmonary pressure and transdiaphragmatic pressure. The hypothesis that occluded inspiratory airway pressure (P_{occl}) and drop in airway pressure in the first 100 ms of an occluded inspiration (P_{0.1}) correlate with lung stress and diaphragm effort and that both parameters would perform well in identifying patients with extremes of lung stress and diaphragm effort was tested in a secondary analysis of data from two clinical trials, a 39-patient primary cohort and a 13-patient validation cohort. Although P_{occl} and P_{0.1} could not be used to calculate the exact values of diaphragm effort and lung stress in the preceding hour in mechanically ventilated critically ill patients, they had good to excellent diagnostic performance in identifying extremes of lung stress and diaphragm effort, with P_{occl} outperforming P_{0.1} in detecting patients with high diaphragm effort. See the accompanying Editorial on [page 235](#). (Summary: M. J. Avram. Image: A. Johnson, Vivo Visuals Studio.)



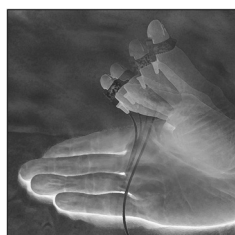
289 Mechanical Power Ratio and Respiratory Treatment Escalation in COVID-19 Pneumonia: A Secondary Analysis of a Prospectively Enrolled Cohort

Tidal volume, minute ventilation, and esophageal pressure measurements help inform diagnosis of patients with acute respiratory failure and monitor their response to therapeutic intervention. Mechanical power quantifies the amount of energy transferred to the respiratory system during mechanical ventilation, and the mechanical power ratio is the ratio between it and the expected baseline mechanical power. The hypothesis that the mechanical power ratio can identify spontaneously breathing patients with higher risk of respiratory failure was tested in a secondary analysis of data from patients with COVID-19 pneumonia. Forty-seven patients were supported with continuous positive airway pressure until transfer to the ward, and 64 underwent treatment escalation to noninvasive or invasive mechanical ventilation. Although the tidal volume was similar in both groups, patients undergoing treatment escalation had higher respiratory rate, minute ventilation, tidal pleural pressure, and mechanical power and lower arterial oxygen tension/fractional inspired oxygen tension. Mechanical power, mechanical power ratio, and pressure-rate index were variables most strongly associated with the need for respiratory treatment escalation. See the accompanying Editorial on [page 238](#). (Summary: M. J. Avram. Image: Generated by the author (of the accompanying Editorial) using DALL•E 2 natural language to image generation AI system.)



299 Predicting Intensive Care Delirium with Machine Learning: Model Development and External Validation

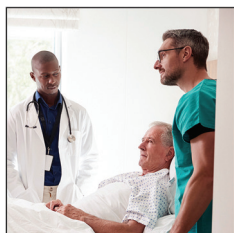
The hypothesis that variables routinely acquired during intensive care would be associated with the probability of delirium onset was tested by developing and validating two models for the prediction of delirium in the intensive care unit (ICU): an early prediction model to identify delirium onset at any time during intensive care using data available early in the ICU stay and a dynamic model to predict the onset of delirium 0 to 12 h in the future. The prediction models were trained and tested using a large multicenter database and externally validated on two large single-center databases. The early prediction model performed better than the modified reference model and calibrated well in a contemporary dataset. The dynamic model had higher discrimination than the reference model and similar or better discrimination compared to published models. Both models generally validated well on the external datasets. Features involving Glasgow Coma Scores, Richmond Agitation Sedation Scale, age, mechanical ventilation, and overall acuity were important in prediction. Length of ICU stay before delirium onset and time of day were important predictors for the dynamic model. (Summary: M. J. Avram. Image: Adobe Stock.)



241 Comparison of Contralateral Acceleromyography and Electromyography for Posttétanic Count Measurement

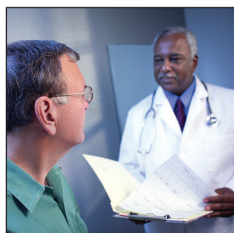
Deep neuromuscular blockade during anesthesia for laparoscopic or robotic surgeries may offer several advantages in terms of patient outcomes and physician surgical experience. Posttétanic count can be used to identify intense neuromuscular block (posttétanic count equal to 0) and deep neuromuscular block (posttétanic count greater than or equal to 1 and train-of-four count equal to 0) and estimate the time to recovery. The agreement of posttétanic counts monitored in contralateral arms by acceleromyography and electromyography was determined in 36 patients given 0.6 mg/kg rocuronium after induction of anesthesia and calibration of the monitors, with additional doses of

0.3 mg/kg if required. Seventy-three percent of 226 pairs of acceleromyography and electromyography posttétanic count measurements indicated the same neuromuscular blockade status (intense or deep block). Of 184 pairs of posttétanic counts of 15 or less, 42 (23%) acceleromyography posttétanic counts were equal to electromyography posttétanic counts, 93 (50%) were more than electromyography counts, and 49 (27%) were less than electromyography counts. (Summary: M. J. Avram. Image: J. P. Rathmell.)



249 Respiratory Effects of Biased Ligand Oliceridine in Older Volunteers: A Pharmacokinetic–Pharmacodynamic Comparison with Morphine

After μ -opioid receptor activation, oliceridine selectively engages the G protein–coupled signaling pathway, which is associated with analgesia, and has reduced engagement of the β -arrestin pathway, which is associated with adverse effects such as respiratory depression. In healthy young males, oliceridine had a higher probability of providing analgesia than producing respiratory depression over the clinically relevant concentration range, while morphine had a higher probability of producing respiratory depression than providing analgesia. Older and somewhat obese individuals of both sexes may be more vulnerable to opioid-induced respiratory depression than younger individuals. The hypothesis that oliceridine and morphine differ in their pharmacodynamic behavior, measured as effect on ventilation at an extrapolated end-tidal P_{CO_2} of 55 mmHg (\dot{V}_{E55}), was tested in a four-arm, double-blind, randomized crossover study of 18 male and female volunteers aged 56 to 87 yr. The effect-site oliceridine concentration causing a 50% depression of \dot{V}_{E55} was 39% higher than that of morphine. The onset and offset of the respiratory effect of oliceridine was five times faster than that of morphine. (Summary: M. J. Avram. Image: Adobe Stock.)



264 Extended-age Out-of-sample Validation of Risk Stratification Index 3.0 Models Using Commercial All-payer Claims

The Risk Stratification Index (RSI) 3.0 is a well-validated and calibrated suite of predictive algorithms that uses diagnostic, procedural, and demographic information available at the time of admission to predict health outcomes during hospitalization and after discharge. The RSI 3.0 models were developed and out-of-sample validated in Medicare fee-for-service patients who were mostly at least 65 yr old. The performance of seven RSI 3.0 models developed in Medicare patients and applied to younger and healthier 2017 Utah (55,109 admissions from 40,710 subjects) and Oregon (21,213 admissions from 16,951 subjects) state populations were compared to those of the out-of-sample Medicare validation analysis to determine how well the RSI 3.0 models

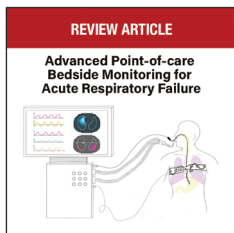
perform when applied to out-of-sample younger and healthier adult populations. The models included in the analysis were selected to demonstrate performance of predictors for clinically and economically meaningful outcomes spanning a broad range of incidences. Performance measures for all endpoints exceeded prespecified minimum acceptable performance standards and were similar to or better than those obtained on the Medicare population. (Summary: M. J. Avram. Image: Thinkstock Images.)



312 Multidisciplinary Pain Management: A Tale of Two Outcomes (Classic Paper Revisited)

The Multidisciplinary Pain Clinic started at the University of Washington by John J. Bonica, M.D., in 1960 evolved over the years, becoming the Pain Center in 1978. John D. Loeser, M.D., the author of this Classic Paper Revisited article, became director of the Pain Center in 1982 where he and Wilbert Fordyce, Ph.D., designed and implemented a 3-week inpatient treatment program for patients with chronic intractable pain, labeled “the structured program,” which became a model for chronic pain treatment not only in the United States but also throughout the world. It has been the model for a wide network of Scandinavian pain treatment programs that provide universal access to multidisciplinary care for acute, chronic, and cancer-related pain to this day. Although

pain programs were developed in many institutions in the United States, without government support few survived the economic health care chaos in the United States. The Classic Paper, published in 1999 in *Acta Anaesthesiologica Scandinavica*, provides an analysis of developments in chronic pain management in both the United States and the Nordic countries. (Summary: M. J. Avram. Image: J. P. Rathmell.)



317 Advanced Point-of-care Bedside Monitoring for Acute Respiratory Failure (Review Article)

Advanced point-of-care respiratory monitoring tools may provide insights on pathologic changes in the respiratory system produced by underlying disease in patients with acute respiratory failure and support clinicians in providing mechanical ventilation while protecting the lungs and respiratory muscles. Such monitoring is focused on assessing lung aeration and morphology, lung recruitment and overdistention, ventilation–perfusion distribution, inspiratory effort, respiratory drive, respiratory muscles contraction, and patient–ventilator asynchrony. Advanced respiratory monitoring involves several noninvasive or minimally invasive technologies, safely applicable at the bedside, to conduct an in-depth evaluation of the lung and respiratory muscles. The present review provides an updated description of those tools, including assessment of esophageal pressure, assessment of electrical activity of the diaphragm, electrical impedance tomography, and ultrasound of the lung and respiratory muscles. (Summary: M. J. Avram. Image: From original article.)

TABLE OF CONTENTS

ANESTHESIOLOGY

Volume 138

Issue 3

March 2023

This Month in ANESTHESIOLOGY.....A1

Science, Medicine, and the Anesthesiologist.....A13

Infographics in AnesthesiologyA17

Editorial

Monitoring Respiratory Effort and Lung-distending Pressure

Noninvasively during Mechanical Ventilation: Ready for Prime Time

J. Dianti, E. C. Goligher.....235

Paradox of Power: Dynamic Tools to Predict Respiratory Failure in Spontaneously Breathing Patients

D. R. Calabrese, M. J. London.....238

Perioperative Medicine

CLINICAL SCIENCE

Comparison of Contralateral Acceleromyography and Electromyography for Posttetanic Count Measurement

H. Joo, S. Cho, J. W. Lee, W. J. Kim, H. J. Lee, J. H. Woo, G. Lee, H. J. Baik.....241

The agreement of posttetanic counts monitored in contralateral arms by acceleromyography and electromyography was determined in 35 patients given 0.6 mg/kg rocuronium after induction of anesthesia and calibration of the monitors, with additional doses of 0.3 mg/kg if required. Seventy-three percent of 226 pairs of acceleromyography– and electromyography–posttetanic count measurements indicated the same neuromuscular blockade status (intense or deep block). Of 184 pairs of posttetanic counts of 15 or less, 42 (23%) acceleromyography–posttetanic counts were equal to electromyography–posttetanic counts, 93 (50%) were more than electromyography counts, and 49 (27%) were less than electromyography counts.

Respiratory Effects of Biased Ligand Oliceridine in Older Volunteers: A Pharmacokinetic–Pharmacodynamic Comparison with Morphine

P. Simons, R. van der Schrier, M. van Lemmen, S. Jansen, K. W. K. Kuipers, M. van Velzen, E. Sarton, T. Nicklas, C. Michalsky, M. A. Demitrack, M. Fossler, E. Olofsen, M. Niesters, A. Dahan.....249

The hypothesis that oliceridine and morphine differ in their pharmacodynamic behavior, measured as effect on ventilation at an extrapolated end-tidal P_{CO_2} of 55 mmHg (\dot{V}_{E55}), was tested in a four-arm, double-blind, randomized crossover study of eighteen 56- to 87-yr-old male and female volunteers. The effect-site oliceridine concentration causing a 50% depression of \dot{V}_{E55} was 39% higher than that of morphine. The onset and offset of the respiratory effect of oliceridine was five times faster than that of morphine.

Extended-age Out-of-sample Validation of Risk Stratification Index 3.0 Models Using Commercial All-payer Claims

S. Greenwald, G. F. Chamoun, N. G. Chamoun, D. Clain, Z. Hong, R. Jordan, P. J. Manberg, K. Maheshwari, D. I. Sessler264

In two different statewide databases, Risk Stratification Index 3.0 models worked well in younger and healthier adults.

Critical Care Medicine

CLINICAL SCIENCE

Performance of Noninvasive Airway Occlusion Maneuvers to Assess Lung Stress and Diaphragm Effort in Mechanically Ventilated Critically Ill Patients

H. J. de Vries, P. R. Tuinman, A. H. Jonkman, L. Liu, H. Qiu, A. R. J. Girbes, Y. Zhang, A. M. E. de Man, H.-J. de Grooth, L. Heunks.....274

◇ Refers to This Month in ANESTHESIOLOGY

◆ Refers to Editorial

🔊 This article has an Audio Podcast

🌐 See Supplemental Digital Content

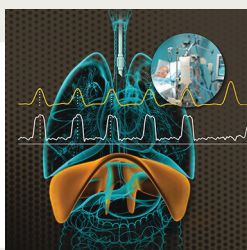
📺 CME Article

🎬 This article has a Video Abstract

🔍 Readers' Toolbox

👁️ This article has a Visual Abstract




🔓 OPEN This article is Open Access





ON THE COVER: Monitoring and controlling lung stress and diaphragm effort has been hypothesized to limit lung injury and diaphragm injury. In this issue of ANESTHESIOLOGY, de Vries *et al.* hypothesized that noninvasively measurable correlates would have strong discriminative performance in identifying extremes of lung stress and diaphragm effort. In an accompanying editorial, Dianti and Goligher examined the history of respiratory effort and proposed that these routine noninvasive measurements should become standard practice in the management of patients receiving mechanical ventilation. Cover illustration: A. Johnson, Vivo Visuals Studio.

- de Vries *et al.*: Performance of Noninvasive Airway Occlusion Maneuvers to Assess Lung Stress and Diaphragm Effort in Mechanically Ventilated Critically Ill Patients, p. 274
- Dianti and Goligher: Monitoring Respiratory Effort and Lung-distending Pressure Noninvasively during Mechanical Ventilation: Ready for Prime Time, p. 235

A secondary analysis of two previous studies evaluated the ability of two transient inspiratory airway occlusion maneuvers (Pocc, the total drop in airway pressure during an occlusion, and P0.1, the drop in the first 100 ms) obtained from the mechanical ventilator to predict either diaphragm effort or lung stress. Neither P0.1 nor Pocc should be used to predict exact values for diaphragm effort or lung distending pressure. However, both maneuvers can reliably identify patients with low or high extremes in diaphragm effort and lung stress, where Pocc outperforms P0.1 based on the areas under the receiver operating characteristic curves.

- 


Mechanical Power Ratio and Respiratory Treatment Escalation in COVID-19 Pneumonia: A Secondary Analysis of a Prospectively Enrolled Cohort
S. Gattarello, S. Coppola, E. Chiodaroli, T. Pozzi, L. Camporota, L. Saager, D. Chiumello, L. Gattinoni289

Despite similar spontaneous tidal volumes, escalated patients had higher respiratory rate, minute ventilation, pleural pressure, and mechanical power ratios. Mechanical power, its ratio with the expected baseline value, and the pressure-rate index had the greatest associations with treatment escalation.

- 

Predicting Intensive Care Delirium with Machine Learning: Model Development and External Validation
K. D. Gong, R. Lu, T. S. Bergamaschi, A. Sanyal, J. Guo, H. B. Kim, H. T. Nguyen, J. L. Greenstein, R. L. Winslow, R. D. Stevens299


In a multicenter electronic health record database of 22,234 intensive care unit (ICU) patients from 2014 to 2015, delirium was identified using the Confusion Assessment Method for the ICU screen or Intensive Care Delirium Screening Checklist. Static and dynamic machine learning algorithms were trained, tested, and externally validated to predict the onset of delirium during the ICU stay. The static model using data from the first 24 h after ICU admission to predict delirium at any point during the ICU stay demonstrated higher discrimination compared with a widely cited reference model. The dynamic model was able to predict delirium up to 12 h in advance with reasonable discrimination and calibration.

Education

CLASSIC PAPER REVISITED

- 
Multidisciplinary Pain Management: A Tale of Two Outcomes
S. H. Butler, J. D. Loeser312

IMAGES IN ANESTHESIOLOGY

- 
Difficult Airway Management in Neonates: Fiberoptic Intubation via Laryngeal Mask Airway
J. J. Thomas, M. Lingruen, A. Reddy, K. H. Chan316

REVIEW ARTICLE

- 

Advanced Point-of-care Bedside Monitoring for Acute Respiratory Failure
G. Cammarota, R. Simonte, F. Longhini, S. Spadaro, L. Vetrugno, E. De Robertis317

Advanced respiratory monitoring involves several mini- or noninvasive tools, applicable at bedside, that have the potential to support clinicians in the management of acute respiratory failure toward the protection of the lung and respiratory muscles and the personalization of ventilatory strategy.

CORRESPONDENCE

- Hypotension and Cardiac Surgical Outcomes: Comment**
R. Descamps, A. Denisenko, M.-O. Fischer335

- Hypotension and Cardiac Surgical Outcomes: Reply**
V. Rangasamy, M. A. de la Hoz, B. Subramaniam336

- Alternative Sleep Apnea Treatment: Comment**
A. Roy, M. Mandal, P. Bhakta, B. O'Brien, A. M. Esquinas337

- Alternative Sleep Apnea Treatment: Reply**
Y. Sakaguchi, N. Nozaki-Taguchi, S. Isono338

Reviews of Educational Materials

- We Are All Perfectly Fine: A Memoir of Love, Medicine and Healing**
K. E. McGoldrick340

Erratum 342

Retraction 343

Careers & Events A19

INSTRUCTIONS FOR AUTHORS

The most recently updated version of the Instructions for Authors is available at www.anesthesiology.org. Please refer to the Instructions for the preparation of any material for submission to ANESTHESIOLOGY.

Manuscripts submitted for consideration for publication must be submitted in electronic format via Editorial Manager (<https://www.editorialmanager.com/aln>). Detailed directions for submission and the most recent version of the Instructions for Authors can be found on the Journal's Web site (<http://www.anesthesiology.org>). Books and educational materials for review should be sent to Alan Jay Schwartz, M.D., M.S.Ed., Director of Education, Department of Anesthesiology and Critical Care Medicine, The Children's Hospital of Philadelphia,

34th Street and Civic Center Blvd., Room 9327, Philadelphia, Pennsylvania 19104-4399. Article-specific permission requests are managed with Copyright Clearance Center's Rightslink service. Information can be accessed directly from articles on the journal Web site. More information is available at <http://anesthesiology.pubs.asahq.org/public/rightsandpermissions.aspx>. For questions about the Rightslink service, e-mail customer-care@copyright.com or call 877-622-5543 (U.S. only) or 978-777-9929. Advertising and related correspondence should be addressed to Advertising Manager, ANESTHESIOLOGY, Wolters Kluwer Health, Inc., Two Commerce Square, 2001 Market Street, Philadelphia, Pennsylvania 19103 (Web site: <http://www.wkand-center.com/>). Publication of an advertisement in an ASA publication or on an ASA website does not constitute endorsement or evaluation by ASA or by ASA's publishing partners of the product or service described therein or of any representations or claims made by the advertiser with respect to the product or service.

ANESTHESIOLOGY (ISSN 0003-3022) is published monthly by Wolters Kluwer Health, Inc., 1800 Dual Highway, Suite 201, Hagerstown, MD 21740-6636. Business office: Two Commerce Square, 2001 Market Street, Philadelphia, PA 19103. Periodicals postage paid at Hagerstown, MD, and at additional mailing offices. Copyright © 2023, the American Society of Anesthesiologists. All Rights Reserved.

Annual Subscription Rates: *United States*—\$1175 Individual, \$2990 Institution, \$461 In-training. *Rest of World*—\$1238 Individual, \$3320 Institution, \$461 In-training. Single copy rate \$312. Subscriptions outside of North America must add \$58 for airfreight delivery. Add state sales tax, where applicable. The GST tax of 7% must be added to all orders shipped to Canada (Wolters Kluwer Health, Inc.'s GST Identification #895524239, Publications Mail Agreement #1119672). Indicate in-training status and name of institution. Institution rates apply to libraries, hospitals, corporations, and partnerships of three or more individuals. Subscription prices outside the United States must be prepaid. Prices subject to change without notice. Subscriptions will begin with currently available issue unless otherwise requested. Visit us online at www.lww.com.

Individual and in-training subscription rates include print and access to the online version. Online-only subscriptions for individuals (\$389) and persons in training (\$389) are available to nonmembers and may be ordered by downloading a copy of the Online Subscription FAXback Form from the Web site, completing the information requested, and faxing the completed form to 301-223-2400. Institutional rates are for print only; online subscriptions are available via Ovid. Institutions can choose to purchase a print and online subscription together for a discounted rate. Institutions that wish to purchase a print subscription, please contact Wolters Kluwer Health,

Inc., 1800 Dual Highway, Suite 201, Hagerstown, MD 21740-6636; phone: 800-638-3030; fax: 301-223-2400. Institutions that wish to purchase an online subscription or online with print, please contact the Ovid Regional Sales Office near you or visit www.ovid.com/site/index.jsp and select Contact and Locations.

Address for non-member subscription information, orders, or change of address: Wolters Kluwer Health, Inc., 1800 Dual Highway, Suite 201, Hagerstown, MD 21740-6636; phone: 800-638-3030; fax: 301-223-2400.

Address for member subscription information, orders, or change of address: Members of the American Society of Anesthesiologists receive the print and online journal with their membership. To become a member or provide a change of address, please contact the American Society of Anesthesiologists, 1061 American Lane, Schaumburg, Illinois 60173-4973; phone: 847-825-5586; fax: 847-825-1692; e-mail: membership@ASAhq.org. For all other membership inquiries, contact Wolters Kluwer Health, Inc., Customer Service Department, P.O. Box 1610, Hagerstown, MD 21740; phone: 800-638-3030; fax: 301-223-2400.

Postmaster: Send address changes to ANESTHESIOLOGY, P.O. BOX 1610, Hagerstown, MD 21740.

Advertising: Please contact Kelle Gray, National Account Manager, Health Learning, Research & Practice, Medical Journals, Wolters Kluwer Health, Inc.; phone: 843-261-4221; e-mail: Kelle.Gray@wolterskluwer.com. For classified advertising: Dave Wiegand, Recruitment Advertising Representative, Wolters Kluwer Health, Inc.; phone: 847-361-6128; e-mail: Dave.Wiegand@wolterskluwer.com.

Challenge your thinking with Summaries of Emerging Evidence SEE



You are caring for a recent lung transplant recipient in the intensive care unit who is intubated and on mechanical ventilation. According to a recent review article, which of the following interventions is MOST appropriate for this patient?

- (A) Normalize tidal volume to 6 mL/kg of donor predicted body weight
- (B) Maintain positive end-expiratory pressure (PEEP) above 15 H₂O
- (C) Maintain pH below 7.25

Find out if you answered correctly:
asahq.org/SEE39A-Sample

Zero in on key learning from
30+ scientific medical journals—
and earn up to 60 CME credits.
SEE 2023 Volume 39A is available now!

ANESTHESIOLOGY

Trusted Evidence: Discovery to Practice®

The Official Journal of the American Society of Anesthesiologists anesthesiology.org

Mission: Promoting scientific discovery and knowledge in perioperative, critical care, and pain medicine to advance patient care.

EDITOR-IN-CHIEF

Evan D. Kharasch, M.D., Ph.D.
Editor-in-Chief, ANESTHESIOLOGY
Department of Anesthesiology
Duke University
Durham, North Carolina
Tel: 1-800-260-5631
E-mail: editorial-office@anesthesiology.org

PAST EDITORS-IN-CHIEF

Henry S. Ruth, M.D., 1940–1955
Ralph M. Tovell, M.D., 1956–1958
James E. Eckenhoff, M.D., 1959–1962
Leroy D. Vandam, M.D., 1963–1970
Arthur S. Keats, M.D., 1971–1973
Nicholas M. Greene, M.D., 1974–1976
C. Philip Larson, Jr., M.D., 1977–1979
John D. Michenfelder, M.D., 1980–1985
Lawrence J. Saidman, M.D., 1986–1996
Michael M. Todd, M.D., 1997–2006
James C. Eisenach, M.D., 2007–2016

COVER ART

James P. Rathmell, M.D., Boston, Massachusetts
Annemarie B. Johnson,
Medical Illustrator, Winston-Salem, North Carolina

For reprint inquiries and purchases, please contact
reprintsolutions@wolterskluwer.com in North America, and
healthlicensing@wolterskluwer.com for rest of world.

Anesthesiology is abstracted or indexed in Index Medicus/MEDLINE, Science Citation Index/SciSearch, Current Contents/Clinical Medicine, Current Contents/Life Sciences, Reference Update, EMBASE/Excerpta Medica, Biological Abstracts (BIOSIS), Chemical Abstracts, Hospital Literature Index, and Comprehensive Index to Nursing and Allied Health Literature (CINAHL).

The affiliations, areas of expertise, and conflict-of-interest disclosure statements for each Editor and Associate Editor can be found on the Journal's Web site (www.anesthesiology.org).

CME EDITORS

Leslie C. Jameson, M.D.
Dan J. Kopacz, M.D.

EDITORIAL OFFICE

Rebecca Benner, Managing Editor
E-mail: managing-editor@anesthesiology.org
Loretta Pickett, Assistant Managing Editor
Gabrielle McDonald, Digital Communications Specialist
Caitlin Washburn
ANESTHESIOLOGY Journal
1061 American Lane
Schaumburg, IL 60173-4973
Tel: 1-800-260-5631
E-mail: editorial-office@anesthesiology.org

WOLTERS KLUWER HEALTH PUBLICATION STAFF

Ryan Shaw, Senior Publisher
Cheryl Stringfellow, Senior Journal Production Editor
Laura Mitchell, Journal Production Editor
Lori Querry, Journal Production Associate
Kelle Gray, National Account Manager

ASA OFFICERS

Michael W. Champeau, M.D., FAAP, FASA, President
Ronald L. Harter, M.D., FASA, President-Elect
Randall M. Clark, M.D., FASA, Immediate Past President
Donald E. Arnold, M.D., FASA, First Vice President

All articles accepted for publication are done so with the understanding that they are contributed exclusively to this Journal and become the property of the American Society of Anesthesiologists. Statements or opinions expressed in the Journal reflect the views of the author(s) and do not represent official policy of the American Society of Anesthesiologists unless so stated.

ANESTHESIOLOGY

Trusted Evidence: Discovery to Practice®

The Official Journal of the American Society of Anesthesiologists anesthesiology.org

Mission: Promoting scientific discovery and knowledge in perioperative, critical care, and pain medicine to advance patient care.

EDITOR-IN-CHIEF

Evan D. Kharasch, M.D., Ph.D., Durham, North Carolina

ASSISTANT EDITOR-IN-CHIEF

Michael J. Avram, Ph.D., Chicago, Illinois

EXECUTIVE EDITORS

Deborah J. Culley, M.D., Philadelphia, Pennsylvania
Andrew Davidson, M.B.B.S., M.D., Victoria, Australia
Jerrold H. Levy, M.D., Durham, North Carolina
Laszlo Vutskits, M.D., Ph.D., Geneva, Switzerland

EDITORS

Brian T. Bateman, M.D., Stanford, California
Amanda A. Fox, M.D., M.P.H., Dallas, Texas
Yandong Jiang, M.D., Ph.D., Houston, Texas
Sachin Kheterpal, M.D., M.B.A., Ann Arbor, Michigan
Martin J. London, M.D., San Francisco, California
Kristin Schreiber, M.D., Ph.D., Boston, Massachusetts
Jamie W. Sleigh, M.D., Hamilton, New Zealand

STATISTICAL EDITOR

Timothy T. Houle, Ph.D., Boston, Massachusetts

CREATIVE AND MULTIMEDIA EDITOR

James P. Rathmell, M.D., Boston, Massachusetts

ASSOCIATE EDITORS

Takashi Asai, M.D., Ph.D., Osaka, Japan
Beatrice Beck-Schimmer, M.D., Zurich, Switzerland
James M. Blum, M.D., Atlanta, Georgia
Sorin J. Brull, M.D., Jacksonville, Florida
Chad Michael Brummett, M.D., Ann Arbor, Michigan
John Butterworth, M.D., Richmond, Virginia
Maxime Cannesson, M.D., Ph.D., Los Angeles, California

Maurizio Cereda, M.D., Boston, Massachusetts
Vincent W. S. Chan, M.D., Toronto, Canada
Steven P. Cohen, M.D., Baltimore, Maryland
Melissa L. Coleman, M.D., Hershey, Pennsylvania
Albert Dahan, M.D., Ph.D., Leiden, The Netherlands
Sharon Einav, M.Sc., M.D., Jerusalem, Israel
Douglas Eleveld, M.D., Groningen, The Netherlands
Holger K. Eltzschig, M.D., Ph.D., Houston, Texas
Charles W. Emala, Sr., M.D., M.S., New York, New York
David Faraoni, M.D., Ph.D., Houston, Texas
Ana Fernandez-Bustamante, M.D., Ph.D., Aurora, Colorado
Julia Alejandra Gálvez Delgado, M.D., M.B.I., Omaha, Nebraska
Laurent Glance, M.D., Rochester, New York
Stephen T. Harvey, M.D., Nashville, Tennessee
Harriet W. Hopf, M.D., Salt Lake City, Utah
Vesna Jevtovic-Todorovic, M.D., Ph.D., M.B.A., Aurora, Colorado
Ru-Rong Ji, Ph.D., Durham, North Carolina
Cor J. Kalkman, M.D., Utrecht, The Netherlands
Karim Ladha, M.D., M.Sc., Toronto, Canada
Meghan Lane-Fall, M.D., M.H.S.P., Philadelphia, Pennsylvania
Adam B. Lerner, M.D., Boston, Massachusetts
Kate Leslie, M.B.B.S., M.D., M.Epi., Melbourne, Australia
Philipp Lirk, M.D., Ph.D., Boston, Massachusetts
George A. Mashour, M.D., Ph.D., Ann Arbor, Michigan
Michael Mazzeffi, M.D., M.P.H., M.Sc., Charlottesville, Virginia
Daniel McIsaac, M.D., M.P.H., Ottawa, Canada
Jane S. Moon, M.D., Los Angeles, California
Jochen D. Muehlschlegel, M.D., M.M.Sc., Boston, Massachusetts
Paul S. Myles, M.B., B.S., M.P.H., M.D., Melbourne, Australia
Peter Nagele, M.D., M.Sc., Chicago, Illinois
Mark D. Neuman, M.D., M.Sc., Philadelphia, Pennsylvania
Craig Palmer, M.D., Tucson, Arizona
Alexander Proekt, M.D., Ph.D., Philadelphia, Pennsylvania
Cyril Rivat, M.D., Montpellier, France
Jeffrey Sall, M.D., Ph.D., San Francisco, California
Warren S. Sandberg, M.D., Ph.D., Nashville, Tennessee
Alan Jay Schwartz, M.D., M.S.Ed., Philadelphia, Pennsylvania
Daniel I. Sessler, M.D., Cleveland, Ohio
Allan F. Simpao, M.D., M.B.I., Philadelphia, Pennsylvania
Nikolaos J. Skubas, M.D., Cleveland, Ohio

ANESTHESIOLOGY

Trusted Evidence: Discovery to Practice®

The Official Journal of the American Society of Anesthesiologists anesthesiology.org

Mission: Promoting scientific discovery and knowledge in perioperative, critical care, and pain medicine to advance patient care.

Ken Solt, M.D., Boston, Massachusetts

David A. Story, M.B.B.S., B.Med.Sci., M.D., Parkville, Australia

Michel Struys, M.D., Ph.D., Groningen, The Netherlands

Eric Sun, M.D., Ph.D., Palo Alto, California

BobbieJean Sweitzer, M.D., Fairfax, Virginia

Marcos F. Vidal Melo, M.D., Ph.D., New York, New York

Suellen Walker, Ph.D., London, United Kingdom

Jonathan P. Wanderer, M.D., M.Phil., Nashville, Tennessee

Duminda N. Wijeyesundera, M.D., Ph.D., Toronto, Canada

Hannah Wunsch, M.D., M.Sc., Toronto, Canada

Michael Zaugg, M.D., M.B.A., Edmonton, Canada

VISUAL TEAM

Christina Boncyk, M.D., Nashville, Tennessee

Holly B. Ende, M.D., Nashville, Tennessee

Julia Alejandra Gálvez Delgado, M.D., M.B.I., Omaha, Nebraska

Daniel Larach, M.D., Nashville, Tennessee

Olivia Nelson, M.D., Philadelphia, Pennsylvania

James P. Rathmell, M.D., Boston, Massachusetts

Allan F. Simpao, M.D., M.B.I., Philadelphia, Pennsylvania

Jonathan Tan, M.D., M.P.H., M.B.I., Los Angeles, California

Naveen Vanga, M.D., Houston, Texas

Jonathan P. Wanderer, M.D., M.Phil., Nashville, Tennessee

Annemarie B. Johnson, Medical Illustrator, Winston-Salem,
North Carolina

Terri Navarette, Graphic Artist, Schaumburg, Illinois

AUDIO TEAM

Julia Alejandra Gálvez Delgado, M.D., M.B.I., Omaha, Nebraska

Young-Tae Jeon, M.D., Seoul, Korea

Yandong Jiang, M.D., Ph.D., Houston, Texas

Rie Kato, M.D., D. Phil., Kanagawa, Japan

James P. Rathmell, M.D., Boston, Massachusetts

Cyril Rivat, M.D., Montpellier, France

BobbieJean Sweitzer, M.D., Fairfax, Virginia

Henrique F. Vale, M.D., Jackson, Mississippi

SOCIAL MEDIA TEAM

Rita Agarwal, M.D., Palo Alto, California

Sean Barnes, M.B.A., M.D., Baltimore, Maryland

Gregory Bryson, M.D., B.Sc., M.Sc., Ottawa, Canada

Nabil Elkassabany, M.D., Philadelphia, Pennsylvania

Alana Flexman, M.D., Vancouver, Canada

Julia Alejandra Gálvez Delgado, M.D., M.B.I., Omaha, Nebraska

Harriet W. Hopf, M.D., Salt Lake City, Utah

Ruth Landau, M.D., New York City, New York

Edward R. Mariano, M.D., M.A.S., Palo Alto, California

Emily Sharpe, M.D., Rochester, Minnesota

Sasha Shillcutt, M.D., M.S., Lincoln, Nebraska

Caitlin Sutton, M.D., Houston, Texas

Allan F. Simpao, M.D., M.B.I., Philadelphia, Pennsylvania

Ankeet Udani, M.D., M.S.Ed., Durham, North Carolina

the
ANESTHESIOLOGY
annual meeting

American Society of Anesthesiologists®

SAN FRANCISCO | OCTOBER 13-17, 2023



The best learning opportunity of the year is heading to the Golden City!

San Francisco has inspired countless startups, action movies, and foodie trends. Now let it inspire you! Join us in San Francisco, October 13–17, for everything new in anesthesiology. Refresh your clinical knowledge, explore new research and innovations, engage face-to-face with leaders and peers, and shape the future of patient care.

Sign up now to stay in the loop:
asahq.org/annualmeeting



Downloaded from /anesthesiology/issue/139/3 by guest on 19 April 2024

Instructions for Obtaining ANESTHESIOLOGY Continuing Medical Education (CME) Credit

CME Editors: Leslie C. Jameson, M.D., and Dan J. Kopacz, M.D.

ANESTHESIOLOGY's Journal CME is open to all readers. To take part in ANESTHESIOLOGY Journal-based CME, complete the following steps:

1. Read the accreditation information presented on this page.
2. Read this month's articles designated for credit (listed below) in either the print or online edition.
3. Register at <http://www.asahq.org/shop-asa>. In the category, search for Journal CME. ASA members can self-enroll for easy access to the CME course. Nonmembers will need to provide payment. This month's exam can be accessed directly at: www.asahq.org/JCME2023MAR. A full list of available courses is at www.ASAHQ.org/JCME.
4. Complete the activity posttest and course evaluation.
5. Claim a maximum of 1 *AMA PRA Category 1 Credit™* by the credit claiming deadline.

Accreditation Information

Purpose: The focus of ANESTHESIOLOGY Journal-based CME is to educate readers on current developments in the science and clinical practice of anesthesiology.

Target Audience: ANESTHESIOLOGY Journal-based CME is intended for anesthesiologists. Researchers and other healthcare professionals with an interest in anesthesiology may also participate.

Accreditation and Designation Statements: The American Society of Anesthesiologists is accredited by the Accreditation Council for Continuing Medical Education to provide continuing medical education for physicians.

The American Society of Anesthesiologists designates this journal-based activity for a maximum of 1 *AMA PRA Category 1 Credits™*. Physicians should claim only the credit commensurate with the extent of their participation in the activity.

Maintenance of Certification in Anesthesiology™ program and MOCA® are registered trademarks of the American Board of Anesthesiology®. MOCA 2.0® is a trademark of the American Board of Anesthesiology®.

This activity contributes to the CME component of the American Board of Anesthesiology's redesigned Maintenance of Certification in Anesthesiology™ (MOCA®) program, known as MOCA 2.0®. Please consult the ABA website, <http://www.theABA.org>, for a list of all MOCA 2.0 requirements.

Rates

Two options are available:

	ASA Member	Non-member
Annual Fee	\$0	\$126

Payment may be made using Visa or MasterCard.

Please direct any questions about Journal-based CME to: EducationCenter@asahq.org

Date of Release: February 2023

Expiration Date: February 2026

This Month's ANESTHESIOLOGY Journal-based CME Article

Read the article by Cammarota *et al.* entitled "Advanced Point-of-care Bedside Monitoring for Acute Respiratory Failure" on page 317. The CME exam can be accessed directly at: www.asahq.org/JCME2023MAR.

Learning Objectives

After successfully completing this activity, the learner will be able to select respiratory monitoring tests to evaluate a patient's lung aeration and morphology, regional ventilation-perfusion distribution, and pleural pressure.

Disclosures

This journal article has been selected for and planned as a journal CME activity, which is designated for *AMA PRA Category 1 Credit™*. The authors disclosed relationships in keeping with ANESTHESIOLOGY's requirements for all journal submissions. All relationships journal authors disclosed to ANESTHESIOLOGY are disclosed to learners, even those relationships that are not relevant financial relationships, per the ACCME's requirements for CME activities.

Editor-in-Chief: Evan D. Kharasch, M.D., Ph.D., has disclosed no relevant financial relationships with commercial interests.

CME Editors: Leslie C. Jameson, M.D., has disclosed no relevant financial relationships with commercial interests. Dan J. Kopacz, M.D., has disclosed having stock with Solo-Dex, Inc.

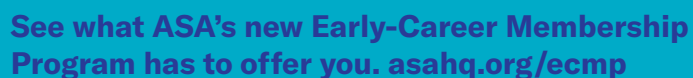
ASA Staff: Kari Lee and Anne Farace have disclosed no relevant financial relationships with commercial interests.

Disclaimer

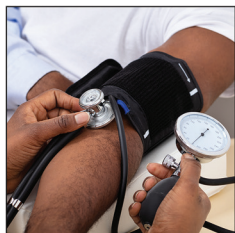
The information provided in this activity is for continuing education purposes only and is not meant to substitute for the independent medical judgment of a healthcare provider relative to diagnostic and treatment options of a specific patient's medical condition.

DOI: 10.1097/ALN.0000000000004494

And it's just for YOU. Start with one three- year membership—just \$299. Pile on FREE premium education and event registrations—valued up to \$4,600. Add timely clinical and career resources just as you need them.



Key Papers from the Most Recent Literature Relevant to Anesthesiologists



Intensive blood pressure control after endovascular thrombectomy for acute ischaemic stroke (ENCHANTED2/MT): A multicentre, open-label, blinded-end-point, randomised controlled trial. *Lancet* 2022; 400:1585–96. PMID: 36341753.

Best practice for systolic blood management after acute ischemic stroke managed with endovascular thrombectomy is uncertain. This open-label, blinded-endpoint trial conducted at 44 tertiary hospitals in China randomized 821 adults (July 2020 to March 2022) with persistently elevated systolic blood pressure (140 mmHg or higher for more than 10 min) after reperfusion with endovascular thrombectomy for acute ischemic stroke due to intracranial large-vessel occlusion. Treatment arms were either more (systolic blood pressure target less than 120 mmHg) or less intensive treatment (target, 140 to 180 mmHg) from 1 h through 72 h. The primary outcome was functional recovery using the modified Rankin scale (range 0 [no symptoms] to 6 [death]) at 90 days. The trial was terminated early given safety concerns (initial target, 2,257 subjects). Subjects in the more intensive treatment group (407) were more likely to sustain poor functional outcome than those in the less intensive group (406), common odds ratio 1.37 [95% CI, 1.07 to 1.76]. Patients in this group also had higher risk of early neurologic deterioration (common odds ratio, 1.53 [95% CI, 1.18 to 1.97]) and major disability at 90 days (odds ratio, 2.07 [95% CI, 1.47 to 2.93]). No significant differences in symptomatic intracerebral hemorrhage were found between groups nor in serious adverse events, recurrent ischemic events, or mortality between groups. (Article Selection: Martin J. London, M.D. Image: Adobe Stock.)

Take home message: This large, multicenter, randomized trial of more *versus* less intensive systolic blood pressure control over a 72-h period after endovascular thrombectomy induced reperfusion for acute large-vessel occlusion ischemic stroke was terminated early due to a higher incidence of poor functional outcomes with more intensive systolic blood pressure management.



Elective surgery system strengthening: Development, measurement, and validation of the surgical preparedness index across 1632 hospitals in 119 countries. *Lancet* 2022; 400:1607–17. PMID: 36328042.

The COVID-19 pandemic has had a detrimental impact on surgery and anesthesia services, particularly with regard to backlogs in elective surgery. To address the robustness of external stressors to surgical capability, The Lancet Commission on Global Surgery developed and validated a novel index, the surgical preparedness index, a measure of the worldwide fragility of planned surgical services. Initially, the index was developed through an international consensus process of 69 clinicians defining 23 prioritized core indicators (11 facilities and consumables, 2 staffing issues, 2 prioritization abilities, 8 systems parameters) with a score range from 23 (least prepared) to 115 (most prepared). This index was then assessed over a 2-month period in 2021 at 1,632 hospitals in 119 high-, middle-, and low-income countries (mean score for all sites was 84, and 89, 82, and 67 for high-, middle-, and low-income countries, respectively). To assess stability to stress (*e.g.*, COVID-19) the surgical volume before and after was calculated (surgical volume ratio). Overall, 75% of hospitals did not maintain their expected ratio, with the greatest reduction occurring in high- and middle-income centers. A linear mixed-effect regression model analysis demonstrated correlation of a 10-point increase in the index with a 4% increase in surgical volume ratio, independent of the income status. (Article Selection: Beatrice Beck-Schimmer, M.D. Image: J. P. Rathmell.)

Take home message: Based on assessment of four key domains of surgical preparedness, the newly developed surgical preparedness index can identify important areas for improvement in surgical and anesthesia care delivery associated with disruption of expected surgical volume in the face of external stressors.



Oxygen-saturation targets for critically ill adults receiving mechanical ventilation. *N Engl J Med* 2022; 387:1759–69. PMID: 36278971.

The optimal oxygen-saturation targets for critically ill adults requiring invasive mechanical ventilation are controversial. This study was a pragmatic, cluster-randomized, cluster-crossover trial at a single academic center (emergency department and medical intensive care unit) that randomized patients to a low (90%; range, 88 to 92%), intermediate (94%; range, 92 to 96%), or high saturation target (98%; range, 96 to 100%). Saturation was assessed by pulse oximetry. Other details of management were left to treating clinicians. Patients were enrolled over a 36-month period with exception of a 2-month pause during the COVID-19 pandemic. The primary outcome was the number of days alive and free of mechanical ventilation (ventilator-free days) through day 28. The secondary outcome was death by day 28. A total of 2,541 patients were analyzed (median ages, 57 to 59 yr; female, 45 to 47%; sepsis, 28 to 34%). There was no difference in the primary outcome between groups: low saturation (20 days; interquartile range, 0 to 25 days), intermediate saturation (21 days; interquartile range, 0 to 25 days), and high saturation (21 days; interquartile range, 0 to 26 days); $P = 0.81$. Likewise, there was no difference in in-hospital death by day 28 (35% vs. 34% vs. 33%). Adverse events (cardiac arrest, arrhythmia, myocardial infarction, stroke, and pneumothorax) were similar between groups. (Article Selection: Martin J. London, M.D. Image: J. P. Rathmell.)

Take home message: In a large, cluster-randomized, single-center trial, the use of a lower, intermediate, or higher oxygen saturation target during invasive mechanical ventilation did not influence the number of ventilator-free days at 28 days after randomization.



Effect of regular, low-dose, extended-release morphine on chronic breathlessness in chronic obstructive pulmonary disease: The BEAMS randomized clinical trial. JAMA 2022; 328:2022–32. PMID: 36413230.

Opioids are known to relieve symptoms of breathlessness; however their role in treating this symptom in patients with chronic obstructive pulmonary disease is uncertain. This multicenter (20 Australian centers), double-blind, placebo-controlled randomized clinical trial evaluated the impact of low-dose, extended-release oral morphine on chronic breathlessness in these patients with a modified Medical Research Council score of 3 to 4 after 1 week of treatment. Subjects were randomized 1:1:1 (8 mg/d, 16 mg/d, or placebo during week 1). At weeks 2 and 3, an additional 8 mg/d was added to the prior week's dose. The primary outcome

was the change in the intensity of breathlessness using a numerical rating scale (0 [none] to 10 [worst or most intense]) comparing the mean baseline score to the mean score after week 1 of treatment *versus* the placebo group. Daily step count by actigraphy device was assessed at week 3. A total of 156 subjects were analyzed (median age, 72 yr; 48% female); 138 (88%) completed treatment at week 1. There was no significant difference in the primary outcome at week 1 between groups: 8 mg morphine *versus* placebo (mean breathlessness score difference, -0.3 [95% CI, -0.9 to 0.4]); 16 mg morphine *versus* placebo (mean difference, -0.3 [95% CI, -1.0 to 0.4]). No difference was noted in the daily step count assessment. (Article Selection: Martin J. London, M.D. Image: Adobe Stock.)

Take home message: In a randomized trial of ambulatory chronic obstructive lung disease patients with chronic severe breathlessness, low-dose, extended-release morphine at two doses did not significantly reduce intensity of breathlessness after 1 week of treatment.



Early active mobilization during mechanical ventilation in the ICU. N Engl J Med 2022; 387:1747–58. PMID: 36286256.

Early active mobilization of intensive care unit (ICU) patients requiring mechanical ventilation is postulated to enhance outcome. This international multicenter trial (49 hospitals, six countries) randomized 750 adult ICU patients undergoing mechanical ventilation to early mobilization (sedation minimization and daily physiotherapy) or usual care. The primary outcome was the number of days alive and out of the hospital at 180 days after randomization. Key secondary outcomes included mortality (180 days) and patient-reported outcome measures. The study cohorts were similar (mean age, 61 vs. 60 yr; female, 35% vs. 40%; unplanned admission, 82% vs. 84%; sepsis, 66% vs. 66%). The mean \pm SD daily duration of mobilization was 21 ± 15 min *versus* 9 ± 9 min; intervention *versus* usual care (difference, 12 min/day; 95% CI, 10 to 14). There was no difference in the primary outcome between groups: median, 143 days (interquartile range, 21 to 161 days) vs. 145 days (interquartile range, 51 to 164 days); absolute difference, -2 days; 95% CI, -10 to 6 days; $P = 0.62$. Among secondary outcomes, neither death by day 180 (23% vs. 20%, odds ratio, 1.15; 95% CI, 0.81 to 1.65) nor patient-reported outcomes among survivors were different. Adverse events potentially due to mobilization were higher in reported in the early-mobilization group, 9% vs. 4% ($P = 0.005$). (Article Selection: Martin J. London, M.D. Image: J. P. Rathmell.)

Take home message: This international multicenter trial failed to detect an advantage to early mobilization in patients requiring mechanical ventilation on the number of days patients were alive and out of the hospital at 180 days relative to usual care. The intervention was associated with an increase in adverse events.



Electroacupuncture vs sham electroacupuncture in the treatment of postoperative ileus after laparoscopic surgery for colorectal cancer: A multicenter, randomized clinical trial. JAMA Surg 2023; 158:20–7. PMID: 36322060.

Despite widespread adoption of enhanced recovery after surgery protocols, postoperative ileus remains a problem with regard to adequate recovery after colorectal resection. The role of electroacupuncture in reducing ileus has not been studied. This multicenter (four Chinese tertiary centers) sham-controlled trial randomized adults undergoing primary laparoscopic resection of colorectal cancer with an enhanced recovery after surgery protocol to four sessions (30 min/day for 4 days after surgery) of electroacupuncture (five acupoints) or sham (four non-acupoints, no electrical stimulation). The primary outcome was the time to first defecation. Secondary outcomes included other patient-reported outcome measures, length of postoperative hospital stay, readmission rate within 30 days, and incidence of postoperative complications and adverse events. A total of 248 patients (mean age, 60 yr; 62% male) were analyzed. The primary outcome was significantly shorter in the treatment group (median [interquartile range] times to defecation 76 h [68 to 97 h] vs. 90 h [74 to 100 h]; mean difference, -8.8 ; 95% CI, -15.8 to -1.7 ; $P = 0.003$). Of the secondary outcomes, time to first flatus, tolerability of semiliquid diet, and solid food were significantly less as was prolonged ileus (risk ratio, 0.51; 95% CI, 0.27 to 0.95; $P = 0.03$). Other secondary outcomes were not different. There were no severe adverse events. (Article Selection: Martin J. London, M.D. Image: Adobe Stock.)

Take home message: In a multicenter trial of Chinese patients undergoing laparoscopic colon resection using enhanced recovery after surgery protocols, those receiving electroacupuncture for 4 days postoperatively had significantly shorter time to first defecation *versus* a sham procedure.



Surgery or endovascular therapy for chronic limb-threatening ischemia. N Engl J Med 2022; 387:2305–16. PMID: 36342173.

The relative roles of either endovascular therapy or surgical revascularization as initial therapies for chronic limb-threatening ischemia are not well delineated. This international, randomized trial of 1,830 patients with infrainguinal peripheral artery disease and limb ischemia studied two parallel cohorts: (1) patients with a single segment of great saphenous vein usable for surgery and (2) patients requiring an alternative bypass conduit. Within each cohort, patients were randomized (1:1) to surgical or endovascular treatment. The primary outcome was a composite of either a major adverse limb event (amputation above the ankle), a major limb reintervention (new bypass graft or graft revision, thrombectomy, or thrombolysis), or all-cause mortality. In cohort 1 (median follow-up, 2.7 yr), the primary outcome was significantly lower in the surgical group than in the endovascular group (43% vs. 57%; hazard ratio, 0.68; 95% CI, 0.59 to 0.79; $P < 0.001$). In cohort 2 (median follow-up, 1.6 yr), there was no significant difference (43% vs. 48%; hazard ratio, 0.79; 95% CI, 0.58 to 1.06; $P = 0.12$). There were no differences in the incidence of adverse events in any of the groups. (Article Selection: Martin J. London, M.D. Image: Adobe Stock.)

Take home message: In a large multicenter study of patients with infrainguinal peripheral artery disease and chronic limb-threatening ischemia, those with a great saphenous vein adequate for surgery had significantly less risk of a major adverse limb event or death relative to those undergoing endovascular therapy, while those without an adequate conduit did not.



Routine sterile glove and instrument change at the time of abdominal wound closure to prevent surgical site infection (ChEETAh): A pragmatic, cluster-randomised trial in seven low-income and middle-income countries. Lancet 2022; 400:1767–76. PMID: 36328045.

The effectiveness of changing gloves and instruments before wound closure in reducing postoperative abdominal surgical site infections is unclear. This multicenter, cluster-randomized trial in seven low- and middle-income African countries randomized clusters of patients undergoing abdominal surgery (consecutive adults and children undergoing elective or emergent abdominal surgery for a clean-contaminated, contaminated, or dirty operation) to standard practice (42 clusters) or intervention (change of gloves and instruments before wound closure for the entire scrub team [39 clusters]). The primary outcome was surgical site infection within 30 days after surgery using U.S. Centers for Disease Control and Prevention criteria and an intent-to-treat analysis. From June 2020 to April 2022, 81 clusters of 13,301 patients (7,157 routine vs. 6,144 intervention) were randomly assigned. Overall, 89% were adults, 46% underwent elective surgery, 61% underwent surgery that was clean-contaminated. Glove and instrument change occurred in 0.8% of standard practice versus 98.3% in the intervention group. The primary outcome was significantly lower in the intervention group (16% vs. 19%; adjusted risk ratio, 0.87; 95% CI, 0.79 to 0.95; $P = 0.0032$). Prespecified subgroup analyses did not show any evidence of heterogeneity of treatment effect. (Article Selection: Martin J. London, M.D. Image: Adobe Stock.)

Take home message: This multicenter, cluster-randomized trial in low- and middle-income African countries demonstrated significantly lower 30-day surgical site infection in patients undergoing abdominal surgery when scrub teams changed gloves and instruments before abdominal wound closure.



Buprenorphine versus methadone for opioid use disorder in pregnancy. N Engl J Med 2022; 387:2033–44. PMID: 36449419.

The impact of buprenorphine therapy for opioid use disorder during pregnancy relative to methadone has not been well established. This retrospective cohort study of Medicaid enrollees (2000 to 2018) evaluated maternal and neonatal outcomes between those receiving either drug during early pregnancy (up to gestational week 19), late pregnancy (from gestational week 20 through the day before delivery), and within 30 days before delivery. Of 2,548,372 successful pregnancies analyzed, 10,704 females were exposed to buprenorphine and 4,387 to methadone in early pregnancy, 11,272 were exposed to buprenorphine and 5,056 to methadone in late pregnancy, and 9,976 were exposed to buprenorphine and 4,597 to methadone in the 30 days before delivery. Neonatal abstinence syndrome was significantly lower in infants exposed to buprenorphine versus methadone, 52% vs. 69% (adjusted relative risk, 0.73; 95% CI, 0.71 to 0.75) in the 30 days before delivery. Preterm birth, 14% versus 25%, (adjusted relative risk, 0.58; 95% CI, 0.53 to 0.62); small size for gestational age, 12% versus 15% (adjusted relative risk, 0.72; 95% CI, 0.66 to 0.80); and low birth weight, 8% versus 15% (adjusted relative risk, 0.56; 95% CI, 0.50 to 0.63) were also lower. No significant differences were noted in the frequency of cesarean section, 34% versus 33% (adjusted relative risk, 1.02; 95% CI, 0.97 to 1.08) or severe maternal complications, 3.3% versus 3.5% (adjusted relative risk, 0.91; 95% CI, 0.74 to 1.13). (Article Selection: Martin J. London, M.D. Image: J. P. Rathmell.)

Take home message: Among females enrolled in Medicaid, buprenorphine use for opioid use disorder was associated with a lower risk of adverse neonatal outcomes compared to methadone, while no significant differences were noted in assessed adverse maternal outcomes.



Association between preoperative hemodialysis timing and postoperative mortality in patients with end-stage kidney disease. *JAMA* 2022; 328:1837–48. PMID: 36326747.

There is a paucity of data on the timing of dialysis in patients with end-stage kidney disease before elective surgery. This retrospective cohort study analyzed the timing of dialysis with 90-day postoperative mortality in 1,147,846 surgical procedures (2011 to 2018) among 346,828 Medicare patients (median age, 65 yr) using the United States Renal Data System, a national registry of all patients treated with hemodialysis, linking records to Medicare claims. The distribution of timing intervals of dialysis to surgery was 65% 1-day, 25% 2-day, and 10% 3-day intervals. The primary outcome of all-cause 90-day postoperative mortality was 3.0% overall. Longer intervals between hemodialysis and surgery were significantly associated with higher risk: 2 days *versus* 1 day: absolute risk, 4.7% *versus* 4.2%; adjusted hazard ratio, 1.14 (95% CI, 1.10 to 1.18); 3 days *versus* 1 day: absolute risk, 5.2% *versus* 4.2%; adjusted hazard ratio, 1.25 (95% CI, 1.19 to 1.31); and 3 days *versus* 2 days: absolute risk, 5.2% *versus* 4.7%; adjusted hazard ratio, 1.09 (95% CI, 1.04 to 1.13). Hemodialysis on the same day as surgery was associated with a significantly lower hazard of mortality *versus* no same-day hemodialysis (absolute risk, 4.0% for same-day hemodialysis *vs.* 4.5% for no same-day hemodialysis; adjusted hazard ratio, 0.88 [95% CI, 0.84 to 0.91]). (Article Selection: Bobbie Jean Sweitzer, M.D. Image: Adobe Stock.)

Take home message: Lengthier intervals between hemodialysis and elective surgery are significantly associated with higher postoperative mortality in Medicare patients with end-stage renal disease.

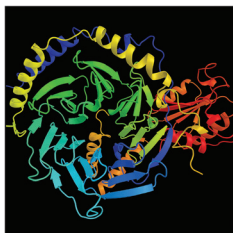


Transcriptomics-based network medicine approach identifies metformin as a repurposable drug for atrial fibrillation. *Cell Rep Med* 2022; 3:100749. PMID: 36223777.

The drug treatment of atrial fibrillation is only partially effective, and there is a need to develop new medications with alternative mechanisms of action. Use of network medicine methods could link drug targets, the human proteome, and disease modules, thus guiding repurposing of existing drugs. Transcriptomic data of human left atrium tissue obtained from 251 patients undergoing elective cardiac surgery was compared with drug-induced gene signatures from pluripotent cardiomyocytes. The results were then validated using a large-scale pharmacoepidemiologic dataset. There were 491 differentially expressed genes, coding for a number

of atrial fibrillation-specific proteins and covering a wide range of cellular functions. Nine potential drug candidates that reversed dysregulated gene expression were identified from the network proximity of 2,891 drug targets (phenformin, metformin, furosemide, metacycline, rofecoxib, dantrolene, dapamide, alclometasone, and streptozocin). Five cohort propensity score comparisons (total $n = 7720$) were performed from a large Enterprise electronic data warehouse comparing metformin to the four commonly used antidiabetic oral agents (and their combination), finding that metformin was associated with a 52% reduced likelihood of atrial fibrillation (odds ratio, 0.48; 95% CI, 0.36 to 0.64; $P < 0.001$). (Article Selection: Jamie Sleight, M.D. Image: J. P. Rathmell.)

Take home message: Metformin action on dysregulated gene networks associated with atrial fibrillation and pharmacoepidemiologic analyses suggest that it could potentially be used as a therapeutic agent.



State-selective modulation of heterotrimeric $G\alpha_s$ signaling with macrocyclic peptides. *Cell* 2022; 185:3950–65.e25. PMID: 36170854.

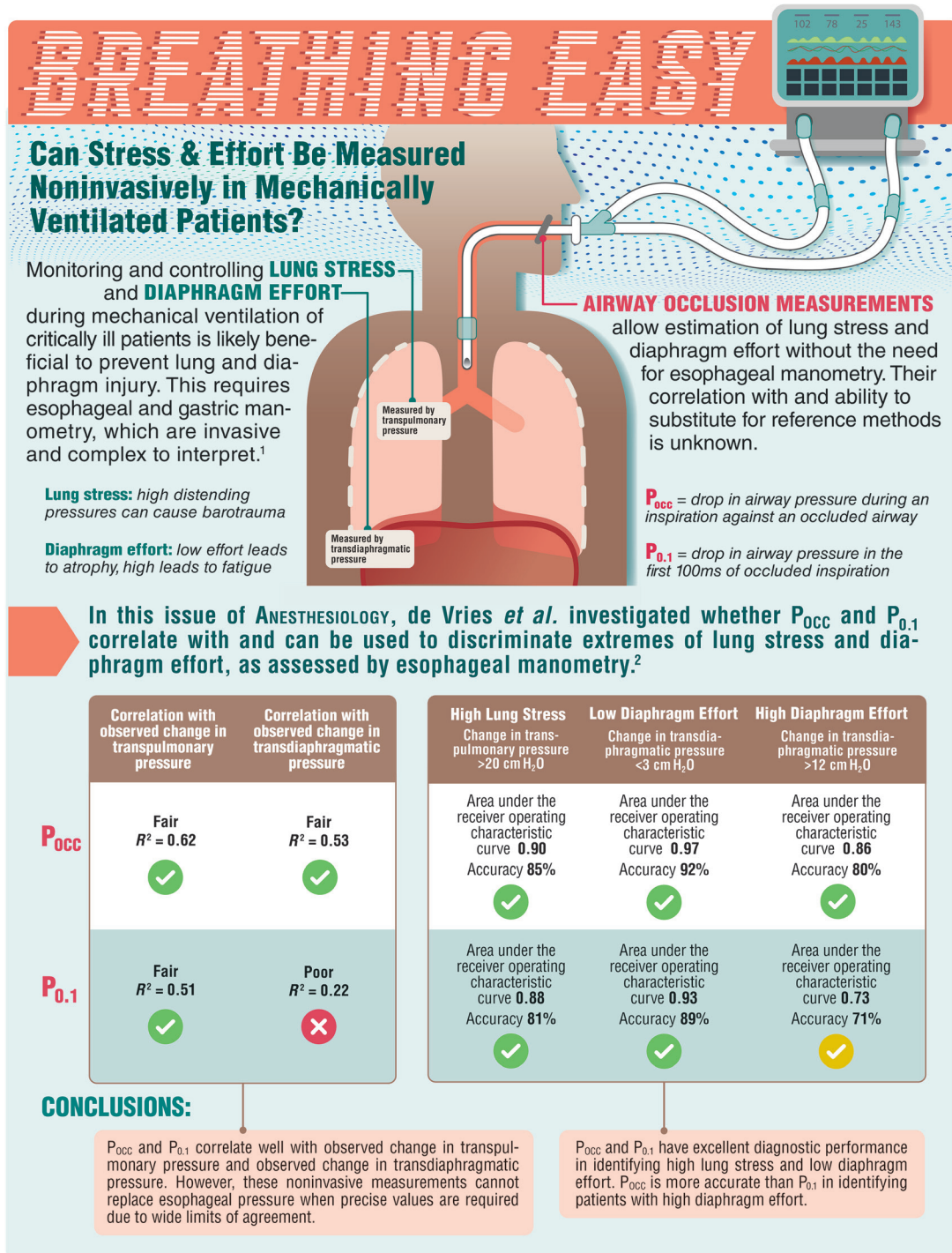
G-protein-coupled receptors are unique to eukaryotic cells and are important drug targets, with one-third of all Food and Drug Administration–approved drugs eliciting their biological effects through them. The ligand-activated seven-transmembrane domain receptors couple with G-proteins (heterotrimers) replacing GDP in G-protein's α subunit by GTP, which induces dissociation of the α subunit together with the bound GTP from the β and γ subunits, to further target intracellular functional proteins, particularly adenylyl cyclase as in the case of $G\alpha_s$. The intrinsic GTPase activity of the α subunit forms GDP, resulting in the reconstitution of the heterotrimer and termination of signaling. To date, direct targeting of G-proteins,

specifically their GTPase activity, was challenging. By screening a library of cyclic peptides, two macrocyclic peptides, GN13 and GD20, were found to specifically interact with $G\alpha_s$. GN13 prevented the interaction of $G\alpha_s$ with adenylyl cyclase, reducing β_2 -adrenergic receptor-induced activation of adenylyl cyclase and the generation of its second messenger cAMP ("inhibition of the $G\alpha_s$ ON-state"). In contrast, GD20 specifically interacted with the GDP-bound inactive conformation of $G\alpha_s$, preventing the dissociation of GDP. It also blocked the binding of $G\alpha_s$ to the $G\beta\gamma$ dimer, resulting in enhanced receptor-dependent $G\beta\gamma$ -signaling as evidenced by prolonged K^+ -channel activation ("blockage of the $G\alpha_s$ OFF-state with prolonged $G\beta\gamma$ activation"). (Article Selection: Michael Zaugg, M.D., M.B.A. Image: Adobe Stock.)

Take home message: Given the myriad physiologic cellular processes mediated by G-protein-coupled receptors, targeting specific G-proteins by macrocyclic peptides in a nucleotide state-selective manner to modulate intracellular signaling is a key step closer in the development of a highly promising entirely new class of drugs.

INFOGRAPHICS IN ANESTHESIOLOGY

Complex Information for Anesthesiologists Presented Quickly and Clearly



Infographic created by Holly B. Ende, Vanderbilt University Medical Center; James P. Rathmell, Brigham and Women's Health Care/Harvard Medical School; and Jonathan P. Wanderer, Vanderbilt University Medical Center. Illustration by Annemarie Johnson, Vivo Visuals Studio. Address correspondence to Dr. Ende: holly.ende@vmc.org.

- Dianti J, Goligher EC: Monitoring respiratory effort and lung-distending pressure noninvasively during mechanical ventilation: Ready for prime time. *ANESTHESIOLOGY* 2023; 138:235–7
- de Vries HJ, Tuinman PR, Jonkman AH, Liu L, Qiu H, Girbes ARJ, Zhang YR, de Man AME, de Groot H-J, Heunks L: Performance of noninvasive airway occlusion maneuvers to assess lung stress and diaphragm effort in mechanically ventilated critically ill patients. *ANESTHESIOLOGY* 2023; 138:274–88



American Society of
Anesthesiologists®

Make this year your year.

Become a Fellow of the American
Society of Anesthesiologists®

See the Criteria:
asahq.org/fasa



“ Leadership matters.
There will be times you will
wish that someone else is the
skipper, but it is during those
times you are needed most. ”

Joseph Dominguez
MD, FASA



“ I sought FASA because
many of the people I
admired in my field carried
this distinction. I knew that
they worked hard and made
meaningful contributions
to their field, and I wanted
to be amongst them! ”

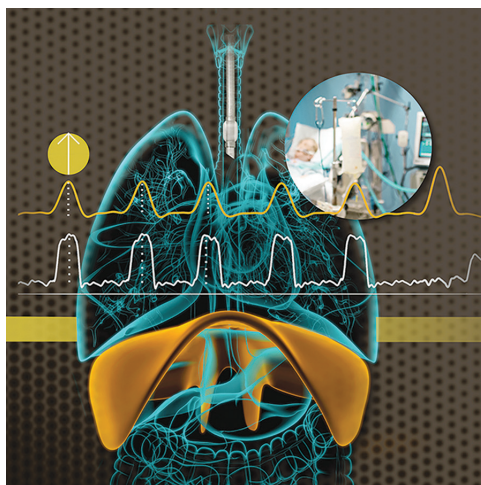
Elisha Peterson
MD, FASA

ASA
FELLOW

Monitoring Respiratory Effort and Lung-distending Pressure Noninvasively during Mechanical Ventilation: Ready for Prime Time

Jose Dianti, M.D., Ewan C. Goligher, M.D., Ph.D., F.R.C.P.C.

Monitoring and managing spontaneous breathing during mechanical ventilation is a routine clinical challenge for clinicians caring for patients with acute respiratory failure. When the respiratory muscles contract in synchrony with the ventilator, the pressure applied to the lung by the respiratory muscles adds to the pressure applied by the ventilator, increasing the total pressure applied across the lung. Respiratory effort is often excessive in patients with acute respiratory failure,¹ and the resulting high lung-distending pressures may further worsen lung injury (a phenomenon referred to as patient self-inflicted lung injury).² Vigorous respiratory efforts can also cause diaphragm myotrauma. On the other hand, when respiratory effort is insufficient, patients are at high risk for diaphragm disuse atrophy. Given increasing evidence of the physiologic and clinical relevance of these problems, respiratory effort merits close attention in mechanically ventilated patients.³ Traditionally, monitoring respiratory effort and lung-distending pressure during spontaneous breathing requires esophageal manometry to assess pleural pressure swings. However, this technique is not routinely employed in clinical practice as it requires dedicated equipment and expertise to correctly acquire and interpret the signals. Simple, noninvasive techniques using ventilator-based maneuvers to monitor respiratory effort would therefore be of great value.



“[Inspiratory occlusion pressure and airway occlusion pressure are] simple and non-invasive methods to monitor the risk of lung and diaphragm injury in patients with acute respiratory failure.”

novel features of this work. First, the authors directly quantify diaphragmatic effort, rather than respiratory effort; this is relevant since transdiaphragmatic pressure is the relevant index of muscular activity. Second, the authors validate P_{occ} and P_{0.1} with reference to a prolonged recording of the reference standard measurement (1 h *vs.* a few minutes, as in previous studies); this suggests that these measurements reflect lung- and diaphragm-protective targets over hours, rather than merely minutes. Third, the authors

In this edition of *ANESTHESIOLOGY*, de Vries *et al.*⁴ evaluated the performance of two noninvasive techniques for monitoring respiratory effort and lung-distending pressure: the inspiratory occlusion pressure (P_{occ}), and the airway occlusion pressure in the first 100 ms (P_{0.1}). Using data from 38 patients enrolled in a randomized trial testing a strategy to facilitate safe spontaneous breathing during mechanical ventilation, they demonstrate the utility of these measurements to monitor diaphragmatic effort and lung-distending pressure during mechanical ventilation. Specifically, they show that P_{occ} and P_{0.1} can accurately detect (1) very low diaphragmatic effort, (2) very high diaphragmatic effort, and (3) potentially injurious levels of transpulmonary driving pressure or transpulmonary mechanical power. There are several key

Image: A. Johnson, Vivo Visuals Studio.

This editorial accompanies the article on p. 274. This article has a related Infographic on p. A17. This article has an audio podcast.

Accepted for publication December 22, 2022.

Jose Dianti, M.D.: Interdepartmental Division of Critical Care Medicine, University of Toronto, Toronto, Canada; Division of Respiriology, Department of Medicine, University Health Network, Toronto, Canada.

Ewan C. Goligher, M.D., Ph.D., F.R.C.P.C.: Interdepartmental Division of Critical Care Medicine, and Department of Physiology, University of Toronto, Toronto, Canada; Division of Respiriology, Department of Medicine, University Health Network, Toronto, Canada; Toronto General Hospital Research Institute, Toronto, Canada.

Copyright © 2023, the American Society of Anesthesiologists. All Rights Reserved. *Anesthesiology* 2023; 138:235–7. DOI: 10.1097/ALN.0000000000004489

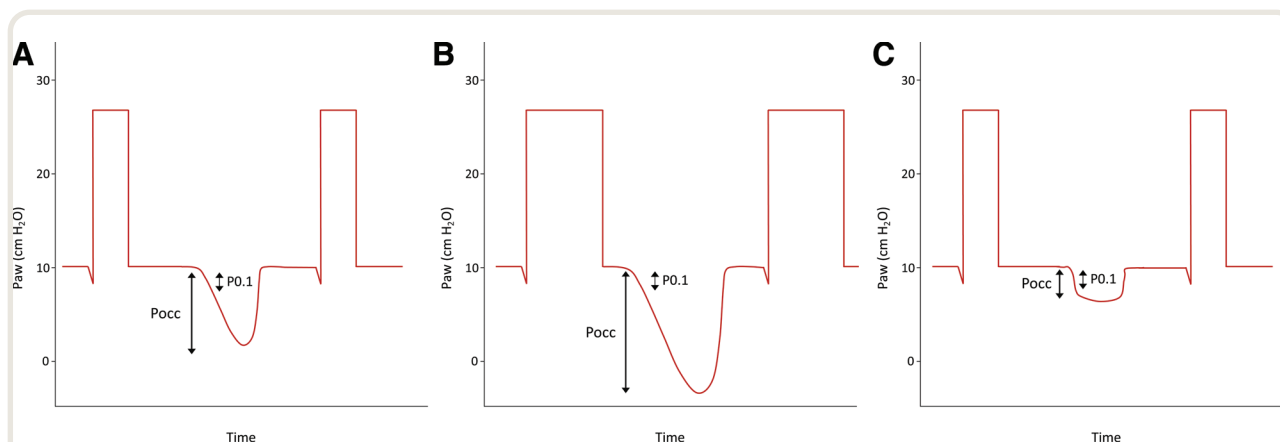


Fig. 1. Theoretical factors affecting the relationship between respiratory drive ($P_{0.1}$) and respiratory effort (Pocc). In contrast to respiratory effort, respiratory drive is not affected by respiratory system mechanics or respiratory muscle dysfunction. The Pocc will therefore vary according inspiratory time (A vs. B) and according to respiratory muscle strength (A vs. C), while $P_{0.1}$ is relatively unaffected across each clinical scenario. P_{aw} , airway pressure; Pocc, inspiratory occlusion pressure; $P_{0.1}$, airway occlusion pressure in the first 100 ms.

derived and validated a method for predicting lung-distending pressure from $P_{0.1}$. Fourth, they also derived and validated a method for computing transpulmonary mechanical power from $P_{0.1}$ and Pocc. Overall, the work by de Vries *et al.* provides definitive confirmation of the relevance of these simple, noninvasive maneuvers to monitor respiratory effort and lung-distending pressure during assisted mechanical ventilation and highlight their potential utility to guide a lung- and diaphragm-protective ventilation strategy.

Airway occlusion pressure in the first 100 ms is a well-known maneuver described several decades ago by Whitelaw *et al.*,⁵ but Pocc was described only recently⁶ and is not as widely employed in clinical practice. Pocc measures the magnitude of the pressure generated by the respiratory muscles against the occluded airway. An end-expiratory occlusion maneuver is applied and maintained for the duration of a single breath (fig. 1). The maneuver is somewhat analogous to measurement of maximal inspiratory pressure on the ventilator (also sometimes called negative inspiratory force), except that the occlusion is being used to estimate the pressure generated during tidal breathing rather than during maximal volitional efforts. The resulting pressure deflection generated by the respiratory muscles can be used to estimate the pleural pressure swing using an empirically derived correction factor. The lung-distending pressure (dynamic transpulmonary driving pressure) during spontaneous breathing can then be estimated by adding the measured airway pressure swing (peak pressure—positive end-expiratory pressure) to the estimated pleural pressure swing. This study confirms and significantly extends our knowledge of the value and interpretation of this technique. A simple Pocc calculator for use at the bedside is available at <https://pocc.coemv.ca>.

One of the important features of the work by de Vries *et al.* is that they provide a head-to-head comparison of the

utility of Pocc and $P_{0.1}$ for monitoring respiratory effort and lung-distending pressure. Airway occlusion pressure in the first 100 ms is technically a measure of the respiratory drive, but since respiratory effort (the amplitude of respiratory muscle force generation during a given breath) is dependent on the presence and magnitude of respiratory drive, it makes sense that drive and effort would be correlated. de Vries *et al.* confirm a previous finding that $P_{0.1}$ can accurately detect insufficient respiratory effort but is less accurate to detect elevated respiratory effort.⁷ Various factors can explain why elevated respiratory effort is less reliably detected by $P_{0.1}$. The relationship between respiratory drive and respiratory effort depends on (1) the inspiratory time (for a given level of respiratory drive—a longer inspiration will lead to greater peak respiratory effort) and (2) diaphragm strength or force-generating capacity: a patient with diaphragmatic weakness may have elevated respiratory drive but be capable of generating only relatively small respiratory efforts (fig. 1). Despite this limitation, the authors found that $P_{0.1}$ can detect elevated lung-distending pressure with reasonable accuracy using an empirically derived correction factor. Overall, $P_{0.1}$ and Pocc provide complementary information about spontaneous breathing. Of note, Esnault *et al.* reported that both $P_{0.1}$ and Pocc predicted a higher risk of failed transition from controlled to assisted ventilation in COVID-19 acute respiratory distress syndrome.⁸

The study by de Vries *et al.* substantially strengthens the growing body of data on the validity of both $P_{0.1}$ and Pocc as simple and noninvasive methods to monitor the risk of lung and diaphragm injury in patients with acute respiratory failure. Analogous to routine measurement of plateau pressure and driving pressure during passive ventilation, $P_{0.1}$ and Pocc provide invaluable information on the safety and appropriateness of mechanical ventilation. The impact of a lung- and diaphragm-protective ventilation strategy guided

by these noninvasive measurements on patient-centered outcomes remains to be determined in clinical trials (www.practicalplatform.org), but clinicians may find them immediately useful for monitoring mechanical ventilation in routine clinical practice.

Competing Interests

Dr. Goligher is a member of the Clinical Advisory Board of LungPacer (Exton, Pennsylvania), which markets pulmonary therapy products. He reports receiving personal fees from Vyaire (Mettawa, Illinois), which markets ventilators and other critical care products; Getinge (Solna, Sweden), a medical technology company that markets ventilators; and BioAge (Richmond, California), which markets health and wellness products and services. Dr. Dianti is not supported by, nor maintains any financial interest in, any commercial activity that may be associated with the topic of this article.

Correspondence

Address correspondence to Dr. Goligher: ewan.goligher@utoronto.ca

References

1. Dianti J, Fard S, Wong J, Chan TCY, Sorbo LD, Fan E, Amato MBP, Granton J, Burry L, Reid WD, Zhang B, Ratano D, Keshavjee S, Slutsky AS, Brochard LJ, Ferguson ND, Goligher EC: Strategies for lung- and diaphragm-protective ventilation in acute hypoxemic respiratory failure: A physiological trial. *Crit Care* 2022; 26:259
2. Brochard L, Slutsky A, Pesenti A: Mechanical ventilation to minimize progression of lung injury in acute respiratory failure. *Am J Resp Crit Care Med* 2017; 195:438–42
3. Goligher EC, Dres M, Patel BK, Sahetya SK, Beitler JR, Telias I, Yoshida T, Vaporidi K, Grieco DL, Schepens T, Grasselli G, Spadaro S, Dianti J, Amato M, Bellani G, Demoule A, Fan E, Ferguson ND, Georgopoulos D, Guérin C, Khemani RG, Laghi F, Mercat A, Mojoli F, Ottenheijm CAC, Jaber S, Heunks L, Mancebo J, Mauri T, Pesenti A, Brochard L: Lung and diaphragm-protective ventilation. *Am J Respir Crit Care Med* 2020; 202:950–61
4. de Vries HJ, Tuinman PR, Jonkman AH, Liu L, Qiu H, Girbes ARJ, Zhang Y, de Man AME, de Grooth H-J, Heunks L: Performance of noninvasive airway occlusion maneuvers to assess lung stress and diaphragm effort in mechanically ventilated critically ill patients. *ANESTHESIOLOGY* 2023; 138:274–88
5. Whitelaw WA, Derenne J-P, Milic-Emili J: Occlusion pressure as a measure of respiratory center output in conscious man. *Resp Physiol* 1975; 23:181–99
6. Bertoni M, Telias I, Urner M, Long M, Sorbo LD, Fan E, Sinderby C, Beck J, Liu L, Qiu H, Wong J, Slutsky AS, Ferguson ND, Brochard LJ, Goligher EC: A novel non-invasive method to detect excessively high respiratory effort and dynamic transpulmonary driving pressure during mechanical ventilation. *Crit Care* 2019; 23:346
7. Telias I, Junhasavasdikul D, Rittayamai N, Piquilloud L, Chen L, Ferguson ND, Goligher EC, Brochard L: Airway occlusion pressure as an estimate of respiratory drive and inspiratory effort during assisted ventilation. *Am J Respir Crit Care Med* 2020; 201:1086–98
8. Esnault P, Cardinale M, Hraiech S, Goutorbe P, Baumstrack K, Prud'homme E, Bordes J, Forel J-M, Meaudre E, Papazian L, Guervilly C: High respiratory drive and excessive respiratory efforts predict relapse of respiratory failure in critically ill patients with COVID-19. *Am J Respir Crit Care Med* 2020; 202:1173–8

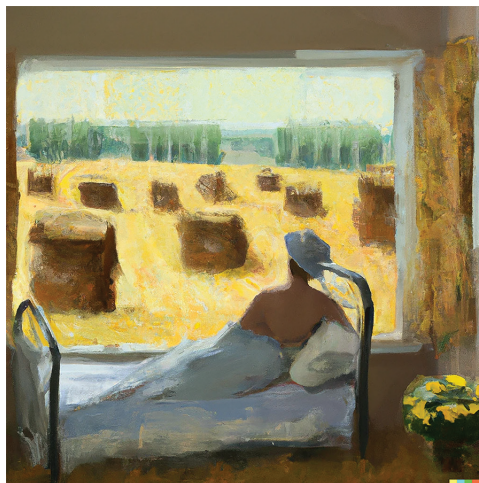
Paradox of Power: Dynamic Tools to Predict Respiratory Failure in Spontaneously Breathing Patients

Daniel R. Calabrese, M.D., Martin J. London, M.D.

THE impressionist artist Claude Monet painted a series of haystacks, *Les Meules à Giverny*. He famously produced 14 paintings in a single day as he noted that the sun changed position every 7 min.¹ Much as observations of color are subject to the influence of atmospheric conditions on the refraction of light, our assessments of complex biologic systems may also change with differences in perspective. While static measurements, such as PaO_2 or plateau pressure, are heavily relied upon for their diagnostic value, dynamic measurements can reveal additional insights into disease trajectory or treatment response.

In this issue of *ANESTHESIOLOGY*, Gattarello *et al.* provide thought provoking data on the value of mechanical power and other dynamic measures of respiratory function in spontaneously breathing COVID-19 patients in acute respiratory failure.² They performed a secondary analysis of a prospective cohort of 111 patients hospitalized with COVID-19 pneumonia at a single center between September 2020 and December 2021. All patients were supported with continuous positive airway pressure. An esophageal balloon catheter estimated the pleural pressure (esophageal inspiratory pressure – esophageal expiratory pressure), and tidal volume (V_T) and respiratory rate (RR) were measured with a novel noninvasive impedance device.³

It is well established that limiting V_T to 6 to 8 ml/kg of ideal body weight improves survival during acute respiratory distress syndrome, but it is unclear if these targets are appropriate for all patients given heterogeneity in regional



“Mechanical power has emerged as a potential *unifying* predictor of ventilator-induced lung injury.”

lung compliance.⁴ Recently, mechanical power has emerged as a potential *unifying* predictor of ventilator-induced lung injury. Mechanical power is a measurement, in joules per minute, of the energy required to move the lungs from rest to a given point on the respiratory system pressure–volume curve. During mechanical ventilation, airway pressure is delivered to overcome the resistive and elastic forces of the respiratory system to generate thoracic expansion. Ventilator-induced lung injury is associated with mechanical power, potentially dependent on V_T , in experimental models,^{5–7} and increased mechanical power is associated with mortality among mechanically ventilated patients with acute respiratory distress syndrome, independent of driving pressure.^{8,9} However, among spon-

taneously breathing patients, it has been unknown whether differences in mechanical power may identify patients at risk for progression of acute lung injury.

To address this gap, Gattarello *et al.* estimated mechanical power with a validated equation using RR, V_T , and pleural pressure. The authors offered a novel definition of *ideal mechanical power* as the power needed for a normal minute ventilation, figured as 0.1 times the ideal body weight (kg). Two recently introduced indices, the ratio of oxygen index and the pressure–rate index, were also measured, with the former more easily applied at the bedside.^{10,11} The primary outcome of treatment escalation, defined as any increase in respiratory support beyond continuous positive airway pressure, was left to the discretion of the attending physician with institutional guidance based on the COVID-19

Image: Generated by the author using DALL•E 2 natural language to image generation AI system.

This editorial accompanies the article on p. 289. This article has an audio podcast.

Accepted for publication December 23, 2022.

Daniel R. Calabrese, M.D.: University of California-San Francisco, San Francisco, California; San Francisco Veterans Affairs Medical Center, San Francisco, California.

Martin J. London, M.D.: University of California-San Francisco; San Francisco, California; San Francisco Veterans Affairs Medical Center, San Francisco, California.

Copyright © 2023, the American Society of Anesthesiologists. All Rights Reserved. *Anesthesiology* 2023; 138:238–40. DOI: 10.1097/ALN.0000000000004490

pandemic. The authors used the area under the receiver operating characteristics curve (AUC) to test the association between each predictor and the binary need for respiratory treatment escalation.

Gattarello *et al.* report clear differences in initial ventilatory parameters in the group of patients eventually requiring respiratory treatment escalation higher than continuous positive airway pressure characterized by lower Pao_2 , worse $\text{Pao}_2/\text{fraction of inspired oxygen}$, higher minute ventilation, higher RR, higher pleural pressure, and higher lung elastance on the first day of hospitalization. All values of the tested dynamic parameters were worse in patients requiring more respiratory support: mechanical power, in absolute and relative values; the ratio of oxygen index; and the pressure–rate index. Mechanical power and the pressure–rate index had the highest AUC for determining need of respiratory treatment escalation, but the ratio of oxygen index had a similar but smaller receiver operating characteristic curve area. These findings identify mechanical power as a potentially sensitive instrument for discerning which spontaneously breathing patients with acute respiratory failure are at risk for escalation in care.

A strength of this study is that it is an analysis of prospective data collected with sophisticated tools and carefully applied to the latest existing mathematical constructs of mechanical power. Stated limitations by the authors included that the statistical approach was not selected to assess superiority of the various indices in predicting the primary outcome. Thus, questions remain about whether mechanical power performs better in identifying an at-risk group than less complex indices of respiratory failure, more readily applied at the bedside, such as the ratio of oxygen index. Of particular concern, the primary study outcome of respiratory escalation is quite broad, is inclusive of other noninvasive support, and may not be clinically meaningful, although the authors' justification that guidelines developed specifically for the COVID-19 pandemic were widely applied appears sound. Further, acknowledging resource limitations during the COVID-19 pandemic, patients in this study were supported on continuous positive airway pressure, whereas high-flow nasal canula is a more accepted initial therapy for respiratory failure.¹² Therefore, additional work is required to best establish the association between mechanical power in spontaneously breathing patients and important clinical outcomes such as the need for mechanical ventilation or, of primary importance, mortality. Broad adoption of this complex approach hinges on evidence of relevance in other common non-COVID-19 causes of respiratory failure, such as sepsis, and with models adjusted for potentially confounding demographic variables, such as age or comorbid respiratory disease.

Based on these findings, one immediate question is whether the clinician should incorporate mechanical power measurements into practice. One potential barrier is the challenge of how best to normalize mechanical power between patients who vary in baseline differences in the

measured parameters given age, sex, and body size. The authors showed no differences in distributions of gas volume or tissue mass on computed tomography chest imaging between the cohorts of patients. However, the question remains of how to account for lung disease heterogeneity within individual patients. Others have proposed normalizing mechanical power to dynamic lung compliance, which would better control for these differences.¹³ Here the authors derived a novel and untested value, *ideal mechanical power* as a function of height and sex, which would control for thoracic size. Which normalization approach will ultimately allow broad clinical application of mechanical power remains to be answered.

There are additional technical considerations regarding the measurement and application of mechanical power. Gattarello *et al.* measure mechanical power with a validated equation that largely reflects inspiratory power. Experts debate whether to include the expiratory component of mechanical power, which may be especially important in spontaneously breathing patients. Quantifying mechanical power as the area under the pressure–volume loop may more comprehensively capture the ventilation cycle, as others have shown discrepant values when comparing these two approaches.¹⁴ Additional work is also needed to ascertain how widely used treatment modalities, such as proning or high-flow nasal canula, may influence mechanical power in spontaneously breathing patients. Finally, data from experimental models are needed to establish whether mechanical power is a marker of lung disease severity or a mediator of lung injury during spontaneous breathing.

As Claude Monet showed in the French countryside, serial observations of complex systems yield novel insights. Intriguingly, mechanical power may be a more dynamic assessment of lung injury, though practical questions remain to be answered before it may supplant conventional clinical approaches and more established indicators of disease severity.

Research Support

Dr. Calabrese is supported with funding from the Cystic Fibrosis Foundation (Bethesda, Maryland), the American Society of Transplantation (Mt. Laurel, New Jersey), and the VA Office of Research and Development (IK2BX005301; Washington, D.C.).

Competing Interests

The authors are not supported by, nor maintain any financial interest in, any commercial activity that may be associated with the topic of this article.

Correspondence

Address correspondence to Dr. Calabrese: daniel.calabrese@ucsf.edu

References

- House J: *Monet: Nature into Art*. New Haven, Connecticut, Yale University Press, 1986
- Gattarello S, Coppola S, Chiodaroli E, Pozzi T, Camporota L, Saager L, Chiumello D, Gattinoni L: Mechanical power ratio and respiratory treatment escalation in COVID-19 pneumonia: A secondary analysis of a prospectively enrolled cohort. *ANESTHESIOLOGY* 2023; 138:289–98
- Galvagno SM, Brayanov J, Corneille MG, Voscopoulos CJ, Sordo S, Ladd D, Freeman J: Non-invasive respiratory volume monitoring in patients with traumatic thoracic injuries. *Trauma* 2015; 17:219–23
- Meyer NJ, Gattinoni L, Calfee CS: Acute respiratory distress syndrome. *Lancet* 2021; 398:622–37
- Moraes L, Silva PL, Thompson A, Santos CL, Santos RS, Fernandes MVS, Morales MM, Martins V, Capelozzi VL, de Abreu MG, Pelosi P, Rocco PRM: Impact of different tidal volume levels at low mechanical power on ventilator-induced lung injury in rats. *Front Physiol* 2018; 9:318
- Cressoni M, Gotti M, Chiurazzi C, Massari D, Algieri I, Amini M, Cammaroto A, Brioni M, Montaruli C, Nikolla K, Guanziroli M, Dondossola D, Gatti S, Valerio V, Vergani GL, Pugini P, Cadringer P, Gagliano N, Gattinoni L: Mechanical power and development of ventilator-induced lung injury. *ANESTHESIOLOGY* 2016; 124:1100–8
- Santos RS, Maia LA, Oliveira MV, Santos CL, Moraes L, Pinto EF, Samary CDS, Machado JA, Carvalho AC, Fernandes MVS, Martins V, Capelozzi VL, Morales MM, Koch T, Gama de Abreu M, Pelosi P, Silva PL, Rocco PRM: Biologic impact of mechanical power at high and low tidal volumes in experimental mild acute respiratory distress syndrome. *ANESTHESIOLOGY* 2018; 128:1193–206
- Tonna JE, Peltan I, Brown SM, Herrick JS, Keenan HT, Grissom CK, Presson AP, Vasques F: Mechanical power and driving pressure as predictors of mortality among patients with ARDS. *Intensive Care Med* 2020; 46:1941–3
- Serpa Neto A, Deliberato RO, Johnson AEW, Bos LD, Amorim P, Pereira SM, Cazati DC, Cordioli RL, Correa TD, Pollard TJ, Schettino GPP, Timenetsky KT, Celi LA, Pelosi P, Gama de Abreu M, Schultz MJ, PROVE Network Investigators: Mechanical power of ventilation is associated with mortality in critically ill patients: An analysis of patients in two observational cohorts. *Intensive Care Med* 2018; 44:1914–22
- Costa ELV, Slutsky AS, Brochard LJ, Brower R, Serpa-Neto A, Cavalcanti AB, Mercat A, Meade M, Morais CCA, Goligher E, Carvalho CRR, Amato MBP: Ventilatory variables and mechanical power in patients with acute respiratory distress syndrome. *Am J Respir Crit Care Med* 2021; 204:303–11
- Roca O, Caralt B, Messika J, Samper M, Sztrymf B, Hernández G, García-de-Acilu M, Frat JP, Masclans JR, Ricard JD: An index combining respiratory rate and oxygenation to predict outcome of nasal high-flow therapy. *Am J Respir Crit Care Med* 2019; 199:1368–76
- Frat J-P, Thille AW, Mercat A, Girault C, Ragot S, Perbet S, Prat G, Boulain T, Morawiec E, Cottureau A, Devaquet J, Nseir S, Razazi K, Mira J-P, Argaud L, Chakarian J-C, Ricard J-D, Wittebole X, Chevalier S, Herblant A, Fartoukh M, Constantin J-M, Tonnelier J-M, Pierrot M, Mathonnet A, Béduneau G, Deléage-Métreau C, Richard J-CM, Brochard L, Robert R: High-flow oxygen through nasal cannula in acute hypoxemic respiratory failure. *N Engl J Med* 2015; 372:2185–96
- Ghiani A, Paderewska J, Sainis A, Crispin A, Walcher S, Neurohr C: Variables predicting weaning outcome in prolonged mechanically ventilated tracheotomized patients: a retrospective study. *J Intensive Care* 2020; 8:19
- Wu S-H, Kor C-T, Mao IC, Chiu C-C, Lin K-H, Kuo C-D: Accuracy of calculating mechanical power of ventilation by one commonly used equation. *J Clin Monit Comput* 2022; 36:1753–9

ANESTHESIOLOGY

Comparison of Contralateral Acceleromyography and Electromyography for Posttetananic Count Measurement

Hyunyoung Joo, M.D., Sooyoung Cho, M.D., Ph.D.,
Jong Wha Lee, M.D., Ph.D., Won Joong Kim, M.D., Ph.D.,
Hyun Jung Lee, M.D., Ph.D., Jae Hee Woo, M.D., Ph.D.,
Giyeon Lee, M.D., Hee Jung Baik, M.D., Ph.D.

ANESTHESIOLOGY 2023; 138:241–8

EDITOR'S PERSPECTIVE

What We Already Know about This Topic

- Deep neuromuscular blockade during anesthesia for laparoscopic or robotic surgeries may offer several advantages in terms of patient outcomes and physician surgical experience
- Posttetanic count can be used to identify intense neuromuscular block (posttetanic count equal to 0) and deep neuromuscular block (posttetanic count greater than or equal to 1 and train-of-four count equal to 0) and estimate the time to recovery

What This Article Tells Us That Is New

- The agreement of posttetanic counts monitored in contralateral arms by acceleromyography and electromyography was determined in 35 patients given 0.6 mg/kg rocuronium after induction of anesthesia and calibration of the monitors, with additional doses of 0.3 mg/kg if required
- Seventy-three percent of 226 pairs of acceleromyography– and electromyography–posttetanic count measurements indicated the same neuromuscular blockade status (intense or deep block)
- Of 184 pairs of posttetanic counts of 15 or less, 42 (23%) acceleromyography–posttetanic counts were equal to electromyography–posttetanic counts, 93 (50%) were more than electromyography counts, and 49 (27%) were less than electromyography counts

ABSTRACT

Background: Electromyography has advantages over mechanomyography and acceleromyography. Previously, agreement of the train-of-four counts between acceleromyography and electromyography was found to be fair. The objective of this study was to assess the agreement of posttetanic count including agreement of neuromuscular blockade status (intense block, posttetanic count equal to 0; or deep block, posttetanic count 1 or greater and train-of-four count equal to 0) between acceleromyography and electromyography.

Methods: Thirty-six patients, aged 20 to 65 yr, participated in this study. A dose of 0.6 mg/kg rocuronium, with additional dose of 0.3 mg/kg if required, was administered to the patients. The train-of-four and posttetanic counts were monitored in the contralateral arm using electromyography at the first dorsal interosseus or adductor pollicis, and acceleromyography at the adductor pollicis. Posttetanic count measurements were performed at 6-min intervals; the responses were recorded until the train-of-four count reached 1. The authors evaluated the agreement of degree of neuromuscular blockade (intense or deep block) and that of posttetanic count between acceleromyography and electromyography.

Results: The authors analyzed 226 pairs of measurements. The percentage agreement indicating the same neuromuscular blockade status (intense or deep block) between acceleromyography and electromyography was 73%. Cohen's kappa coefficient value was 0.26. After excluding data with acceleromyography–posttetanic counts greater than 15, a total of 184 pairs of posttetanic counts were used to evaluate the agreement between the two monitoring methods. For acceleromyography–posttetanic count, 42 (23%) pairs had the same electromyography–posttetanic count, and 93 (50%) pairs had more than the electromyography–posttetanic count. The mean posttetanic count on electromyography was 38% (95% CI, 20 to 51%) lower than that on acceleromyography ($P = 0.0002$).

Conclusions: Acceleromyography frequently counted more twitches than electromyography in posttetanic count monitoring. Acceleromyography– and electromyography–posttetanic counts cannot be used interchangeably to assess the degree of neuromuscular blockade.

(*ANESTHESIOLOGY* 2023; 138:241–8)

Neuromuscular monitoring, particularly quantitative twitch monitoring, is recommended during anesthesia and recovery.¹ Although acceleromyography is easily and widely used clinically, it has some limitations in that the thumb must be unrestricted and free to move and the baseline train-of-four ratio is often greater than 1.0.^{1–3} Electromyography has many advantages over mechanomyography or acceleromyography; free movement of the

This article is featured in "This Month in Anesthesiology," page A1. This article has a visual abstract available in the online version. The work presented in this article has been presented at KoreAnesthesia 2021, The 98th Annual Scientific Meeting of the Korean Society of Anesthesiologists, in Busan, Republic of Korea, November 4, 2021.

Submitted for publication May 25, 2022. Accepted for publication December 2, 2022. Published online first on December 15, 2022.

Hyunyoung Joo, M.D.: Department of Anesthesiology and Pain Medicine, Daniel Hospital, Bucheon, Republic of Korea.

Sooyoung Cho, M.D., Ph.D.: Department of Anesthesiology and Pain Medicine, College of Medicine, Ewha Womans University, Seoul, Republic of Korea.

Jong Wha Lee, M.D., Ph.D.: Department of Anesthesiology and Pain Medicine, College of Medicine, Ewha Womans University, Seoul, Republic of Korea.

Won Joong Kim, M.D., Ph.D.: Department of Anesthesiology and Pain Medicine, College of Medicine, Ewha Womans University, Seoul, Republic of Korea.

Copyright © 2023, the American Society of Anesthesiologists. All Rights Reserved. *Anesthesiology* 2023; 138:241–8. DOI: 10.1097/ALN.0000000000004466

thumb is not required, no preload is needed, and it is less dependent on the maintenance of intraoperative normothermia.^{1,4} Recently, several freestanding electromyography monitors have become commercially available.

Previous studies evaluated the agreement of train-of-four counts or ratios between acceleromyography and electromyography. Results showed that agreement of train-of-four counts between acceleromyography and electromyography was fair, and that acceleromyography underestimated the electromyography–train-of-four count.⁵ However, another study showed that acceleromyography was less precise than electromyography and overestimated the electromyography–train-of-four ratio.⁶

Recently, robotic and laparoscopic surgeries have been increasing, and the burden of recovery from deep neuromuscular blockade has been reduced by the use of sugammadex.⁷ Thus, the desire to maintain deep neuromuscular blockade during these surgeries is increasing; deep neuromuscular blockade creates a good surgical field, requires low carbon dioxide inflation pressure, and reduces postoperative pain.^{8–10} Although the evidence for routine use of deep neuromuscular blockade for laparoscopic surgery is insufficient,¹¹ posttetanic count measurement is important for clinical situations requiring maintenance of deep neuromuscular blockade.

However, to our knowledge, the comparison of posttetanic counting by acceleromyography and electromyography has not been well studied. The objective of this study was to assess the agreement of posttetanic counts, including agreement of neuromuscular blockade status (intense block, posttetanic count equal to 0; or deep block, posttetanic count 1 or greater and train-of-four count equal to 0)¹² between acceleromyography and electromyography.

Materials and Methods

This study was conducted at Ewha Womans University Mokdong Hospital (Seoul, Republic of Korea) from October 12, 2020, to February 23, 2021. Thirty-six patients, aged 23 to 65 yr, American Society of Anesthesiologists Physical Status I or II, scheduled for various elective surgeries that require positioning for more than 90 min under general anesthesia in the supine position with both arms abducted, were enrolled. The Institutional Review Board of Ewha Womans University Mokdong Hospital (Institutional Review Board No. 2020-06-001-002, Seoul, Republic of Korea) approved

the study protocol on August 13, 2020, and written informed consent was obtained from all the patients. This trial was registered in the Clinical Trial Registry of Korea (<http://cris.nih.go.kr>, KCT0005444, posted on October 6, 2020; principal investigator, Hee Jung Baik, M.D., Ph.D.) before enrolling the first participant. Patients were excluded if they had neuromuscular, neurologic, or renal disease or body mass index greater than 25 kg/m².¹³

For neuromuscular blockade monitoring, we used acceleromyography (Philips IntelliVue Neuro Muscular Transmission Module 865383, Philips Healthcare, The Netherlands) and electromyography (TwitchView Monitor, Blink Device Company, USA) monitors that stimulated the ulnar nerves to obtain a twitch response from the adductor pollicis muscle for acceleromyography and the first dorsal interosseus or adductor pollicis muscle for electromyography. According to the Good Clinical Research Practice guidelines for neuromuscular monitoring,¹³ acceleromyography was performed using two electrodes (3M Red Dot electrode 2248-50, 3M Healthcare, USA) placed 3 to 6 cm apart over the ulnar nerve. An acceleration transducer was attached to the thumb and moved freely without preload. The second through the fourth fingers were attached to the arm board with surgical tape.^{13–15} Electromyography electrode array was applied according to the manufacturers' guidelines, and we did not fix the patient's hand for electromyography monitoring. To reduce arm-to-arm variation, we attached both acceleromyography and electromyography electrodes to the dominant and nondominant arms in equal proportions using a computer-generated randomization table (Random Allocation Software, version 1.0; developed by M. Saghaei, Isfahan University of Medical Sciences, Iran).^{16,17}

Effect-site concentration–target–controlled infusions of propofol and remifentanyl were used for total intravenous anesthesia. After the patient was unconscious, acceleromyography and electromyography were calibrated using built-in calibration functions to determine the supramaximal current for nerve stimulation. Train-of-four stimulation at the supramaximal current was performed immediately before administration of 0.6 mg/kg IV rocuronium to the patients. Thereafter, train-of-four stimulation was given at 12-s intervals until tracheal intubation was performed when the train-of-four count was 0 to 3. If the patient's diaphragmatic or limb movement or cough was observed during or after tracheal intubation, or posttetanic count was not 0, an additional dose of rocuronium (0.3 mg/kg) was injected after intubation. When the train-of-four count was 0, the posttetanic count stimulus was performed at 6-min intervals, and the responses were recorded until the first twitch response in the train-of-four stimulus (T1) appeared. All patients were placed under an upper body forced air warming blanket (Bair Hugger, Augustine Medical Inc., USA), and the central temperatures were monitored in the nasopharynx and maintained greater than 36°C.

Hyun Jung Lee, M.D., Ph.D.: Department of Anesthesiology and Pain Medicine, Ewha Womans University Seoul Hospital, Seoul, Republic of Korea.

Jae Hee Woo, M.D., Ph.D.: Department of Anesthesiology and Pain Medicine, College of Medicine, Ewha Womans University, Seoul, Republic of Korea.

Giyar Lee, M.D.: Department of Anesthesiology and Pain Medicine, Ewha Womans University Mokdong Hospital, Seoul, Republic of Korea.

Hee Jung Baik, M.D., Ph.D.: Department of Anesthesiology and Pain Medicine, College of Medicine, Ewha Womans University, Seoul, Republic of Korea.

Statistical Analysis

The normality of continuous data was tested using the Kolmogorov–Smirnov test and quantile–quantile plot evaluation. Data are expressed as number (percentage) for categorical data and mean \pm SD for normally distributed data or median [interquartile range] for nonnormally distributed data. For paired measurements, comparisons of supramaximal stimuli current and the time for train-of-four count to reach 0 after rocuronium injection between acceleromyography and electromyography monitoring were analyzed using the Wilcoxon signed-rank test. Cohen’s kappa statistic was used to assess the agreement of the neuromuscular blockade status (intense or deep block) between acceleromyography and electromyography monitoring. To evaluate the relationship between acceleromyography–posttetanic count *versus* electromyography–posttetanic count, a scatter plot was presented. The maximum number of stimuli for posttetanic count monitoring of acceleromyography used in this study was 20, and that of electromyography was 15. Therefore, to evaluate the agreement of posttetanic counts between acceleromyography and electromyography monitoring, we excluded data with acceleromyography–posttetanic counts greater than 15. Owing to the nature of the data, Poisson regression analysis was performed to establish the percentage

limits. It considered both correlations between paired measurements and between multiple measurements in the same subject. If overdispersion was suspected, negative binomial Poisson regression analysis was performed. Statistical analyses were performed using SPSS software (SPSS for Windows, Version 22.0, IBM Corp., USA) and R statistical software version 3.6.2 (R Foundation for Statistical Computing, Austria). P value < 0.05 was considered statistically significant. PASS software (PASS 11, NCSS, LLC, USA)¹⁸ was used to calculate the sample size of 142 measurements to achieve a power of 90% and an alpha of 0.05, with a dropout rate of 20% when the null hypothesis was “no agreement” and the expected kappa coefficient was 0.3.¹⁹ This strategy was based on the results of a previous study comparing train-of-four agreement between acceleromyography and electromyography.⁵ Since an average of four measurements per patient was expected to be possible, we enrolled 36 patients.

Results

Of the enrolled 36 patients, one patient was excluded from statistical analysis because of measurement failure (fig. 1). Patient characteristics are shown in table 1. No significant difference was observed in the amplitude of the supramaximal stimulus (mA; median [interquartile range]) between

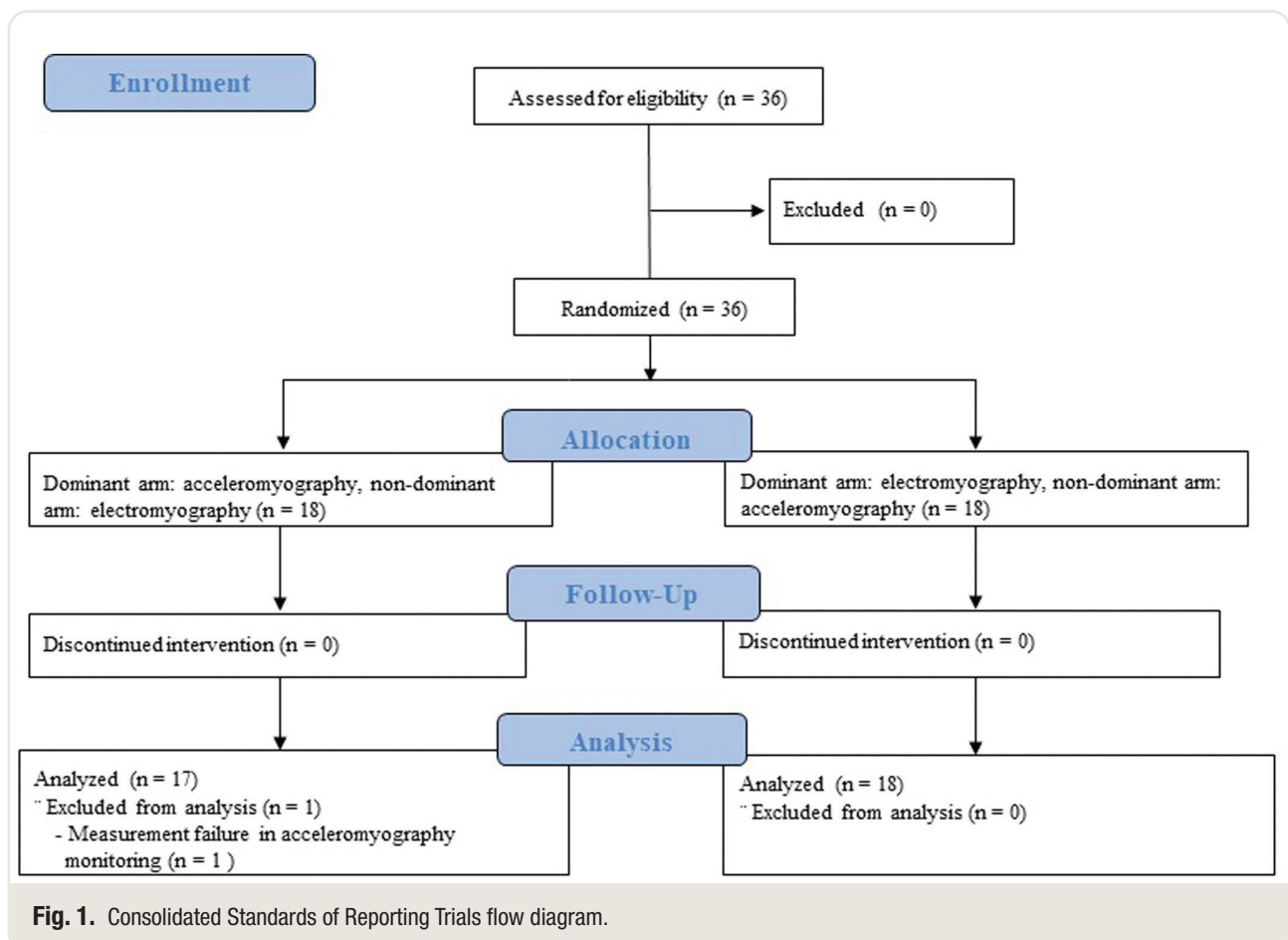


Table 1. Demographic Data

Patients (n = 35)	
Sex	
Men	19 (54%)
Women	16 (46%)
Age, yr	53 [47–62]
Height, cm	165.4 ± 7.8
Weight, kg	63.1 ± 9.3
Body mass index, kg/m ²	22.9 ± 2.1
ASA Physical Status	
I	15 (43%)
II	20 (57%)
Dominant arm	
Right	35 (100%)
Left	0
Study arm	
Dominant arm: acceleromyography, nondominant arm: electromyography	17 (49%)
Dominant arm: electromyography, nondominant arm: acceleromyography	18 (51%)

Data are number of patients (%), mean ± SD, or median [interquartile range]. ASA, American Society of Anesthesiologists.

acceleromyography (60 [50–60] mA) and electromyography (48 [48–54] mA; $P = 0.518$). The time from administration of rocuronium to the start of posttetananic count measurement when the train-of-four count reached 0 was not significantly different between acceleromyography (180 [120–320] s) and electromyography (150 [100–255] s; $P = 0.248$).

We analyzed 226 pairs of posttetananic count measurements. The percentage agreement indicating the same neuromuscular blockade status (intense or deep block) between acceleromyography and electromyography was 73%, and Cohen's kappa coefficient (95% CI) was 0.26 (0.12 to 0.40; table 2). The kappa coefficient showed positive value, thus indicating that the actual agreement for intense or deep block between acceleromyography and electromyography is greater than agreement by chance.

Figure 2 shows a scatter plot of acceleromyography–posttetananic count *versus* electromyography–posttetananic count. This shows that the range of electromyography–posttetananic count values measured to correspond to

acceleromyography–posttetananic count is very wide. Forty-two out of 226 pairs were excluded for the comparison of posttetananic count between the two monitors because electromyography–posttetananic count had a maximum value of 15. For acceleromyography, out of 184 pairs, 42 (23%) acceleromyography–posttetananic counts were equal to electromyography–posttetananic counts, 93 (50%) were more than electromyography–posttetananic counts, and 49 (27%) were less than electromyography–posttetananic counts (fig. 3). The mean posttetananic count on electromyography was 38% (95% CI, 20 to 51%) lower than that on acceleromyography (table 3).

Discussion

The main findings of this study are as follows: (1) The percentage agreement indicating the same neuromuscular blockade status (intense or deep block) between acceleromyography and electromyography was 73%, and Cohen's kappa coefficient was 0.26, which indicated that the actual agreement for intense or deep block between acceleromyography and electromyography was greater than coincidence. (2) For posttetananic count, 23% and 50% of acceleromyography–posttetananic counts were equal to and greater than electromyography–posttetananic counts, respectively, which indicated that acceleromyography frequently counted more twitches than electromyography for posttetananic counts. (3) The mean posttetananic count on electromyography was 38% lower than that on acceleromyography.

Currently, the importance of objective neuromuscular monitoring during and after anesthesia is emphasized. Among the objective neuromuscular monitoring devices, mechanomyography is impractical for clinical use despite being the accepted standard for neuromuscular monitoring. Acceleromyography is the most widely used clinically, but it is not interchangeable with mechanomyography or electromyography.^{5,6,20–22} The electromyography–train-of-four ratio obtained at the first dorsal interosseus muscle is reportedly equivalent to mechanomyography during the recovery phase.^{2,4,23} Several studies have shown that acceleromyography–train-of-four counts and ratios are not interchangeable with electromyography.^{5,6,22}

Table 2. Agreement of Intense Block or Deep Block between Acceleromyography and Electromyography

		Electromyography			Cohen's Kappa Coefficient (95% CI)
		Intense Block	Deep Block	Total	
Acceleromyography	Intense block	22 (10%)	16 (7%)	38	0.26 (0.12–0.46)
	Deep block	45 (20%)	143 (63%)	188	
	Total	67	159	226	

Data are number of measurements (%). Intense block, posttetananic count equal to 0; deep block: posttetananic count 1 or greater and train-of-four count equal to 0.

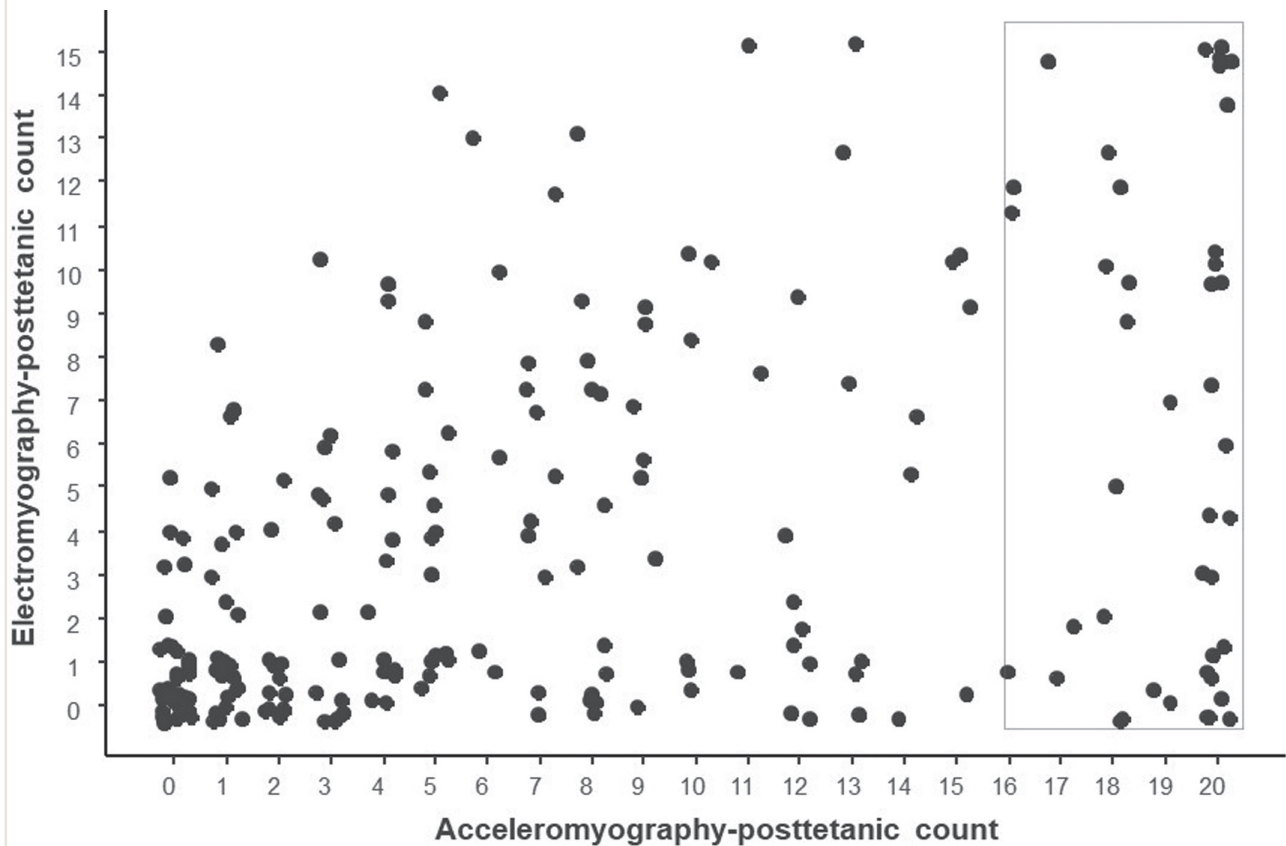


Fig. 2. Scatter plot of acceleromyography–posttetanic count versus electromyography–posttetanic count. Out of all 226 pairs, 42 (in the rectangular box) showed an acceleromyography–posttetanic count number of 16 or more.

The use of deep neuromuscular blockade during anesthesia in laparoscopic or robotic surgeries may have several advantages in terms of patient outcomes and physician surgical experience. Posttetanic count can be used to estimate the extent of intense to deep neuromuscular block and time to recovery.^{24,25} Dhonneur *et al.* demonstrated that posttetanic count at the adductor pollicis was a better indicator of early diaphragmatic recovery than train-of-four at the corrugator supercilii, and a posttetanic count at the adductor pollicis of 5 or less corresponded to deep neuromuscular block of the diaphragm.¹⁵ Fernando *et al.* also showed that the neuromuscular blockade of adductor pollicis should be intense (posttetanic count equal to 0) to ensure total diaphragmatic paralysis.²⁶ Therefore, posttetanic count monitoring is useful for achieving and maintaining deep neuromuscular blockade during these surgeries.

However, to date, the agreement of posttetanic count between acceleromyography and electromyography has not been well studied. This study aimed to verify the agreement between acceleromyography and electromyography for posttetanic count measurements to evaluate whether the two devices were clinically interchangeable determining the status of neuromuscular blockade (intense or deep block).

Our results showed that the percentage agreement indicating the same neuromuscular block status (intense or deep block) between acceleromyography and electromyography was 73%, and that Cohen's kappa coefficient value was 0.26, which indicates greater agreement than coincidence. This is consistent with the results of a study by Bowdle *et al.* for train-of-four response, which showed that the value of Cohen's kappa coefficient between acceleromyography and electromyography was fair (kappa = 0.38).⁵

We also performed pairwise comparisons of the posttetanic count using acceleromyography and electromyography. Twenty-three percent of acceleromyography–posttetanic counts were equal to electromyography–posttetanic counts, and 50% were greater. This indicates that compared with electromyography, acceleromyography frequently counted more twitches for the posttetanic count. Previous studies also have shown clinically significant differences between electromyography and acceleromyography with respect to train-of-four count⁵ and train-of-four ratio.^{6,22} These differences are attributed to several factors, including differences in monitoring devices used, differences in the side of the monitored arm (ipsilateral or contralateral), whether examiners apply preload to the thumb and/or restrain

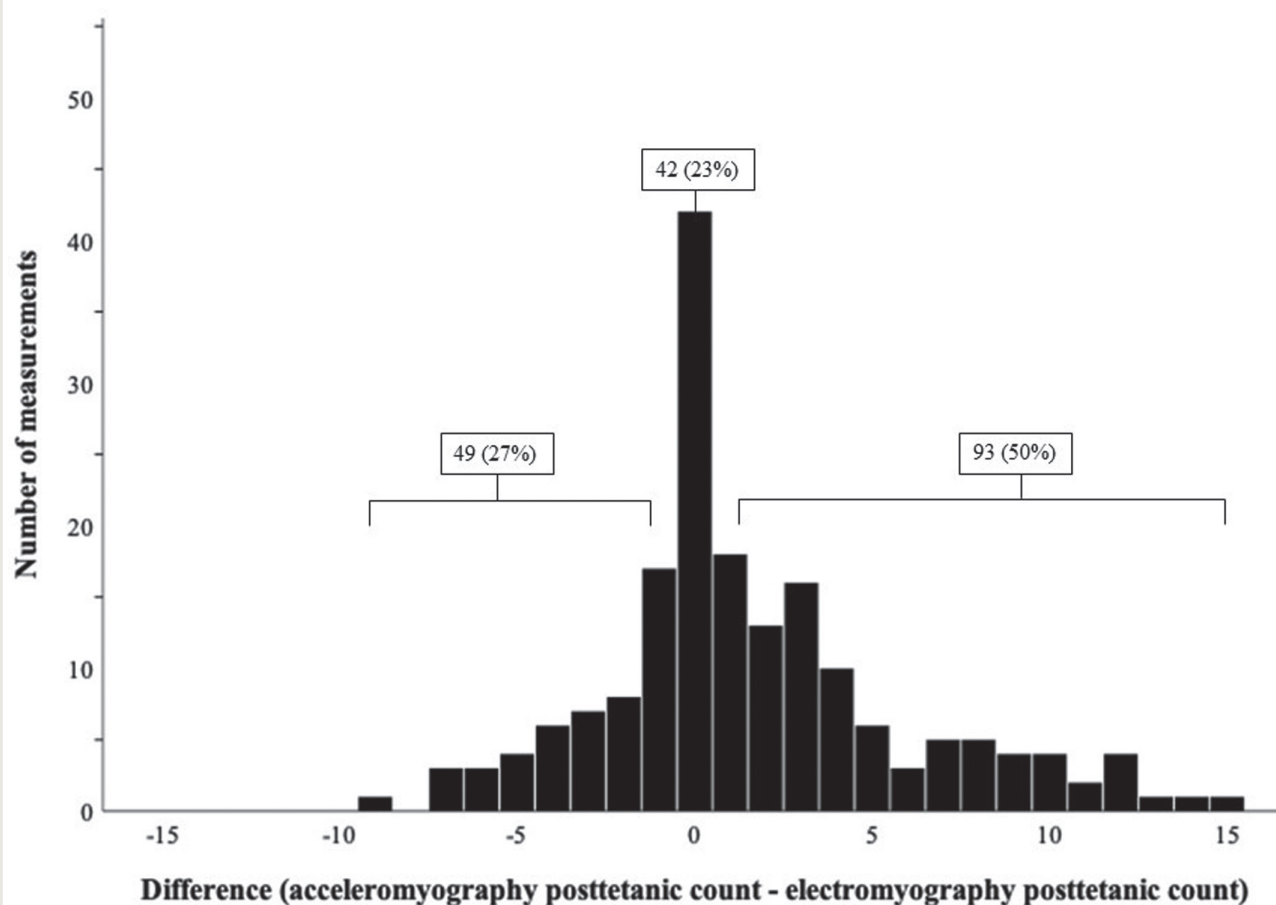


Fig. 3. Distribution of difference between acceleromyography–posttetanic count and electromyography–posttetanic count. For acceleromyography, 23% of acceleromyography–posttetanic counts were equal to electromyography–posttetanic counts, 50% were more than, and 27% were less than electromyography–posttetanic counts.

Table 3. Percentage Limits of Posttetanic Counts between Acceleromyography and Electromyography Estimated by the Poisson Model

	Estimated Ratio	Lower 95% CI	Upper 95% CI	P Value
Electromyography	0.62 [0.57–0.68]	0.49	0.80	0.0002
Acceleromyography	Reference			

Estimated ratio [interquartile range] and 95% CI were obtained from the negative binomial Poisson regression analysis.

finger movement during acceleromyography monitoring, and whether examiners normalize acceleromyography values. Among several electromyography twitch monitors, the TwitchView monitor has been validated to most closely resemble mechanomyographic assessment of the train-of-four ratio compared to acceleromyography (Stimpod, Xavant Technology, South Africa).² In addition, train-of-four counting by electromyography (TwitchView) or palpation were more similar to mechanomyography than acceleromyography (Stimpod).⁵ Moreover, in comparison between

electromyography monitors, the GE Healthcare electromyography monitor showed the greater train-of-four count and ratio than those measured by the TwitchView monitor.²⁷ However, the agreement of the TwitchView with mechanomyography for posttetanic count has not been well evaluated. In addition, the use of the Philips IntelliVue acceleromyography monitor in evaluating the twitch response has not been well studied for comparison to mechanomyography or electromyography. Our finding that the scatter in the posttetanic count data was very large (fig. 2)

could be attributed to either of the two monitors. This concern can be addressed by further studies, in which the TwitchView electromyography— and the Philips IntelliVue acceleromyography—posttetanic counting are compared to mechanomyography and/or palpation. Although we may not be able to draw clear conclusions based on past studies and lack of studies, our finding that acceleromyography (Philips IntelliVue Neuro Muscular Transmission Module) counted the greater posttetanic count compared to electromyography using the TwitchView suggests that anesthesiologists may administer higher doses of muscle relaxants when monitoring neuromuscular function using acceleromyography than electromyography; therefore, this should be considered for the maintenance of deep neuromuscular blockade with posttetanic count monitoring during laparoscopic or robotic surgeries.

Considering the nature of the data shown in figure 2, Poisson regression analysis performed to establish percentage limits showed that the mean posttetanic count on electromyography was 38% lower than that on acceleromyography (table 3). This result seems to be related to the finding that the ratio belonging to the acceleromyography—deep block and the electromyography—intense block (20%) was approximately three times higher than that in the opposite case (7%) (table 2).

This study had several limitations. First, the acceleromyography and electromyography for posttetanic count were compared in the contralateral arms. Because the electromyography electrodes of the TwitchView monitor used in this study occupied a large area, they could not be attached to the arm on the same side as the acceleromyography electrodes. Considering that arm-to-arm variation is a possible source of variation when monitors are compared on opposite arms, we applied both acceleromyography and electromyography monitors to the dominant and nondominant arms in equal proportions. This may have reduced the differences due to arm-to-arm variations. However, Claudius *et al.* found that there was no mean bias between the arms.¹⁶ Second, the patient's hand temperature was not monitored. However, we monitored and maintained the patient's nasopharyngeal temperature within the normal range (36.0 to 37.0°C) using a forced-air warming blanket. Third, the number of data pairs analyzed for the agreement of intense block or deep block and the agreement of posttetanic count between the two monitors were 226 and 184, respectively. These numbers may seem relatively small; however, they exceeded 142 measurements determined from the sample size calculation. Future studies with more measurements are required. Fourth, we did not compare acceleromyography and electromyography with mechanomyography or twitch response by manual palpation for posttetanic count monitoring. Therefore, we do not know which monitor is more accurate for posttetanic counts between acceleromyography and electromyography. Further studies are needed to clarify this point. Fifth, we simply compared acceleromyography

with electromyography for posttetanic count and did not observe any relationship with clinical issues to surgical stimuli, including intra-abdominal pressure to secure an appropriate surgical field, peak airway pressure, patient outcome, and the surgeon's satisfaction during laparoscopic or robotic surgeries. Future research could investigate whether electromyography or acceleromyography is a more suitable device in these respects.

In conclusion, this observational study demonstrated that acceleromyography (Philips IntelliVue) frequently counted more twitches than electromyography (TwitchView) in posttetanic count monitoring, and the posttetanic counts measured using acceleromyography and electromyography are not interchangeable for assessing the degree of neuromuscular blockade.

Acknowledgments

The authors thank Hye Ah Lee, Ph.D. (Clinical Trial Center, Mokdong Hospital, Ewha Womans University, Seoul, Republic of Korea), for her assistance in statistical analysis. The authors also thank Editage (Seoul, South Korea, www.editage.co.kr) for English language editing.

Research Support

Support was provided solely from institutional and/or departmental sources.

Competing Interests

The authors declare no competing interests.

Correspondence

Address correspondence to Dr. Baik: 1071 Anyangcheon-ro, Yangcheon-gu, Seoul, 07985, Republic of Korea. baikhj@ewha.ac.kr. This article may be accessed for personal use at no charge through the Journal Web site, www.anesthesiology.org.

References

1. Naguib M, Brull SJ, Kopman AF, Hunter JM, Fülesdi B, Arkes HR, Elstein A, Todd MM, Johnson KB: Consensus statement on perioperative use of neuromuscular monitoring. *Anesth Analg* 2018; 27:71–80
2. Bowdle A, Bussey L, Michaelsen K, Jelacic S, Nair B, Togashi K, Hulvershorn J: A comparison of a prototype electromyograph vs. a mechanomyograph and an acceleromyograph for assessment of neuromuscular blockade. *Anaesthesia* 2020; 75:87–95
3. Suzuki T, Fukano N, Kitajima O, Saeki S, Ogawa S: Normalization of acceleromyographic train-of-four ratio by baseline value for detecting residual neuromuscular block. *Br J Anaesth* 2006; 96:44–7

4. Engbaek J, Skovgaard LT, Friis B, Kann T, Viby-Mogensen J: Monitoring of the neuromuscular transmission by electromyography (I). Stability and temperature dependence of evoked EMG response compared to mechanical twitch recordings in the cat. *Acta Anaesthesiol Scand* 1992; 36:495–504
5. Bowdle A, Bussey L, Michaelsen K, Jelacic S, Nair B, Togashi K, Hulvershorn J: Counting train-of-four twitch response: Comparison of palpation to mechanomyography, acceleromyography, and electromyography. *Br J Anaesth* 2020; 124:712–7
6. Liang SS, Stewart PA, Phillips S: An ipsilateral comparison of acceleromyography and electromyography during recovery from nondepolarizing neuromuscular block under general anesthesia in humans. *Anesth Analg* 2013; 117:373–9
7. Abrishami A, Ho J, Wong J, Yin L, Chung F: Sugammadex, a selective reversal medication for preventing postoperative residual neuromuscular blockade. *Cochrane Database Syst Rev* 2009:CD007362
8. Raval AD, Deshpande S, Rabar S, Koufopoulou M, Neupane B, Iheanacho I, Bash L, Horrow J, Fuchs-Buder T: Does deep neuromuscular blockade during laparoscopy procedures change patient, surgical, and healthcare resource outcomes? A systematic review and meta-analysis of randomized controlled trials. *PLoS One* 2020; 15:e0231452.
9. Torensma B, Martini CH, Boon M, Olofsen E, in 't Veld B, Liem RSL, Knook MTT, Swank DJ, Dahan A: Deep neuromuscular block improves surgical conditions during bariatric surgery and reduces postoperative pain: A randomized double blind controlled trial. *PLoS One* 2016; 11:e0167907.
10. Martini CH, Boon M, Bevers RF, Aarts LP, Dahan A: Evaluation of surgical conditions during laparoscopic surgery in patients with moderate vs deep neuromuscular block. *Br J Anaesth* 2014; 112:498–505.
11. Kopman AF, Naguib M: Is deep neuromuscular block beneficial in laparoscopic surgery? No, probably not. *Acta Anaesthesiol Scand* 2016; 60:717–22
12. Claudius C, Fuchs-Buder T: Neuromuscular monitoring, Miller's Anesthesia, 9th edition. Edited by Gropper MA, Cohen NH, Eriksson LI, Fleisher LA, Leslie K, Wiener-Kronish JP. Philadelphia, Elsevier Saunders, 2020, pp 1354–61
13. Fuchs-Buder T, Claudius C, Skovgaard LT, Eriksson LI, Mirakhur RK, Viby-Mogensen J: 8th International Neuromuscular Meeting: Good clinical research practice in pharmacodynamics studies of neuromuscular blocking agents II: The Stockholm revision. *Acta Anaesthesiol Scand* 2007; 51:789–808
14. Murphy GS: Neuromuscular monitoring in the perioperative period. *Anesth Analg* 2018; 126:464–8
15. Dhonneur G, Kirov K, Motamed C, Amathieu R, Kamoun W, Slavor V, Ndoko SK: Post-tetanic count at adductor pollicis is a better indicator of early diaphragmatic recovery than train-of-four count at corrugator supercilii. *Br J Anaesth* 2007; 99:376–9
16. Claudius C, Skovgaard LT, Viby-Mogensen J: Arm-to-arm variation when evaluating neuromuscular block: An analysis of the precision and the bias and agreement between arms when using mechanomyography or acceleromyography. *Br J Anaesth* 2010; 105:310–7
17. Saghaei M: Random allocation software for parallel group randomized trials. *BMC Med Res Methodol* 2004; 4:26
18. Bujang MA, Baharum N: Guidelines of the minimum sample size requirements for Cohen's kappa. *Epidemiol Biostat Public Health* 2017; 14:e12267-1-10
19. Landis JR, Koch GG: The measurement of observer agreement for categorical data. *Biometrics* 1977; 33:159–74
20. Claudius C, Viby-Mogensen J: Acceleromyography for use in scientific and clinical practice: A systematic review of the evidence. *ANESTHESIOLOGY* 2008; 108:1117–40
21. Claudius C, Skovgaard LT, Viby-Mogensen J: Is the performance of acceleromyography improved with preload and normalization? A comparison with mechanomyography. *ANESTHESIOLOGY* 2009; 110:1261–70
22. Kopman AF, Chin W, Cyriac J: Acceleromyography vs. electromyography: An ipsilateral comparison of the indirectly evoked neuromuscular response to train-of-four stimulation. *Acta Anaesthesiol Scand* 2005; 49:316–22
23. Engbaek J, Roed J, Hangaard N, Viby-Mogensen J: The agreement between adductor pollicis mechanomyogram and first dorsal interosseous electromyogram. A pharmacodynamic study of rocuronium and vecuronium. *Acta Anaesthesiol Scand* 1994; 38:869–78
24. Viby-Mogensen J, Howardy-Hansen P, Chraemmer-Jorgensen B, Ording H, Engbaek J, Nielsen A: Posttetanic count (PTC): A new method of evaluating an intense non-depolarizing neuromuscular blockade. *ANESTHESIOLOGY* 1981; 55:458–61
25. El-Orbany MI, Joseph NJ, Ramez Salem M: The relationship of posttetanic count and train-of-four responses during recovery from intense cis-atracurium-induced neuromuscular blockade. *Anesth Analg* 2003; 97:80–4
26. Fernando PUE, Viby-Mogensen J, Bonsu AK, Tamilarasan A, Muchhal KK, Lambour A: Relationship between posttetanic count and response to carinal stimulation during vecuronium-induced neuromuscular blockade. *Acta Anaesthesiol Scand* 1987; 31:593–6
27. Bussey L, Jelacic S, Togashi K, Hulvershorn J, Bowdle A: Train-of-four monitoring with the TwitchView monitor electromyograph compared to the GE NMT electromyograph and manual palpation. *J Clin Monit Comput* 2021; 35:1477–83

ANESTHESIOLOGY

Respiratory Effects of Biased Ligand Oliceridine in Older Volunteers: A Pharmacokinetic–Pharmacodynamic Comparison with Morphine

Pieter Simons, M.D., Rutger van der Schrier, M.D., Maarten van Lemmen, B.Sc., Simone Jansen, M.D., Kiki W.K. Kuijpers, B.Sc., Monique van Velzen, Ph.D., Elise Sarton, M.D., Ph.D., Todd Nicklas, M.S.N., Cathy Michalsky, M.Sc., Mark A. Demitrack, M.D., Michael Fossler, Pharm.D., Ph.D., F.C.P., Erik Olofsen, Ph.D., Marieke Niesters, M.D., Ph.D., Albert Dahan, M.D. Ph.D.

ANESTHESIOLOGY 2023; 138:249–63

EDITOR'S PERSPECTIVE

What We Already Know about This Topic

- After μ -opioid receptor activation, oliceridine selectively engages the G protein–coupled signaling pathway, which is associated with analgesia, and has reduced engagement of the β -arrestin pathway, which is associated with adverse effects such as respiratory depression
- In healthy young males, oliceridine had a higher probability of providing analgesia than producing respiratory depression over the clinically relevant concentration range, while morphine had a higher probability of producing respiratory depression than providing analgesia
- Older and somewhat obese individuals of both sexes may be more vulnerable to opioid-induced respiratory depression than younger individuals

What This Article Tells Us That Is New

- The hypothesis that oliceridine and morphine differ in their pharmacodynamic behavior, measured as effect on ventilation at an extrapolated end-tidal P_{CO_2} of 55 mmHg (\dot{V}_{E55}), was tested in a four-arm, double-blind, randomized crossover study of eighteen 56- to 87-yr-old male and female volunteers
- The effect-site oliceridine concentration causing a 50% depression of \dot{V}_{E55} was 39% higher than that of morphine
- The onset and offset of the respiratory effect of oliceridine was five times faster than that of morphine

ABSTRACT

Background: Oliceridine is a G protein–biased μ -opioid, a drug class that is associated with less respiratory depression than nonbiased opioids, such as morphine. The authors quantified the respiratory effects of oliceridine and morphine in elderly volunteers. The authors hypothesized that these opioids differ in their pharmacodynamic behavior, measured as effect on ventilation at an extrapolated end-tidal P_{CO_2} at 55 mmHg, \dot{V}_{E55} .

Methods: This four-arm double-blind, randomized, crossover study examined the respiratory effects of intravenous 0.5 or 2 mg oliceridine and 2 or 8 mg morphine in 18 healthy male and female volunteers, aged 55 to 89 yr, on four separate occasions. Participants' *CYP2D6* genotypes were determined, hypercapnic ventilatory responses were obtained, and arterial blood samples were collected before and for 6 h after treatment. A population pharmacokinetic–pharmacodynamic analysis was performed on \dot{V}_{E55} , the primary end-point; values reported are median \pm standard error of the estimate.

Results: Oliceridine at low dose was devoid of significant respiratory effects. High-dose oliceridine and both morphine doses caused a rapid onset of respiratory depression with peak effects occurring at 0.5 to 1 h after opioid dosing. After peak effect, compared with morphine, respiratory depression induced by oliceridine returned faster to baseline. The effect-site concentrations causing a 50% depression of \dot{V}_{E55} were 29.9 ± 3.5 ng/ml (oliceridine) and 21.5 ± 4.6 ng/ml (morphine), the blood effect-site equilibration half-lives differed by a factor of 5: oliceridine 44.3 ± 6.1 min and morphine 214 ± 27 min. Three poor *CYP2D6* oliceridine metabolizers exhibited a significant difference in oliceridine clearance by about 50%, causing higher oliceridine plasma concentrations after both low- and high-dose oliceridine, compared with the other participants.

Conclusions: Oliceridine and morphine differ in their respiratory pharmacodynamics with a more rapid onset and offset of respiratory depression for oliceridine and a smaller magnitude of respiratory depression over time.

(*ANESTHESIOLOGY* 2023; 138:249–63)

In-hospital use of opioids is associated with multiple adverse events, prolonged length of stay, and opioid-related readmissions.^{1–4} Particularly respiratory depression from potent opioids is associated with not only respiratory depression, but also cardiorespiratory collapse and death.⁵ Despite these adverse effects, opioids remain the cornerstone of pharmacotherapy for moderate-to-severe acute pain because of their efficacy.⁶ One strategy to mitigate opioid-induced adverse events is the development of safer opioids,^{7–11} e.g., opioids that produce less respiratory depression and lead to less addiction or abuse. One example of this strategy is the development of oliceridine that was recently approved by regulatory authorities in the United States for the treatment of postoperative pain.^{7,8} It differs from other

This article is featured in "This Month in Anesthesiology," page A1. This article has a visual abstract available in the online version.

Submitted for publication June 30, 2022. Accepted for publication December 2, 2022. Published online first on December 20, 2022.

Pieter Simons, M.D.: Department of Anesthesiology, Leiden University Medical Center, Leiden, The Netherlands.

Copyright © 2023, the American Society of Anesthesiologists. All Rights Reserved. *Anesthesiology* 2023; 138:249–63. DOI: 10.1097/ALN.0000000000004473

opioids in that it is assumed that, after activation of the μ -opioid receptor, oliceridine is biased toward the G-protein intracellular pathway, which is predominantly associated with analgesia, and shows limited recruitment of the β -arrestin pathway, which is associated with opioid-related adverse events (e.g., respiratory depression and tolerance).^{8,9,12} Theoretically, this would suggest that oliceridine has a lower probability of respiratory depression than, for example, morphine, a full μ -opioid receptor agonist without bias toward the G-protein pathway. This was indeed observed in a study that examined the antinociceptive and respiratory effects of oliceridine *versus* morphine and showed a higher probability of antinociception *versus* respiratory depression for oliceridine while the reverse was true for morphine.¹³ In that study, healthy young volunteers were studied. In the current study, we tested older and somewhat obese individuals (age range 55 to 90 yr, body mass index up to 34 kg/m²) because such individuals are an increasing part of our clinical caseload, and opioids in these older individuals possibly may have a higher potency for respiratory depression than in younger individuals. In the current sample of such older individuals, we performed a population pharmacokinetic–pharmacodynamic modeling study on the effect of intravenous oliceridine *versus* morphine on ventilation at an extrapolated end-tidal carbon dioxide concentration of 55 mmHg (\dot{V}_{E55}), the main endpoint of the study. We hypothesized that oliceridine and morphine differ in their pharmacodynamic behavior, measured as effect on ventilation at an extrapolated end-tidal P_{CO_2} of 55 mmHg.

Rutger van der Schrier, M.D.: Department of Anesthesiology, Leiden University Medical Center, Leiden, The Netherlands.

Maarten van Lemmen, B.Sc.: Department of Anesthesiology, Leiden University Medical Center, Leiden, The Netherlands.

Simone Jansen, M.D.: Department of Anesthesiology, Leiden University Medical Center, Leiden, The Netherlands.

Kiki W. K. Kuipers, B.Sc.: Department of Anesthesiology, Leiden University Medical Center, Leiden, The Netherlands.

Monique van Velzen, Ph.D.: Department of Anesthesiology, Leiden University Medical Center, Leiden, The Netherlands.

Elise Sarton, M.D., Ph.D.: Department of Anesthesiology, Leiden University Medical Center, Leiden, The Netherlands.

Todd Nicklas, M.S.N.: Trevena Inc., Chesterbrook, Pennsylvania.

Cathy Michalsky, M.Sc.: Trevena Inc., Chesterbrook, Pennsylvania.

Mark A. Demitrack, M.D.: Trevena Inc., Chesterbrook, Pennsylvania.

Michael Fossler, Pharm.D., Ph.D., F.C.P.: Trevena Inc., Chesterbrook, Pennsylvania.

Erik Olofsen, Ph.D.: Department of Anesthesiology, Leiden University Medical Center, Leiden, The Netherlands.

Marieke Niesters, M.D., Ph.D.: Department of Anesthesiology, Leiden University Medical Center, Leiden, The Netherlands.

Albert Dahan, M.D., Ph.D.: Department of Anesthesiology, Leiden University Medical Center, Leiden, The Netherlands; PainLess Foundation, Leiden, The Netherlands.

Materials and Methods

Ethics and Registration

The study was performed at a single site after approval of the protocol by the medical ethics committee of the Leiden University Medical Center, METC Leiden–Den Haag–Delft (under identifier P21.025) and the Central Committee on Research Involving Human Subjects (competent authority) in The Hague, The Netherlands (identifier NL75790.058.21). The study was performed from June 29, 2021, to January 4, 2022, in the Anesthesia and Pain Research Unit of the Department of Anesthesiology at Leiden University Medical Center. The study was registered in the trial register of the Dutch trial registry, currently available at the World Health Organization International Clinical Trials Registry Platform (<https://trialsearch.who.int>), under identifier NL9524 on June 2, 2021. The principal investigator of the study was Albert Dahan, M.D., Ph.D. The study was conducted in accordance with current Good Clinical Practice Guidelines and adhered to the principles of the Declaration of Helsinki. Before enrollment, all subjects gave oral and written informed consent. Thereafter, their medical history was obtained, and a physical examination was performed. The whole project was monitored by an independent data input monitor and a data safety monitoring committee.

Participants

Healthy volunteers of either sex were recruited to participate in the study. Inclusion criteria were age 55 yr or older; body mass index in the range 19 to 35 kg/m² (inclusive); absence of any significant medical, neurologic, or psychiatric illness as determined by the investigators; and willing and able to sign a written informed consent. The inclusion process was aimed to include an equal number of men and women, include half of the participants with an age of 65 yr or older, and a third of subjects with a body mass index range of 30 to 35 kg/m², to represent an average elective surgical population. The main exclusion criteria were intolerance, hypersensitivity, or recent (less than 1 month) exposure to opioids; a positive drug test or breath alcohol test on screening or subsequent study visits; inability to perform the study procedures as tested during screening; cognitive impairment as determined by the short version of the Mini Mental Status Examination (score less than 24); any clinically significant laboratory abnormality; abnormalities on the electrocardiogram including a corrected QT interval greater than 450 ms; alcohol intake of more than 4 units per day; participation in a drug trial in the 30 days before screening; or any other condition that in the opinion of the investigator would complicate or compromise the study or the well-being of the subject.

Study Design

The following study drugs were administered on 4 separate study days, at least 1 week apart in a double-blind,

randomized order: 0.5 mg low-dose oliceridine (Trevena Inc., USA), 2.0 mg high-dose oliceridine, 2.0 mg low-dose morphine hydrochloride (Centrafarm BV, Etten-Leur, The Netherlands), or 8.0 mg high-dose morphine hydrochloride. The study drugs were administered intravenously for over 60 s. The study drugs were prepared by the pharmacy and dispensed to the study team in identical, unmarked, numbered (subject and visit numbers) syringes on the morning of the experiment. Randomization was performed using a computer-generated randomization list; the list was available to the pharmacy and the data safety monitoring committee. Unblinding was only justified in case of drug-related serious adverse events.

The choice of the opioid doses was based on earlier clinical studies. Available oliceridine and morphine comparative data from the literature suggest that oliceridine is 6.7 times more potent than morphine in the cold pressor test and 3.3 times more potent in pupil constriction as derived from a phase 1 study obtained in younger adults (less than 50 yr),¹⁴ and 4 times more potent in decreasing pain intensity as derived from a phase 2 study in 144 postoperative patients (age range 18 to 75 yr).¹⁵ Based on these observations, we consider that the doses used in our study (2 mg and 8 mg morphine and 0.5 and 2 mg oliceridine) are equianalgesic.

Before each visit, participants were asked to fast for at least 8 h. Upon arrival in the research unit, the subjects were screened for the use of illicit substances by using a urine dipstick (Alere Toxicology Plc., Oxfordshire, United Kingdom), and screened for alcohol use with a breath analysis test (AlcoHawk CA-120, USA). Thereafter, the participants received an intravenous catheter in the median cubital vein of the left or right arm and an arterial line in the left or right radial artery. The arterial line was connected to a FloTrac Sensor and HemoSphere (Edwards Lifesciences, USA) for hemodynamic monitoring. Finally, a 3-lead electrocardiogram (Datex Cardiopac, Helsinki, Finland) and a finger probe for pulse oximetry (Masimo Corporation, USA) were placed.

Respiratory Measurements.

After a short period of relaxation, the ventilatory response to hypercapnia was measured by using a modified rebreathing method.^{16–18} During respiratory testing, the subjects were semirecumbent and breathed through a face mask positioned over the mouth and nose. The face mask was connected to a pneumotachograph and pressure transducer system (Hans Rudolph Inc., USA) to measure ventilation on a breath-to-breath basis. Inspired and expired carbon dioxide concentrations were measured at the mouth using a Datex Capnomac (Datex, Finland). After a 4-min period of relaxed breathing of room air, the subjects were coached to hyperventilate for 2 to 3 min while breathing a hyperoxic gas mixture ($\text{FIO}_2 = 1$), followed by normal breathing for 30 s of the hyperoxic gas mixture, after which rebreathing from a 6-l balloon containing 7% carbon dioxide in

93% oxygen was initiated. The rebreathing period lasted for 3 to 4 min. We obtained eight responses, one before any drug administration, and 30 min, 1, 2, 3, 4, 5, and 6 h after drug infusion. The following breath-to-breath data were collected: minute ventilation, end-tidal oxygen and carbon dioxide concentration, and oxygen saturation.

Blood Sampling and Analysis.

At the following time points, 2 ml blood was drawn from the arterial line for determination of oliceridine or morphine and morphine-6-glucuronide concentrations: 0 (predose) 2, 5, 10, 15, 30, and 45 min, and 1, 1.5, 2, 3, 4, 5, and 6 h (postdose). Plasma samples were shipped to Labcorp Bioanalytical Services LLC, Indianapolis, Indiana, for analysis.

Oliceridine plasma concentrations were quantified using a validated high-performance liquid chromatography with tandem mass spectrometry bioanalytical assay.^{7,13} Oliceridine and the internal standard TRV0110813A:2 (tri-deutero ¹³C-labeled oliceridine) were extracted from human plasma containing K₂EDTA by supported-liquid extraction. The lower limit of quantitation for oliceridine in human plasma was 0.05 ng/ml, with linearity demonstrable up to 50 ng/ml (upper limit of quantitation), using a 50-μl sample volume. Mean coefficient of variation among the various analytical runs ranged from 5.9 to 7.1% with bias ranging from 0.5 to 5.5% and accuracy from 100.5 to 105.5%. Oliceridine metabolites were not measured because none of them are pharmacologically active.

Morphine and morphine-6-glucuronide concentrations were determined by a validated high-performance liquid chromatography with tandem mass spectrometry method, after solid-phase extraction of morphine and internal standard morphine-d₃ and morphine-6-glucuronide and internal standard morphine-6β-D-glucuronide-d₃ from human plasma containing K₂EDTA. The lower limits of quantitation for morphine and morphine-6-glucuronide in human plasma were both 0.5 ng/ml, with linearity demonstrable up to 250 ng/ml (upper limit of quantitation), using a 50-μl sample volume. For morphine, the mean coefficient of variations among the analytical runs ranged from 5.2 to 7.5% with bias ranging from 0.5 to 3.2% and accuracy from 100.5 to 103.2%. For morphine-6-glucuronide, the mean coefficient of variations ranged from 5.2 to 6.8% with bias ranging from 0.5 to 5.6% and accuracy from 100.5 to 105.6%. The assay has not been published previously, but see Dahan *et al.*¹³

To determine the drug metabolizer status of the participants, one additional blood sample was drawn for determination of the *CYP2D6* genotype. Genotyping was performed by the ISO15189-accredited laboratory of the Leiden University Medical Center Pharmacy and Toxicology Department using the TAG *CYP2D6* Kit v3 (Luminex Corporation, Den Bosch, The Netherlands). *CYP2D6*-haplotypes and copy number variants were determined.¹⁹

Adverse Events

Side effects were evaluated on an 11-point visual analog scale (0 to 10) for the following items: nausea (none to severe), sedation (none to most intense), dizziness (none to most severe), lightheadedness (none to most severe), drug likability (5 was equivocal, under 5 was do not like, over 5 was like). Additionally, we scored occurrence vomiting (yes/no). These items were queried at baseline, $t = 45$ min, and subsequently at 1-h intervals until $t = 345$ min after drug administration. Also, adverse effects spontaneously reported by the participant or observed by the investigators were recorded.

Data Analysis

Data analysis was performed in several steps. First, \dot{V}_{E55} or ventilation at an extrapolated end-tidal PCO_2 of 55 mmHg (units l/min) was calculated from the slope of the ventilatory response to hypercapnia. The slope was determined in R (the R-Foundation for Statistical Computing, www.r-project.org) by fitting all ventilation-end-tidal PCO_2 data points of the linear part of the ventilatory response to hypercapnia curve to the equation $S = \text{Ventilation}(t) / [\text{end-tidal } \text{PCO}_2(t) - B]$, where S is the slope of the ventilatory response to hypercapnia and B the apneic threshold or extrapolated end-tidal PCO_2 at zero ventilation; this process was automated in R.²⁰ Next, the population pharmacokinetic data were analyzed, followed by a population pharmacokinetic-pharmacodynamic analysis using \dot{V}_{E55} , the main endpoint of the study, as pharmacodynamic input to the model.

Pharmacokinetic-Pharmacodynamic Analysis.

The pharmacokinetics and pharmacodynamics of oliceridine and morphine were analyzed with NONMEM VII (Icon Plc., USA), a software package for nonlinear mixed-effects modeling, using a population approach. Although measured in plasma, morphine-6-glucuronide was not included in the analyses, because previous studies indicated a rather low potency of morphine-6-glucuronide on generating respiratory effects in individuals with a normal renal function with a potency ratio of approximately 1:20 for depression of isohypercapnic ventilation and 1:50 for isocapnic hypoxic ventilation.²¹ The pharmacokinetic data were analyzed using three-compartment models. The following analysis sequence was applied: initialization using iterative two-stage, parameter estimation using stochastic approximation expectation maximization, objective function evaluation using importance sampling, and a final No U-Turn sampling Bayesian step using noninformative priors to visualize and quantify parameter uncertainty.

The early samples at 2 min after infusion showed considerable variability. Because infusion was done manually for 1 min, it was hypothesized that this could be caused, at least in part, by variability of the infusion duration. Therefore, NONMEM's parameter of the infusion duration (D_1) was set up to be an estimable parameter.

Body weight and, for oliceridine, the metabolizer status based on the genotype of the *CYP2D6* gene, were incorporated as covariates in the pharmacokinetic analyses. The change in NONMEM's objective function value was tested to assess whether weight *via* allometric scaling improved the fit (because this requires no extra parameters, incorporating allometric scaling would be preferable with any decrease in the objective function value). For metabolizer status, the clearance for each nonnormal status was tested for statistically significant difference from the clearance for the normal status (change in objective function value of at least 6.63; $P < 0.01$).

Allometric scaling using standard powers of weight (1 for volumes and 0.75 for clearances) was assumed *a priori* and implemented in the pharmacokinetic models.²² During model evaluation, it was checked that incorporating allometric scaling indeed reduced NONMEM's objective function value and that it decreased the dependence of interindividual variability terms on weight. To quantify the hysteresis between the arterial drug concentration and effect, an effect site is postulated characterized by a first-order process with rate constant ke_0 and half-life $t_{1/2}ke_0 (= \ln 2/ke_0)$.

The ventilatory effects of oliceridine and morphine were modeled using an inhibitory sigmoid E_{MAX} model. Ventilation at an extrapolated isohypercapnic level of 55 mmHg (\dot{V}_{E55}) was modeled as follows:

$$\dot{V}_{E55}(t) = \dot{V}_{E55} \text{ at baseline} - \dot{V}_{E55} \text{ at baseline} \times \left[\frac{C_E(t)^\gamma}{C_{50}^\gamma} \right] / \left[1 + \frac{C_E(t)^\gamma}{C_{50}^\gamma} \right]$$

where baseline is the value before any drug administration, $C_E(t)$ is the effect-site concentration at time t , C_{50} the effect-site concentration causing a 50% depression of \dot{V}_{E55} , and γ a shape parameter, which was fixed to 1 in the analyses. The same estimation steps were followed as was done for the pharmacokinetic analyses. To determine whether the models adequately described the data, goodness-of-fit plots were created and inspected. To allow a visual predictive check of the final pharmacokinetic or pharmacodynamic models, the normalized prediction discrepancies were estimated. Parameter estimates are reported as median \pm standard error of the estimate; $P < 0.01$ was considered significant.

No formal sample size analysis was performed. A previous study from our laboratory enrolled 15 subjects and was able to detect a significant difference between two opioids (oxycodone and tapentadol) on \dot{V}_{E55} in a young healthy population (mean difference 5 l/min, 95% CI -7 to -3 l/min).²³ In the current study, we planned to enroll 18 subjects to consider some variability in the data obtained from an older sample and possible withdrawal of up to 3 subjects.

The time to peak effect after a bolus dose is determined by both the blood-effect-site equilibration half-life and the pharmacokinetics.²⁴ This composite measure may be

useful for the design of target-controlled infusion systems where the available models from the literature are evaluated. From the estimated parameters for both oliceridine and morphine, we calculated the time to peak effect using the method described in Minto *et al.*²⁴ implemented in R (the root of the derivative of the effect-site concentration function of time after a unit bolus dose).

Simulations.

We simulated the effect of multiple doses to reach a level of respiration depression of maximal 65% of isohypercapnic baseline ventilation in a typical 70-kg patient. The simulations were performed in R using implementation of the final models and estimated typical population parameters with simulated data obtained at 1-min intervals. After a bolus dose, a subsequent sequence of doses, three to four per hour, mimicking patient-controlled analgesia, was simulated while advancing simulated time considering a lockout time of 6 min. Three runs were done: one for morphine and two for oliceridine with normal and low elimination clearance. The bolus dose was 10 times and 3 times higher than the subsequent repetitive dose (10:1 and 1.5:0.5), for morphine and oliceridine, respectively, as applied clinically.^{14,15}

Results

A total of 341 individuals responded to an online mailing for participation in our study. Twenty-two were assessed for eligibility of which 4 were excluded because they did not show up on the first study day ($n = 1$), they met exclusion criteria ($n = 2$), or they declined to participate ($n = 1$). Eighteen subjects (9 men and 9 women) were enrolled in the study and randomly assigned; 17 subjects successfully

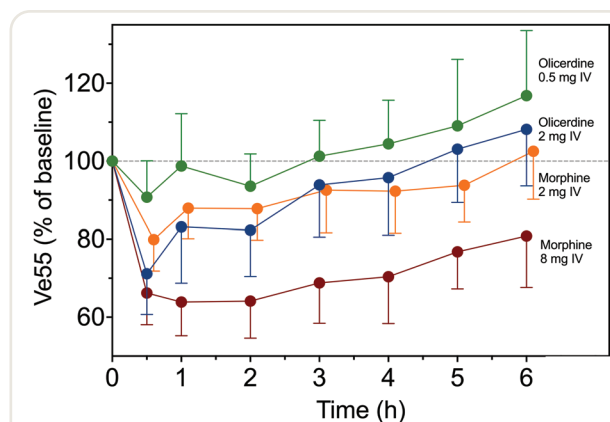


Fig. 1. Ventilation at an extrapolated carbon dioxide partial pressure of 55 mmHg, \dot{V}_{55} , for the four treatment arms (green, 0.5 mg oliceridine; blue, 2 mg oliceridine; orange, 2 mg morphine; and red, 8 mg morphine). Data are averaged percentage of baseline \pm 95% CI.

completed the trial. One male subject withdrew consent after the second visit because of a (transient) painful hematoma that developed at the location of the vascular access line after the subject returned home; his data are included in the analyses. All other subjects completed the study without any serious or unexpected adverse effects. The mean age

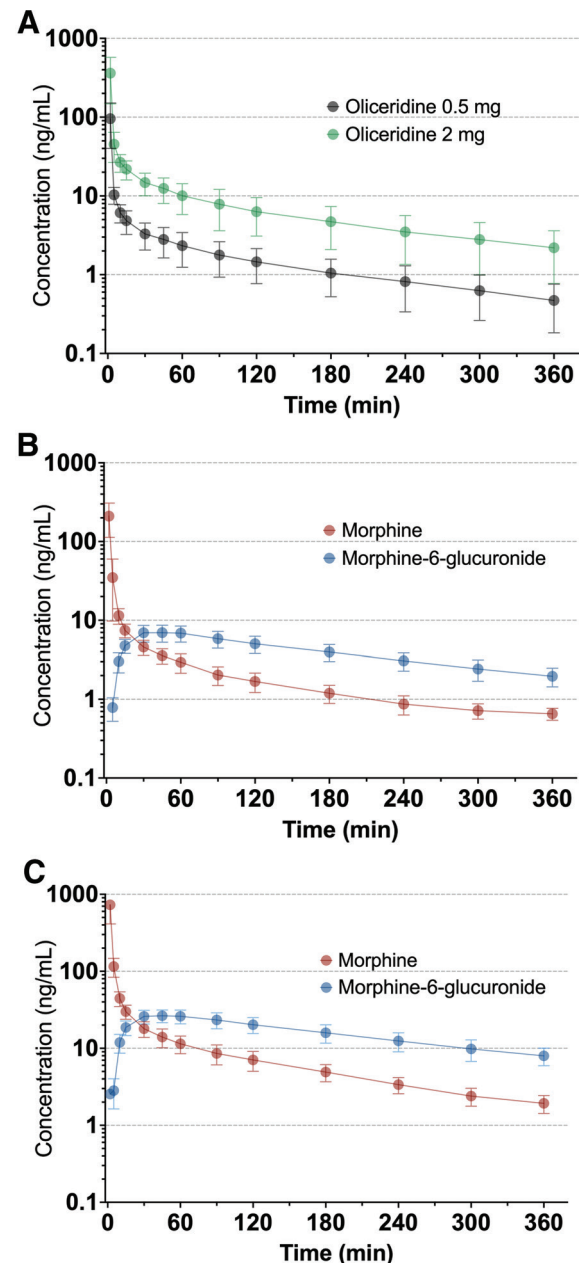


Fig. 2. Mean pharmacokinetic data \pm 95% CI after intravenous administration of morphine and oliceridine. (A) 0.5 mg oliceridine (gray symbols) and 2 mg oliceridine (green symbols). (B) 2 mg morphine (red symbols) and morphine-6-glucuronide (blue symbols). (C) 8 mg morphine (red symbols) and morphine-6-glucuronide (blue symbols).

of the participants was 71 yr (range 56 to 87 yr), height 170 cm (155 to 189 cm), and body mass index 26 kg/m² (20 to 34 kg/m²). Five subjects, with age range 69 to 75 yr, had a body mass index greater than 30 kg/m² (mean value 33 kg/m², with range 32 to 34 kg/m²); the other subjects (age range 56 to 87 yr) had a mean body mass index of 24 kg/m² (20 to 29 kg/m²).

Primary Endpoint: Opioid Effect on \dot{V}_{E55}

The effect of oliceridine and morphine on mean isohypercapnic ventilation, \dot{V}_{E55} , are given in figure 1. The dynamic patterns observed after the opioid infusions were different for the two opioids. High-dose oliceridine and high- and low-dose morphine showed a rapid drop in \dot{V}_{E55} , an indication of rapid onset of respiratory depression, *i.e.*, within 30 min of administration. High-dose oliceridine and low-dose morphine returned toward baseline within 3 h, and high-dose morphine lagged behind, and a slow return toward baseline (more than 6 h) was observed. Low-dose oliceridine did not produce any significant respiratory depression. In contrast to \dot{V}_{E55} after high-dose morphine, \dot{V}_{E55} after low- and high-dose oliceridine infusion had mean values greater than pre-drug baseline values from $t = 4$ h on.

Population Pharmacokinetic Analyses

The average plasma concentrations of oliceridine, morphine, and morphine-6-glucuronide are given in figure 2.

Goodness-of-fit plots (individual and population predicted *versus* measured data, conditional weighted residuals *versus* time, and normalized prediction discrepancy errors *versus* time) are given in figure 3; the population predicted pharmacokinetic outcomes and measured plasma concentrations of each individual of the four treatment arms are given in figure 4. Inspection of the data fits and goodness-of-fit plots indicate that the three-compartment models adequately described the data of both opioids. The estimated pharmacokinetic model parameter estimates are given in table 1. For all 4 treatment arms, the infusion rate parameter (D_1) was not significantly different from 1, but its variability was significantly different from 0. Fixing it to zero had a marked effect on the remaining variability parameters and also on the population estimates. Therefore, including variability on D_1 likely reduced the bias on all parameter estimates. The decrease in NONMEM's objective function value was 141 and 139 points for morphine and oliceridine, respectively. Weight had an effect on the pharmacokinetic parameters *via* allometric scaling, indicated by a decrease in objective function value of 43 and 24 points for morphine and oliceridine, respectively.

With respect to the *CYP2D6* genotype, 10 subjects were classified as normal oliceridine metabolizers (2 functional alleles), 4 as intermediate metabolizer (heterozygous with one functional allele), 3 as poor metabolizer (with two alleles lacking activity due to $\ast 4/\ast 4$, $\ast 3/\ast 4$, and $\ast 4/\ast 4$ with

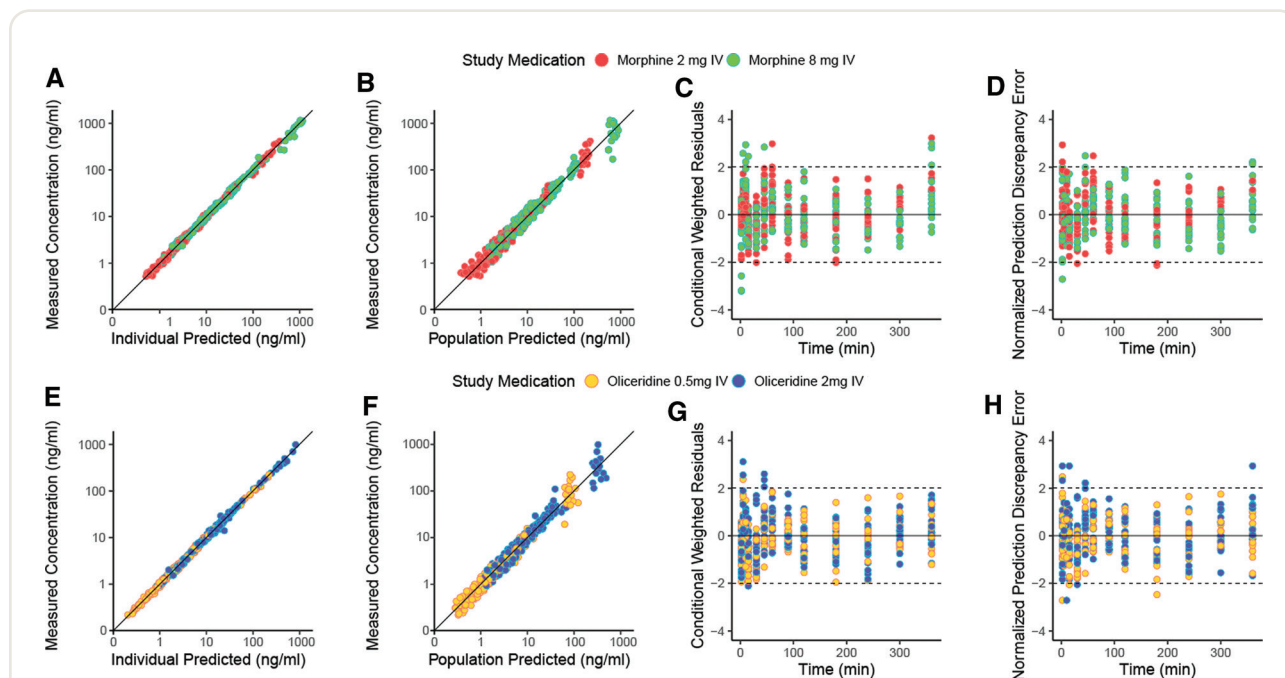


Fig. 3. Goodness-of-fit plots of the pharmacokinetic data analyses for morphine (A to D) and oliceridine (E to H). (A and E) Measured concentration *versus* individual predicted concentration. (B and F) Measured concentration *versus* population predicted concentration. (C and G) Conditional weighted residuals *versus* time. (D and H) Normalized prediction discrepancy error *versus* time. Dotted lines represent the upper and lower limits of the 95% CI. Red symbols, 2 mg morphine; green symbols, 8 mg morphine; blue symbols, 0.5 mg oliceridine; yellow symbols, 2 mg oliceridine.

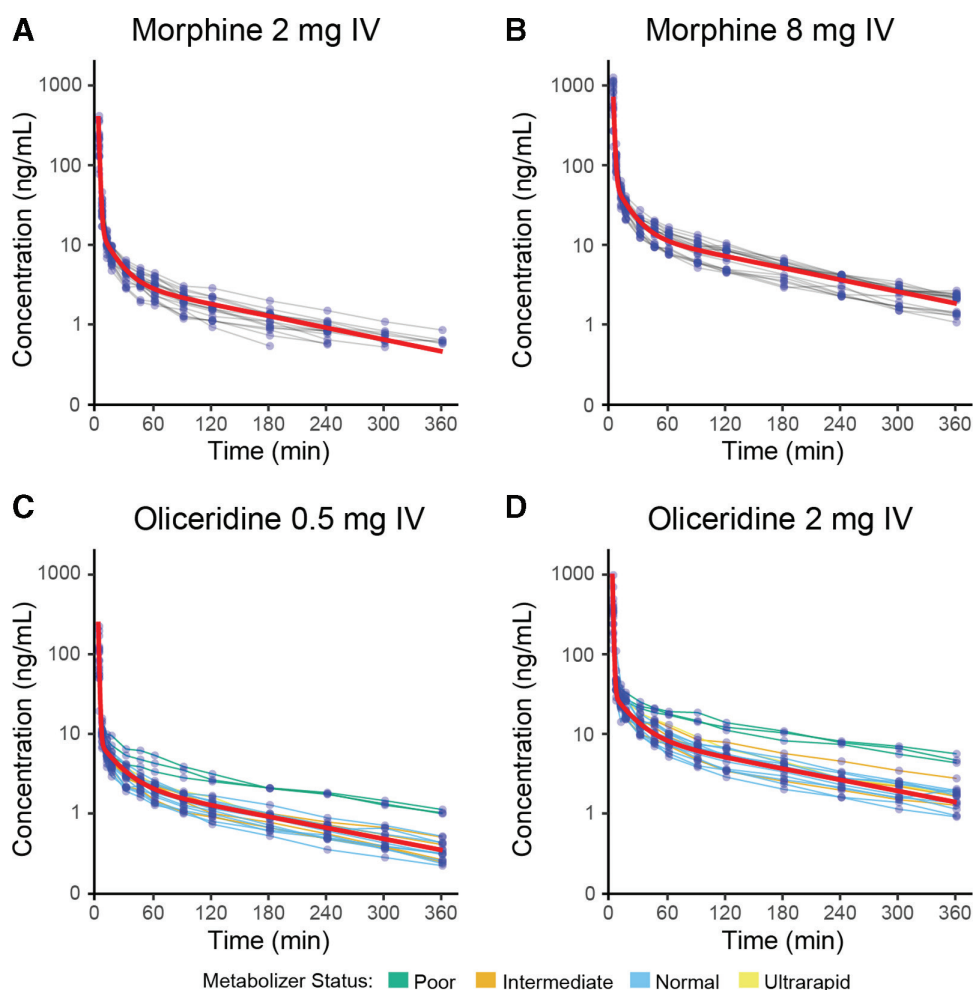


Fig. 4. The population pharmacokinetic model outcome (red lines) and the observed pharmacokinetic data points of each individual versus time for 2 mg morphine (A), 8 mg morphine (B), 0.5 mg oliceridine (C), and 2 mg oliceridine (D). For oliceridine the status of the *CYP2D6* genotype is given: poor metabolizer (green), intermediate metabolizer (dark yellow), normal metabolizer (blue), and ultrarapid metabolizer (yellow).

*3 = 2549delA and *4 = 100C>T, 1661G>T, 1846G>A, 2850C>T, or 4180G>C) and 1 as ultrarapid metabolizer (more than two functional alleles).²⁵ A significant difference in clearance (CL_T) by about 50% was observed in the three poor oliceridine metabolizers. This caused higher plasma concentrations in these three subjects after both low- and high-dose oliceridine compared with the other participants (fig. 4, C and D).

Pharmacodynamic Analyses

The population predicted pharmacodynamic outcomes and measured pharmacodynamic data points (\dot{V}_{E55}) of each individual of the four treatment arms are illustrated in figure 5, and goodness-of-fit plots are given in figure 6. Inspection of the data fits and goodness-of-fit plots indicate that the pharmacodynamic model adequately described the data of both opioids. The estimated pharmacodynamic

model parameter estimates are given in table 2. Two relevant observations are that oliceridine displays a 39% higher C_{50} value than morphine, and the two drugs differ by a factor of 5 in their onset/offset times ($t_{1/2ke0}$) with oliceridine being 5 times more rapid than morphine in the transition from plasma to effect site. The time to peak effect was 10.5 min and 56.0 min for oliceridine and morphine, respectively. For both drugs, parameter γ was not significantly different from 1 and therefore fixed to 1.

Simulations

Results of the simulation study are given in figure 7. They show the effect of multiple dosing aimed at a steady state in effect to maximal depression of 65% of baseline isohypercapnic ventilation. Irrespective of genotype (oliceridine), the differences in pharmacokinetic and pharmacodynamic properties result in less variation in the effect-site concentrations

Table 1. Pharmacokinetic Parameter Estimates

Parameter \pm SEE		Between-Subject Variability $\omega^2 \pm$ SEE	Interoccasion Variability $\nu^2 \pm$ SEE
Oliceridine			
V_1 , l/70 kg	1.1 \pm 0.1		0.07 \pm 0.03
V_2 , l/70 kg	5.6 \pm 0.5		
V_3 , l/70 kg	45.3 \pm 1.8		0.01 \pm 0.01
CL_1 , l/h at 70 kg	33.1 \pm 1.5	0.02 \pm 0.01	0.006 \pm 0.003
CL_2 , l/h at 70 kg	22.8 \pm 2.3	0.04 \pm 0.02	0.02 \pm 0.01
CL_3 , l/h at 70 kg	27.6 \pm 2.0	0.05 \pm 0.03	
D_1 , min	1		0.83 \pm 0.43
CL_1^{PM} , l/h at 70 kg	17.8 \pm 1.5		
σ^2	0.009 \pm 0.001		
Morphine			
V_1 , l/70 kg	3.3 \pm 0.3	0.05 \pm 0.02	
V_2 , l/70 kg	7.1 \pm 0.6		
V_3 , l/70 kg	90.2 \pm 3.7	0.02 \pm 0.01	
CL_1 , l/h at 70 kg	80.1 \pm 2.3	0.016 \pm 0.004	
CL_2 , l/h at 70 kg	35.8 \pm 2.3		
CL_3 , l/h at 70 kg	51.4 \pm 2.4		
D_1 , min	1.0	1.1 \pm 0.5	
σ^2	0.012 \pm 0.001		

CL_1 , the clearance from compartment 1 with CL_1^{PM} is CL_1 of the oliceridine poor metabolizer; CL_2 and CL_3 , the intercompartmental clearances between compartments 1 and 2 and 1 and 3, respectively; D_1 , the infusion duration; ω^2 , intersubject variability; SEE, standard error of the estimate; σ^2 , measure of residual variability; V_1 , V_2 , and V_3 , the volumes of compartments 1, 2 and 3, respectively.

for morphine (difference between peaks and valleys 1 ng/ml) *versus* oliceridine (5 ng/ml) and variation in ventilation for morphine (difference between peaks and valleys 2% of baseline) *versus* oliceridine (7%). For morphine, in a 24-h period, the total drug dose given is 27 mg, which is made up of an initial bolus dose of 10 mg followed by 17 1-mg doses. For oliceridine in normal and poor metabolizers, the initial bolus dose was 1.5 mg followed by 20 doses of 0.5 mg in normal metabolizers (total dose given 11.5 mg) and 11 doses of 0.5 mg in poor metabolizers (total dose 7 mg). This indicates that less oliceridine was needed in poor than in normal metabolizers to induce a similar level of respiratory depression.

Adverse Effects

All reported and observed adverse effects are given in table 3. At low dose and high dose, the total number of events was similar between opioids. Most frequently reported events were dizziness, lightheadedness, somnolence, and horizontal vertigo after oliceridine administration, and nausea, lightheadedness, dizziness, and somnolence following morphine (all occurring on at least 8 visits). The queried adverse events are given in figure 8. It shows the more protracted occurrence of events after morphine than oliceridine.

Discussion

We studied oliceridine and morphine and measured isohypercapnic ventilation at an end-tidal P_{CO_2} of 55 mmHg as a biomarker of drug effect in a sample of moderately

overweight older men and women. Our main observations were as follows: (1) there was a 30% difference in respiratory potency between oliceridine and morphine with a 50% reduction of \dot{V}_{E55} (C_{50}) observed at 29.9 ± 3.5 ng/ml oliceridine and 21.1 ± 4.6 ng/ml morphine; (2) oliceridine had a 5-times faster onset and offset of respiratory effect than morphine (blood-effect-site equilibration half-life, $t_{1/2ke0}$, 44 ± 6 min for oliceridine *versus* 214 ± 27 min for morphine); and (3) oliceridine metabolism was dependent on the *CYP2D6* enzyme genotype. Simulations revealed that about 40% less oliceridine is needed to achieve the same level of respiratory depression in poor metabolizers compared with normal metabolizers over 24 h.

The study was conducted in older subjects as opposed to the more typically young and healthy study population. Previously, we studied healthy young volunteers (18 to 30 yr) to determine the respiratory effects of a range of opioids, including morphine, morphine-6-glucuronide, oxycodone, fentanyl, and buprenorphine.^{20,21,23,26} Although these studies are of interest from a pharmacologic perspective, the current study sample is clinically more relevant, because patients aged 55 yr and older comprise the vast majority of patients in anesthetic practice. The differences in estimated model parameters indicate that, on bolus dose administration, oliceridine produces respiratory depression more rapidly than morphine, but the oliceridine effect wears off more quickly. In clinical practice, often higher opioid doses are administered than in our experimental study. This may be necessary, for example, to achieve rapid pain relief. Because we did not obtain pain data in our study (see next

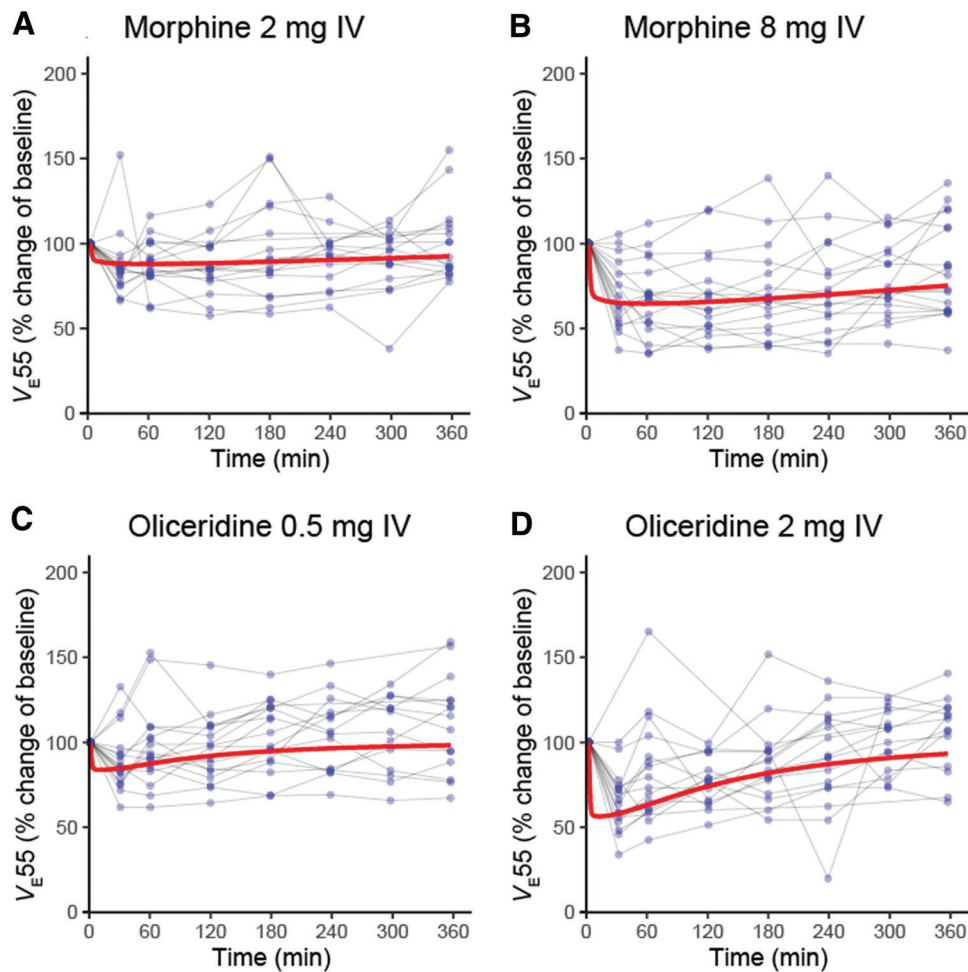


Fig. 5. The population pharmacodynamic model outcome (red lines) and the measured pharmacodynamic data points (V_{E55}) of each individual versus time for 2 mg morphine (A), 8 mg morphine (B), 0.5 mg oliceridine (C), and 2 mg oliceridine (D). Data are averaged percentage of baseline \pm 95% CI.

paragraph), we remain uninformed how the ventilatory effects that we observed relate to the antinociceptive effects. This requires further study.

Previously, Dahan *et al.*¹³ analyzed respiratory and antinociceptive oliceridine and morphine data in a younger cohort of healthy male volunteers (19 to 50 yr) to construct utility functions or therapeutic indices of the two opioids. They showed superiority for oliceridine compared with morphine in the utility $U = P(A) - P(R)$, where $P(A)$ is the probability for analgesia and $P(R)$ is the probability for respiratory depression. In the current study, we had planned to construct similar utility functions and therefore measured antinociceptive responses (cold pressor and electrical pain tests, data not shown) in our subjects. However, we experienced early on that the older subjects had difficulty scoring the applied noxious stimuli. They consistently were insensitive to the intense cold-water stimuli (1.5°C) and we did not detect a dose- or time-dependent effect

in the electrical pain assay. We therefore discarded the antinociceptive data obtained in the study. We demonstrated earlier that volunteers (mean age 37 yr, body mass index under 30 kg/m²) were not able to reliably score thermal or electrical stimuli after opioid administration.²⁷ This may be even worse in the elderly because the nociceptive fibers in the skin are affected by the normal aging process and there is also evidence for functional alterations in pain-processing regions in the brain of elderly individuals.^{28,29} Additionally, we showed that a sample of predominantly women with morbid obesity (mean age 43 yr, body mass index range 43 kg/m²) were hypoalgesic to noxious stimuli and had difficulty grading thermal and electrical stimuli.³⁰ All of these factors could have impacted the pain measurement in our current study.

It was not possible to compare the respiratory safety of oliceridine and morphine in the older subjects of the present study because of our inability to construct utility

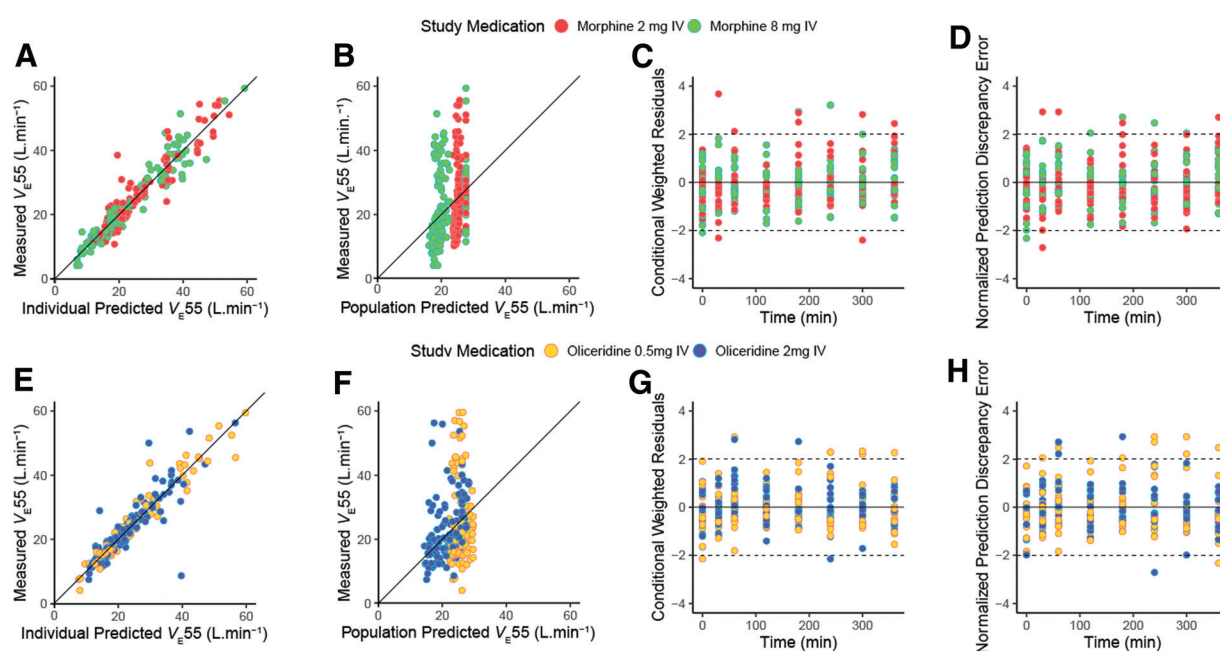


Fig. 6. Goodness-of-fit plots of the pharmacodynamic data analyses for morphine (A to D) and oliceridine (E to H). (A and E) Measured concentration *versus* individual predicted concentration. (B and F) Measured concentration *versus* population predicted concentration. (C and G) Conditional weighted residuals *versus* time. (D and H) Normalized prediction discrepancy error *versus* time. Dotted lines represent the upper and lower limits of the 95% CI. Top panels: red symbols, 2 mg morphine; green symbols, 8 mg morphine. Bottom panels: yellow symbols, 0.5 mg oliceridine; blue symbols, 2 mg oliceridine.

Table 2. Pharmacodynamic Parameter Estimates

Parameter ± SEE		Between-subject Variability $\omega^2 \pm \text{SEE}$	Interoccasion Variability $\nu^2 \pm \text{SEE}$
Oliceridine \dot{V}_{E55}			
Baseline, l/min	28.3 ± 3.3	0.21 ± 0.10	0.07 ± 0.03
$t_{1/2\text{ke0}}$, min	44.3 ± 6.1		
C_{50} , ng/ml	29.9 ± 3.5		
σ^2	15.1 ± 5.7	1.95 ± 0.82	
Morphine \dot{V}_{E55}			
Baseline, l/min	27.8 ± 3.1	0.20 ± 0.08	0.05 ± 0.02
$t_{1/2\text{ke0}}$, min	214 ± 27		
C_{50} , ng/ml	21.5 ± 4.6	0.49 ± 0.28	1.81 ± 0.55
σ^2	6.7 ± 1.7		

C_{50} , effect-site concentration causing 50% respiratory depression; SEE, standard error of the estimate; ω^2 , intersubject variability; σ^2 , a measure of residual variability; $t_{1/2\text{ke0}}$, blood to effect-site equilibration half-life; \dot{V}_{E55} , extrapolated ventilation at an end-tidal Pco_2 of 55 mmHg.

functions. This is particularly so because respiratory depression is related to drug dose and plasma concentration, speed of drug infusion, timing of measurement and underlying pain, which are considered in the utility function. Similarly, a comparison with our previous study in younger volunteers should be made with caution given the many differences in protocol, such as inclusion of only male subjects, venous sampling, and a different respiratory test in the

earlier study.¹³ Despite these differences, a comparison of respiratory potency ratios (C_{50} oliceridine)/(C_{50} morphine) remains meaningful. The ratio equaled 1.4 in the current study and was 1.6 in the cohort of younger men.¹³ This shows that the potency ratio is maintained over the age ranges studied (19 to 50 yr and 56 to 87 yr). Further, the estimated blood–effect site equilibration half-lives are in the same range as observed in earlier morphine and oliceridine

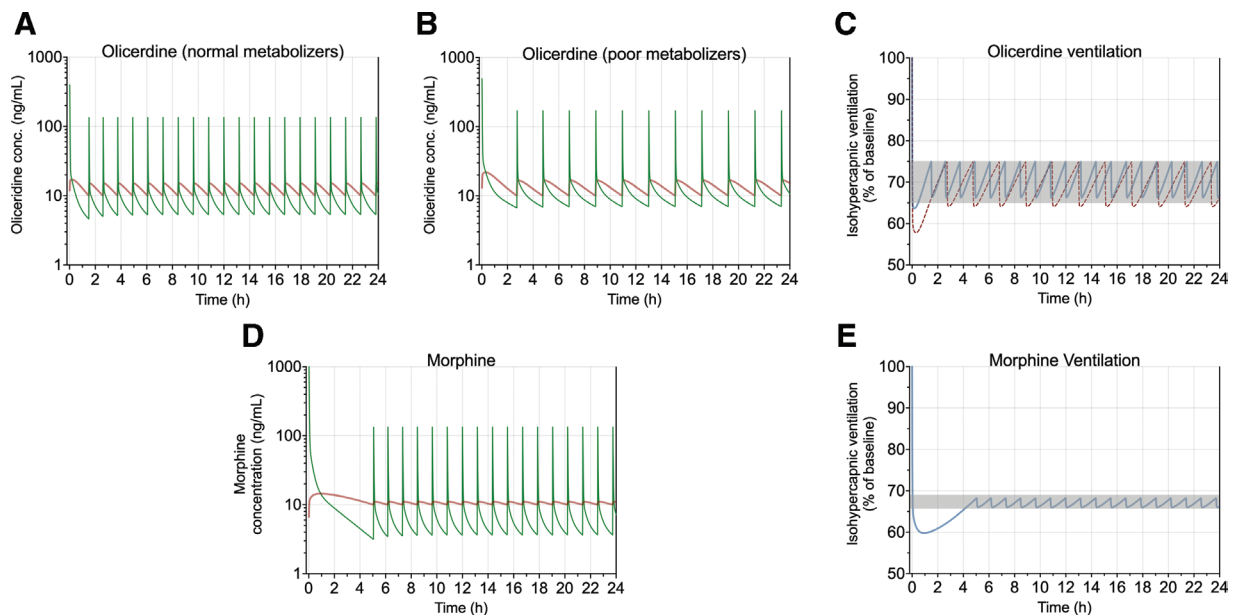


Fig. 7. Simulation study of the effect of multiple doses of oliceridine and morphine, mimicking patient-controlled analgesia and aimed at a maximum level of respiratory depression of 65% of baseline ventilation. (A) Oliceridine pharmacokinetics in normal metabolizers. (B) Oliceridine pharmacokinetics in poor metabolizers. (C) Ventilation in normal (blue line) and poor oliceridine metabolizers (red broken line). The gray area indicates the ventilation variability. (D) Morphine pharmacokinetics. (E) Ventilation following morphine. (A, B, and D) Green lines depict plasma concentration; red lines effect-site concentrations. (C and E) Gray areas depict the ventilation variability.

Table 3. Adverse Effects

	Oliceridine 0.5 mg	Oliceridine 2 mg	Morphine 2 mg	Morphine 8 mg
Apnea*				1
Bradycardia			1	3
Dizziness	4	12	4	7
Drowsiness	1	1	1	2
Flushing		3	1	2
Headache	3	6	4	4
Hoarseness				1
Lightheadedness	5	8	3	8
Myalgia shoulders				1
Nausea (without vomiting)		6	2	10
Nausea and vomiting		1	2	5
Numbness shoulders			1	
Paresthesia extremities		1	1	3
Paresthesia whole body		1		
Pruritis at injection site		1	2	1
Rigidity of the thorax				1
Shivering			1	
Slurred speech		2		1
Somnolence	4	7	2	6
Syncope	1		1	1
Vertigo (horizontal)	2	6		3
Vertigo (vertical)		4		2
Total	20	59	26	62

Data are n (subjects).

*Cessation of breathing for at least 30 s.

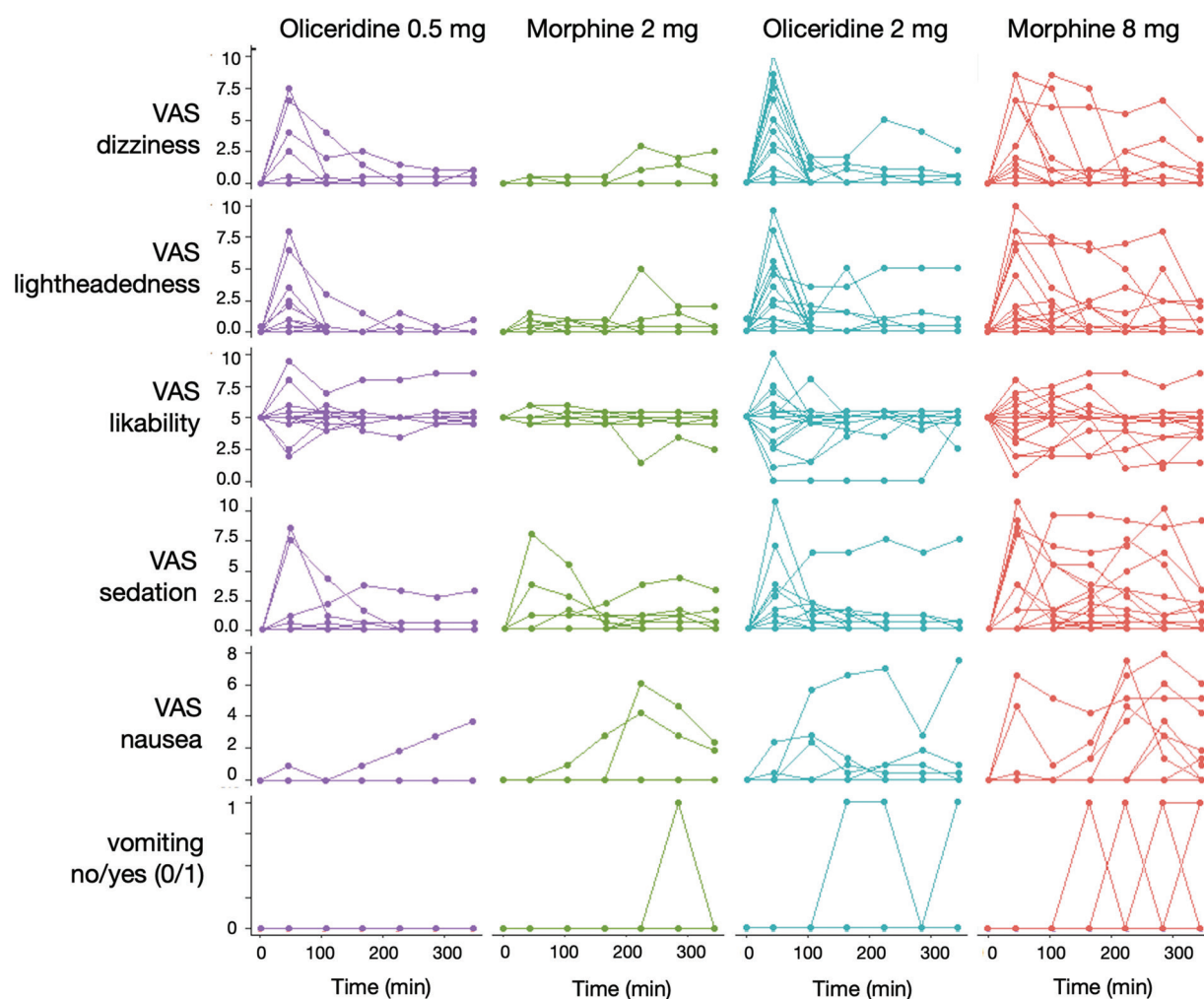


Fig. 8. Adverse events, queried on a visual analog scale for dizziness, lightheadedness, drug likability, sedation, nausea, and vomiting. For drug likability, the score ranges from 0 = I do not like this drug to 10 = I do like this drug, with 5 an equivocal score = I do like/I do not like. VAS, visual analog scale.

respiratory studies.^{13,21,31,32} Additional studies in preferably acute pain patients, comparing multiple age cohorts, on pain relief and respiration are needed for definite conclusions.

The pharmacokinetic profile of oliceridine was altered in three poor metabolizers related to the *CYP2D6* genotype. All three had a significantly lower clearance (CL_r) with higher plasma oliceridine concentrations than the other *CYP2D6* genotypes. Similar observations were reported earlier.³³ In reviewing the pharmacokinetic data, we also need to consider the effects of age and body mass index. Among other physiologic changes, at an increasing age, glomerular filtration rate is reduced and there is a shift in the distribution of fat and muscle mass.^{34,35} The latter may account for the decreased morphine compartmental volumes compared with volumes reported in younger volunteers with mean age 26 yr.³⁶ Similar observations were made for remifentanyl showing reduced compartmental volumes with increasing age.³⁷ Our oliceridine pharmacokinetic parameter estimates

agree with the pooled analysis of seven oliceridine data sets in acute pain patients of which more than half had an age range of 40 to 65 yr.⁷ For morphine, a possible age-related reduction in renal function may cause accumulation of morphine-6-glucuronide, morphine's active metabolite, and subsequently enhance respiratory depression.³⁸ In our sample, all subjects had a glomerular filtration rate greater than 60 ml/min and a normal liver function.

The morphine and oliceridine C_{50} values (table 2) are lower than previously reported in several studies in younger volunteers.³² For example, we earlier observed a C_{50} for morphine respiratory effect of about 45 ng/ml in young volunteers in their twenties.³⁹ Although we did not perform a direct comparison among different age cohorts, these observations point toward an increase in respiratory potency with increasing age for the two tested opioids. Our findings are consistent with earlier studies showing enhanced desired and undesired opioid effect with increasing age.^{37,40–42} For potent synthetic opioids,

the age effect is well documented. For example, Scott *et al.*⁴³ found that the fentanyl dose requirements to produce a similar electroencephalographic effect decreases by 50% at an increasing age (from 20 to 89 yr) in male patients. Similar observations were made for remifentanyl.³⁷ Cepeda *et al.*⁴² showed that the risk for postoperative respiratory depression rises with increasing age in 8,855 surgical patients receiving an opioid (fentanyl, meperidine, or morphine) for postoperative pain. Compared with younger patients (16 to 45 yr), those aged 61 to 70 yr, 71 to 80 yr, and 81 yr and older had, respectively, a 2.8, 5.4, and 8.7 times higher risk for the development of respiratory depression. The physiologic basis of the increased opioid respiratory sensitivity with age remains unknown but may be related to an age-dependent imbalance between excitatory and inhibitory neuronal pathways within the respiratory networks of the brainstem after opioid receptor activation.⁴⁴ Possibly excitatory pathways are less active in the elderly, leading to increased sensitivity of the ventilatory control system to opioids.

\dot{V}_{E55} versus Slope of the Hypercapnic Ventilatory Response

We measured the non-steady-state ventilatory response to carbon dioxide according to Read,¹⁶ Rebuck,¹⁷ and Florian *et al.*¹⁸ Rather than using the slope of the response curve as our primary endpoint, we used ventilation at an end-tidal P_{CO_2} of 55 mmHg (\dot{V}_{E55}) calculated from the slope (S) and the x -axis intercept (B) as follows: $\dot{V}_{E55} = [S \times (55 - B)]$; S and B are estimated from the regression of the breath-to-breath P_{CO_2} ventilation data. As is apparent from the formula, \dot{V}_{E55} considers the slope and the position of the hypercapnic response curve. Opioids are known to decrease the slope and shift the response curve to the right, both of which are signs of respiratory depression. We and others earlier used \dot{V}_{E55} to reliably express opioid effects on ventilatory control.^{18,20,23} We chose a rebreathing rather than a steady-state technique to quantify the opioid effect on the hypercapnic ventilatory response to enable rapid and frequent testing over time. The steady-state technique is more cumbersome and takes 30 to 40 min to complete.²⁰ We previously argued that, in contrast to the steady-state technique, the rebreathing technique causes a reduction of the response slope due to a decrease in the differences between end-tidal (and arterial) P_{CO_2} and the CO_2 content in the rebreathing balloon (7%) after opioid administration.^{45,46} However, the opioid-induced rise in end-tidal P_{CO_2} is due to the opioid respiratory effect, and, consequently, the reduced slope is a sign of respiratory depression that becomes apparent because of methodologic issues. A reduced slope is often not observed using a nonrebreathing steady-state technique.^{47,48} Interestingly, opioids cause a rightward shift of the steady-state hypercapnic response curve, but the effect of opioids on \dot{V}_{E55} seems independent of the method used to measure the hypercapnic ventilatory response.⁴⁸

In conclusion, our population pharmacokinetic-pharmacodynamic analysis, performed in older individuals,

shows that oliceridine has a more rapid onset/offset of respiratory depression, as defined by parameter $t_{1/2k_{e0}}$, combined with a 30% lesser potency for respiratory depression, as defined by parameter C_{50} , than morphine.

Research Support

Support was provided from institutional and/or departmental sources and from Trevena Inc., Chesterbrook, Pennsylvania. Dr. Dahan received funding from the Dutch Research Council (Nederlandse Organisatie voor Wetenschappelijk Onderzoek, The Hague, The Netherlands) in the framework of the NWA-ORC Call for research project TAPTOE, Tackling and preventing the opioid epidemic (NWA.1160.18.300).

Competing Interests

T. Nicklas, C. Michalsky, and Dr. Demitrack are or were (Dr. Fossler) employees of Trevena Inc., Chesterbrook, Pennsylvania, at the time of performance of the study. Dr. Fossler is currently employed at Cytel Inc., Cambridge, Massachusetts, a consulting firm for the pharmaceutical industry. The Anesthesia & Pain Research Unit of the Department of Anesthesiology, Leiden University Medical Center (Leiden, The Netherlands) received/receives funding from AMO Pharma Ltd. (Leeds, United Kingdom), Bedrocan BV (Groningen, The Netherlands), Grünenthal GmbH (Stolberg, Germany), and Medtronic (Minneapolis, Minnesota), and MSD Nederland BV (Haarlem, The Netherlands). Dr. Dahan received consultancy and/or speaker fees from Enalare Therapeutics Inc. (Princeton, New Jersey), Grünenthal BV (Breukelen, The Netherlands), Medasense Biometrics Ltd. (Ramat Gan, Israel), Trevena Inc., MSD Nederland BV, LTS Lohmann Therapie Systeme AG (Andernach, Germany), and awards and/or grants from the U.S. Food and Drug Administration (Silver Spring, Maryland) and from the Netherlands Organisation for Health Research and Development (ZonMW, The Hague, The Netherlands). Dr. Sarton received support from the Federation Medical Specialists (Utrecht, The Netherlands) for updating national guidelines.

Reproducible Science

Full protocol available at: a.dahan@lumc.nl. Raw data available at: a.dahan@lumc.nl.

Correspondence

Address correspondence to Dr. Dahan, Department of Anesthesiology, Leiden University Medical Center, PO Box 9600, 2300 RC Leiden, The Netherlands. a.dahan@lumc.nl. This article may be accessed for personal use at no charge through the Journal Web site, www.anesthesiology.org.

References

- Paul AK, Smith CG, Rahmattullah M, Nissapatorn V, Wilairatana P, Spetea M, Gueven N, Diteis N: Opioid analgesia and opioid-induced adverse effects: A review. *Pharmaceut (Basel)* 2021; 14:1091
- Shafi S, Collinsworth AW, Copeland LA, Ogola GA, Qiu T, Kouznetsova M, Liao IC, Ners N, Pham AT, Wan GJ, Masica AL: Association of opioid-related adverse drug events with clinical and cost outcomes among surgical patients in a large integrated health care delivery system. *JAMA Surg* 2018; 153:757–63
- Kessler ER, Shah M, Grushkus SK, Raju A: Cost and quality implications of opioid-based postsurgical pain control using administrative claims data from a large health system: Opioid-related adverse events and their impact on clinical and economic outcomes. *Pharmacotherapy* 2013; 33:383–91
- Boom M, Niesters M, Sarton E, Aarts L, Smith TW, Dahan A: Non-analgesic effects of opioids: Opioid-induced respiratory depression. *Curr Pharm Des* 2012; 18:5994–6004
- Mann J, Samieegohar M, Chaturbedi A, Zikle J, Han X, Ahmadi SF, Eshleman A, Janowsky A, Wolfrum K, Swanson T, Bloom S, Dahan A, Olofsen E, Florian J, Strauss D, Li Z: Development of a translational model to assess the impact of opioid overdose and naloxone dosing on respiratory depression and cardiac arrest. *Clin Pharmacol Ther* 2022; 112:1020–32
- Kharasch ED, Avram MJ, Clark JD: Rational perioperative opioid management in the era of the opioid epidemic. *ANESTHESIOLOGY* 2020; 132:603–5
- Fossler MJ, Sadler BM, Farrell C, Burt DA, Pitsiu M, Skobieranda F, Soergel DG: Oliceridine (TRV130), a novel G protein-biased ligand at the mu-opioid receptor, a predictable relationship between plasma concentrations and pain relief. I: Development of pharmacokinetic/pharmacodynamic model. *J Clin Pharmacol* 2018; 58:750–61
- Dewire SM, Yamashita DS, Rominger DH, Liu G, Cowan CL, Graczyk TM, Chen XT, Pitis PM, Gotchev D, Yuan C, Koblish M, Lark MW, Violoin JD: A G protein-biased ligand at the μ -opioid receptor is potently analgesic with reduced gastrointestinal and respiratory dysfunction compared with morphine. *J Pharmacol Exp Ther* 2013; 344:708–17
- Manglik A, Lin H, Aryal DK, McCorvy JD, Dengler D, Corder G, Levit A, Kling RC, Bernat V, Hübner H, Huang XP, Sassano MF, Giguère PM, Löber S, Duan D, Scherrer G, Kobilka BK, Gmeiner P, Roth BL, Shoichet BK: Structure-based discovery of opioid analgesics with reduced side effects. *Nature* 2016; 537:185–90
- Raehal KM, Walker JKL, Bohn LM: Morphine side effects in β -arrestin 2 knockout mice. *J Pharmacol Ther* 2005; 314:1195–2001
- Gillis A, Gondin AB, Kliewer A, Lim HD SJ, Alamein C, Manandhar P, Santiago M, Fritzwancker S, Schmiedel F, Katte TA, Reekie T, Grimsey NL, Kassiou M, Kellam B, Krasel C, Halls ML, Connor M, Lane JR, Schulz S, Christie MJ, Canals M: Low intrinsic efficacy for G protein activation can explain the improved side effect profiles of new opioid agonists. *Sci Signal* 2020; 13:eaaz3140
- Stahl EL, Bohn LM: Low intrinsic efficacy alone cannot explain the improved side effect profiles of new opioid agonists. *Biochemistry* 2022; 61:1923–35
- Dahan A, van Dam CJ, Niesters M, van Velzen M, Fossler MJ, Demitrack MA, Olofsen E: Benefit and risk evaluation of biased μ -receptor agonist oliceridine versus morphine. *ANESTHESIOLOGY* 2020; 133:559–68
- Soergel G, Subach RS, Burnam N, Lark MW, James IE, Sadler BM, Skobieranda F, Violin JD, Webster LR: Biased agonism of the μ -opioid receptor by TRV130 increases analgesia and reduces on-target adverse effects vs. morphine: A randomized, double-blind, placebo-controlled, crossover study in healthy volunteers. *Pain* 2014; 155:1829–35
- Viscusi ER, Webster I, Kuss M, Daniels S, Bolognese JA, Zuckerman S, Soergel DG, Subach RA, Cook E, Skobieranda F: A randomized, phase-2 study investigating TRV130, a biased-ligand of the mu-opioid receptor, for intravenous treatment of pain. *Pain* 2016; 157:264–72
- Read DJ: A clinical method for assessing the ventilatory response to carbon dioxide. *Australas Ann Med* 1967; 16:20–32
- Rebuck AS: Measurement of ventilatory response to CO₂ by rebreathing. *Chest* 1976; 70:118–21
- Florian J, van der Schrier R, Gershuny V, Davis MC, Wang C, Han X, Burkhart K, Prentice K, Shah A, Raczy R, Patel V, Matta M, Ismaiel OA, Weaver J, Boughner R, Ford K, Rouse R, Stone M, Sanabria C, Dahan A, Strauss DG: Effect of paroxetine or quetiapine combined with oxycodone on ventilation: A randomized clinical trial. *JAMA* 2022; 328:1405–14
- Henriques BC, Buchner A, Hu X, Wang Y, Yavorsky V, Wallace K, Dong R, Martens K, Carr MS, Asl BB, Hague J, Sivapalan S, Maier W, Dernovsek MZ, Henigsberg N, Hauser J, Souery D, Cattaneo A, Mors O, Rietschel M, Pfeffer G, Hume S, Aitchison KJ: Methodology for clinical genotyping of CYP2D6 and CYP2C19. *Transl Psychiatry* 2021; 11:596 (2022 corrected version)
- van der Schrier R, Roozkrans M, Olofsen E, Aarts L, van Velzen M, de Jong M, Dahan A, Niesters M: Influence of ethanol on oxycodone-induced respiratory depression: A dose-escalating study in young and elderly volunteers. *ANESTHESIOLOGY* 2017; 126:534–42
- Romberg R, Olofsen E, Sarton E, Teppema L, Dahan A: Pharmacodynamic effect of morphine-6-glucuronide versus morphine on hypoxic and hypercapnic breathing in healthy volunteers. *ANESTHESIOLOGY* 2003; 99:788–98

22. Holford NH: A size standard for pharmacokinetics. *Clin Pharmacokinet* 1996; 30:329–32
23. van der Schrier R, Jonkman K, van Velzen M, Olofsen E, Drewes AM, Dahan A, Niesters M: An experimental study comparing the respiratory effects of tapentadol and oxycodone in healthy volunteers. *Br J Anaesth* 2017; 119:1169–77
24. Minto CF, Schnider TW, Gregg KM, Henthorn TK, Shafer SL: Using the maximum effect site concentration to combine pharmacokinetics and pharmacodynamics. *ANESTHESIOLOGY* 2003; 99:324–33
25. Caudle KE, Sangkuhl K, Whirl-Carrillo M, Swen JJ, Haider CE, Klein TE, Gammal RS, Relling MV, Scott SA, Hertz DL, Guchelaar HJ, Gaedigk A: Standardizing CYP2D6 genotype to phenotype translation: Consensus recommendations from the clinical pharmacogenetics implementation consortium and Dutch pharmacogenetics working group. *Clin Transl Sci* 2020; 13:116–24
26. Olofsen E, Algera M, Moss L, Dobbins RL, Groeneveld GJ, van Velzen M, Niesters M, Dahan A, Laffont C: Modelling buprenorphine reduction of fentanyl-induced respiratory depression. *JCI Insight* 2022; 7:e156973
27. Oudejans LCJ, van Velzen M, Olofsen E, Beun R, Dahan A, Niesters M: Translation of random painful stimuli into numerical responses in fibromyalgia and perioperative patients. *Pain* 2016; 157:128–36
28. Kemp J, Després O, Pabayle T, Dufour A: Differences in age-related effects on myelinated and unmyelinated peripheral fibres: A sensitivity and evoked potential study. *Eur J Pain* 2014; 18:482–8
29. Tseng MT, Chiang MC, Yazhuo K, Chao CC, Tseng WYI, Hsieh ST: Effect of aging on the cerebral processing of thermal pain in the human brain. *Pain* 2013; 154:2120–9
30. Torensma B, Oudejans L, van Velzen M, Swank D, Niesters M, Dahan A: Pain sensitivity and pain scoring in patients with morbid obesity. *Surg Obes Relat Dis* 2017; 13:788–95
31. Lötsch J, Skarke C, Schmidt H, Grösch S, Geisslinger G: The transfer half-life of morphine-6-glucuronide from plasma to effect site assessed by pupil size measurement in healthy volunteers. *ANESTHESIOLOGY* 2001; 95:1329–38
32. Martini CH, Olofsen E, Yassen A, Aarts L, Dahan A: Pharmacokinetic-pharmacodynamic modeling in acute and chronic pain: An overview of the recent literature. *Exp Rev Clin Pharmacol* 2011; 4:719–2
33. Fossler MJ, Sadler BM, Farrell C, Burt DA, Pitsiu M, Skobierdanda F, Soergel DG: Oliceridine, a novel G protein-biased ligand at the μ -opioid receptor, demonstrates a predictable relationship between plasma concentrations and pain relief. II: Simulation of potential phase 3 study designs using a pharmacokinetic/pharmacodynamic model. *J Clin Pharmacol* 2018; 58:762–70
34. Boss GR, Seegmiller JE: Age-related physiological changes and their clinical significance. *West J Med* 1981; 135:434–40
35. Dodds C, Kumar CM, Veering BTh: *Oxford Textbook of Anaesthesia for the Elderly Patient*. Oxford: Oxford University Press; 2014.
36. Lötsch J, Stockmann A, Kobal G, Brune K, Waibel R, Schmidt N, Geisslinger G: Pharmacokinetics of morphine and its glucuronides after intravenous infusion of morphine and morphine-6-glucuronide in healthy volunteers. *Clin Pharmacol Ther* 1996; 60:316–25
37. Minto CF, Schnider TW, Shafer SL: Pharmacokinetics and pharmacodynamics of remifentanyl. II. Model application. *ANESTHESIOLOGY* 1997; 86:24–33
38. van Crugten JT, Somogyi AA, Nation RL, Reynolds GR: The effect of age on the disposition and antinociceptive response of morphine and morphine-6 β -glucuronide in the rat. *Pain* 1997; 71:199–205
39. Olofsen E, van Dorp E, Teppma L, Aarts L, Smith T, Dahan A, Sarton E: Naloxone reversal of morphine- and morphine-6-glucuronide-induced respiratory depression in humans. *ANESTHESIOLOGY* 2010; 212:1417–27
40. Vuyk J: Pharmacodynamics in the elderly. *Best Pract Res Clin Anaesthesiol* 2003; 17:207–18
41. Bowie MW, Slattum PW: Pharmacodynamics in older adults: A review. *Am J Geriatr Pharmacother* 2007; 5:263–303
42. Cepeda MS, Farrar T, Baumgarten M, Boston R, Carr DB, Strom BL: Side effects of opioids during short-term administration: Effect of age, gender and race. *Clin Pharmacol Ther* 2003; 74:102–12
43. Scott JC, Stanski DR: Decreased fentanyl and alfentanil dose requirements with age; a simultaneous pharmacokinetic and pharmacodynamic evaluation. *J Pharmacol Exp Ther* 1987; 240:159–66
44. Dahan A, van der Schrier R, Smith T, Aarts L, van Velzen M, Niesters M: Averting opioid-induced respiratory depression without affecting analgesia. *ANESTHESIOLOGY* 2018; 128:1027–37
45. Dahan A, Berkenbosch A, DeGoede J, Olivier ICW, Bovill JG: On a pseudo-rebreathing technique to assess the ventilatory sensitivity to carbon dioxide in man. *J Physiol* 1990; 423:615–29
46. Berkenbosch A, DeGoede J, Olivier CN, Schuitmaker JJ: A pseudo-rebreathing technique for assessing the ventilatory response to carbon dioxide in cats. *J Physiol* 1986; 381:483–95
47. Berkenbosch A, Bovill JG, Dahan A, DeGoede J, Olivier ICW: The ventilatory CO₂ sensitivities from Read's rebreathing method and the steady-state method are not equal in man. *J Physiol* 1989; 411:367–77
48. Bourke DL, Warley A: The steady-state and rebreathing methods compared during morphine administration in humans. *J Physiol* 1989; 419:509–17

ANESTHESIOLOGY

Extended-age Out-of-sample Validation of Risk Stratification Index 3.0 Models Using Commercial All-payer Claims

Scott Greenwald, Ph.D., George F. Chamoun, B.S.,
Nassib G. Chamoun, M.S., David Clain, B.S., Zhenyu Hong, M.S.,
Richard Jordan, Ph.D., Paul J. Manberg, Ph.D.,
Kamal Maheshwari, M.D., Daniel I. Sessler, M.D.

ANESTHESIOLOGY 2023; 138:264–73

EDITOR'S PERSPECTIVE

What We Already Know about This Topic

- Risk Stratification Index 3.0 predictive analytical models provide risk profiles at hospital admission from individual administrative claims histories. These models were generated and validated in a population that was mostly more than 65 yr old.

What This Article Tells Us That Is New

- In two different statewide databases, Risk Stratification Index 3.0 models worked well in younger and healthier adults.

The Risk Stratification Index 3.0 (Health Data Analytics Institute, Inc., USA) suite of predictive models is a broadly applicable set of risk adjustment measures that use administrative claims data to predict health outcomes

ABSTRACT

Background: The authors previously reported a broad suite of individualized Risk Stratification Index 3.0 (Health Data Analytics Institute, Inc., USA) models for various meaningful outcomes in patients admitted to a hospital for medical or surgical reasons. The models used International Classification of Diseases, Tenth Revision, trajectories and were restricted to information available at hospital admission, including coding history in the previous year. The models were developed and validated in Medicare patients, mostly age 65 yr or older. The authors sought to determine how well their models predict utilization outcomes and adverse events in younger and healthier populations.

Methods: The authors' analysis was based on All Payer Claims for surgical and medical hospital admissions from Utah and Oregon. Endpoints included unplanned hospital admissions, in-hospital mortality, acute kidney injury, sepsis, pneumonia, respiratory failure, and a composite of major cardiac complications. They prospectively applied previously developed Risk Stratification Index 3.0 models to the younger and healthier 2017 Utah and Oregon state populations and compared the results to their previous out-of-sample Medicare validation analysis.

Results: In the Utah dataset, there were 55,109 All Payer Claims admissions across 40,710 patients. In the Oregon dataset, there were 21,213 admissions from 16,951 patients. Model performance on the two state datasets was similar or better than in Medicare patients, with an average area under the curve of 0.83 (0.71 to 0.91). Model calibration was reasonable with an R^2 of 0.93 (0.84 to 0.97) for Utah and 0.85 (0.71 to 0.91) for Oregon. The mean sensitivity for the highest 5% risk population was 28% (17 to 44) for Utah and 37% (20 to 56) for Oregon.

Conclusions: Predictive analytical modeling based on administrative claims history provides individualized risk profiles at hospital admission that may help guide patient management. Similar predictive performance in Medicare and in younger and healthier populations indicates that Risk Stratification Index 3.0 models are valid across a broad range of adult hospital admissions.

(*ANESTHESIOLOGY* 2023; 138:264–73)

including mortality, prolonged hospitalization, and adverse events during hospitalization and after discharge.¹ This well-validated and calibrated broad suite of predictive algorithms uses diagnostic, procedural, and demographic

This article is featured in "This Month in Anesthesiology," page A1. Supplemental Digital Content is available for this article. Direct URL citations appear in the printed text and are available in both the HTML and PDF versions of this article. Links to the digital files are provided in the HTML text of this article on the Journal's Web site (www.anesthesiology.org). This article has a visual abstract available in the online version.

Submitted for publication July 25, 2022. Accepted for publication December 12, 2022. Published online first on December 20, 2022.

Scott Greenwald, Ph.D.: Health Data Analytics Institute, Dedham, Massachusetts.

George F. Chamoun, B.S.: Health Data Analytics Institute, Dedham, Massachusetts.

Nassib G. Chamoun, M.S.: Health Data Analytics Institute, Dedham, Massachusetts.

David Clain, B.S.: Health Data Analytics Institute, Dedham, Massachusetts.

Zhenyu Hong, M.S.: Health Data Analytics Institute, Dedham, Massachusetts.

Richard Jordan, Ph.D.: Health Data Analytics Institute, Dedham, Massachusetts.

Paul J. Manberg, Ph.D.: Health Data Analytics Institute, Dedham, Massachusetts.

Kamal Maheshwari, M.D.: Department of Outcomes Research, and Department of General Anesthesiology, Cleveland Clinic, Cleveland, Ohio.

Daniel I. Sessler, M.D.: Department of Outcomes Research, Cleveland Clinic, Cleveland, Ohio.

Copyright © 2023, the American Society of Anesthesiologists. All Rights Reserved. *Anesthesiology* 2023; 138:264–73. DOI: 10.1097/ALN.0000000000004477

information over time to anticipate evolution of health conditions based solely on administrative claims and demographic data available at the time of admission.

A limitation of Risk Stratification Index 3.0 models is that they were developed and out-of-sample validated in Medicare fee-for-service patients who are mostly age 65 yr or older. An obvious question is whether Risk Stratification Index 3.0 models are comparably predictive in other populations, especially those that are younger and healthier. Our goal was to determine how well seven Risk Stratification Index 3.0 models developed in Medicare patients perform when applied to out-of-sample younger and healthier adult populations.

Materials and Methods

As described elsewhere,¹ Risk Stratification Index 3.0 models were developed on the Centers for Medicare & Medicaid Services (Baltimore, Maryland) Research Identifiable File data on a remote server using the SAS Enterprise Guide (version 7.15; SAS Institute Inc., USA) under a Centers for Medicare & Medicaid Services data use agreement (No. 51870). The models are extensions of previously published Risk Stratification Index versions 1.0 and 2.0.^{2,3}

Subject Selection

Our reference study design was an extension of the previously described out-of-sample validation in all 2017 to 2019 hospitalized Medicare fee-for-service and dual-eligible (Medicaid and Medicare) beneficiaries.¹ Briefly, in that study, admissions were excluded if patient age on admission was either younger than 18 or older than 99 yr, records had missing or inconsistent data (e.g., missing sex or birthdate information, or had different sex, birth dates, or mortality dates [if applicable] reported in source files), or patients had either discontinuous Part A or Part B Medicare coverage or had Part C coverage in the year before admission (fig. 1A). Claims data during the year before the admission were used to characterize the patient history. Admissions were considered “planned” when designated elective, and were otherwise considered “unplanned.” Claims data during the 90 days after admission characterized outcomes. Model performance results from the 2019 Medicare out-of-sample validation cohort were used as the baseline performance comparator for the current study.

Some U.S. states consolidate medical and pharmacy claims data submitted voluntarily by healthcare insurance carriers in what are commonly called All Payer Claims Databases.⁴ These registries contain medical and pharmacy claims along with insurance enrollment and health provider data for a large fraction of each state’s population. The Utah Office of Health Care Statistics (Salt Lake City, Utah) and the Oregon Office of Health Analytics (Portland, Oregon) have each established progressive and well-defined All Payer Claims data external access programs and were thus selected for analysis. We used the

available claims files from 2017, with cases selected as shown in figure 1, B and C.

Our analysis plan was approved by the Utah Department of Health & Human Services Institutional Review Board (Salt Lake City, Utah; No. 544) with a waiver of informed consent requirements. State data were housed on a local server using R software (3.6.0; available at <https://cran.r-project.org/src/base>, accessed January 6, 2023) under separate data use agreements with each party. Data were handled consistent with our data use agreements, which required suppression of metrics in downloaded tables for populations smaller than 11 individuals.

This report follows the Transparent Reporting of a Multivariable Prediction Model for Individual Prognosis or Diagnosis reporting guideline.⁵

Outcomes Selection

For our Risk Stratification Index 3.0 validation analysis, we included a suite of 10 models that predict excess length of stay and adverse events, selected to demonstrate performance of predictors for clinically and economically meaningful outcomes spanning a broad range of incidences. Cardiac complications, kidney injury, sepsis, pneumonia, and respiratory failure were defined using International Classification of Diseases, Tenth Revision (ICD-10), diagnosis and procedure codes⁶ along with information about their associated claim, such as the setting and revenue center. Additionally, we considered whether codes were primary or secondary.

As reported previously, endpoint definitions were derived using published methods for classifying events using administrative data.¹ Events were identified between admission and discharge (for in-hospital endpoints) and/or between admission and 90 days thereafter (for 90-day endpoints). In-hospital mortality was defined by any-cause death between admission and discharge.

The state datasets did not include sufficient information to determine length of stay, discharge location, or vital status after discharge (for example, date of death). We were therefore unable to compare these three outcomes to the Medicare analysis. The state datasets also did not include race of included subjects, precluding description of the population’s racial characteristics.

Model Development

As previously presented, medical history was represented by a set of variables indicating the presence or absence of individual and categories of ICD-10 diagnostic and procedure codes. We used a custom procedure to reduce 69,000 potential ICD-10 diagnostic codes to a representative subset of 4,426 codes by collapsing rare codes into their parent codes to avoid overfitting. ICD-10 diagnostic codes were additionally represented by their corresponding default Clinical Classifications Software Refined category.⁷ Similarly, ICD-10 procedure codes were represented by their corresponding default Clinical Classifications Software

category.⁸ Temporal information relative to a prediction date was encoded using two sets of these variables representing the presence or absence of relevant codes in the past 90 or 365 days.

Outcomes were indexed to the date of inpatient admission, and claims within the preceding 365 days were included in our models. The only information used from

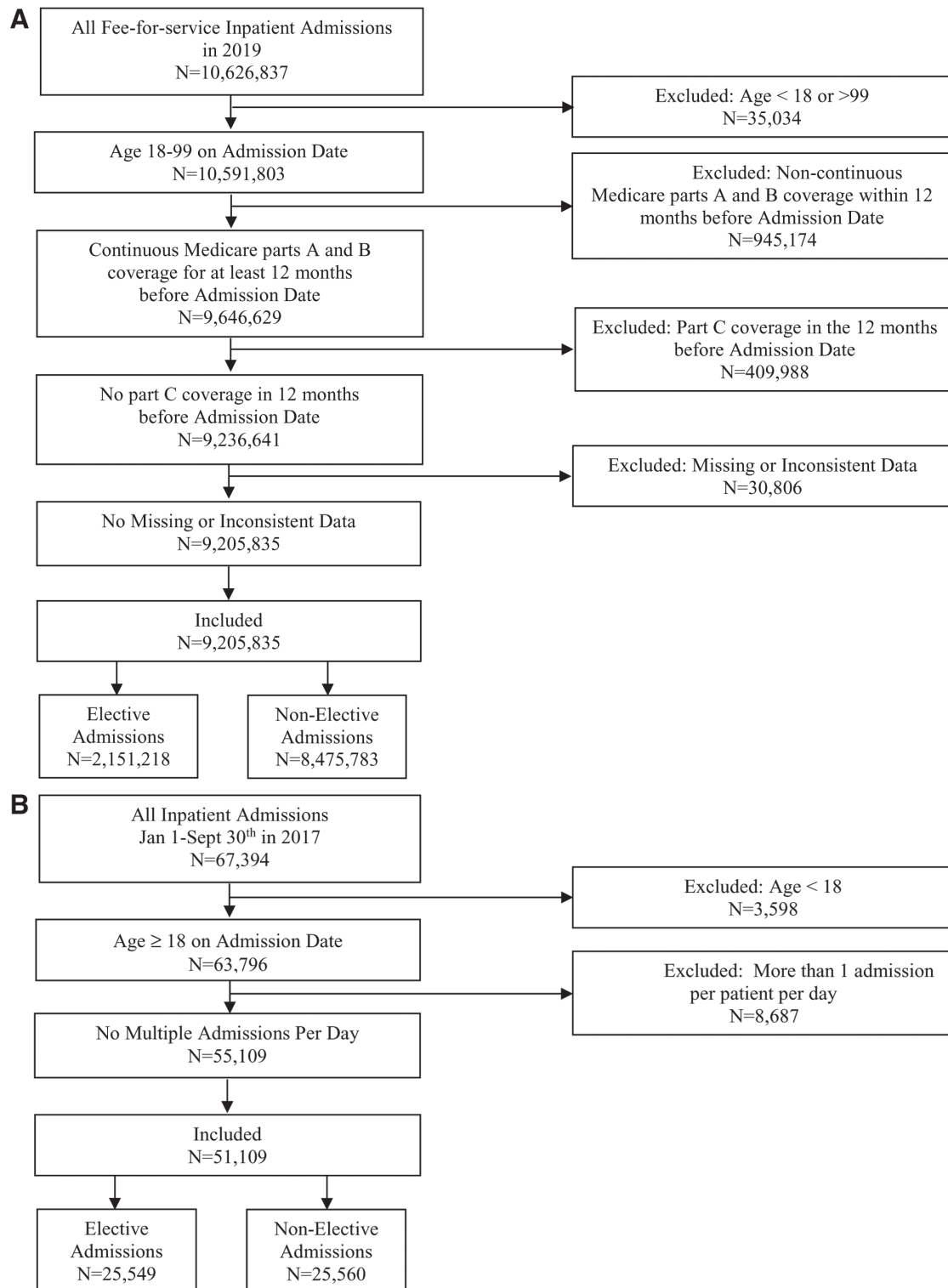


Fig. 1. Cohorts selection diagrams for (A) 2019 Medicare dataset; (B) Utah All Payer Claims Database dataset; (continued)

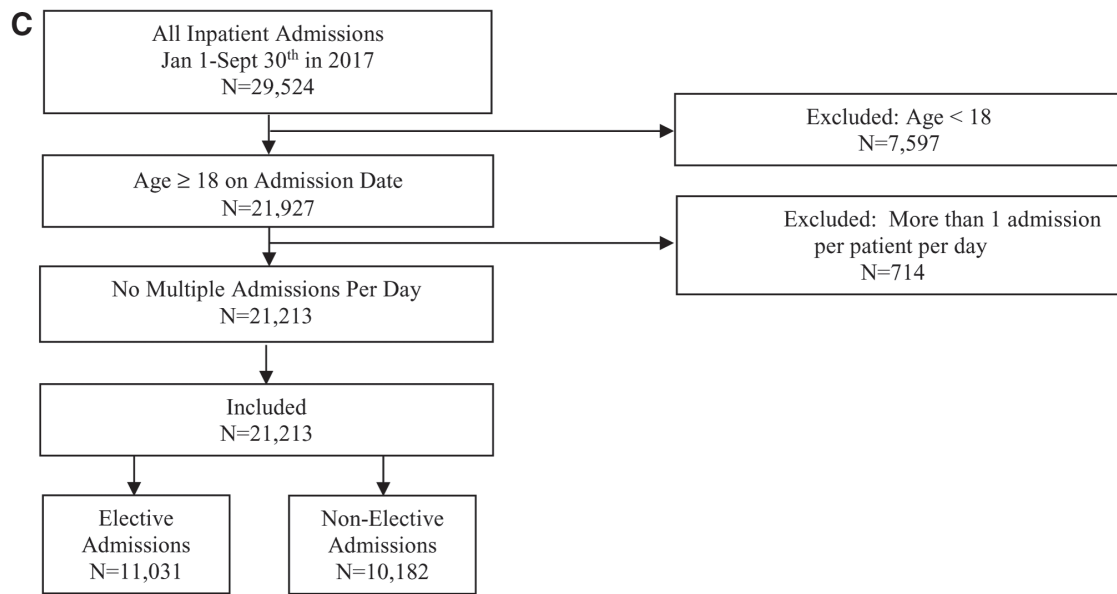


Fig.1. (continued) (C) Oregon All Payer Claims Database dataset.

the day of admission was the admitting diagnosis (not the principal diagnosis) along with the principal procedure for planned admissions. We also included age at the time of admission. We did not include present-on-admission codes because these are usually coded during or after discharge and are thus not actually available upon admission.

Logistic regression models were trained with the SAS HPLOGISTIC procedure using log-log linkage and backwards fast selection of covariates, keeping those with a $P < 0.01$ significance level. The HPLOGISTIC CODE statement option was used to generate SAS code for subsequent use in a SAS DATA step to apply the model to score new data. We used the asymmetric log-log link function because such models handle skewed extreme value distributions associated with rare events better than symmetrical link functions.⁹ There were nonlinear interactions by sex and admission type between ICD-10 codes and various outcomes that precluded using a single logistic model for each outcome. We therefore constructed an overall model for each outcome, designated an ensemble model, that was based on coefficients from four models depending on sex and admission status.

Model Application

Our general approach was to apply our final Medicare-derived models prospectively on each of the two out-of-population state datasets separately to document performance on each of the prospective age validation datasets. Model predictions for each state database were generated in two steps. First, a data file similar in format

to that used for model development was created to house the patient demographic and medical history for each admission. Second, the SAS code generated by the SAS HPLOGISTIC procedure during model development was applied to the medical history data file in a SAS DATA step to compute model predictions.

Performance Metrics

Overall discrimination performance was evaluated using the mean and 95% CI for area under the receiver operating characteristics curve (AUC). To compare model detection performance consistently across various endpoints, we compared sensitivity for each model at an alert threshold corresponding to the highest 5% risk fraction of the population.

Calibration performance for each endpoint was evaluated using observed and predicted incidences of subpopulations in bins along the full continuum of risk. We computed R^2 goodness-of-fit values between observed and predicted incidences using all bins having more than 100 subjects. We similarly computed the slope and intercept of the best-fit line and the overall observed-to-predicted ratio. In the primary calibration analysis, we assessed calibration performance using subpopulations in steps of 1% resolution of risk. This approach used assessments of variable-sized populations at equal increments of risk. In a secondary analysis, we assessed calibration performance using decile subpopulations based on risk. This second approach used assessments of similarly sized populations at variable increments of risk.

We *a priori* applied the same minimum acceptable performance criteria as were used in our previous validation study using two metrics to reject clinically nonviable models.

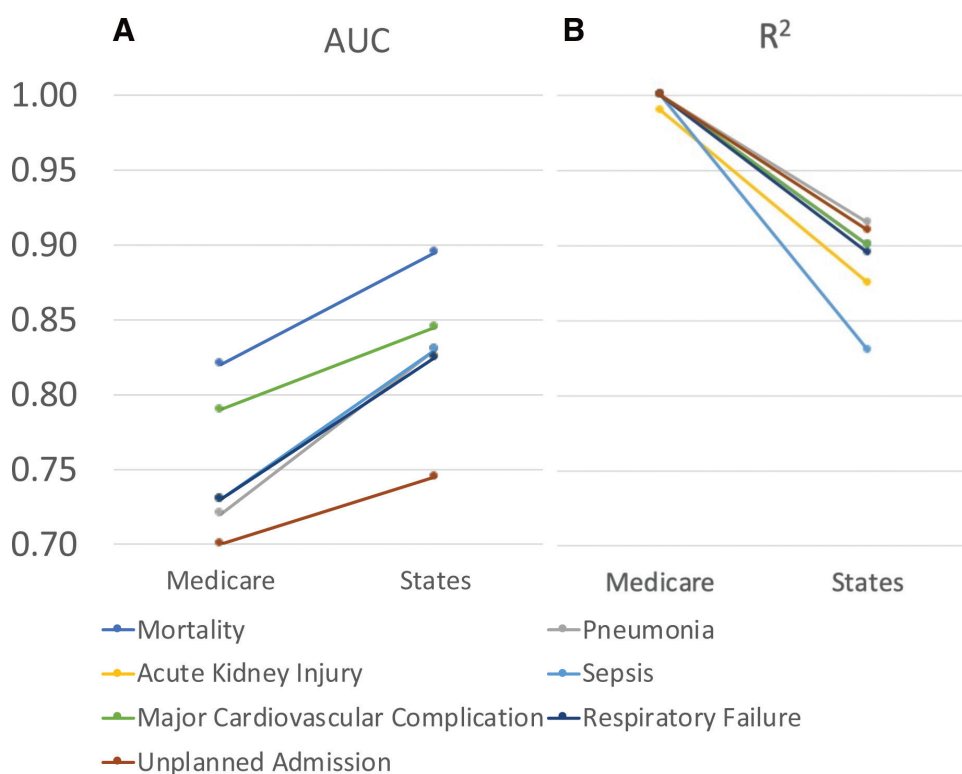


Fig. 2. Performance characteristics on Medicare and combined state admissions. (A) Area under the receiver operating characteristics curve (AUC). (B) R^2 .

Model acceptance required (1) a reasonably accurate overall classification performance defined by an AUC 0.70 or greater; and (2) relatively accurate prediction defined by an observed-to-expected ratio near 1 over the full risk continuum (*i.e.*, calibration R^2 greater than 0.80). The conservative 0.7 minimum acceptance threshold for AUC was based on consultation with clinical advisors and a literature review indicating the acceptability of numerous perioperative machine-learning models with c-statistics in the 0.7 to 0.8 range.^{10,11} Because no *a priori* hypotheses were tested, we did not estimate required sample size, but instead used all eligible cases available in the two state files for the selected years.

Results

There were a total of 9,205,835 admissions eligible from 5,336,265 Medicare beneficiaries for analysis in 2019 used previously for model validation. For the Utah dataset, there were 55,109 admissions from 40,710 subjects, and for Oregon, there were 21,213 admissions from 16,951 subjects. The fraction of surgical admissions was 26% in our Medicare population, 26% in Utah's and 24% in Oregon's. As expected, the state populations were younger than the Medicare population, with the mean Medicare age being 74 yr *versus* 58 yr for Utah and 44 yr for Oregon (table 1). As might thus be expected, the incidence of various morbid

outcomes was less, confirming that the state populations were also healthier. A consequence of the populations being healthier is that there were fewer diagnostic claims per subject in each of the state datasets.

Prospective classification and primary calibration performance characteristics for binary event predictors in the state datasets are summarized in tables 2 and 3. Secondary calibration performance characteristics are summarized in Supplemental Table 1 (<http://links.lww.com/ALN/C1000>). Calibration results reported in the main manuscript body are solely from the primary analysis. The observed incidence of endpoints ranged from 0.7% for pneumonia to 10.8% for unplanned readmissions within 90 days and were all considerably less than comparable incidences observed in the Medicare population.

The mean and range of AUCs across all seven outcomes were 0.83 (0.71 to 0.91). The mean and range of the calibration goodness-of-fit (R^2) were 0.89 (0.71 to 0.97). The receiver operator characteristics and calibration curves for each endpoint model for each of the state datasets are provided in the Supplemental Digital Content (<http://links.lww.com/ALN/C1000>). For the highest 5% risk population, the mean and range of sensitivity were 32% (17 to 56%).

Prediction of short-term (*e.g.*, in-hospital) events frequently outperforms prediction of longer-term (*e.g.*, after discharge) events. As expected, the inpatient mortality

Table 1. Mean and Interquartile of Age, and Percentage of Men, Percentage of Surgical Cases, Percentage of Unplanned Admissions, Average Number of Previous Claims per Admission, and Percentage of Admissions with No Previous Claims within 1 yr of Admission Date for the 2019 Medicare and 2017 Utah and Oregon Datasets.

Characteristic	Medicare Dataset	Utah Dataset	Oregon Dataset
No. of admissions	9,205,835	55,109	21,213
Surgical cases, % (No.)	26 (2,428,690)	26 (16,679)	24 (5,306)
No. of Individuals	5,336,265	40,710	16,951
Age, mean [interquartile range]	74 [68–83]	58 [35–76]	44 [31–58]
Age > 65 yr, % (No.)	80.9 (7,444,716)	43.1 (23,722)	0.5 (103)
Men, % (No.)	46 (4,267,427)	36 (20,060)	33 (7,092)
Unplanned admissions, % (No.)	80 (1,846,670)	46 (25,560)	48 (10,182)
Number of claims within 1 yr before admission, mean [interquartile range]	77 [32–101]	40.1 [16–48]	43.9 [17–55]
Admissions with no claims within 1 yr before admission, % (No.)	0 (10,648)	0 (0)	0 (0)

Neither state provided race information. The percentage of surgical cases was derived by first establishing a pairing between each principal diagnosis code and its most common admission type as defined by the Diagnostic Related Group (*i.e.*, medical or procedural/surgical case) using the Medicare Dataset, and then applying the mapping to identify the surgical cases in the three datasets.

predictive model showed the best performance across the Medicare (AUC, 0.82), Utah (AUC, 0.89) and Oregon (AUC, 0.90) datasets, with especially high sensitivity at the top 5% threshold (Medicare, 30.1%; Utah, 44.1%; Oregon, 56.5%). The calibration metrics, however, were lower in the state datasets because of endpoint detection issues as explained in the Discussion section (Utah R^2 , 0.93; Oregon R^2 , 0.85) than in the Medicare population (R^2 , 1.00). Calibration results were generally similar whether assessed using subpopulations at percent increments of risk in the primary analysis (table 3) or using decile subpopulations based on risk in the secondary analysis (Supplemental Table 1, <http://links.lww.com/ALN/C1000>).

Five 90-day adverse event models (pneumonia, acute kidney injury, sepsis, major cardiovascular complications, and respiratory failure) all showed a similar pattern of somewhat higher state AUC (0.80 to 0.86 *vs.* 0.72 to 0.79) and sensitivity (20 to 47% *vs.* 16 to 24%) performance results relative to the Medicare population (fig. 2). The model for 90-day unplanned admissions showed the lowest, but still acceptable, performance across all datasets (AUC: 0.70 to 0.78; sensitivity: 11.6% to 19.9%).

Discussion

We present the performance of Risk Stratification Index 3.0 predictive models for seven endpoints when applied prospectively to two large out-of-sample state datasets comprised of younger and healthier subjects who are more representative of the overall adult U.S. population requiring hospital admission. For all the endpoints, performance measures including AUC, R^2 , and sensitivity at the top 5% risk all were similar or better than the performance obtained on just the Medicare population. These results support the conclusion that our models are robust and widely applicable to the broad U.S. adult population including relatively young and health subjects. One factor contributing to Risk Stratification Index

3.0 models being so robust is that they were trained on more than 18 million hospital admissions and validated on more than 9 million out-of-sample Medicare admissions.

An intriguing observation is that models built on an older Medicare population generally performed as well or better when applied to younger and healthier subjects. One explanation may be that older individuals often have concomitant conditions that may contribute to risk in complex ways, whereas younger patient usually have fewer chronic conditions and thus a statistically cleaner risk profile linkage to the primary admission diagnosis. For example, we observed that the average Medicare beneficiary had an average of 77 medical claims recorded in the year before admission, whereas patients in Utah had only 40, and Oregon patients had only 44.

We also note that the incidence of the seven adverse outcomes described in this study was much lower in the younger and healthier state populations. The Oregon dataset showed the lowest event rates, consistent with the lower average age of that population. This dataset also showed slightly better performance metrics, thereby suggesting a complex interaction between lower age, fewer events, and better model performance metrics. However, this pattern is insufficiently consistent to conclude with certainty that these predictive models work best on young, otherwise healthy populations.

The state datasets we used differed from the Medicare database in a number of important ways. For example, the Oregon dataset did not (based on policy) include any Medicare-eligible subjects, and both datasets contained a sizeable number of pregnancy-related admissions. Furthermore, neither state database is curated as well as the Medicare registry. We confirmed the presence of several data quality issues first identified in a 2017 report by The Agency for Healthcare Research and Quality,¹² most notably the presence of duplicate records and missing data fields. We also identified coding differences, including an

Table 2. Classification Performance of Risk Stratification Index Models on Out-of-sample Medicare and State Admissions

Period	Endpoint	Incidence, % (No.)			AUC (95% CI)			Sensitivity at Top 5% Threshold (95% CI)		
		Medicare	Utah	Oregon	Medicare	Utah	Oregon	Medicare	Utah	Oregon
In-hospital	Mortality	2.8 (259,144)	1.2 (634)	0.8 (170)	0.82 (0.82–0.82)	0.89 (0.88–0.90)	0.90 (0.88–0.93)	30.1 (29.9–30.3)	44.1 (40.2–48.0)	56.5 (49.0–64.0)
	Discharge to facility	35.9 (3,308,992)	N/A	N/A	0.79 (0.79–0.79)	N/A	N/A	12.2 (12.2–12.2)	N/A	N/A
90 days after admission	Pneumonia	3.9 (363,078)	2.6 (1,427)	0.7 (143)	0.72 (0.72–0.72)	0.83 (0.82–0.84)	0.83 (0.80–0.87)	18.5 (18.4–18.6)	30.1 (27.7–32.5)	46.9 (38.7–55.1)
	Acute kidney injury	5.5 (503,672)	5.8 (3,217)	1.6 (335)	0.73 (0.73–0.73)	0.80 (0.80–0.81)	0.85 (0.84–0.87)	16.3 (16.2–16.4)	20.1 (18.7–21.5)	34.0 (28.9–39.1)
	Sepsis	5.8 (534,402)	3.2 (1,786)	1.6 (333)	0.73 (0.73–0.73)	0.81 (0.80–0.82)	0.85 (0.83–0.87)	18.7 (18.6–18.8)	27.9 (25.8–30.0)	36.6 (31.4–41.8)
	Major cardiovascular com- plication	6.0 (551,203)	2.9 (1,591)	1.4 (300)	0.79 (0.79–0.79)	0.83 (0.82–0.84)	0.86 (0.85–0.88)	24.1 (24.0–24.2)	30.2 (27.9–32.5)	41.3 (35.7–46.9)
	Respiratory failure	6.3 (582,587)	4.4 (2,447)	1.7 (360)	0.73 (0.73–0.73)	0.81 (0.80–0.82)	0.84 (0.82–0.86)	20.0 (19.9–20.1)	26.7 (24.9–28.5)	36.4 (31.4–41.4)
	Unplanned admission	28.0 (2,578,303)	10.8 (5,931)	9.7 (2,051)	0.70 (0.70–0.70)	0.71 (0.70–0.72)	0.78 (0.77–0.79)	11.6 (11.6–11.6)	16.8 (15.8–17.8)	19.9 (18.2–21.6)
	Including discharge to facility	11.8 (3,5–20.1)	N/A	N/A	0.75 (0.72–0.78)	N/A	N/A	18.9 (15.0,22.9)	N/A	N/A
	Excluding discharge to facility	8.3 (1.8–14.8)	4.4 (2.1–6.8)	2.5 (0.1–4.9)	0.75 (0.71–0.78)	0.81 (0.77–0.85)	0.84 (0.82–0.87)	19.9 (15.4–24.3)	28.0 (21.5–34.5)	36.8 (30.4–47.2)
	Overall mean (95% CI)									

Metrics include endpoint, observation window (either in-hospital or within 90 days after admission), incidence, area under the receiver operating characteristics curve (AUC), and sensitivity. Endpoints include acute kidney injury, sepsis, respiratory failure, unplanned hospitalization, discharge to facility status, major cardiovascular event, mortality, and pneumonia. Endpoints in the table are ordered by increasing incidence within their corresponding event period (*i.e.*, in-hospital or 90 days after admission). AUC, area under the receiver operating characteristics curve. N/A, not available.

Table 3. Calibration Performance of Risk Stratification Models on Out-of-sample Medicare and State Admissions

Period	Endpoint	Calibration Metrics* R^2			Calibration Estimates (Intercept/Slope)		
		Medicare	Utah	Oregon	Medicare	Utah	Oregon
In-hospital	Mortality	1.00	0.93	0.87	0.00/0.94	−0.01/0.90	0.00/0.92
90 days after admission	Discharge to facility	1.00	N/A	N/A	0.00/1.00	N/A	N/A
	Pneumonia	1.00	0.97	0.86	0.00/0.89	−0.02/2.28	−0.01/0.84
	Acute kidney injury	0.99	0.84	0.91	0.01/0.87	0.03/1.64	−0.01/0.89
	Sepsis	1.00	0.95	0.71	0.01/0.92	−0.01/1.75	−0.01/0.90
	Major cardiovascular complication	1.00	0.95	0.85	0.01/0.93	−0.01/1.75	0.00/1.23
	Respiratory failure	1.00	0.93	0.86	0.01/0.90	−0.02/2.11	−0.01/0.77
Overall mean (95% CI)	Unplanned admission	1.00	0.95	0.87	0.00/0.98	−0.05/1.16	−0.04/1.02
	Including discharge to facility	1.00 (1.00 to 1.00)	N/A	N/A	0.01 (0.00 to 0.01)/ 0.93 (0.90 to 0.96)	N/A	N/A
	Excluding discharge to facility	1.00 (1.00 to 1.00)	0.93 (0.90 to 0.96)	0.85 (0.80 to 0.89)	0.01 (0.00 to 0.01)/ 0.92 (0.89 to 0.95)	−0.01 (−0.03 to 0.00)/ 1.66 (1.29 to 2.02)	−0.01 (−0.02 to 0.00)/ 0.94 (0.83 to 1.05)

Statistics are calculated using observations per percent risk of adverse event. Metrics include endpoint, observation window (either in-hospital or within 90 days after admission), R^2 goodness-of-fit, estimates of intercept and slope of best fit regression line. Endpoints include acute kidney injury, sepsis, respiratory failure, unplanned hospitalization, discharge to facility status, major cardiovascular event, mortality, and pneumonia. Endpoints in the table are ordered by increasing incidence within their corresponding event period (*i.e.*, in-hospital or 90 days after admission).

*Calibration metrics: R^2 goodness-of-fit between observed and expected incidences among subpopulations using bins of 0.01 resolution of predicted risk, excluding the top 1% of subjects with highest risk. Slope and intercept: estimates of the regression line coefficients (*i.e.*, best fit line between actual and expected observations).

unexplained near absence of certain codes (such as for dialysis) in the Utah state database. The absence of codes used to identify endpoints impacts their apparent incidence (*e.g.*, missing dialysis codes associated with chronic kidney disease are unavailable to exclude false detection of acute kidney injury, resulting in the inflation of the apparent incidence of acute kidney injury). This inflation in turn degrades the “actual”-to-expected performance in those datasets. Taking the example of acute kidney injury in the Utah dataset, the apparent incidence is inflated to nearly twice that observed in a similar Utah population in the Medicare database (results not shown). Consequently, the calibration plot demonstrates that the rank ordering of the prediction is tightly preserved as desired, although the slope of the calibration curve markedly differs from unity. Although database limitations might make these state registries unsuitable for developing reliable new predictive models, they nonetheless provided a rigorous external validation test set.

Our overall calibration results met our prespecified acceptance criteria; however, additional refinements in the calibration of some models may be considered to optimize performance in datasets comprised of populations with observed event rates different than those in the development Medicare set. Our results indicate that our models work reasonably well even with the sort of imperfect datasets that might be encountered with clinical implementation.

A limitation of our analysis is that we were unable to evaluate our models for discharge destination, excess length

of stay, and 90-day mortality because requisite data were not included in the state registries. While we present model validations applicable to broad U.S. adult populations, we did not include children. Children differ substantially from adults in rarely having serious chronic conditions. Furthermore, they are hospitalized for different reasons. Our models should therefore be properly validated in pediatric patients and refined as necessary for this special population. Future research will be needed to document applicability to other sources of diagnostic and procedural histories, such as electronic medical records, registries, health information exchanges, or institutional data warehouses. The potential impact of COVID-19 and associated disruptions in health-care delivery on model performance must also be assessed in future research. International Classification of Disease coding in the United States is generally reliable since it is guided by well-enforced federal regulations. Less rigorous application would degrade Risk Stratification Index 3.0 predictions.

Our model validation consisted of prospectively testing previously developed models on two out-of-sample state datasets and shows that predictions exceeded our prespecified minimum acceptable performance standards. We did not employ either a “non-inferiority” or a “superiority” design because our goal was to determine whether the models can be applied successfully to other populations—especially younger and healthier patients who better represent typical U.S. hospitalized patients. Our results indicate

that they can. Although this work externally validates the models, it is currently not clear if the application of the models will be feasible across all settings in real time or, if applied, improves either efficiency or patient outcomes. We are currently testing deployment of these models for a number of clinical applications to address these open questions.

Fortunately, there are current and impending ways to electronically acquire a patient's billing record to help near real-time implementation of the models. A number of recent rulings have driven development and adoption of tools that enable and access to claims data (<https://www.federalregister.gov/documents/2020/05/01/2020-05050/medicare-and-medicaid-programs-patient-protection-and-affordable-care-act-interoperability>). Existing application programming interfaces enable payer-to-patient access (e.g., Blue Button technology [<https://bluebutton.cms.gov/>]), payer-to-provider access (e.g., Beneficiary Claims Data application programming interfaces for accountable care organization access [<https://bcda.cms.gov/>]; Data at the Point of Care or Physician access [<https://dpc.cms.gov>, in pilot stage]), and provider-to-provider access (e.g., Epic's Care Everywhere [<https://www.epic.com/interoperability/ehr-interoperability-from-anywhere>]). These application programming interfaces and the electronic health records of the local institution (for the current medical history) allow users to access or construct the claims stream for our predictors and clinical support software. We anticipate that these policies will help drive access to claims data from multiple additional payer organizations and facilitate more widespread practical access to the predictive models based on administrative claims.

As an example, the models described in this manuscript are undergoing field testing at several major institutions, including the Cleveland Clinic (Cleveland, Ohio). While code latency could theoretically lead to underprediction of risk, real-time implementation of the models permits code feeds from multiple sources such as the Beneficiary Claims Data application programming interfaces (<https://bcda.cms.gov/>), which are updated weekly, or directly from local EPIC sources, which can update faster. Future research is needed to define whether using Risk Stratification Index 3.0 predictive modeling at admission improves clinical efficiency and patient outcomes.

In summary, we demonstrate that a suite of predictive Risk Stratification Index 3.0 models developed using a very large population of Medicare fee-for-service beneficiaries, mostly older than 65 yr, also performs well when applied prospectively to two large out-of-sample state datasets that include younger and healthier subjects.

Acknowledgments

The authors thank Thomas DeRito, B.S. (Health Data Analytics Institute, Dedham, Massachusetts), for technical assistance in querying the state databases and conducting certain statistics.

Research Support

Funded by the Health Data Analytics Institute (Dedham, Massachusetts).

Competing Interests

G. F. Chamoun, N. G. Chamoun, D. Clain, Z. Hong, and Drs. Greenwald, Manberg, and Jordan are employees of the Health Data Analytics Institute (Dedham, Massachusetts). Dr. Sessler is a consultant and shareholder in the company. Dr. Maheshwari declares no competing interests.

Correspondence

Address correspondence to Dr. Sessler: Department of Outcomes Research, Anesthesiology Institute, Cleveland Clinic, 9500 Euclid Ave — L1-407, Cleveland, Ohio 44195. DS@OR.org. This article may be accessed for personal use at no charge through the Journal Web site, www.anesthesiology.org.

Supplemental Digital Content

Supplemental Digital Content, <http://links.lww.com/ALN/C1000>

Supplemental Figure 1. Performance characteristics: in-hospital mortality.

Supplemental Figure 2. Performance characteristics: 90-day pneumonia.

Supplemental Figure 3. Performance characteristics: 90-day acute kidney injury.

Supplemental Figure 4. Performance characteristics: 90-day sepsis.

Supplemental Figure 5. Performance characteristics: 90-day cardiovascular complications.

Supplemental Figure 6. Performance characteristics: 90-day respiratory failure.

Supplemental Figure 7. Performance characteristics: 90-day unplanned admission.

Supplemental Table 1. Calibration Performance of Risk Stratification Models on Out-of-sample Medicare and State Admissions (Risk Decile Groups).

References

1. Greenwald S, Chamoun GF, Chamoun NG, Clain D, Hong Z, Jordan R, Manberg PJ, Maheshwari K, Sessler DI: Risk Stratification Index 3.0, a broad set of models for predicting adverse events during and after hospital admission. *ANESTHESIOLOGY* 2022; 137:673–86
2. Sessler DI, Sigl JC, Manberg PJ, Kelley SD, Schubert A, Chamoun NG: Broadly applicable risk stratification system for predicting duration of hospitalization and mortality. *ANESTHESIOLOGY* 2010; 113:1026–37

3. Chamoun GF, Li L, Chamoun NG, Saini V, Sessler DI: Validation and calibration of the Risk Stratification Index. *ANESTHESIOLOGY* 2017; 126:623–30
4. Agency for Healthcare Research and Quality. All-Payer Claims Databases. Available at <https://www.ahrq.gov/data/apcd/index.html>. Accessed June 1, 2022.
5. Collins GS, Reitsma JB, Altman DG, Moons KG: Transparent Reporting of a multivariable prediction model for Individual Prognosis or Diagnosis (TRIPOD): The TRIPOD statement. *Ann Intern Med* 2015; 162:55–63
6. Centers for Medicare & Medicaid Services. International Classification of Diseases, Tenth Revision. Available at <https://www.cms.gov/medicare/coding/icd10>. Accessed February 28, 2021.
7. Agency for Healthcare Research and Quality. Clinical Classification Software Refined (CCSR). Available at https://www.hcup-us.ahrq.gov/toolssoftware/ccsr/ccs_refined.jsp. Accessed August 21, 2021.
8. Agency for Healthcare Research and Quality. Clinical Classification Software ICD-10-PCS (beta version). Available at <https://www.hcup-us.ahrq.gov/toolssoftware/ccs10/ccs10.jsp>. Accessed August 21, 2021.
9. Van der Paal B: A Comparison of Different Methods for Modelling Rare Events Data, Department of Applied Mathematics, Computer Science and Statistics. Ghent, University of Ghent, 2014, pp 70
10. Centers for Disease Control and Prevention. ICD-10-CM Official Coding and Reporting Guidelines April 1, 2020 through September 30, 2020. Available at <https://www.cdc.gov/nchs/data/icd/COVID-19-guidelines-final.pdf>. Accessed February 16, 2021.
11. Bellini V, Valente M, Bertorelli G, Pifferi B, Craca M, Mordonini M, Lombardo G, Bottani E, Del Rio P, Bignami E: Machine learning in perioperative medicine: A systematic review. *J Anesth Analg Crit Care* 2022; 2:2
12. Bardach N LG, Wade E, Dean M, Shultz E, McDonald K, Dudley RA: Final Report: All-Payer Claims Databases Measurement of Care: Systematic Review and Environmental Scan of Current Practices and Evidence (report AHRQ publication No. 17-0022-2-EF). Available at <https://www.ahrq.gov/sites/default/files/publications/files/envscanlitrev.pdf>. Accessed June 1, 2022.

ANESTHESIOLOGY

Performance of Noninvasive Airway Occlusion Maneuvers to Assess Lung Stress and Diaphragm Effort in Mechanically Ventilated Critically Ill Patients

Heder J. de Vries, M.D., Pieter R. Tuinman, M.D., Ph.D., Annemijn H. Jonkman, Ph.D., Ling Liu, M.D., Ph.D., Haibo Qiu, M.D., Ph.D., Armand R. J. Girbes, M.D., Ph.D., YingRui Zhang, M.D., Angelique M. E. de Man, M.D., Ph.D., Harm-Jan de Grooth, M.D., Ph.D., Leo Heunks, M.D., Ph.D.

ANESTHESIOLOGY 2023; 138:274–88

EDITOR'S PERSPECTIVE

What We Already Know about This Topic

- Recent research suggests that optimization of diaphragmatic effort and avoidance of excessive lung stress may facilitate liberation from mechanical ventilation in critically ill patients
- Low diaphragmatic effort has been associated with rapid development of disuse atrophy, and excessive effort may result in muscle injury, increased lung stress, and pendelluft (displaced ventilation from recruited to nonrecruited lung regions)
- Monitoring transdiaphragmatic and transpulmonary pressures may facilitate accurate assessment of diaphragmatic effort and lung stress, respectively, but requires esophageal and gastric manometry, an overly complex process for routine clinical practice

What This Article Tells Us That Is New

- A secondary analysis of two previous studies evaluated the ability of two transient inspiratory airway occlusion maneuvers (Pocc, the total drop in airway pressure during an occlusion, and P0.1, the drop in the

ABSTRACT

Background: Monitoring and controlling lung stress and diaphragm effort has been hypothesized to limit lung injury and diaphragm injury. The occluded inspiratory airway pressure (Pocc) and the airway occlusion pressure at 100 ms (P0.1) have been used as noninvasive methods to assess lung stress and respiratory muscle effort, but comparative performance of these measures and their correlation to diaphragm effort is unknown. The authors hypothesized that Pocc and P0.1 correlate with diaphragm effort and lung stress and would have strong discriminative performance in identifying extremes of lung stress and diaphragm effort.

Methods: Change in transdiaphragmatic pressure and transpulmonary pressure was obtained with double-balloon nasogastric catheters in critically ill patients (n = 38). Pocc and P0.1 were measured every 1 to 3 h. Correlations between Pocc and P0.1 with change in transdiaphragmatic pressure and transpulmonary pressure were computed from patients from the first cohort. Accuracy of Pocc and P0.1 to identify patients with extremes of lung stress (change in transpulmonary pressure > 20 cm H₂O) and diaphragm effort (change in transdiaphragmatic pressure < 3 cm H₂O and >12 cm H₂O) in the preceding hour was assessed with area under receiver operating characteristic curves. Cutoffs were validated in patients from the second cohort (n = 13).

Results: Pocc and P0.1 correlate with change in transpulmonary pressure ($R^2 = 0.62$ and 0.51 , respectively) and change in transdiaphragmatic pressure ($R^2 = 0.53$ and 0.22 , respectively). Area under receiver operating characteristic curves to detect high lung stress is 0.90 (0.86 to 0.94) for Pocc and 0.88 (0.84 to 0.92) for P0.1. Area under receiver operating characteristic curves to detect low diaphragm effort is 0.97 (0.87 to 1.00) for Pocc and 0.93 (0.81 to 0.99) for P0.1. Area under receiver operating characteristic curves to detect high diaphragm effort is 0.86 (0.81 to 0.91) for Pocc and 0.73 (0.66 to 0.79) for P0.1. Performance was similar in the external dataset.

Conclusions: Pocc and P0.1 correlate with lung stress and diaphragm effort in the preceding hour. Diagnostic performance of Pocc and P0.1 to detect extremes in these parameters is reasonable to excellent. Pocc is more accurate in detecting high diaphragm effort.

(*ANESTHESIOLOGY* 2023; 138:274–88)

first 100 ms) obtained from the mechanical ventilator to predict either diaphragm effort or lung stress

- Neither P0.1 nor Pocc should be used to predict exact values for diaphragm effort or lung distending pressure
- However, both maneuvers can reliably identify patients with low or high extremes in diaphragm effort and lung stress, where Pocc outperforms P0.1 based on the areas under the receiver operating characteristic curves

This article is featured in "This Month in Anesthesiology," page A1. This article is accompanied by an editorial on p. 235. This article has a related Infographic on p. A17. Supplemental Digital Content is available for this article. Direct URL citations appear in the printed text and are available in both the HTML and PDF versions of this article. Links to the digital files are provided in the HTML text of this article on the Journal's Web site (www.anesthesiology.org). This article has an audio podcast. This article has a visual abstract available in the online version. Part of the data in this article was presented as an abstract for the Pleural Pressure Working Group meeting (PLUG; October 2021, online).

Submitted for publication May 16, 2022. Accepted for publication November 26, 2022. Published online first on December 15, 2022.

Heder J. de Vries, M.D.: Department of Intensive Care Medicine, Amsterdam UMC, location VUmc, Amsterdam, The Netherlands; Amsterdam Cardiovascular Sciences Research Institute, Amsterdam UMC, Amsterdam, The Netherlands.

Copyright © 2023, the American Society of Anesthesiologists. All Rights Reserved. *Anesthesiology* 2023; 138:274–88. DOI: 10.1097/ALN.0000000000004467

Implementation of lung-protective ventilation with low tidal volumes has improved outcomes of critically ill patients,^{1,2} likely by limiting lung stress and strain caused by excessive regional volume expansion and distending (driving) pressures of the alveoli.^{3,4} It has been proposed that monitoring and controlling diaphragm effort in addition to lung stress may further benefit ventilated patients.^{5,6} The rationale is that absence of diaphragm effort during mechanical ventilation rapidly leads to disuse atrophy and weakness,^{7,8} which can be ameliorated by keeping the diaphragm active.^{9,10} Preventing high effort may limit diaphragm injury and fatigue¹¹ and reduce sources of lung stress such as lung edema and pendelluft.^{12,13}

The reference methods to assess lung stress and diaphragm effort are esophageal and gastric manometry to calculate the transpulmonary pressure and transdiaphragmatic pressure,^{14–16} which is seldom used in clinical practice due to invasiveness and complexity.¹ Two measurements based on airway occlusion maneuvers have recently been evaluated as proposed noninvasive estimates for lung stress and respiratory muscle effort. The occluded inspiratory airway pressure (Pocc), also known as the expiratory occlusion pressure, is the drop in airway pressure during an inspiration against an occluded airway. Pocc correlates with total respiratory muscle pressure and lung stress, albeit with wide limits of agreement.^{17,18} The drop in airway pressure in the

first 100 ms of an occluded inspiration (P0.1) has recently been compared with respiratory effort as well.¹⁹ Despite the moderate correlations, the parameters were proposed to be useful in identifying patients with extremes of respiratory muscle effort.

However, several questions remain regarding the validity of Pocc and P0.1. First, the relation of Pocc and P0.1 to diaphragm effort is unknown. Second, performance of P0.1 to detect potentially injurious lung stress has not been reported. Third, the correlation of Pocc and P0.1 with mechanical power, an advanced parameter for lung stress, is unknown. Finally, the performance of Pocc and P0.1 have not been compared with each other in the same cohorts.

Therefore, our aim was to validate and compare Pocc and P0.1 as measurements for lung stress and diaphragm effort in invasively ventilated critically ill patients. We hypothesized that Pocc and P0.1 correlate with lung stress and diaphragm effort, and that both parameters would have good diagnostic performance in identifying patients with extremes of lung stress and diaphragm effort.

Materials and Methods

Study Design

This diagnostic study is a secondary analysis on data from two clinical trials: a randomized controlled trial conducted in The Netherlands (NCT 03527797)²⁰ and a physiologic trial conducted in China (NCT 01663480).²¹ This analysis was not registered *a priori*. The article is reported according to the STARD guidelines.²²

Patients

The primary cohort was recruited at the mixed medical-surgical intensive care unit (ICU) of a tertiary university hospital (Amsterdam UMC, location VUmc, Amsterdam, The Netherlands), and consisted of patients ($n = 39$) with acute respiratory failure ventilated with a spontaneous mode of mechanical ventilation (either pressure support or neurally adjusted ventilatory assist) with an expected duration of ventilation of at least 48 h.²⁰ The external validation cohort was recruited at another academic hospital (South East University, Nanjing, China) and consisted of patients ($n = 13$) ventilated in neurally adjusted ventilatory assist mode at different neurally adjusted ventilatory assist levels.²¹ Both cohorts were convenience samples.

Procedures and Signal Analysis

In the primary cohort flow, volume (time-integral of flow), airway opening pressure, esophageal pressure, gastric pressure, transdiaphragmatic pressure (gastric pressure minus esophageal pressure), and transpulmonary pressure (airway opening pressure minus esophageal pressure) were recorded continuously for 24 h with a flow sensor and a double-balloon nasogastric catheter (Nutrivent, Sidam,

Pieter R. Tuinman, M.D., Ph.D.: Department of Intensive Care Medicine, Amsterdam UMC, location VUmc, Amsterdam, The Netherlands; Amsterdam Cardiovascular Sciences Research Institute, Amsterdam UMC, Amsterdam, The Netherlands.

Annemijn H. Jonkman, Ph.D.: Department of Intensive Care Medicine, Amsterdam UMC, location VUmc, Amsterdam, The Netherlands; Amsterdam Cardiovascular Sciences Research Institute, Amsterdam UMC, Amsterdam, The Netherlands; Department of Intensive Care Medicine, Erasmus University Medical Center, Rotterdam, The Netherlands.

Ling Liu, M.D. Ph.D.: Jiangsu Provincial Key Laboratory of Critical Care Medicine, Department of Critical Care Medicine, Zhongda Hospital, School of Medicine, Southeast University, Nanjing, China.

Haibo Qiu, M.D. Ph.D.: Jiangsu Provincial Key Laboratory of Critical Care Medicine, Department of Critical Care Medicine, Zhongda Hospital, School of Medicine, Southeast University, Nanjing, China.

Armand R. J. Girbes, M.D., Ph.D.: Department of Intensive Care Medicine, Amsterdam UMC, location VUmc, Amsterdam, The Netherlands.

YingRui Zhang, M.D.: Department of Critical Care Medicine, Fujian Provincial Hospital, Fujian Provincial Center for Critical Care Medicine, Fujian Medical University, Fuzhou, Fujian, China.

Angelique M. E. de Man, M.D., Ph.D.: Department of Intensive Care Medicine, Amsterdam UMC, location VUmc, Amsterdam, The Netherlands.; Amsterdam Cardiovascular Sciences Research Institute, Amsterdam UMC, Amsterdam, The Netherlands.

Harm-Jan de Grooth, M.D., Ph.D.: Department of Intensive Care Medicine, Amsterdam UMC, location VUmc, Amsterdam, The Netherlands; Amsterdam Cardiovascular Sciences Research Institute, Amsterdam UMC, Amsterdam, The Netherlands.

Leo Heunks, M.D., Ph.D.: Department of Intensive Care Medicine, Amsterdam UMC, location VUmc, Amsterdam, The Netherlands; Amsterdam Cardiovascular Sciences Research Institute, Amsterdam UMC, Amsterdam, The Netherlands; Department of Intensive Care Medicine, Erasmus University Medical Center, Rotterdam, The Netherlands.

Italy) connected to a dedicated signal acquisition system (MP160, BIOPAC Systems Inc, USA) as described previously.²³ Airway occlusions lasting 2 to 3 s were performed at baseline and were repeated every 1 to 3 h (fig. 1) to assess correct positioning and filling of the esophageal balloons and to calculate Pocc and P0.1. End-inspiratory occlusions lasting 2 to 3 s were performed at baseline and were repeated every 4 to 6 h to calculate the elastance of the chest wall and lungs in semistatic conditions. Patients in the external validation cohort had a nasogastric catheter (NeuroVent Research, Toronto, Canada) to record esophageal, gastric, transdiaphragmatic, and transpulmonary pressure and the electrical activity of the diaphragm. The patients received multiple expiratory occlusions at baseline, after which the neurally adjusted ventilatory assist level (*i.e.*, cm H₂O of inspiratory support above positive end-expiratory pressure per microvolt of electrical activity of the diaphragm) was increased gradually to induce a wide range of diaphragm effort in the subjects. Airway occlusion maneuvers lasting 2 to 3 s were repeated at each neurally adjusted ventilatory assist level.²¹ All recordings with airway occlusion maneuvers with a ratio of the change in airway opening pressure-to-change in esophageal pressure less than 0.8 or more than 1.2 were discarded because the esophageal pressure-based measurements were deemed unreliable due to inadequate balloon filling or positioning.^{14,24} In this article, the term “diaphragm effort” refers to diaphragm pressure output (transdiaphragmatic pressure), and respiratory drive to the intensity of respiratory center output to the diaphragm.

Signal Analyses

Signal analyses for the current study were performed with a custom software (Matlab 2021a, MathWorks, USA) as described previously,²⁰ and are shown in figure 1 and figure E1 (<http://links.lww.com/ALN/C991>). Comprehensive description of the signal analysis including calculation of mechanical power is available in the Supplemental Digital Content (<http://links.lww.com/ALN/C989>). In this study, we have adopted the term “occluded inspiratory airway pressure” for Pocc instead of “expiratory occlusion pressure” to reflect that the measurement is obtained during inspiration.

Statistical Analysis

Descriptive statistics are expressed as mean \pm SD, median [interquartile range], or count (percentages), as appropriate. The reference parameters were averaged per hour before each occlusion in each subject. Normality of distributions was assessed visually on normal-probability plots. Log transformations were used to transform distributions to normal if required. Sample size calculations were not performed. Biologic variability of change in transdiaphragmatic pressure, change in total respiratory muscle pressure, and the

ratio of the two was estimated by calculating the coefficient of variation (SD/mean) of the respective parameters in each hour of the recordings, averaged for each subject.

The steps shown in figure 2 were taken consecutively to assess the diagnostic accuracy of Pocc and P0.1 to assess lung stress and diaphragm effort. First, the conversion factors to estimate change in transpulmonary pressure, transpulmonary mechanical power, and change in transdiaphragmatic pressure from Pocc and P0.1 were obtained with internal bootstrap procedures as described previously in the primary cohort.¹⁷ The bootstrap procedure randomly selected half of the patients in each loop, after which repeated-measures mixed models were used to obtain the optimal coefficient to convert Pocc and P0.1 into the reference parameters (change in transpulmonary pressure, transpulmonary mechanical power, or change in transdiaphragmatic pressure). The mean coefficient factor after 1,000 loops was selected as the final conversion factor for each respective measure; the CI is reported to show variability of this factor in the different loops of the bootstrap.

Next, correlations between the observed and predicted lung stress and diaphragm effort (based on Pocc and P0.1) were calculated using the obtained conversion factors and were compared with the reference standards with the methods of Bland and Altman in the primary cohort.²⁵ Within-subject limits of agreement were calculated with repeated-measure mixed models as described previously.¹⁷ The within-subject explained variance (R^2) was calculated with the methods described by Nakagawa and Schielzeth.²⁶ Correlations with R^2 less than 0.30 were defined as poor, 0.31 to 0.50 as moderate, 0.51 to 0.80 as fair, 0.81 to 0.90 as strong, and greater than 0.90 as very strong.

Additionally, the discriminative power of Pocc and P0.1 to detect extremes of lung stress and diaphragm effort were calculated using standard formulas and by constructing the receiver operating characteristic curves in the primary and external cohort.²⁷ The limits for high lung stress were set at change in transpulmonary pressure > 20 cm H₂O^{5,14} and transpulmonary mechanical power > 12 J/min²⁸ based on recent consensus statements. The limits for low and high diaphragm effort were set at less than 3 cm H₂O and greater than 12 cm H₂O, respectively, also based on consensus statements.^{5,6,20} Because no interventional studies have shown that these limits are not injurious in critically ill patients as of yet, additional limits for potentially injurious lung stress and diaphragm effort were analyzed as well (table E1, <http://links.lww.com/ALN/C990>). Areas under the receiver operating characteristic curves between 0.5 and 0.7 were defined as poor, between 0.7 and 0.8 as acceptable, between 0.8 and 0.9 as excellent, and 0.9 or more as outstanding discrimination.²⁹ The cutoffs with the highest Youden J -statistic (sensitivity + specificity – 1) were selected from the ROC curves.³⁰ The CI of the areas under the receiver operating characteristic curves was constructed with the standard error of the Wilcoxon statistic as described previously.³¹

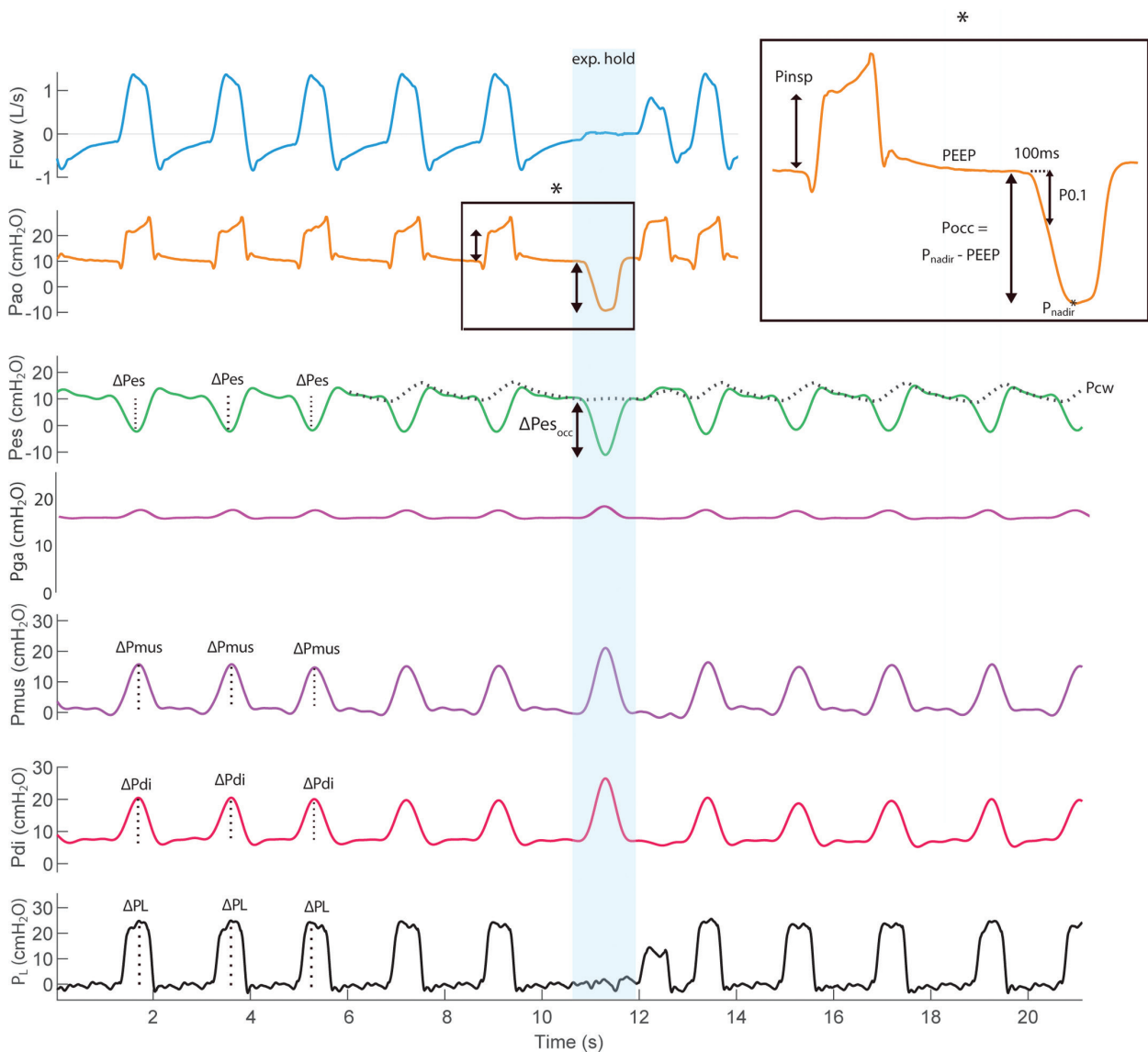


Fig. 1. Line graphs showing flow, airway pressure (Paw), esophageal pressure (Pes) with superimposed chest wall recoil pressure (Pcw), gastric pressure (Pga), total respiratory muscle pressure (Pmus, calculated as $P_{cw} - P_{es}$), transdiaphragmatic pressure (Pdi, calculated as $P_{ga} - P_{es}$) and transpulmonary pressure (P_L , calculated as $P_{aw} - P_{es}$) over time. ΔP_{mus} , ΔP_{di} , and ΔP_L were calculated as the maximal absolute difference in the respective pressure tracings per breath (dotted vertical lines). An expiratory occlusion was administered in the shaded area. The inset shows a zoomed-in portion of airway pressure during the expiratory occlusion and the preceding breath: P_{occ} was calculated as the total drop in airway pressure during the occlusion, whereas the airway occlusion pressure at 100 ms ($P_{0.1}$) was calculated as the drop in the first 100 ms of the occlusion. The inspiratory support provided by the ventilator (P_{insp}) was measured as the plateau airway pressure shortly after inspiratory triggering and pressurization by the ventilator. Pao, airway opening pressure; PEEP, positive end-expiratory pressure; P_{nadir} , the lowest point of the inspiratory effort of the patient.

Next, the overall diagnostic accuracy of P_{occ} and $P_{0.1}$ to identify patients with extremes in lung stress and diaphragm effort was calculated as the proportion of cases that were correctly identified by these cutoffs (i.e., [true positives + true negatives]/all cases) in the primary cohort and in the external validation cohort. Accuracy of different tests was compared with the “N-1” chi-square test.³²

A two-tailed significance level of 5% was used for all statistical analyses. All the statistical analyses were performed in R version 4.0.1 (R Foundation for Statistical Programming, Vienna, Austria). Additional details are available in the Supplemental Digital Content (<http://links.lww.com/ALN/C989>) and figure E2 (<http://links.lww.com/ALN/C992>).

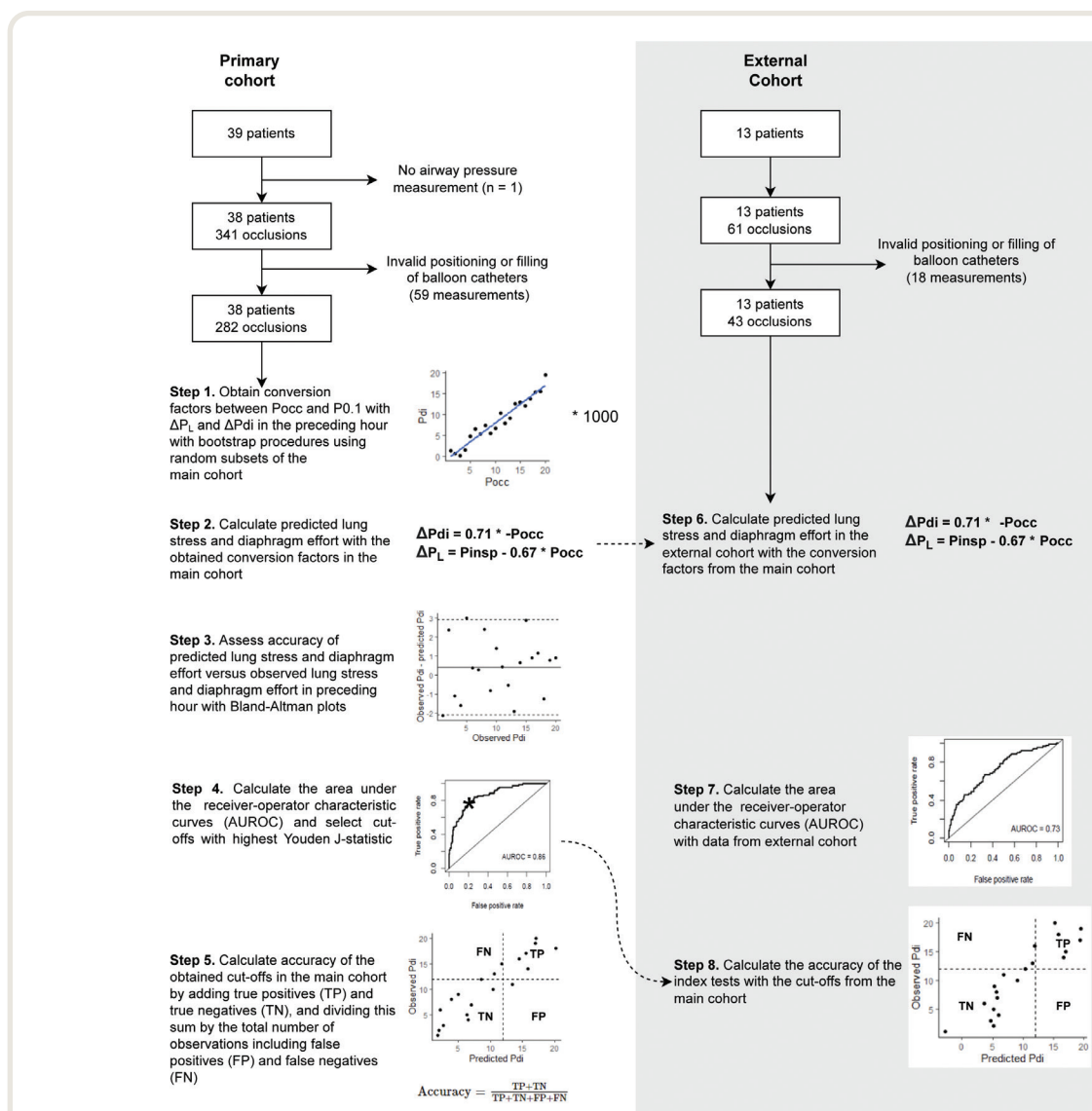


Fig. 2. Diagram of study flow. Occlusion measurements were excluded from analysis if the change in esophageal pressure during the occlusion differed more than 20% from the change in airway pressure because the reference parameters in the preceding hour were deemed unreliable in this case (invalid Baydur maneuver). Data in the *inset graphs* are simulated for illustrative purposes. The conversion factors and cutoffs found in the primary cohort were used in the external cohort to assess external validity. P_{di}, transdiaphragmatic pressure; P_{insp}, inspiratory support provided by the ventilator; P_L, transpulmonary pressure; P_{occ}, occluded inspiratory airway pressure; P_{0.1}, airway occlusion pressure at 100 ms; ΔP_{di} , change in transdiaphragmatic pressure; ΔP_L , change in transpulmonary pressure.

Results

Patient characteristics are summarized in table 1, and patient flow is shown in figure 2. In total, 840,817 breaths obtained in 38 patients during a 24-h period were analyzed from the primary cohort, including 341 occluded inspiration maneuvers from which 282 met the criteria for adequate filling and positioning of the esophageal and gastric balloon that were used for further analysis. Number of recordings with low and high lung stress and diaphragm effort are shown in table 2. The average hourly within-subject coefficients of variation of change in esophageal pressure, transdiaphragmatic pressure,

and total respiratory muscle pressure were $32 \pm 5\%$, $33 \pm 6\%$, and $25 \pm 4\%$, respectively. The average ratio between change in transdiaphragmatic pressure and change in total respiratory muscle pressure was 0.93 ± 0.15 , with a within-subject breath-by-breath coefficient of variation of $48 \pm 12\%$.

Relation between Esophageal Pressure, Total Respiratory Muscle Pressure, and Diaphragm Effort in the Same Breath

Change in total respiratory muscle pressure and change in transdiaphragmatic pressure of individual breaths were

Table 1. Baseline Characteristics

Patient Characteristic	Primary Cohort (n = 38)	External Cohort (n = 13)
Age, yr	65 [51 to 75]	60 [57 to 73]
Sex = female, n (%)	13 (33)	10 (83)
Cause of respiratory failure, n (%)		
Pulmonary adult respiratory distress syndrome	21 (54)	10 (77)
Chronic obstructive pulmonary disease exacerbation	0	1 (8)
Nonpulmonary adult respiratory distress syndrome	14 (36)	0
Cardiogenic shock	3 (7)	2 (15)
Intracranial disease	1 (3)	0
APACHE IV score	85 ± 28	—
Pao ₂ /Fio ₂ ratio at baseline, mmHg	190 ± 54	—
Ventilator settings		
Pressure support, n (%)	37 (95)	0 (0)
Neurally adjusted ventilatory assist, n (%)	2 (5)	13 (100)
Positive end-expiratory pressure, cm H ₂ O	10 [8 to 12]	8 [6 to 10]
Inspiratory support, cm H ₂ O	9 [7 to 15]	12 [10 to 17]
Richmond Agitation and Sedation Scale score	−1 [−3 to 0]	—
Respiratory mechanics		
Tidal volume, ml/kg predicted body weight	7.5 ± 1.8	6.7 ± 1.8
Change in transpulmonary pressure, cm H ₂ O	21 [16 to 25]	17 [10 to 21]
Breathing effort		
Respiratory rate, breaths/min	25 ± 7	23 ± 7
Change in transdiaphragmatic pressure, cm H ₂ O/breath	11 [7 to 14]	7 [5 to 10]
Transdiaphragmatic pressure-time product, cm H ₂ O × s/min	155 [114 to 224]	136 [75 to 180]
Total respiratory muscle pressure during inspiration, cm H ₂ O/breath	12 [9 to 15]	8 [4 to 10]
Total respiratory muscle pressure-time product during inspiration, cm H ₂ O × s/min	205 [168 to 241]	186 [102 to 214]
Occluded inspiratory airway pressure, cm H ₂ O	−15 [−19 to −12]	−11 [−15 to −6]
Airway occlusion pressure at 100 ms, cm H ₂ O	2.4 [1.7 to 3.5]	1.7 [1.2 to 2.4]

Parameters are reported as mean ± SD when distribution was normal in both cohorts, and with median [interquartile range] if distribution was nonparametric in either or both cohorts. Risk scores, oxygenation, and sedation scores were not available in the external cohort. Fio₂, fraction of inspired oxygen.

strongly correlated (change in transdiaphragmatic pressure = $0.85 \times$ change in total respiratory muscle pressure, $R^2 = 0.87$, $P < 0.001$; fig. E3, <http://links.lww.com/ALN/C993>). Converting change in total respiratory muscle pressure into change in transdiaphragmatic pressure with this formula resulted in a bias of less than 0.1 cm H₂O and 95% limits-of-agreement from −4.5 to 4.3 cm H₂O. Change in esophageal pressure and change in transdiaphragmatic pressure of individual breaths were very strongly correlated (change in transdiaphragmatic pressure = $1.08 \times$ change in esophageal pressure, $R^2 = 0.92$, $P < 0.001$; fig. E3, <http://links.lww.com/ALN/C993>). Converting change in esophageal pressure into change in transdiaphragmatic pressure with this formula resulted in a bias of 1.1 cm H₂O with 95% limits-of-agreement from −1.9 to 3.8 cm H₂O.

Relation between Esophageal and Diaphragm Effort in the Preceding Hour

Change in esophageal pressure correlated fairly with diaphragm effort (change in transdiaphragmatic pressure) in the preceding hour (average change in transdiaphragmatic pressure = $1.04 \times$ change in esophageal pressure, $R^2 = 0.79$, $P < 0.001$; fig. 3). Converting change in esophageal pressure into change in transdiaphragmatic pressure with this formula, bias was 0.4 cm H₂O and 95%

limits-of-agreement ranged from −3.5 to +3.7 cm H₂O. Averaging three consecutive change in esophageal pressure measurements improved the correlation slightly ($R^2 = 0.84$, $P < 0.001$; fig. E4, <http://links.lww.com/ALN/C994>). Diagnostic metrics to identify patients with extremes in lung stress and diaphragm effort are shown in table 2. Diagnostic metrics for additional parameters and cutoffs are reported in table E1 (<http://links.lww.com/ALN/C990>).

Relation between the Airway Occlusion Pressure and Lung Stress in the Preceding Hour

The mean conversion factor to predict change in transpulmonary pressure with Pocc was 0.67 (0.64 to 0.71). The predicted lung stress (change in transpulmonary pressure = inspiratory support provided by the ventilator − $0.67 \times$ Pocc) correlated fairly well with the observed lung stress in the preceding hour ($R^2 = 0.62$, $P < 0.001$; fig. 4). Bias was −1.6 cm H₂O. 95% limits-of-agreement ranged from −10.0 to +6.6 cm H₂O.

The conversion factor to predict transpulmonary mechanical power with Pocc was on average 0.93 (0.90 to 0.95). The predicted mechanical power (predicted transpulmonary mechanical power = $0.5 \times$ (inspiratory support − $0.93 \times$ Pocc) \times tidal volume [Vt] \times respiratory rate [RR] \times

Table 2. Diagnostic Performance of Occlusion Maneuvers

Parameter	No. of Observations (% of total)	Predictor	Area under the Receiver Operating Characteristic Curve (95% CI)	Cutoff	Accuracy, %	Sensitivity, %	Specificity, %	Positive Predictive Value, %	Negative Predictive Value, %
Low diaphragm effort, $\Delta P_{di} < 3 \text{ cm H}_2\text{O}$	9 in 4 patients (3%)	ΔP_{es}	0.97 (0.89–1.00)	4 cm H_2O	93	98	88	48	99
		Pocc	0.97 (0.87–1.00)	–7 cm H_2O	92	84	95	31	99
		P0.1	0.93 (0.81–0.99)	1.3 cm H_2O	89	83	89	17	99
High diaphragm effort, $\Delta P_{di} > 12 \text{ cm H}_2\text{O}$	88 in 27 patients (31%)	ΔP_{es}	0.91 (0.87–0.95)	10 cm H_2O	86	89	85	71	92
		Pocc	0.86 (0.81–0.91)	–15 cm H_2O	80	80	76	63	83
		P0.1	0.73 (0.66–0.79)	2.9 cm H_2O	71	57	72	58	72
High lung stress, $\Delta P_L > 20 \text{ cm H}_2\text{O}$	155 in 31 patients (55%)	$P_{insp} - 0.67 \times P_{occ}$	0.90 (0.86–0.94)	22 cm H_2O	85	90	77	86	83
		$P_{insp} + 3.3 \times P0.1$	0.88 (0.84–0.92)	21 cm H_2O	81	89	74	73	89
High power, $MP_L > 12 \text{ J/min}$	199 in 32 patients (71%)	$0.5 \times (P_{insp} - 0.93 \times P_{occ}) \times Vt \times RR \times 0.098$	0.89 (0.85–0.93)	12 J/min	84	63	92	89	56
		$0.5 \times (P_{insp} + 4.7 \times P0.1) \times RR \times Vt \times 0.098$	0.72 (0.66–0.78)	13 J/min	73	69	69	87	42

Total number of observations was 282. Note that no conversion is necessary when using the Pocc and P0.1 cutoffs for low and high diaphragm effort, but that conversion is required to assess lung stress and mechanical power. MP_L , transpulmonary mechanical power; P0.1, airway occlusion pressure at 100 ms; Pao, airway opening pressure; Pes, esophageal pressure; Pdi, transdiaphragmatic pressure; P_L , transpulmonary pressure, calculated as $Pao - Pes$; P_{insp} , inspiratory support provided by the ventilator; Pocc, occluded inspiratory airway pressure; RR, respiratory rate in breaths per minute; Vt, tidal volume in liters; ΔP_{di} , change in transdiaphragmatic pressure; ΔP_{es} , change in esophageal pressure; ΔP_L , change in transpulmonary pressure.

0.098, with Vt in liters) correlated moderately well with the observed mechanical power ($R^2 = 0.47$, $P < 0.001$; fig. 4); bias was 0.4 J/min, 95% limits-of-agreement ranged from –6.4 to 7.6 J/min.

Relation between the Airway Occlusion Pressure and Diaphragm Effort in the Preceding Hour

The conversion factor to predict change in transdiaphragmatic pressure with Pocc was on average 0.71 (0.65 to 0.76). The predicted diaphragm effort (change in transdiaphragmatic pressure = $0.71 \times -P_{occ}$) correlated fairly well with observed diaphragm effort ($R^2 = 0.53$, $P < 0.001$; fig. 4). Bias was 1.2 cm H_2O and 95% limits-of-agreement from –6.4 to +7.6 cm H_2O . Cutoffs and diagnostic metrics are shown in table 2.

Relation between P0.1 and Lung Stress in the Preceding Hour

The conversion factor to predict change in transpulmonary pressure with P0.1 was on average 3.3 (2.4 to 4.1). The predicted lung stress (change in transpulmonary pressure = $3.3 \times P0.1 + \text{inspiratory support}$) correlated fairly well with the observed lung stress in the preceding hour ($R^2 = 0.51$, $P < 0.001$; fig. 5). Bias was –0.6 cm H_2O ; 95% limits-of-agreement ranged from –10.2 to +10.1 cm H_2O .

The conversion factor to predict MP_L with P0.1 was on average 4.7 (4.2 to 5.3). The predicted mechanical power

(predicted transpulmonary mechanical power = $0.5 \times (\text{inspiratory support} + 4.7 \times P0.1) \times RR \times Vt \times 0.098$, with Vt in liters) correlated moderately with the observed mechanical power ($R^2 = 0.35$, $P < 0.001$; fig. 5). Bias was 1.4 J/min, 95% limits-of-agreement ranged from –6.7 to 8.2 J/min.

Relation between P0.1 and Diaphragm Effort in the Preceding Hour

The conversion factor to predict change in transdiaphragmatic pressure with P0.1 was on average 3.5 (2.0 to 4.9). The predicted diaphragm effort (change in transdiaphragmatic pressure = $3.5 \times P0.1$) correlated poorly with observed diaphragm effort ($R^2 = 0.22$, $P < 0.001$; fig. 5). Bias was –0.6 cm H_2O ; 95% limits-of-agreement ranged from –7.3 to 6.2 cm H_2O . Cutoffs and diagnostic metrics are shown in table 2.

External Validation

In total, 14,651 breaths obtained in 13 patients were analyzed in the external validation cohort. The recordings included 61 expiratory occlusions, of which 43 had a Pocc/change in esophageal pressure_{occ} ratio between 0.8 and 1.2 which were used for further analysis (fig. 2). Correlations are shown in figure E5 (<http://links.lww.com/ALN/C995>) and figure E6 (<http://links.lww.com/ALN/C996>). Lung stress was high in 7 of 43 (16%) of the recordings.

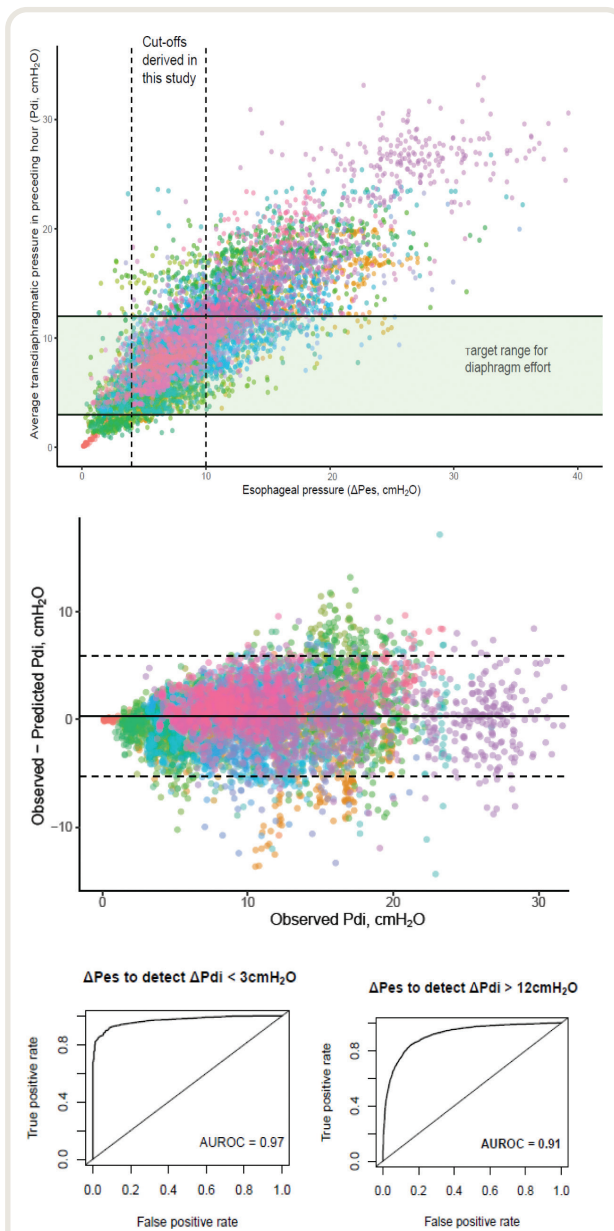


Fig. 3. (Top) Correlation between random tidal swings in esophageal pressure (ΔP_{es}) measurements and diaphragm effort (average tidal swing in transdiaphragmatic pressure, ΔP_{di}) in the preceding hour. Each dot is a measurement ($n = 7,729$); each color represents one subject ($n = 38$). Green shaded area shows the target range for diaphragm effort (ΔP_{di} 3 to 12 cm H_2O). Dashed lines cross the x-axis at the obtained cutoffs (4 and 10 cm H_2O) for detecting $\Delta P_{di} < 3$ cm H_2O and > 12 cm H_2O , respectively. In total, 522 of 7,729 (6.7%) of the recordings had a $\Delta P_{di} < 3$ cm H_2O and 2,749 of 7,729 (35.7%) had a $\Delta P_{di} > 12$ cm H_2O . (Right) Bland-Altman plot of predicted ΔP_{di} based on ΔP_{es} versus observed ΔP_{di} . Solid horizontal line shows bias, dashed lines show 95% limits-of-agreement. (Bottom) Receiver operating characteristic curves of using a random ΔP_{es} measurement to detect average $\Delta P_{di} < 3$ cm H_2O (left) and > 12 cm H_2O (right).

Diaphragm effort was low in 4 of 43 (10%) and high in 3 of 43 (7%) of the recordings. Accuracy of Pocc and P0.1 to identify patients with extremes in lung stress and diaphragm effort was not significantly different in the external cohort compared with the primary cohort (fig. E5, <http://links.lww.com/ALN/C995>, and fig. E6, <http://links.lww.com/ALN/C996>).

Discussion

In the current study we tested the validity of noninvasive airway occlusion maneuvers to quantify lung stress and diaphragm effort in ventilated critically ill patients. Our findings can be summarized as follows: First, Pocc and P0.1 cannot be used to calculate the exact values of diaphragm effort and lung stress in the preceding hour, due to wide limits of agreement between occlusions pressures and the reference standard (esophageal pressure). Second, if the goal is to obtain lung stress and diaphragm effort in purported safe ranges,^{5,6} Pocc and P0.1 have good to excellent diagnostic performance in identifying extremes of lung stress and diaphragm effort. Third, Pocc is at least as reliable as P0.1 in all instances but outperforms P0.1 in detecting patients with high diaphragm effort.

Occlusion Pressures: Estimation of Lung Stress and Breathing Effort versus Identification of Extremes

The predicted lung stress based on Pocc and P0.1 correlates with change in transpulmonary pressure in the preceding hour ($R^2 = 0.62$ and 0.51 , respectively), albeit with wide limits of agreement ranging from 5 to 10 cm H_2O in either direction (figs. 4 and 5). Likewise, Pocc and P0.1 correlate with change in transdiaphragmatic pressure ($R^2 = 0.53$ and 0.22 , respectively) with equally wide limits of agreement. The limits of agreement are likely wide because of variations in breathing effort within subjects over time, and because a single breath is extrapolated to diaphragm effort and/or lung stress over a longer period of time. Pocc and P0.1 can therefore not replace esophageal pressure when precise values are required such as in physiologic studies.

The area under receiver operating characteristic curves of Pocc and P0.1 to identify patients with extremes in lung stress and diaphragm effort are high (table 2). The predicted lung stress and diaphragm effort show considerable heteroscedasticity (fanning out) compared with observed change in transpulmonary pressure and transdiaphragmatic pressure (figs. 4 and 5), meaning that errors are lower at low lung stress and diaphragm effort and greater at higher levels. This provides an explanation for the discrepancy between the wide limits of agreement and the high accuracy; most of the errors are made at higher levels of lung stress and diaphragm effort, where differences of 5 cm H_2O might be less important than at lower levels (e.g., a change in transpulmonary pressure of either 30 or 35 cm H_2O are both far

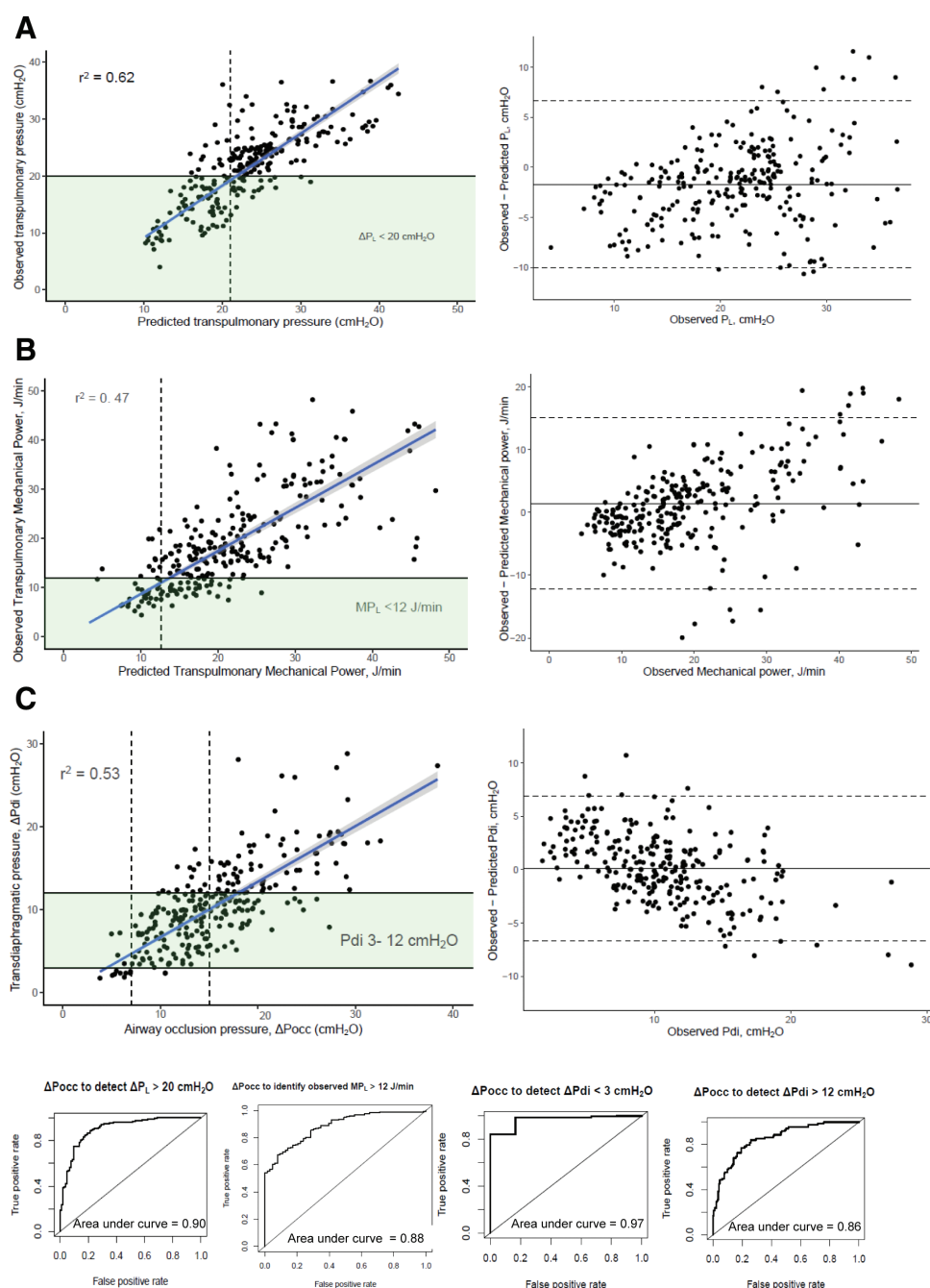


Fig. 4. Change in occluded inspiratory airway pressure (ΔP_{occ}) to assess lung stress and diaphragm effort. *Green shaded areas* show the proposed safe limits for lung stress and diaphragm effort. Note that P_{occ} is presented as a positive number for this plot to preserve a positive correlation, while it is measured as a negative number. (A, *left*) Correlation between the predicted lung stress (ΔP_L [change in transpulmonary pressure] based on P_{occ}) and the observed lung stress in the preceding hour. Each *dot* is a measurement ($n = 282$). *Dashed line* shows the selected cutoff for predicted ΔP_L at 22 cm H₂O. (Right) Bland-Altman plot of predicted ΔP_L based on P_{occ} versus observed ΔP_L . *Solid horizontal line* shows bias; *dashed lines* show 95% limits-of-agreement. (B, *left*) Correlation between predicted transpulmonary mechanical power (MP_L) and observed MP_L in the preceding hour. Each *dot* is a measurement ($n = 282$). *Dashed line* shows the selected cutoff (predicted MP_L of 12 J/min). (right) Bland-Altman plot of predicted MP_L based on P_{occ} versus observed MP_L . *Solid horizontal line* shows bias, *dashed lines* show 95% limits-of-agreement. (C, *left*) Correlation between P_{occ} and the average change in transdiaphragmatic pressure (ΔP_{di}) in the preceding hour. Each *dot* is a measurement ($n = 282$). *Dashed lines* show the selected cutoffs for P_{occ} (-7 and -15 cm H₂O). (Right) Bland-Altman plot showing the predicted diaphragm effort (P_{di} based on ΔP_{occ}) versus observed diaphragm effort. *Solid horizontal line* shows bias, *dashed lines* show 95% limits-of-agreement. (Bottom) Receiver operating characteristic curves of using P_{occ} to identify patients with potentially injurious diaphragm effort and lung stress.

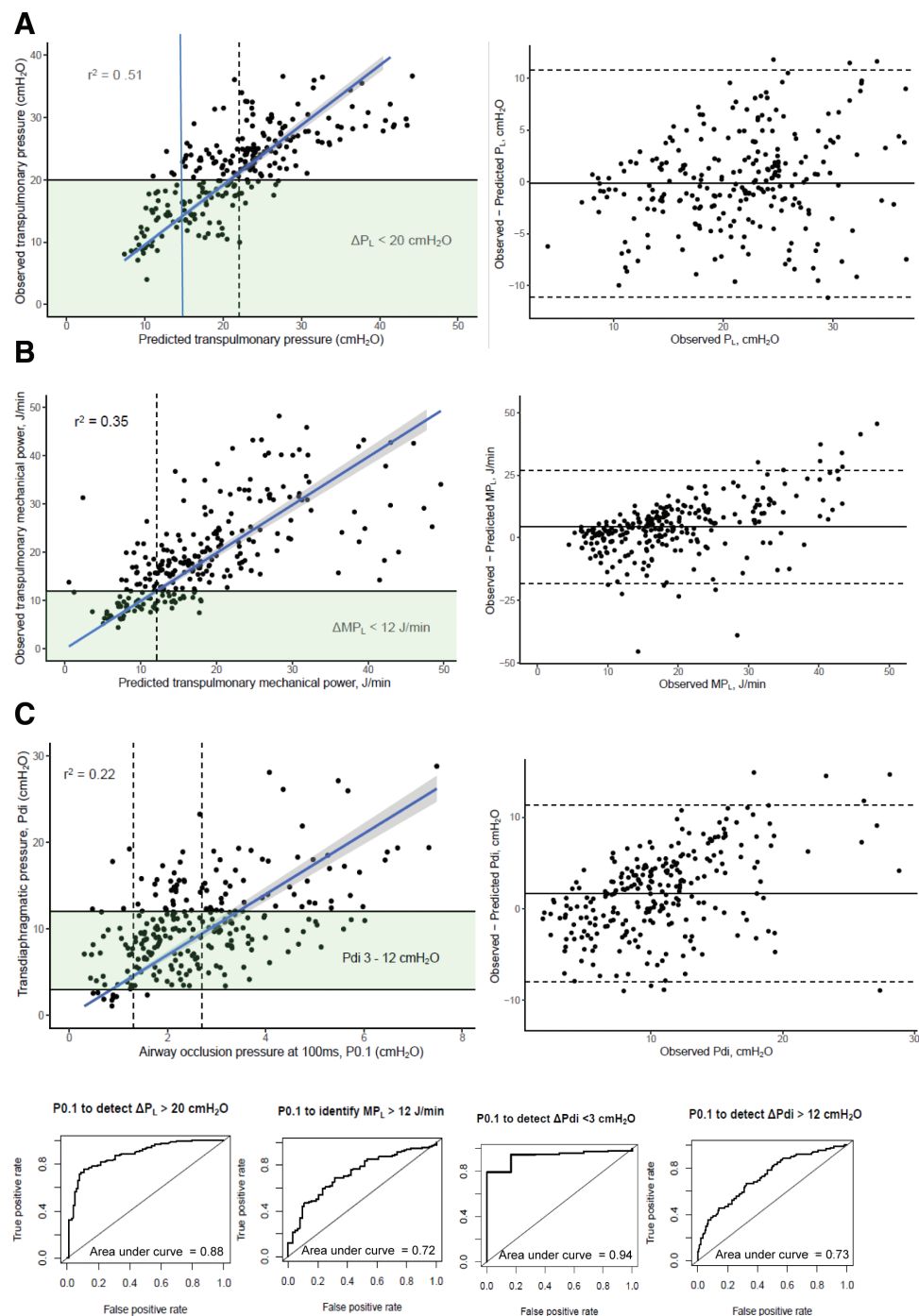


Fig. 5. Airway occlusion pressure at 100 ms (P0.1) to assess lung stress and diaphragm effort. *Green shaded areas* show the proposed safe limits for lung stress and diaphragm effort. (A, *left*) Correlation between the predicted change in transpulmonary pressure (ΔP_L) based on P0.1 and the observed lung stress (ΔP_L) in the preceding hour. Each *dot* is a measurement ($n = 282$). *Dashed line* shows the selected cutoffs (21 cm H₂O). (*Right*) Bland-Altman plot of predicted lung stress (ΔP_L based on P0.1) *versus* observed lung stress. *Solid horizontal line* shows bias; *dashed lines* show 95% limits-of-agreement. (B, *left*) Correlation between predicted transpulmonary mechanical power (MP_L) and observed MP_L in the preceding hour. *Dashed line* shows the selected cut off (predicted MP_L of 12 J/min). Each *dot* is a measurement ($n = 282$). (*Right*) Bland-Altman plot of predicted lung stress (ΔP_L based on P0.1) *versus* observed lung stress. *Solid horizontal line* shows bias, *dashed lines* show 95% limits-of-agreement. (C, *left*) Correlation between ΔP_{occ} and the average transdiaphragmatic pressure (ΔP_{di}) in the preceding hour. Each *dot* is a measurement ($n = 282$). *Dashed lines* show the selected cutoffs (7 and 15 cm H₂O). (*right*) Bland-Altman plot of predicted diaphragm effort (ΔP_{di} based on P0.1) *versus* observed diaphragm effort. *Solid horizontal line* shows bias, *dashed lines* show 95% limits-of-agreement. (*Bottom*) Receiver operating characteristic curves of using P0.1 to identify patients with potentially injurious diaphragm effort and lung stress.

beyond proposed safe values, so precision is less important at this level).

Pocc has higher discriminative power than P0.1 in detecting patients with high transdiaphragmatic pressure in our cohort (area under receiver operating characteristic curves 0.86 *vs.* 0.73, respectively), which might be explained by several factors. First, P0.1 is based on a shorter measurement interval and thus suffers more from high-frequency noise such as cardiac artefacts. Second, factors that cause a time delay in the transmission of pressures between the patient and measurement setup might have more effect on dynamic measurements such as P0.1. Third, properties of the respiratory system and control center might influence the convexity of airway pressure curves, distorting the relation between P0.1 and total respiratory muscle pressure in the same breath.³³

Our data show that Pocc together with tidal volume and respiratory rate may be used to estimate mechanical power, which correlates moderately well to observed mechanical power ($R^2 = 0.47$) as shown in figure 4. Area under receiver operating characteristic curves to detect high mechanical power are acceptable to excellent (table 2).³⁴ Mechanical power has been theorized to better reflect the risk of lung injury than pressure alone in animal studies²⁸ and retrospective cohorts of ICU patients.³⁵ However, the superiority of mechanical power to predict lung injury requires further validation in prospective clinical studies.

Clinical Implications

Lung- and diaphragm-protective mechanical ventilation is an emerging concept for ventilatory management in critically ill patients. The hypothesis is that monitoring and controlling breathing effort and lung stress in critically ill patients could have several benefits: limiting lung stress might hamper development of lung injury, whereas targeting moderate diaphragm effort has been theorized to protect against disuse atrophy while limiting the probability of developing load-induced diaphragm injury.^{5,6} The evidence that absence of diaphragm effort leads to atrophy and weakness is compelling,^{7,8} and maintaining some diaphragm effort reduces diaphragm atrophy in animal studies.^{9,10} Evidence that high diaphragm effort leads to injury is currently based on small sets of experimental human and animal data.^{36–38} Apart from potentially preventing diaphragm injury, limiting excessive diaphragm effort might improve patient comfort by reducing dyspnea,³⁹ and is proposed to reduce regional lung stress by limiting pendelluft.¹² The proposed pathophysiology of diaphragm protective ventilation, including current knowledge gaps, has been covered in depth recently.^{5,40}

State-of-the-art monitoring of lung stress and diaphragm effort requires esophageal (and gastric) pressure measurement, which is not routine performed in clinical practice.¹ Our data show that the Pocc and P0.1 cannot replace esophageal and gastric manometry when precise

values are desired. At best, Pocc and P0.1 give an indication of a range of the true lung stress and diaphragm effort. This range can allow a clinician to identify patients that are most likely to benefit from advanced respiratory monitoring: a patient with a predicted transdiaphragmatic pressure of 20 cm H₂O based on Pocc has an actual change in transdiaphragmatic pressure between 13 and 27 cm H₂O with 95% certainty and could thus benefit from additional monitoring. Additionally, a clinician can use Pocc and P0.1 to estimate whether lung stress and diaphragm effort are likely within proposed safe limits when esophageal manometry is not available by using the cutoffs provided in table 2: 86% of patients with an estimated change in transpulmonary pressure < 22 cm H₂O are expected to have actual lung stress in the proposed safe range (less than 20 cm H₂O), and 89% of patients with a Pocc between –7 and –15 cm H₂O will have diaphragm effort in the proposed safe range (transdiaphragmatic pressure of 3 to 12 cm H₂O). An example of a bedside monitoring protocol based on Pocc and these cutoffs is presented in figure E7 (<http://links.lww.com/ALN/C997>), but prospective studies are required to assess whether using this protocol results in more lung stress and effort in purported safe ranges.

Validity of Transdiaphragmatic Pressure and the Proposed Cutoffs

Transdiaphragmatic pressure, the pressure output of the diaphragm, is the current reference standard to assess diaphragm effort.^{6,14–16,23} Several factors influence a patient's capacity to generate pressure, such as diaphragm weakness before ICU admission⁴¹ and changes in diaphragm geometry due to lung collapse and positive end-expiratory pressure.⁴² Consequently, a certain transdiaphragmatic pressure may require more myofiber recruitment in critically ill patients compared with healthy subjects. Thus, the precise “safe transdiaphragmatic pressure interval” may be patient specific. Furthermore, diaphragm weakness was found to associate strongly to ICU outcomes such as weaning failure in several studies,^{41,43,44} but the correlation was absent in others.^{45,46} Prospective trials are thus required to assess whether diaphragm effort during mechanical ventilation is indeed causally related to ICU outcomes, and not merely a confounder for disease severity.^{47,48} Additionally, further research must assess the optimal cutoffs to prevent lung and diaphragm injury, because the current cutoffs are based only on consensus.

Comparison with Other Studies

The conversion factor to predict lung stress from Pocc in our cohort (0.67) closely matches the conversion factor reported in an earlier study (0.66),¹⁷ suggesting that this factor is generalizable to external populations. Likewise, the conversion factor to predict change in total respiratory muscle pressure with Pocc found in our cohort (0.73,

fig. E8, <http://links.lww.com/ALN/C998>) was very close to value reported previously (0.75).¹⁷ The high accuracy of P0.1 to identify patients with purported insufficient respiratory muscle effort is in agreement with recent studies.^{19,49} Accurately detecting insufficient effort is a novel observation for Pocc, because an earlier study lacked recordings with low effort.¹⁷

Strengths and Limitations

This study has several strengths. We included a heterogeneous group of patients with acute respiratory failure, displaying a wide range of lung stress and diaphragm effort. In contrast to previous studies, we used the reference methods to assess lung stress and diaphragm effort, recorded patients for prolonged periods of time (24 h), included more patients (38 *vs.* 16) and conducted much more occlusion measurements (282 *vs.* 52). We also confirmed the robustness of Pocc and P0.1 in an external cohort. Earlier studies validated the Pocc and P0.1 with total respiratory muscle pressure, which reflects total pressure generation resulting from activation of the diaphragm, accessory muscles and relaxation of the expiratory muscles.^{17,18,50} Transdiaphragmatic pressure may be more linked to studies on diaphragm injury during mechanical ventilation which have demonstrated an association (but not necessarily causation⁴⁷) between *diaphragm* function and clinical outcome.^{41,43} Whether monitoring transdiaphragmatic pressure leads to better outcomes than monitoring total respiratory muscle pressure requires further study. Last, we have estimated the potential magnitude of measurement errors in our study, and found that these likely do not influence our conclusions (Supplemental Digital Content, <http://links.lww.com/ALN/C989>).

Several limitations should be acknowledged. First, the optimal ranges for lung stress and diaphragm effort to prevent both lung injury and diaphragm weakness are unknown and were based on expert consensus. Second, although we used data from two independent centers, performance of Pocc and P0.1 needs to be evaluated in larger cohorts from multiple international centers. Third, earlier reports averaged three consecutive P0.1 measurements to improve reliability.¹⁹ We could not conduct the same analysis as single occlusions were performed in our protocol. We have, however, estimated to which degree averaging multiple consecutive change in esophageal pressure measurements would improve correlations and diagnostic accuracy with change in transdiaphragmatic pressure (fig. 3 and fig. E4, <http://links.lww.com/ALN/C994>), and found the benefit to be relatively minor: averaging three measurements improved R^2 from 0.79 to 0.84, but had little effect on diagnostic performance. Fourth, we used the same external validation cohort as an earlier report validating Pocc.¹⁷ This external cohort had few recordings with low diaphragm effort, underlining the importance of further validation in larger cohorts. Fifth, the external validation cohort ventilated patients exclusively in neurally adjusted

ventilatory assist, which is a proportional mode of ventilation, whereas the primary cohort used mostly pressure support. This likely had little effect on the validity of the Pocc and P0.1, however, because single airway occlusions were found not to affect respiratory drive¹⁷ and the correlations and diagnostic performance were not different in primary cohort and the external cohort (fig. E5, <http://links.lww.com/ALN/C995>, and fig. E6, <http://links.lww.com/ALN/C996>). Finally, 20 to 30% of all recordings in the main cohort and external data set had to be discarded due to our strict quality control for adequate calibration of the esophageal pressure balloons.

Conclusions

This study shows that Pocc and P0.1 cannot predict exact values for lung stress and diaphragm effort in ventilated critically ill patients. Both maneuvers can reliably identify patients with purported low diaphragm effort and high lung stress in the preceding hour. Pocc is more accurate than P0.1 in identifying patients with high diaphragm effort.

Acknowledgments

The authors thank R. H. Driessen, B.Sc., from the Department of Intensive Care Medicine, Amsterdam UMC, location VUmc (Amsterdam, The Netherlands), for database management support.

Research Support

This study was funded by a Ph.D.-research grant to Dr. de Vries from the Amsterdam Cardiovascular Sciences research institute (Amsterdam, The Netherlands). No commercial support was received.

Competing Interests

Dr. Heunks has received research support from Liberate Medical (Crestwood, Kentucky) and speakers fee from Getinge (Göteborg, Sweden). Dr. de Vries has received travel and speaker fees from the Chinese Association of Rehabilitation Medicine (Beijing, China). Dr. Jonkman has received personal fees from Liberate Medical. The other authors declare no competing interests.

Correspondence

Address correspondence to Dr. Heunks: Department of Intensive Care, Erasmus Medical Center, Rotterdam, Postbox 2040, 3000CA, The Netherlands. l.heunks@erasmusmc.nl. This article may be accessed for personal use at no charge through the Journal Web site, www.anesthesiology.org.

Supplemental Digital Content

Supplemental methods and results, <http://links.lww.com/ALN/C989>

Table E1 Additional diagnostic performance, <http://links.lww.com/ALN/C990>

Figure E1 Pressure-volume loopst, <http://links.lww.com/ALN/C991>

Figure E2 Example delayed cycling, <http://links.lww.com/ALN/C992>

Figure E3 Correlations of Pes, Pmus and Pdi, <http://links.lww.com/ALN/C993>

Figure E4 Performance of averaging Pes, <http://links.lww.com/ALN/C994>

Figure E5 Pocc in external cohort2, <http://links.lww.com/ALN/C995>

Figure E6 P0.1 in external cohort, <http://links.lww.com/ALN/C996>

Figure E7 Proposed monitoring protocol, <http://links.lww.com/ALN/C997>

Figure E8 Performance of Pocc for Pmus, <http://links.lww.com/ALN/C998>

References

- Bellani G, Laffey JG, Pham T, Fan E, Brochard L, Esteban A, Gattinoni L, Haren F van, Larsson A, McAuley DE, Ranieri M, Rubenfeld G, Thompson BT, Wrigge H, Slutsky AS, Pesenti A; LUNG SAFE Investigators, the European Society of Intensive Care Medicine Trials Group: Epidemiology, patterns of care, and mortality for patients with acute respiratory distress syndrome in intensive care units in 50 countries. *JAMA* 2016; 315:788–800
- Neto AS, Cardoso SO, Manetta JA, Pereira VGM, Espósito DC, Pasqualucci MdOP, Damasceno MCT, Schultz MJ: Association between use of lung-protective ventilation with lower tidal volumes and clinical outcomes among patients without acute respiratory distress syndrome: a meta-analysis. *JAMA* 2012; 308:1651–9
- Goligher EC, Costa EL V, Yarnell CJ, Brochard LJ, Stewart TE, Tomlinson G, Brower RG, Slutsky AS, Amato MPB: Effect of lowering VT on mortality in acute respiratory distress syndrome varies with respiratory system elastance. *Am J Respir Crit Care Med* 2021; 203:1378–85
- Tobin MJ: The dethroning of 6 ml/kg as the “go-to” setting in acute respiratory distress syndrome. *Am J Respir Crit Care Med* 2021; 204:868–9
- Goligher EC, Dres M, Patel BK, Sahetya SK, Beitler JR, Telias I, Yoshida T, Vaporidi K, Grieco DL, Schepens T, Grasselli G, Spadaro S, Dianti J, Amato M, Bellani G, Demoule A, Fan E, Ferguson ND, Georgopoulos D, Guérin C, Khemani RG, Laghi F, Mercat A, Mojoli F, Ottenheim CAC, Jaber S, Heunks L, Mancebo J, Mauri T, Pesenti A, Brochard L: Lung- and diaphragm-protective ventilation. *Am J Respir Crit Care Med* 2020; 202:950–61
- Goligher EC, Jonkman AH, Dianti J, Vaporidi K, Beitler JR, Patel BK, Yoshida T, Jaber S, Dres M, Mauri T, Bellani G, Demoule A, Brochard L, Heunks L: Clinical strategies for implementing lung and diaphragm-protective ventilation: Avoiding insufficient and excessive effort. *Intensive Care Med* 2020; 46:2314–26
- Levine S, Nguyen T, Taylor N, Friscia ME, Budak MT, Rothenberg P, Zhu J, Sachdeva R, Sonnad S, Kaiser LR, Rubinstein NA, Powers SK, Shrager JB: Rapid disuse atrophy of diaphragm fibers in mechanically ventilated humans. *N Engl J Med* 2008; 358:1327–35
- Jaber S, Petrof BJ, Jung B, Chanques G, Berthet J-P, Rabuel C, Bouyabrine H, Courouble P, Koechlin-Ramonatxo C, Sebbane M, Similowski T, Scheuermann V, Mebazaa A, Capdevila X, Mornet D, Mercier J, Lacampagne A, Philips A, Matecki S: Rapidly progressive diaphragmatic weakness and injury during mechanical ventilation in humans. *Am J Respir Crit Care Med* 2011; 183:364–71
- Jung B, Constantin J-M, Rossel N, Le GC, Sebbane M, Coisel Y, Chanques G, Futier E, Hugon G, Capdevila X, Petrof B, Matecki S, Jaber S: Adaptive support ventilation prevents ventilator-induced diaphragmatic dysfunction in piglet. *ANESTHESIOLOGY* 2010; 112:1435–43
- Sassoon CSH, Zhu E, Caiozzo VJ: Assist-control mechanical ventilation attenuates ventilator-induced diaphragmatic dysfunction. *Am J Respir Crit Care Med* 2004; 170:626–32
- Laghi F, D’Alfonso N, Tobin MJ: Pattern of recovery from diaphragmatic fatigue over 24 hours. *J Appl Physiol* 1995; 79:539–46
- Yoshida T, Torsani V, Gomes S, Santis RRD, Beraldo MA, Costa ELV, Tucci MR, Zin WA, Kavanagh BP, Amato MBP: Spontaneous effort causes occult pendelluft during mechanical ventilation. *Am J Respir Crit Care Med* 2013; 188:1420–7
- Toumpanakis D, Kastis GA, Zacharatos P, Sigala I, Michailidou T, Kouvela M, Glynos C, Divangahi M, Roussos C, Theocharis SE, Vassilakopoulos T: Inspiratory resistive breathing induces acute lung injury. *Am J Respir Crit Care Med* 2010; 182:1129–36
- Mauri T, Yoshida T, Bellani G, Goligher EC, Carteaux G, Rittayamai N, Mojoli F, Chiumello D, Piquilloud L, Grasso S, Jubran A, Laghi F, Magder S, Pesenti A, Loring S, Gattinoni L, Talmor D, Blanch L, Amato M, Chen L, Brochard L, Mancebo J; PLUG—Acute Respiratory Failure section of the European Society of Intensive Care Medicine): Esophageal and transpulmonary pressure in the clinical setting: meaning, usefulness and perspectives. *Intensive Care Med* 2016; 42:1360–73
- Akoumianaki E, Maggiore SM, Valenza F, Bellani G, Jubran A, Loring SH, Pelosi P, Talmor D, Grasso S, Chiumello D, Guérin C, Patroniti N, Ranieri VM,

- Gattinoni L, Nava S, Terragni P-P, Pesenti A, Tobin M, Mancebo J, Brochard L; PLUG Working Group (Acute Respiratory Failure Section of the European Society of Intensive Care Medicine): The application of esophageal pressure measurement in patients with respiratory failure. *Am J Respir Crit Care Med* 2014; 189:520–31
16. Vries H de, Jonkman A, Shi Z-H, Spoelstra-de Man A, Heunks L, Vries H de, Jonkman A, Shi Z-H, Man AS, Heunks L, Vries H de, Jonkman A, Shi Z-H, Man AS, Heunks L: Assessing breathing effort in mechanical ventilation: physiology and clinical implications. *Ann Transl Med* 2018; 6:387
 17. Bertoni M, Telias I, Urner M, Long M, Sorbo LD, Fan E, Sinderby C, Beck J, Liu L, Qiu H, Wong J, Slutsky AS, Ferguson ND, Brochard LJ, Goligher EC: A novel non-invasive method to detect excessively high respiratory effort and dynamic transpulmonary driving pressure during mechanical ventilation. *Crit Care* 2019; 23:346
 18. Roesthuis L, van den Berg M, van der Hoeven H: Non-invasive method to detect high respiratory effort and transpulmonary driving pressures in COVID-19 patients during mechanical ventilation. *Ann Intensive Care* 2021; 11:26
 19. Telias I, Junhasavasdikul D, Rittayamai N, Piquilloud L, Chen L, Ferguson ND, Goligher EC, Brochard L: Airway occlusion pressure as an estimate of respiratory drive and inspiratory effort during assisted ventilation. *Am J Respir Crit Care Med* 2020; 201:1086–98
 20. de Vries H, Jonkman AH, de Grooth HJ, Duitman JW, Girbes ARJ, Ottenheijm CAC, Schultz MJ, van de Ven PM, Zhang Y, de Man AME, Tuinman PR, Heunks LMA: Lung- and diaphragm-protective ventilation by titrating inspiratory support to diaphragm effort: a randomized clinical trial. *Crit Care Med* 2022; 50:192–203
 21. Liu L, Liu S, Xie J-F, Slutsky A, Beck J, Sinderby C, Qiu H: Assessment of patient-ventilator breath contribution during neurally adjusted ventilatory assist in patients with acute respiratory failure. *Crit Care* 2015; 19:43
 22. Cohen JF, Korevaar DA, Altman DG, Bruns DE, Gatsonis CA, Hooft L, Irwig L, Levine D, Reitsma JB, Vet HD, Bossuyt PMM: STARD 2015 guidelines for reporting diagnostic accuracy studies: explanation and elaboration. *BMJ Open* 2016; 6:e012799
 23. American Thoracic Society/European Respiratory Society. ATS/ERS Statement on respiratory muscle testing. *Am J Respir Crit Care Med* 2002; 166:518–624
 24. Baydur A, Behrakis PK, Zin WA, Jaeger M, Milic-Emili J: A simple method for assessing the validity of the esophageal balloon technique. *Am Rev Respir Dis* 1982; 126:788–91
 25. Altman DG, Bland JM: Measurement in medicine: the analysis of method comparison studies. *Stat* 1983; 32:307
 26. Nakagawa S, Schielzeth H: A general and simple method for obtaining R² from generalized linear mixed-effects models. *Methods Ecol Evol* 2013; 4:133–42
 27. Fawcett T: An introduction to ROC analysis. *Pattern Recognit Lett* 2006; 27:861–74
 28. Cressoni M, Gotti M, Chiurazzi C, Massari D, Algieri I, Amini M, Cammaroto A, Brioni M, Montaruli C, Nikolla K, Guanzioli M, Dondossola D, Gatti S, Valerio V, Vergani GL, Pugini P, Cadringer P, Gagliano N, Gattinoni L: Mechanical power and development of ventilator-induced lung injury. *ANESTHESIOLOGY* 2016; 124:1100–8
 29. Hosmer D, Lemeshow S: *Applied Logistic Regression*. John Wiley & Sons, Inc; 2013:177
 30. Youden WJ: Index for rating diagnostic tests. *Cancer* 1950; 3:32–5
 31. Hanley JA, McNeil BJ: The meaning and use of the area under a receiver operating characteristic (ROC) curve. *Radiology* 1982; 143:29–36
 32. Richardson JTE: The analysis of 2×2 contingency tables—yet again. *Stat Med* 2011; 30:890
 33. Whitelaw WA, Derenne JP: Airway occlusion pressure. 1993; 74:1475–83
 34. Gattinoni L, Tonetti T, Cressoni M, Cadringer P, Herrmann P, Moerer O, Protti A, Gotti M, Chiurazzi C, Carlesso E, Chiumello D, Quintel M: Ventilator-related causes of lung injury: The mechanical power. *Intensive Care Med* 2016; 42:1567–75
 35. Costa ELV, Slutsky AS, Brochard LJ, Brower R, Serpa-Neto A, Cavalcanti AB, Mercat A, Meade M, Morais CCA, Goligher E, Carvalho CRR, Amato MBP: Ventilatory variables and mechanical power in patients with acute respiratory distress syndrome. *Am J Respir Crit Care Med* 2021; 204:303–11
 36. Jiang TX, Reid WD, Belcastro A, Road JD: Load dependence of secondary diaphragm inflammation and injury after acute inspiratory loading. *Am J Respir Crit Care Med* 1998; 157:230–6
 37. Reid WD, Belcastro AN: Time course of diaphragm injury and calpain activity during resistive loading. *Am J Respir Crit Care Med* 2000; 162:1801–6
 38. Orozco-Levi M, Lloreta J, Minguella J, Serrano S, Broquetas JM, Gea J: Injury of the human diaphragm associated with exertion and chronic obstructive pulmonary disease. *Am J Respir Crit Care Med* 2001; 164:1734–9
 39. Demoule A, Hajage D, Messika J, Jaber S, Diallo H, Coutrot M, Kouatchet A, Azoulay E, Fartoukh M, Hraïech S, Beuret P, Darmon M, Decavèle M, Ricard JD, Chanques G, Mercat A, Schmidt M, Similowski T, for the REVA Network Research Network in Mechanical Ventilation: Prevalence, intensity, and clinical impact of

- dyspnea in critically ill patients receiving invasive ventilation. *Am J Respir Crit Care Med* 2022; 205:917–26
40. Dres M, Goligher EC, Heunks LMA, Brochard LJ: Critical illness-associated diaphragm weakness. *Intensive Care Med* 2017; 43:1441–52
 41. Demoule A, Jung B, Prodanovic H, Molinari N, Chanques G, Coirault C, Matecki S, Duguet A, Similowski T, Jaber S: Diaphragm dysfunction on admission to the intensive care unit. Prevalence, risk factors, and prognostic impact—A prospective study. *Am J Respir Crit Care Med* 2013; 188:213–9
 42. Jansen D, Jonkman AH, De Vries HJ, Wennen M, Elshof J, Hoofs MA, Van Den Berg M, De Man AME, Keijzer C, Scheffer GJ, Van Der Hoeven JG, Girbes A, Tuinman PR, Marcus JT, Ottenheijm CAC, Heunks L: Positive end-expiratory pressure affects geometry and function of the human diaphragm. *J Appl Physiol* 2021; 131:1328–39
 43. Dres M, Dube BP, Mayaux J, Delemazure J, Reuter D, Brochard L, Similowski T, Demoule A, Dubé B-P, Mayaux J, Delemazure J, Reuter D, Brochard L, Similowski T, Demoule A: Coexistence and impact of limb muscle and diaphragm weakness at time of liberation from mechanical ventilation in medical intensive care unit patients. *Am J Respir Crit Care Med* 2017; 195:57–66
 44. Kim WY, Suh HJ, Hong S-B, Koh Y, Lim C-M: Diaphragm dysfunction assessed by ultrasonography: Influence on weaning from mechanical ventilation*. *Crit Care Med* 2011; 39:2627–30
 45. Laghi F, Cattapan SE, Jubran A, Parthasarathy S, Warshawsky P, Choi YSA, Tobin MJ: Is weaning failure caused by low-frequency fatigue of the diaphragm? *Am J Respir Crit Care Med* 2003; 167:120–7
 46. Yang KL, Tobin MJ: A prospective study of indexes predicting the outcome of trials of weaning from mechanical ventilation. *N Engl J Med* 1991; 324:1445–50
 47. Laghi F, Sassoon CS: Weakness in the critically ill: “Captain of the men of death” or sign of disease severity? *Am J Respir Crit Care Med* 2017; 195:7–9
 48. Goligher EC, Brochard LJ, Reid WD, Fan E, Saarela O, Slutsky AS, Kavanagh BP, Rubenfeld GD, Ferguson ND: Diaphragmatic myotrauma: a mediator of prolonged ventilation and poor patient outcomes in acute respiratory failure. *Lancet Respir Med* 2019; 7:90–8
 49. Telias I, Damiani F, Brochard L: The airway occlusion pressure (P 0.1) to monitor respiratory drive during mechanical ventilation: increasing awareness of a not-so-new problem. *Intensive Care Med* 2018; 44:1532–5
 50. Shi Z-HZ-H, Jonkman A, Vries H de, Jansen D, Ottenheijm C, Girbes A, Spoelstra-de Man A, Zhou J-XJ-X, Brochard L, Heunks L: Expiratory muscle dysfunction in critically ill patients: towards improved understanding. *Intensive Care Med* 2019; 45:1–11

ANESTHESIOLOGY

Mechanical Power Ratio and Respiratory Treatment Escalation in COVID-19 Pneumonia: A Secondary Analysis of a Prospectively Enrolled Cohort

Simone Gattarello, M.D., Ph.D., Silvia Coppola, M.D.,
Elena Chiodaroli, M.D., Tommaso Pozzi, M.D.,
Luigi Camporota, M.D., Leif Saager, M.D.,
Davide Chiumello, M.D., Luciano Gattinoni, M.D., F.R.C.P.

ANESTHESIOLOGY 2023; 138:289–98

EDITOR'S PERSPECTIVE

What We Already Know about This Topic

- Determination of the optimal timing of endotracheal intubation in patients presenting with respiratory failure from COVID-19 pneumonia based on objective physiologic parameters is controversial
- The authors performed a secondary analysis of such patients in which a baseline computed tomography scan was obtained on admission and a battery of routine clinical and more complex derived respiratory parameters were quantified using esophageal manometry and transthoracic electrical impedance including mechanical power, its ratio to the expected baseline value, and the pressure-rate index ($4 \times \text{driving pressure} + \text{respiratory rate}$)
- Associations of the studied parameters with treatment escalation to intubation and mechanical ventilation was assessed using the area under the receiver operator characteristic curve

What This Article Tells Us That Is New

- Despite similar spontaneous tidal volumes, escalated patients had higher respiratory rate, minute ventilation, pleural pressure, and mechanical power ratios
- Mechanical power, its ratio with the expected baseline value, and the pressure-rate index had the greatest associations with treatment escalation

ABSTRACT

Background: Under the hypothesis that mechanical power ratio could identify the spontaneously breathing patients with a higher risk of respiratory failure, this study assessed lung mechanics in nonintubated patients with COVID-19 pneumonia, aiming to (1) describe their characteristics; (2) compare lung mechanics between patients who received respiratory treatment escalation and those who did not; and (3) identify variables associated with the need for respiratory treatment escalation.

Methods: Secondary analysis of prospectively enrolled cohort involving 111 consecutive spontaneously breathing adults receiving continuous positive airway pressure, enrolled from September 2020 to December 2021. Lung mechanics and other previously reported predictive indices were calculated, as well as a novel variable: the mechanical power ratio (the ratio between the actual and the expected baseline mechanical power). Patients were grouped according to the outcome: (1) no-treatment escalation (patient supported in continuous positive airway pressure until improvement) and (2) treatment escalation (escalation of the respiratory support to noninvasive or invasive mechanical ventilation), and the association between lung mechanics/predictive scores and outcome was assessed.

Results: At day 1, patients undergoing treatment escalation had spontaneous tidal volume similar to those of patients who did not (7.1 ± 1.9 vs. 7.1 ± 1.4 mL/kg_{IBW}; $P = 0.990$). In contrast, they showed higher respiratory rate (20 ± 5 vs. 18 ± 5 breaths/min; $P = 0.028$), minute ventilation (9.2 ± 3.0 vs. 7.9 ± 2.4 L/min; $P = 0.011$), tidal pleural pressure (8.1 ± 3.7 vs. 6.0 ± 3.1 cm H₂O; $P = 0.003$), mechanical power ratio (2.4 ± 1.4 vs. 1.7 ± 1.5 ; $P = 0.042$), and lower partial pressure of alveolar oxygen/fractional inspired oxygen tension (174 ± 64 vs. 220 ± 95 ; $P = 0.007$). The mechanical power (area under the curve, 0.738; 95% CI, 0.636 to 0.839; $P < 0.001$), the mechanical power ratio (area under the curve, 0.734; 95% CI, 0.625 to 0.844; $P < 0.001$), and the pressure-rate index (area under the curve, 0.733; 95% CI, 0.631 to 0.835; $P < 0.001$) showed the highest areas under the curve.

Conclusions: In this COVID-19 cohort, tidal volume was similar in patients undergoing treatment escalation and in patients who did not; mechanical power, its ratio, and pressure-rate index were the variables presenting the highest association with the clinical outcome.

(*ANESTHESIOLOGY* 2023; 138:289–98)

In patients with acute respiratory failure, the direct measurement of tidal volume, minute ventilation, and esophageal pressure, as well as their integration with other data such as gas-exchange or radiological variables, provides valuable clinical information to determine the diagnosis and to monitor the clinical response to a therapeutic intervention.¹ Furthermore, such a clinical monitoring may

This article is featured in "This Month in Anesthesiology," page A1. This article is accompanied by an editorial on p. 238. Supplemental Digital Content is available for this article. Direct URL citations appear in the printed text and are available in both the HTML and PDF versions of this article. Links to the digital files are provided in the HTML text of this article on the Journal's Web site (www.anesthesiology.org). This article has a video abstract. This article has an audio podcast. This article has a visual abstract available in the online version.

Submitted for publication July 30, 2022. Accepted for publication November 28, 2022. Published online first on December 26, 2022.

Simone Gattarello, M.D., Ph.D.: Anesthesia and Intensive Care Medicine, IRCCS San Raffaele Scientific Institute, Milan, Italy; and Department of Anesthesiology, University Medical Center Göttingen, Göttingen, Germany.

Copyright © 2022, the American Society of Anesthesiologists. All Rights Reserved. *Anesthesiology* 2023; 138:289–98. DOI: 10.1097/ALN.0000000000004465

allow for the early identification of clinical deterioration. In an era of personalized medicine, a tailored clinical approach is only possible through a careful approach to clinical monitoring, whose invasiveness should be proportional to the specific clinical severity and patients' requirements.

The mechanical power quantifies the amount of energy transferred to the respiratory system during mechanical ventilation, and it depends on the parameters used to set the ventilator and the resulting variables in the respiratory system.² Such energy is entirely provided by the ventilator in controlled mechanical ventilation, while it results from the combination of the energy generated by the respiratory muscles and the energy delivered by the ventilator in supported ventilation.

In this study, we aimed to (1) describe the physiologic characteristics of spontaneously breathing patients with COVID-19 pneumonia, on admission and over the course of hospitalization; (2) compare the respiratory mechanics of patients who underwent treatment escalation with those who did not; and (3) derive a diagnostic receiver operating characteristic model to assess which variables are associated with the need for respiratory treatment escalation.

Materials and Methods

Patient Population

This study is a secondary analysis of a prospective cohort, collected from September 2020 to December 2021, in which the primary objective was to assess whether an increased esophageal pressure was related to the severity of COVID-19 disease and the clinical outcome.¹ All spontaneously breathing patients with COVID-19 infection, confirmed by polymerase chain reaction, and acute respiratory failure supported by continuous positive airway pressure were enrolled in the study, and the current analysis was performed *a posteriori*. All patients were managed in a high-dependency COVID-19 unit and were consecutively enrolled. Of 140 eligible patients, we were able to measure minute ventilation only in the last 111 individuals (see flow chart for patients' enrollment in the supplemental material, <http://links.lww.com/ALN/C988>).

Silvia Coppola, M.D.: Department of Anesthesiology and Intensive Care, ASST Santi Paolo e Carlo, University of Milan, Milan, Italy.

Elena Chiodaroli, M.D.: Department of Anesthesiology and Intensive Care, ASST Santi Paolo e Carlo, University of Milan, Milan, Italy.

Tommaso Pozzi, M.D.: Department of Anesthesiology and Intensive Care, ASST Santi Paolo e Carlo, University of Milan, Milan, Italy.

Luigi Camporota, M.D.: Guy's and St. Thomas' NHS Foundation Trust, Department of Adult Critical Care, London, United Kingdom.

Leif Saager, M.D.: Department of Anesthesiology, University Medical Center Göttingen, Göttingen, Germany; and Outcomes Research Consortium, Cleveland, Ohio.

Davide Chiumello, M.D.: Department of Anesthesiology and Intensive Care, ASST Santi Paolo e Carlo, University of Milan, Milan, Italy.

Luciano Gattinoni, M.D., F.R.C.P.: Department of Anesthesiology, University Medical Center Göttingen, Göttingen, Germany.

The clinical management of the study individuals included standard COVID-19 pharmacologic guidance (see the supplemental material for details on pharmacologic management, <http://links.lww.com/ALN/C988>), which was initiated on admission in all patients. Although the study individuals were undergoing sessions of awake prone positioning, during data collection, each patient was in the supine position (for at least 2h) and supported with continuous positive airway pressure. The study was approved by the local ethical committee (Comitato Etico Milano Area I; 17263/2020-2020/ST/095), and written informed consent was obtained from each individual. The article follows the Strengthening the Reporting of Observational Studies in Epidemiology (STROBE) guidelines.

Study Protocol

All patients were first assessed in the emergency department, where a computed tomography scan was performed in spontaneous breathing and without positive end-expiratory pressure (PEEP), and an arterial blood sample was collected. The patients were then transferred to the high-dependency COVID-19 unit, where continuous positive airway pressure was applied according to local guidance (FiO₂ of 60% and PEEP of 5, 7.5, or 10 cm H₂O, as set by the attending physician). The esophageal pressure was measured using the esophageal-balloon catheter, connected to a data acquisition system (Optivent SIDAM Srl, Modena, Italy), while minute ventilation, respiratory rate, and tidal volume were quantified by a novel impedance-based monitoring device: ExSpirom (Respiratory Motion Inc., Watertown, Massachusetts). Blood gases were sampled from an arterial catheter.

We defined two outcome groups based on whether a patient underwent the escalation of the respiratory support: (1) no treatment escalation (the individual was supported with continuous positive airway pressure from admission in the high-dependency COVID-19 unit until clinical improvement, and then transferred to the ward) and (2) treatment escalation (any additional increase of the respiratory support, either noninvasive or invasive ventilation).

The decision to escalate the ventilatory support, as well as the type of treatment escalation (to either noninvasive or invasive mechanical ventilation), were left to the discretion of the clinical care team in accordance with local institutional guidelines: tachypnea more than 28 breaths/min, esophageal pressure swing higher than 8 cm H₂O, PaO₂/FiO₂ ratio lower than 100, delirium, increase of 2 points in the Work of Breathing score³ or 3 points in the Borg scale,⁴ or intolerance to continuous positive airway pressure. Similarly, the type of treatment escalation (escalation from continuous positive airway pressure to noninvasive or to invasive mechanical ventilation) was left to the decision of the treating clinical team.

Measurements

Tissue Mass and Gas Volume

After semiautomatic contour analysis of the lung computed tomography slices,⁵ the following variables were derived:

tissue mass (g), gas volume (ml), and fractions (%) of over-aerated, normally aerated, poorly aerated, and nonaerated tissue. The estimated baseline gas volume and tissue mass were calculated according to Ibanez *et al.*⁶ and Cressoni *et al.*⁷ (the equations are detailed in the supplemental material, <http://links.lww.com/ALN/C988>).

Tidal Volume and Minute Ventilation

Tidal volume and minute ventilation were quantified by analysis of the variation of the electrical impedance in the respiratory system,⁸ which was validated in acute and postacute patients^{9–12} (see supplemental material for specifics and details, <http://links.lww.com/ALN/C988>).

Esophageal Pressure

Esophageal pressure was determined using the esophageal-balloon catheter, connected to a data acquisition system (Optivent SIDAM Srl; see supplemental material for specifics and details, <http://links.lww.com/ALN/C988>).

The measurement of these variables allowed us to estimate the following ventilatory variables: ventilatory ratio, tidal pleural pressure, dynamic lung elastance, and tidal muscular pressure, which is the pressure exerted on the respiratory system by the respiratory muscles (see the supplemental material for the derivation of equations, <http://links.lww.com/ALN/C988>). In addition, we quantified the mechanical power and its normalization over the expected mechanical power at rest.

Respiratory System Mechanical Power

Respiratory system mechanical power (MP_{RS}) was estimated as follows:

$$MP_{RS} \text{ (J/min)} = 0.098 \times RR \times \left[V_t^2 \times \left(0.714 \times \frac{\Delta P_{pl}}{V_t} + RR \times 0.5 \right) + V_t \times PEEP \right] \quad (1)$$

where 0.098 is the constant that converts $l \cdot \text{cm H}_2\text{O}$ into J/min; RR is the respiratory rate; V_t is the tidal volume; 0.714 is a constant that accounts for the ratio between lung and total elastances (E_L/E_{rs}), that we assumed to equal 0.7¹³; and ΔP_{pl} is the tidal pleural pressure. See the supplemental material (<http://links.lww.com/ALN/C988>) for the full derivation of equation 1.

Mechanical Power Ratio

The mechanical power ratio is the ratio between the actual mechanical power of the respiratory system and the expected baseline mechanical power. The latter was estimated, analogously to the ventilatory ratio,¹⁴ as the power required to obtain a normal minute ventilation (computed as 0.1 times the ideal body weight)¹⁵ by applying an ideal transpulmonary pressure of 5 cm H_2O ¹⁶ at 15 breaths/min and without applied PEEP. The equations we used to quantify the expected baseline mechanical power (MP_{exp}) and the mechanical power ratio (MP ratio) are as follows:

$$MP_{exp} \text{ (J/min)} = 1.47 \times (0.006 \times IBW)^2 \times \left(\frac{3.57}{0.006 \times IBW} + 7.5 \right) \quad (2)$$

$$MP \text{ ratio} = \frac{MP_{RS}}{MP_{exp}} \quad (3)$$

where 1.47, 0.006, 3.57, and 7.5 are conversion constants (see supplemental material for the full derivation, <http://links.lww.com/ALN/C988>), and IBW is the ideal body weight. The mechanical power ratio, in essence, measures the fold increase in mechanical power compared to normal breathing in healthy conditions.

Additional Indexes

The ratio of oxygen saturation measured by pulse oximetry/ FiO_2 to respiratory rate index¹⁷ was calculated as the ratio between oxygen pulse oximetry to the fraction of inspired oxygen, over the respiratory rate. The pressure-rate index¹⁸ was rearranged to account for the spontaneous breathing and for easy comparison with the mechanical power; *i.e.*, for its computation, we used ΔP_{cs} instead of the driving pressure.

Statistical Analysis

We used a convenience sample of all eligible patients during the observation period and did not perform a sample size calculation as no previous data on the distribution of mechanical power ratio on COVID-19 patients is available. The data are reported as means \pm SD or median [interquartile range], as appropriate. The comparison between the two groups was performed using the independent-samples Student's *t* test or Wilcoxon's test, according to the distribution of each variable. Chi-square or Fisher's exact test were used to compare categorical variables. A receiver operating characteristic analysis was performed to assess the area under the curve for each variable, to estimate the association with the outcome. To evaluate the effect of multiple repeated measures in the same population during the time course, we built a model of repeated measures analysis of variance, in which the fixed effect was the need for treatment escalation and the random effect was the individual ID. No adjustment for potential confounders was performed in the statistical analysis because our aim was to assess the association between mechanical power ratio and the clinical outcome in the population as a whole. Two-tailed *P* values less than 0.05 were considered statistically significant. All analyses were performed with R for Statistical Computing 4.0 and SPSS version 25.

Results

A total of 111 adults were enrolled in the study. In table 1, we present the main demographic and anatomic-physiologic characteristics measured in the emergency department before continuous positive airway pressure initiation in patients who underwent ventilatory treatment escalation ($n = 64$) and those

Table 1. Baseline, Demographic, and Clinical Characteristics

Variable	No Treatment Escalation (n = 47)	Treatment Escalation (n = 64)	P Value
Age, yr [range]*	57 [48 to 66] {47}	58 [53 to 67] {64}	0.377
Sex female, n (%)†	18 (38.3) {47}	15 (23.4) {64}	0.091
Height, cm	168 ± 9.4 {41}	171 ± 10.0 {57}	0.210
Weight (actual), kg	84.5 ± 22.5 {41}	83.8 ± 18.3 {56}	0.871
Body mass index, kg/cm ²	29.5 ± 6.7 {41}	28.4 ± 28.4 {57}	0.350
Ideal body weight, kg	62.9 ± 10.2 {41}	65.9 ± 10.3 {56}	0.153
Onset of symptoms to admission, days*	6 [4 to 10] {47}	6 [4 to 8] {64}	0.735
Work of Breathing scale	1.40 ± 0.96 {45}	1.77 ± 1.08 {62}	0.062
Borg's dyspnea score	0.62 ± 1.19 {45}	0.92 ± 1.67 {62}	0.295
Pao ₂ before C-PAP, mmHg	71.7 ± 28.3 {45}	65.3 ± 16.8 {62}	0.145
Paco ₂ before C-PAP, mmHg	32.6 ± 4.6 {45}	32.9 ± 5.7 {62}	0.720
Fio ₂ before C-PAP, %	32.2 ± 2.1 {45}	32.2 ± 2.0 {62}	0.997
Estimated Pao ₂ /Fio ₂ ratio before C-PAP, mmHg	263 ± 81 {45}	246 ± 83 {62}	0.289
Respiratory rate before C-PAP, breaths/min	22 ± 5 {38}	22 ± 5 {49}	0.857
Measured gas volume, ml	2,355 ± 1,072 {41}	2,261 ± 1,059 {57}	0.665
Calculated baseline gas volume, ml	1,892 ± 276 {41}	1,932 ± 265 {61}	0.472
Measured tissue mass, g	1,090 ± 274 {41}	1,138 ± 267 {57}	0.389
Calculated baseline tissue mass, g	997 ± 1 ± 62 {41}	1,040 ± 169 {61}	0.208
Fraction of overaerated, %	9.3 ± 7.4 {41}	9.3 ± 9.3 {57}	0.972
Fraction of normally aerated, %	71.8 ± 7.8 {41}	69.6 ± 9.4 {57}	0.185
Fraction of poorly aerated, %	14.9 ± 7.4 {41}	17.0 ± 9.3 {57}	0.283
Fraction of nonaerated, %	4.0 ± 2.7 {41}	4.4 ± 3.6 {57}	0.503
Days from admission to outcome, days*	6 [6 to 9] {47}	3 [2 to 6] {64}	< 0.001
Intensive care unit length of stay, days*	0 [0] {47}	12 [7 to 18] {64}	
Hospital length of stay, days*	19 [16 to 25] {47}	25 [18 to 33] {64}	0.006
Endotracheal intubation†	0 (0) {47}	23 (35.9) {64}	< 0.001
Mortality†	0 (0) {47}	8 (12.5) {64}	0.020

Unless otherwise specified, values are presented as the means ± SD. The number in curling brackets is the number of individuals (all missing values are either due to missing or insufficient-quality data).

*The values are expressed as median [interquartile range]. †The values are expressed as absolute count and percent.

C-PAP, continuous positive airway pressure; Fio₂, fractional inspired oxygen tension.

who did not (n = 47). As shown, no differences were observed in terms of demographics, time from symptoms onset to the referral to the emergency department, or gas-exchange variables between the two outcome groups. In addition, no differences between groups were observed in terms of measured gas volume and tissue mass and in the fractions of overaerated, normally aerated, poorly aerated, and nonaerated tissue.

On day 1, once continuous positive airway pressure treatment was implemented, the group with no treatment escalation showed higher values of PaO₂ (mean ± SD, 141.5 ± 63.0 *vs.* 111.1 ± 44.3 mmHg; *P* = 0.007) and PaO₂/Fio₂ (220 ± 95 *vs.* 174 ± 64 mmHg; *P* = 0.007; table 2). Paco₂ was similar between groups but at the cost of higher minute ventilation (9.2 ± 3.0 *vs.* 7.9 ± 2.4 L/min; *P* = 0.011), respiratory rate (20 ± 5 *vs.* 18 ± 5 breaths/min; *P* = 0.028), tidal pleural pressure (8.1 ± 3.7 *vs.* 6.0 ± 3.1 cm H₂O; *P* = 0.003), tidal muscular pressure (11.8 ± 5.2 *vs.* 8.5 ± 4.3 cm H₂O; *P* = 0.001), and dynamic lung elastance (19.4 ± 9.7 *vs.* 13.7 ± 6.5 cm H₂O/L; *P* = 0.001) in the treatment escalation group. Ventilatory ratio was comparable, while the absolute mechanical power of the respiratory system (9.9 ± 6.0 *vs.* 6.7 ± 4.3 J/min; *P* = 0.003) and its relative mechanical power ratio (2.4 ± 1.4 *vs.*

1.7 ± 1.5; *P* = 0.042) were higher in the treatment escalation group. The respiratory rate index and the pressure-rate indexes were also significantly different between groups (respectively, in the escalation *vs.* no escalation groups: 7.6 ± 2.0 *vs.* 9.1 ± 2.6, *P* = 0.003; and 53.6 ± 16.0 *vs.* 41.9 ± 1.4, *P* = 0.04).

The variables presenting significant differences between escalation *vs.* nonescalation group the day before the outcome occurred were as follows: respiratory rate (18 ± 5 *vs.* 15 ± 3 breaths/min; *P* = 0.001), PaO₂ (129 ± 61 *vs.* 158 ± 64 mmHg; *P* = 0.025), PaO₂/Fio₂ (201 ± 102 *vs.* 249 ± 83 mmHg; *P* = 0.010), tidal pleural pressure swings (8.9 ± 3.4 *vs.* 5.6 ± 2.0 cm H₂O; *P* < 0.001), mechanical power (9.5 ± 4.7 *vs.* 6.3 ± 3.5 J/min; *P* = 0.003), and its ratio (2.2 ± 1.0 *vs.* 1.5 ± 0.7; *P* = 0.002). Of note, the indexed tidal volume remained similar between groups (7.5 ± 1.6 *vs.* 8.0 ± 2.0 ml/kg_{IBW}; *P* = 0.221; table 2).

The most relevant respiratory variables from the univariate analysis on day 1 were entered in a receiver operating characteristic model to assess their association with the need for treatment escalation (table E1 in supplemental digital content, <http://links.lww.com/ALN/C988>). The mechanical power of the respiratory system and the

Table 2. Lung Mechanics and Gas-Exchange Data

Assessed Variable	First Day of Study			Average Value throughout Study			Day before the Outcome		
	No Treatment Escalation (n = 47)	Treatment Escalation (n = 64)	P Value	No Treatment Escalation (n = 47)	Treatment Escalation (n = 64)	P Value	No Treatment Escalation (n = 47)	Treatment Escalation (n = 64)	P Value
C-PAP FiO_2 , %	66 ± 7 {47}	66 ± 7 {57}	0.750	63 ± 6 {47}	64 ± 7 {50}	0.353	61 ± 8 {47}	66 ± 9 {58}	0.014
C-PAP PEEP, cm H_2O	8.7 ± 1.3 {47}	8.7 ± 1.3 {57}	0.875	8.7 ± 1.1 {47}	8.9 ± 1.2 {51}	0.444	8.8 ± 1.4 {44}	8.8 ± 1.4 {56}	0.956
Tidal volume, ml	443 ± 103 {46}	465 ± 149 {62}	0.370	463 ± 104 {42}	465 ± 116 {49}	0.950	501 ± 147 {45}	489 ± 140 {63}	0.656
Tidal volume/ideal body weight, ml/kg	7.1 ± 1.4 {41}	7.1 ± 1.9 {54}	0.990	7.4 ± 1.2 {38}	7.3 ± 1.6 {42}	0.840	8.0 ± 2.0 {40}	7.5 ± 1.6 {56}	0.221
Respiratory rate, breaths/min	18 ± 5 {46}	20 ± 5 {62}	0.028	17 ± 3 {42}	19 ± 4 {48}	0.016	15 ± 3 {45}	18 ± 5 {63}	< 0.001
Minute ventilation, l/min	7.9 ± 2.4 {46}	9.2 ± 3.0 {62}	0.011	7.9 ± 1.6 {42}	8.4 ± 2.1 {49}	0.137	7.6 ± 2.0 {45}	8.5 ± 2.4 {64}	0.030
Minute ventilation increment, %	111 ± 39 {46}	120 ± 35 {61}	0.227	107 ± 19 {42}	115 ± 24 {48}	0.100	103 ± 23 {45}	111 ± 33 {63}	0.166
PaO_2 , mmHg	141.5 ± 63.0 {46}	111.1 ± 44.3 {62}	0.007	162.3 ± 41.5 {46}	135.8 ± 51.8 {61}	0.004	158 ± 64 {44}	129 ± 61 {60}	0.025
Paco_2 , mmHg	39.1 ± 4.9 {45}	38.1 ± 5.5 {61}	0.327	39.9 ± 4.1 {46}	39.3 ± 4.0 {61}	0.420	40.0 ± 4.9 {44}	39.0 ± 4.7 {60}	0.291
Estimated $\text{PaO}_2/\text{FiO}_2$, mmHg	220 ± 95 {44}	174 ± 64 {58}	0.007	254 ± 66 {46}	213 ± 80 {60}	0.005	249 ± 83 {44}	201 ± 102 {59}	0.010
pH	7.45 ± 0.03 {46}	7.44 ± 0.04 {61}	0.459	7.45 ± 0.02 {46}	7.45 ± 0.02 {61}	0.518	7.46 ± 0.03 {44}	7.45 ± 0.04 {60}	0.119
Tidal pleural pressure, cm H_2O	6.0 ± 3.1 {45}	8.1 ± 3.7 {53}	0.003	6.0 ± 1.9 {45}	8.5 ± 2.8 {41}	< 0.001	5.6 ± 2.0 {32}	8.9 ± 3.4 {38}	< 0.001
Tidal muscular pressure, cm H_2O	8.5 ± 4.3 {44}	11.8 ± 5.2 {51}	0.001	8.6 ± 2.7 {39}	12.2 ± 4.4 {36}	< 0.001	7.8 ± 2.7 {30}	12.8 ± 4.8 {37}	< 0.001
Dynamic elastance – lung, cm $\text{H}_2\text{O}/\text{ml}$	13.7 ± 6.5 {44}	19.4 ± 9.7 {51}	0.001	14.0 ± 5.6 {39}	20.3 ± 7.4 {36}	< 0.001	11.4 ± 4.6 {30}	19.7 ± 8.2 {37}	< 0.001
Ventilatory ratio	1.3 ± 0.4 {40}	1.4 ± 0.4 {53}	0.332	1.2 ± 0.3 {37}	1.3 ± 0.3 {40}	0.485	1.2 ± 0.3 {38}	1.3 ± 0.4 {53}	0.339
Expected baseline mechanical power – respiratory system, J/min	4.2 ± 1.0 {41}	4.5 ± 1.0 {57}	0.144						
Mechanical power, respiratory system, J/min	6.7 ± 4.3 {44}	9.9 ± 6.0 {51}	0.003	6.4 ± 2.3 {39}	9.0 ± 5.0 {36}	0.007	6.3 ± 3.5 {41}	9.5 ± 4.7 {57}	0.003
Mechanical power ratio, respiratory system	1.7 ± 1.5 {39}	2.4 ± 1.4 {45}	0.042	1.5 ± 0.4 {35}	2.2 ± 1.2 {30}	0.003	1.5 ± 0.7 {30}	2.2 ± 1.0 {37}	0.002
ROX index	9.1 ± 2.6 {46}	7.6 ± 2.0 {55}	0.003	9.8 ± 2.3 {41}	8.4 ± 2.4 {35}	0.011	10.9 ± 3.2 {35}	8.7 ± 2.6 {40}	0.002
Pressure-rate index	41.9 ± 13.5 {44}	53.6 ± 16.0 {51}	< 0.001	41.1 ± 8.4 {39}	53.5 ± 14.5 {35}	< 0.001	37.6 ± 8.4 {30}	53.7 ± 14.5 {37}	< 0.001

The table shows the lung mechanics and gas-exchange data summarized as the first day of study, average value throughout the experiment (the average value of all measurement collected from the second day of admission until the day before the outcome), and day before the outcome. The values are presented as means ± SD. The number in curling brackets is the number of individuals (all missing values are either due to missing or insufficient-quality data).

C-PAP, continuous positive airway pressure; FiO_2 , fractional inspired oxygen tension; PEEP, positive end-expiratory pressure; ROX, ratio of oxygen saturation measured by pulse oximetry/ FiO_2 to respiratory rate.

mechanical power ratio showed areas under the curve of 0.738 (95% CI, 0.636 to 0.839; $P < 0.001$) and 0.734 (95% CI, 0.625 to 0.844; $P < 0.001$), while the area under the curve of tidal muscular pressure was 0.700 (95% CI, 0.595 to 0.804; $P < 0.001$). The area under the curve of the respiratory rate index was 0.659 (95% CI, 0.549 to 0.769; $P = 0.006$), while the area under the curve of pressure-rate index was 0.733 (95% CI, 0.631 to 0.835). The relative receiver operating characteristics are shown in figures E1 and E2 of the supplemental material (<http://links.lww.com/ALN/C988>).

Figure 1 depicts the time evolution of $\text{PaO}_2/\text{FiO}_2$ and Paco_2 (indicators of the efficiency of the gas exchanger), the tidal muscular pressure and dynamic lung elastance (indicators of the lung mechanics), and the indexed tidal volume and mechanical power ratio (indicators of the effort undertaken by the patient). The time evolution is detailed in three steps:

(1) record collected on day 1; (2) average of the records collected from day 2 until the day before the outcome; and (3) record collected the day before the outcome. All tested variables but Paco_2 and indexed tidal volume showed significant differences between groups when analyzed at each time point; conversely, when analyzing the evolution of such variables over time, the only variables presenting significant differences were the $\text{PaO}_2/\text{FiO}_2$ ratio and the indexed tidal volume (fig. 1).

Discussion

In a previous study based on the same cohort and data on COVID-19 patients in continuous positive airway pressure, we observed that total lung stress was the best predictive variable of disease evolution¹: patients who required invasive mechanical ventilation had a lower $\text{PaO}_2/\text{FiO}_2$ ratio and greater lung stress. In this study, we were able to assess not

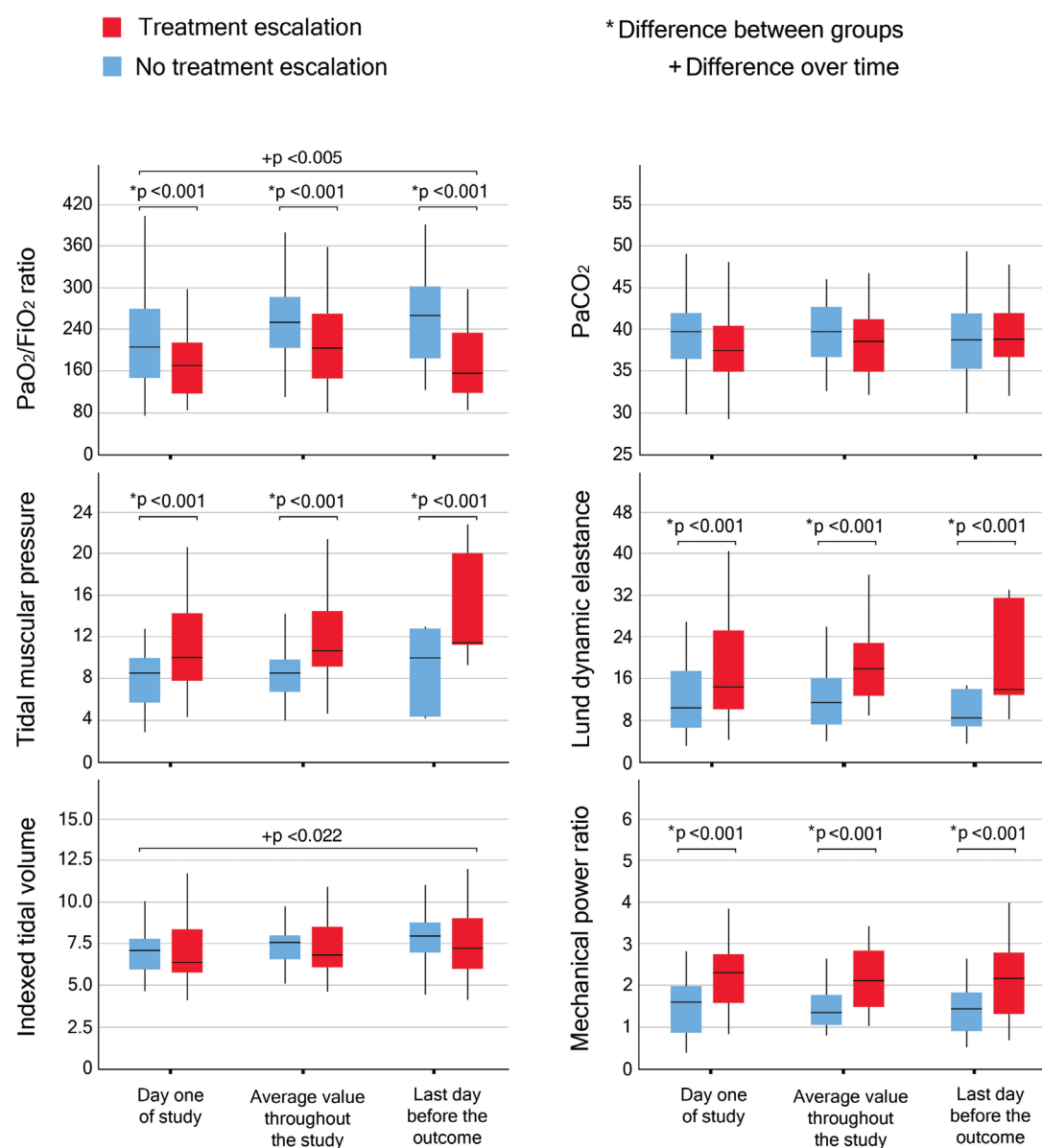


Fig. 1. Time course of PaO₂/fractional inspired oxygen tension (FiO₂) ratio and PaCO₂ (mmHg; *top*), tidal muscular pressure (cm H₂O), and lung dynamic elastance (cm/l; *middle*), indexed tidal volume (ml/kg_{IBW}), and mechanical power ratio (*bottom*). An asterisk indicates difference between groups, while a plus sign refers to difference over time.

only the stress through the esophageal pressure measurement but also tidal volume and respiratory rate, so that we could assess mechanical power, dynamic lung elastance, and muscular pressure (P_{mus}). In addition, we computed two recently described predictive indexes, the respiratory rate index,¹⁷ which is designed to predict high-flow nasal cannulas and continuous positive airway pressure failure, and the pressure-rate index,¹⁸ which combined the two variables most strongly associated with the outcome (driving

pressure and respiratory rate) in a mechanically ventilated population.

The novel information we observed in this current analysis is that the tidal volume, rather unexpectedly, was similar in the two outcome groups. The groups differed, however, in terms of respiratory rate, minute ventilation, and mechanical power. This behavior depicts a clear trend: for the same impairment of the lung structures, as quantified by the lung computed tomography scan, the patients

in the treatment escalation group maintained normal PaCO_2 without increasing the tidal volume, but with a significant increase of the respiratory effort and energy requirement, as shown by the increased esophageal pressure swing, muscular pressure, mechanical power, and minute ventilation. Furthermore, we explored the association between several variables and the need for respiratory treatment escalation, and we identified the mechanical power, the mechanical power ratio, and the pressure-rate index to have the highest area under the curve, respectively: 0.738; 0.734, and 0.733.

This is an interesting finding as most current criteria evaluating the risk failure of noninvasive support are based on a threshold value of tidal volume beyond which the risk of failure is considered high: *i.e.*, 9 to 9.5 ml/kg.^{19,20} On the contrary, the HACOR score (heart rate, acidosis, consciousness, oxygenation, and respiratory rate), used to determine the risk of failure of noninvasive ventilation, does not include the tidal volume but includes respiratory rate, oxygenation, and pH among the respiratory variables.²¹ Although these studies were performed pre-COVID-19 in patients with hypoxemic respiratory failure of mixed etiology, these criteria have been extrapolated in the management of COVID-19. Therefore, the approaches illustrated in this study may improve the detection of risk of failure specifically in COVID-19–related acute hypoxemic respiratory failure.

The escalation of the respiratory treatment from continuous positive airway pressure to noninvasive or invasive mechanical ventilation is usually consequent to a worsening in respiratory conditions. As previously reported, the decision to intubate or not a patient with COVID-19 pneumonia is cumbersome and based on several clinical assessments²²; therefore, to identify all patients presenting unfavorable clinical evolution, we allocated in the poor clinical outcome group all individuals requiring either non-invasive or invasive mechanical ventilation.

In our cohort, most of the respiratory variables were significantly worse in the treatment escalation group (table 2). Unfortunately, it is not possible to discriminate the contribution of the natural course of the disease *versus* the potential lung damage induced by a high-stress ventilation (patient self-induced lung injury) in leading to unfavorable outcome, because the clinical presentation of these conditions is identical: progressive impairment of gas exchange and lung mechanics.²³ However, although it is impossible to discriminate between the changes induced by the COVID-19 disease *per se* and patient self-induced lung injury, we may hypothesize that an increased respiratory effort at admission (higher stress and mechanical power in the treatment escalation group) may contribute to the further deterioration of the lung parenchyma through a vortex that we previously called the “shrinking baby lung,”²⁴ regardless of the severity of impairment as determined by lung computed tomography. Although the

two groups presented comparable patterns at computed tomography analysis, the perfusion derangements should be higher in the group undergoing treatment escalation (lower $\text{PaO}_2/\text{FiO}_2$ ratio at day 1) leading to a higher PaCO_2 . This, in turn, should increase the respiratory effort leading to a higher stress and mechanical power, worsening the inflammation within the lungs and promoting the vortex. Of note, the discrepancy between the expected oxygenation assessed by the lung computed tomography scan (anatomical shunt) and the actual oxygenation is well known,¹ and it seems to be caused by a significant alteration in perfusion, including an increased intrabronchial shunt,²⁵ leading to an excess in venous admixture not explained by the anatomical changes in the lung parenchyma.^{26–29}

In this study, we were able to compute the mechanical power as the patients were monitored with an esophageal balloon, and the tidal volume and minute ventilation were also collected. The total stress may be in part overestimated as it was not computed in static conditions, however, because the mechanical power estimates the energy over time; it should also include the dynamic components. For this reason, and more importantly because the respiratory rate is included in its calculation, the mechanical power may be the most comprehensive variable to quantify the lungs derangements that are actually occurring in the patient. The relevance of respiratory rate is well exemplified in the current study: whether the energetic cost per breath was only slightly different between two study cohorts (as in our cohort: similar tidal volume and different pleural pressure), the inclusion of the respiratory rate in the assessment of the energetic cost for each breath may enhance the signal effect. Of note, the measurement of esophageal pressure is a procedure that could lead to better understanding of the physiologic changes and possibly tailoring the respiratory treatment for a specific subset of patients. However, there are challenges associated with the wider adoption of this monitoring techniques, due to familiarity and invasiveness, and therefore decision-making needs to be informed by wider clinical risk–benefit ratio.

One of the unsolved problems referring to the mechanical power is its normalization; attempts were done by referring it to the respiratory system compliance,³⁰ but the conceptual problem of the variable relationship between compliance and functional residual capacity still persists. Indeed, it is worth recalling that the mechanical power is necessary for life (*i.e.*, it cannot be zero); therefore, more than the quantification of mechanical power in different individuals, the real issue is to quantify its relative “excess.” In this article, we tried to normalize the mechanical power by relating it to the expected normal mechanical power for a given individual, using the same approach of the ventilatory ratio. We referred to a ventilation of 0.1 l/(kg · min), airway resistances of 10 cm $\text{H}_2\text{O}/(\text{ml} \cdot \text{s})$, a respiratory rate of 15 breaths/min and an I:E ratio of 1:2. In this setting, a

70-kg individual at rest would require a mechanical power of 4.84 J/min, a value that is consistent with the reports in the literature.³¹ Using this approach, it is possible to quantify the excess and defect of the actual mechanical power. In our cohort, the mechanical power ratio of patients undergoing the escalation of the respiratory treatment was nearly 50% greater compared to patients with favorable outcome.

Limitations

The major limitation of the current study is the use of clinical criteria and the lack of a protocolized hard criteria when escalating the respiratory support. This may have led to variations in practice such that some patients received escalation later than anticipated or when other clinical criteria—not captured by respiratory parameters—occurred. However, all patients were admitted to a high-dependency COVID-19 unit, where clinical activities are focused on COVID-19 patients, and the clinical management is standardized according to the institutional protocols. Conversely, one of its strengths is the combination of tidal volume and esophageal pressure measurements in spontaneous breathing patients, allowing the calculation of mechanical power and its relative ratio. We also recognize that all measurements, taken in dynamic condition, cannot equate to the usual static assessment. This limitation, however, is mandatory during spontaneous breathing and may present the advantage of a more realistic assessment of the energy required by the patient to sustain the breathing process. Although the use of local institutional guidelines should have minimized the risk of bias, it is possible that some unrecognized bias was present during the study. Because of the design and set-up of the study, we used average values to compare different groups and time points, and this could lead to regression artifact into the analysis. Another limitation is the assumption that the ratio between lung and total elastances equals 0.7. However, because in the early stages of COVID-19, pneumonia lung mechanics are usually preserved,¹ we do not expect this ratio to be significantly different from 0.7 when assessed in our population. Finally, we cannot exclude that an obese patient in a semirecumbent position may present some degree of flow limitation and, consequently, auto-PEEP.

Conclusions

In our cohort of spontaneously breathing COVID-19 patients, the patients' respiratory pattern was comparable between groups and within the limits of lung protective strategy. Our study points out the paramount importance of respiratory rate and tidal pleural pressure, both usually ignored when lung protective strategy is applied, in modifying the outcome. Among all assessed variables, mechanical power and mechanical power ratio had the highest area under the curve when assessing the clinical outcome.

Acknowledgments

The authors thank all the nurses and physicians at Ospedale San Paolo (Milan, Italy) who helped with data collection and patient care. They are also grateful to Respiratory Motion Inc. (Watertown, Massachusetts) for providing the ExSpirom monitors.

Research Support

Supported by institutional and/or departmental sources and from Sartorius AG (Göttingen, Germany) through an unrestricted grant for lung injury-related research to the Department of Anesthesiology, University Medical Center Göttingen, Göttingen, Germany.

Competing Interests

Dr. Gattinoni reports a consultancy for General Electrics (Boston, Massachusetts) and SIDAM (Modena, Italy). He also receives lecture fees from ESTOR (Pero, Italy) and Mindray (Darmstadt, Germany). Dr. Saager has received payments from the Surgical Company Netherlands (Amersfoort, The Netherlands) for consultancy work. The other authors declare no competing interests.

Correspondence

Address correspondence to Dr. Gattinoni: University Medical Center Göttingen, Robert Koch Strasse 40, Göttingen, Germany. gattinoniluciano@gmail.com. This article may be accessed for personal use at no charge through the Journal Web site, www.anesthesiology.org.

Supplemental Digital Content

Supplemental Material, <http://links.lww.com/ALN/C988>

References

1. Coppola S, Chiumello D, Busana M, Giola E, Palermo P, Pozzi T, Steinberg I, Roli S, Romitti F, Lazzari S, Gattarello S, Palumbo M, Herrmann P, Saager L, Quintel M, Meissner K, Camporota L, Marini JJ, Centanni S, Gattinoni L: Role of total lung stress on the progression of early COVID-19 pneumonia. *Intensive Care Med* 2021; 47:1130–9
2. Gattinoni L, Tonetti T, Cressoni M, Cadringer P, Herrmann P, Moerer O, Protti A, Gotti M, Chiurazzi C, Carlesso E, Chiumello D, Quintel M: Ventilator-related causes of lung injury: The mechanical power. *Intensive Care Med* 2016; 42:1567–75
3. Apigo M, Schechtman J, Dhliwayo N, Tameemi M, Gazmuri RJ: Development of a Work of Breathing scale and monitoring need of intubation in COVID-19 pneumonia. *Critical Care* 2020; 24:477
4. Borg G, Ljunggren G, Ceci R: The increase of perceived exertion, aches and pain in the legs, heart

- rate and blood lactate during exercise on a bicycle ergometer. *Eur J Appl Physiol Occup Physiol* 1985; 54:343–9
5. Herrmann P, Busana M, Cressoni M, Lotz J, Moerer O, Saager L, Meissner K, Quintel M, Gattinoni L: Using artificial intelligence for automatic segmentation of CT lung images in acute respiratory distress syndrome. *Front Physiol* 2021; 12:676118
 6. Ibanez J, Raurich JM: Normal values of functional residual capacity in the sitting and supine positions. *Intensive Care Med* 1982; 8:173–7
 7. Cressoni M, Gallazzi E, Chiurazzi C, Marino A, Brioni M, Menga F, Cigada I, Amini M, Lemos A, Lazzarini M, Carlesso E, Cadringher P, Chiumello D, Gattinoni L: Limits of normality of quantitative thoracic CT analysis. *Crit Care* 2013; 17:R93
 8. Voscopoulos C, Brayanov J, Ladd D, Lalli M, Panasyuk A, Freeman J: Special article: Evaluation of a novel noninvasive respiration monitor providing continuous measurement of minute ventilation in ambulatory subjects in a variety of clinical scenarios. *Anesth Analg* 2013; 117:91–100
 9. Schumann R, Harvey B, Zahedi F, Bonney I: Minute ventilation assessment in the PACU is useful to predict postoperative respiratory depression following discharge to the floor: A prospective cohort study. *J Clin Anesth* 2019; 52:93–8
 10. Galvagno SM, Brayanov JB, Corneille MG, Voscopoulos CJ, Sordo S, Ladd D, Freeman JE: Non-invasive respiratory volume monitoring in patients with traumatic thoracic injuries. *Trauma* 2015; 17:219–23
 11. Qiu C, Cheng E, Winnick SR, Nguyen VT, Hou FC, Yen SS, Custodio GD, Dang JH, LaPlace D, Morkos A, Chung EP, Desai VN: Respiratory volume monitoring in the perioperative setting across multiple centers. *Respir Care* 2020; 65:482–91
 12. Voscopoulos CJ, MacNabb CM, Brayanov J, Qin L, Freeman J, Mullen GJ, Ladd D, George E: The evaluation of a non-invasive respiratory volume monitor in surgical patients undergoing elective surgery with general anesthesia. *J Clin Monit Comput* 2015; 29:223–30
 13. Gattinoni L, Carlesso E, Cadringher P, Valenza F, Vagginelli F, Chiumello D: Physical and biological triggers of ventilator-induced lung injury and its prevention. *Eur Respir J* 2003; 47:15s–25s
 14. Sinha P, Fauvel NJ, Singh S, Soni N: Ventilatory ratio: A simple bedside measure of ventilation. *Br J Anaesth* 2009; 102:692–7
 15. Nunn JF: Ventilation nomograms during anaesthesia. *Anaesthesia* 1960; 15:65
 16. Butler J, Caro CG, Alcalá R, Dubois AB: Physiological factors affecting airway resistance in normal subjects and in patients with obstructive respiratory disease. *J Clin Invest* 1960; 39:584–91
 17. Roca O, Caralt B, Messika J, Samper M, Sztrymf B, Hernandez G, Garcia-de-Acila M, Frat JP, Masclans JR, Ricard JD: An index combining respiratory rate and oxygenation to predict outcome of nasal high-flow therapy. *Am J Respir Crit Care Med* 2019; 199:1368–76
 18. Costa E, Slutsky A, Brochard L, Brower R, Serpa-Neto A, Cavalcanti A, Mercat A, Meade M, Morais C, Goligher E, Carvalho C, Amato M: Ventilatory variables and mechanical power in patients with acute respiratory distress syndrome. *Am J Respir Crit Care Med* 2021; 204:303–11
 19. Carteaux G, Millán-Guilarte T, De Prost N, Razazi K, Abid S, Thille AW, Schortgen F, Brochard L, Brun-Buisson C, Mekontso Dessap A: Failure of noninvasive ventilation for de novo acute hypoxemic respiratory failure: Role of tidal volume. *Crit Care Med* 2016; 44:282–90
 20. Frat JP, Ragot S, Girault C, Perbet S, Prat G, Boulain T, Demoule A, Ricard JD, Coudroy R, Robert R, Mercat A, Brochard L, Thille AW; REVA network: Effect of non-invasive oxygenation strategies in immunocompromised patients with severe acute respiratory failure: A post-hoc analysis of a randomised trial. *Lancet Respir Med* 2016; 4:646–52
 21. Duan J, Han X, Bai L, Zhou L, Huang S: Assessment of heart rate, acidosis, consciousness, oxygenation, and respiratory rate to predict noninvasive ventilation failure in hypoxemic patients. *Intensive Care Med* 2017; 43:192–9
 22. Tobin M: The criteria used to justify endotracheal intubation of patients with COVID-19 are worrisome. *Can J Anaesth* 2021; 68:258–9
 23. Mascheroni D, Kolobow T, Fumagalli R, Moretti MP, Chen V, Buckhold D: Acute respiratory failure following pharmacologically induced hyperventilation: An experimental animal study. *Intensive Care Med* 1988; 15:8–14
 24. Marini JJ, Gattinoni L: Time course of evolving ventilator-induced lung injury: the “shrinking baby lung.” *Crit Care Med* 2020; 48:1203–9
 25. Galambos C, Bush D, Abman SH: Intrapulmonary bronchopulmonary anastomoses in COVID-19 respiratory failure. *Eur Respir J* 2021; 58:2004397
 26. Busana M, Giosa L, Cressoni M, Gasperetti A, Di Girolamo L, Martinelli A, Sonzogni A, Lorini L, Palumbo MM, Romitti F, Gattarello S, Steinberg I, Herrmann P, Meissner K, Quintel M, Gattinoni L: The impact of ventilation-perfusion inequality in COVID-19: A computational model. *J Appl Physiol* (1985) 2021; 130:865–76
 27. Gattinoni L, Gattarello S, Steinberg I, Busana M, Palermo P, Lazzari S, Romitti F, Quintel M, Meissner K, Marini JJ, Chiumello D, Camporota L: COVID-19

- pneumonia: Pathophysiology and management. *Eur Respir Rev* 2021; 30:210138.
28. Herrmann J, Mori V, Bates JHT, Suki B: Modeling lung perfusion abnormalities to explain early COVID-19 hypoxemia. *Nat Commun* 2020; 11:4883
 29. Ackermann M, Verleden SE, Kuehnel M, Haverich A, Welte T, Laenger F, Vanstapel A, Werlein C, Stark H, Tzankov A, Li WW, Li VW, Mentzer SJ, Jonigk D: Pulmonary vascular endothelialitis, thrombosis, and angiogenesis in COVID-19. *N Engl J Med* 2020; 383:120–8
 30. Ghiani A, Paderewska J, Walcher S, Tsitouras K, Claus Neurohr C, Kneidinger N: Mechanical power normalized to lung–thorax compliance indicates weaning readiness in prolonged ventilated patients. *Sci Rep* 2022; 12:6
 31. Rehder K, Marsh HM: Respiratory Mechanics during Anesthesia and Mechanical Ventilation, *Handbook of Physiology*. Hoboken, Wiley; pp 737–52.

ANESTHESIOLOGY REFLECTIONS FROM THE WOOD LIBRARY-MUSEUM

Emanuel Papper's Ph.D.: Anesthesia's Romantic Ideals



Later in life, Emanuel M. Papper, M.D., Ph.D. (1915 to 2002), would describe his tenure as Chair of the newly independent Department of Anesthesiology at Columbia University as a time “as exciting as Camelot must have been in ancient Britain.” After 17 productive years, followed by 12 more as Dean of the University of Miami School of Medicine, Papper would seize a unique opportunity to combine two loves—anesthesia and British culture. At age 75, he received his Ph.D. in English at the University of Miami for a dissertation on British Romantic poetry and the birth of surgical anesthesia. Given the description of anesthetic gases like ether as early as 1540, Papper wondered why anesthesia was not “discovered” until 1846. He argued that British Romanticism, by celebrating individualism, the pursuit of happiness, and the beauty of nature, popularized the concept of freedom from suffering as an intrinsic human right. Thus, the Romantics prepared society to seek and to embrace the advent of anesthesia. Artist John Constable’s *Salisbury Cathedral from the Meadows* (1831, above) reflects Romanticism’s deep connection with nature—at times a symbol of turbulence (clouds, above), at others a wellspring of tranquility, health, and hope (rainbow, above). (Papper EM. *Perspect Biol Med* 1992; 35:401–15. Artwork © Tate. CC-BY-NC-ND 3.0). (Copyright © the American Society of Anesthesiologists’ Wood Library-Museum of Anesthesiology. www.woodlibrarymuseum.org)

Jane S. Moon, M.D., Assistant Clinical Professor, Department of Anesthesiology and Perioperative Medicine, University of California, Los Angeles, California.

ANESTHESIOLOGY

Predicting Intensive Care Delirium with Machine Learning: Model Development and External Validation

Kirby D. Gong, M.S.E., Ryan Lu, B.S., M.D., Ph.D.,
Teya S. Bergamaschi, M.S.E., Ph.D., Akaash Sanyal, M.S.E.,
Joanna Guo, B.S., Han B. Kim, M.S.E., Hieu T. Nguyen, B.S., Ph.D.,
Joseph L. Greenstein, Ph.D., Raimond L. Winslow, Ph.D.,
Robert D. Stevens, M.D.

ANESTHESIOLOGY 2023; 138:299–311

EDITOR'S PERSPECTIVE

What We Already Know about This Topic

- Existing intensive care unit (ICU) delirium prediction models consider a parsimonious set of clinical variables, lack dynamic prediction capability, and have received limited external validation

What This Manuscript Tells Us That Is New

- In a multicenter electronic health record database of 22,234 intensive care unit (ICU) patients from 2014 to 2015, delirium was identified using the Confusion Assessment Method for the ICU screen or Intensive Care Delirium Screening Checklist
- Static and dynamic machine learning algorithms were trained, tested, and externally validated to predict the onset of delirium during the ICU stay
- The static model using data from the first 24 h after ICU admission to predict delirium at any point during the ICU stay demonstrated higher discrimination compared with a widely cited reference model
- The dynamic model was able to predict delirium up to 12 h in advance with reasonable discrimination and calibration

ABSTRACT

Background: Delirium poses significant risks to patients, but countermeasures can be taken to mitigate negative outcomes. Accurately forecasting delirium in intensive care unit (ICU) patients could guide proactive intervention. Our primary objective was to predict ICU delirium by applying machine learning to clinical and physiologic data routinely collected in electronic health records.

Methods: Two prediction models were trained and tested using a multicenter database (years of data collection 2014 to 2015), and externally validated on two single-center databases (2001 to 2012 and 2008 to 2019). The primary outcome variable was delirium defined as a positive Confusion Assessment Method for the ICU screen, or an Intensive Care Delirium Screening Checklist of 4 or greater. The first model, named "24-hour model," used data from the 24 h after ICU admission to predict delirium any time afterward. The second model designated "dynamic model," predicted the onset of delirium up to 12 h in advance. Model performance was compared with a widely cited reference model.

Results: For the 24-h model, delirium was identified in 2,536 of 18,305 (13.9%), 768 of 5,299 (14.5%), and 5,955 of 36,194 (11.9%) of patient stays, respectively, in the development sample and two validation samples. For the 12-h lead time dynamic model, delirium was identified in 3,791 of 22,234 (17.0%), 994 of 6,166 (16.1%), and 5,955 of 28,440 (20.9%) patient stays, respectively. Mean area under the receiver operating characteristics curve (AUC) (95% CI) for the first 24-h model was 0.785 (0.769 to 0.801), significantly higher than the modified reference model with AUC of 0.730 (0.704 to 0.757). The dynamic model had a mean AUC of 0.845 (0.831 to 0.859) when predicting delirium 12 h in advance. Calibration was similar in both models (mean Brier Score [95% CI] 0.102 [0.097 to 0.108] and 0.111 [0.106 to 0.116]). Model discrimination and calibration were maintained when tested on the validation datasets.

Conclusions: Machine learning models trained with routinely collected electronic health record data accurately predict ICU delirium, supporting dynamic time-sensitive forecasting.

(*ANESTHESIOLOGY* 2023; 138:299–311)

Delirium is common in the acute care setting and particularly in intensive care units (ICUs), affecting up to 35% of hospitalized patients and up to 80% of patients requiring intensive care,¹ and costing an estimated \$164

This article is featured in "This Month in Anesthesiology," page A1. Supplemental Digital Content is available for this article. Direct URL citations appear in the printed text and are available in both the HTML and PDF versions of this article. Links to the digital files are provided in the HTML text of this article on the Journal's Web site (www.anesthesiology.org). This article has a visual abstract available in the online version. Part of the data in this article was presented at the 50th Critical Care Congress, February 3, 2021, held virtually; the International Anesthesia Research Society Annual Meeting, May 15, 2021, held virtually; the European Society of Intensive Care Medicine's Linking Innovation Vision Excellence Science (LIVES) 2021, October 3, 2021, held virtually; Neurocritical Care Society Annual Meeting, October 26, 2021, held virtually.

Submitted for publication March 21, 2022. Accepted for publication December 8, 2022. Published online first on December 20, 2022.

Kirby D. Gong, M.S.E.: Johns Hopkins University School of Medicine, Baltimore, Maryland.

Ryan Lu, B.S., M.D., Ph.D.: Northwestern University, Evanston, Illinois.

Teya S. Bergamaschi, M.S.E., Ph.D.: Massachusetts Institute of Technology, Cambridge, Massachusetts.

Akaash Sanyal, M.S.E.: Johns Hopkins University, Baltimore, Maryland.

Joanna Guo, B.S.: Johns Hopkins University, Baltimore, Maryland.

Copyright © 2023, the American Society of Anesthesiologists. All Rights Reserved. *Anesthesiology* 2023; 138:299–311. DOI: 10.1097/ALN.0000000000004478

billion annually in healthcare expenditures.² The onset of delirium in hospitalized patients has been independently associated with poor short-term and long-term health outcomes, and research aimed at preventing or treating delirium is regarded as a public health priority.³

Approximately 30 to 40% of delirium cases might be amenable to delirium-reduction strategies.⁴ Multicomponent interventions focusing on device and catheter removal, promotion of normal sleep-wake cycles, and early mobilization are cost-effective methods for preventing and treating delirium.⁴ In critically ill patients, implementation of a structured bundle of treatments has been associated with a 40% reduction in delirium in a multisite cohort of more than 15,000 critically ill patients,⁵ and use of the α_2 agonist dexmedetomidine could decrease delirium risk by up to 48% in ICU patients requiring sedation. Although these approaches are promising, ICU delirium may be underrecognized and misdiagnosed.⁷ Delirium screening is inconsistent in many health systems and, even when consistently deployed, may not capture relevant events due to the acute onset and fluctuating nature of the disorder.⁸

Research during the past two decades has identified a number of delirium risk factors, some of which may be modifiable.³ The ability to predict delirium onset in high-risk individuals might allow preventive or treatment strategies to be implemented in a more targeted or even personalized fashion. Here, we created two models to predict delirium: an early prediction model to identify delirium onset at any time during intensive care by using data available early in the ICU stay, and a dynamic model to predict the onset of delirium 0 to 12 h in the future. We hypothesized that physiologic and clinical variables routinely acquired during intensive care would be associated with the probability of delirium onset.

Materials and Methods

The overarching goal was to predict the onset of ICU delirium by training machine learning models with physiologic and clinical features routinely available at the bedside. If our primary hypothesis is correct, we will reject the null hypothesis that physiologic and clinical variables routinely acquired during intensive care have no relation to the probability of delirium onset. Research followed the Transparent Reporting of a Multivariable Prediction Model for Individual Prognosis checklist,⁹ a copy of which is provided in table E1 of the Supplemental Digital Content (<http://links.lww.com/ALN/C999>). The model pipeline is schematized in figure E1 in the Supplemental Digital Content

(<http://links.lww.com/ALN/C999>). All code is available on GitHub at <https://github.com/ryanlu41/delirium>.

The data analysis and statistical plan for the first 24-h model development were written and recorded in the investigators' files before data were accessed, while additional model development occurred after the data were accessed. This included determining which patients developed delirium in the development dataset and extracting features guided by domain expertise. The distribution differences of these features were compared using Mann-Whitney U tests (for nonparametric comparison of continuous feature means in two independent samples), or chi-square tests (for comparison of proportions in categorical data). All analyses use a *P*-value threshold of 0.05 for significance. Statistical and machine learning software packages used are detailed in subsequent sections.

Data Sources

Research in this report was performed on three fully deidentified publicly available datasets made available *via* the Massachusetts Institute of Technology (Cambridge, Massachusetts) PhysioNet repository¹⁰: the Philips eICU Collaborative Research Database (hereafter referred to as the development dataset), the third version of Medical Information Mart for Intensive Care (often abbreviated as MIMIC-III, and hereafter referred to as validation dataset 1), and the fourth version of Medical Information Mart for Intensive Care (often abbreviated as MIMIC-IV, and hereafter referred to as validation dataset 2). The former was used for model training and testing, while the latter two were used for external validation. The development dataset is a multicenter electronic health record–based database containing granular data on 200,859 admissions to ICUs from between 2014 and 2015 at 208 hospitals located in the United States.¹¹ Validation dataset 1 comprises electronic health record data from 61,532 ICU stays at Beth Israel Deaconess Medical Center in Boston, Massachusetts, from 2001 to 2012.¹² Validation dataset 2 comprises electronic health record data from 76,943 ICU stays at Beth Israel Deaconess Medical Center from 2008 to 2019.¹³ Both validation datasets likely do have some overlap in data due to being from the same hospital and having several years in common.

Data in both validation databases have been deidentified, and the institutional review boards of Massachusetts Institute of Technology (number 0403000206) and Beth Israel Deaconess Medical Center (number 2001-P-001699/14) both approved the use of the database for research. Because the database does not contain protected health information, a waiver of the requirement

Han B. Kim, M.S.E.: Johns Hopkins University School of Medicine, Baltimore, Maryland.

Hieu T. Nguyen, B.S., Ph.D.: Johns Hopkins University School of Medicine, Baltimore, Maryland.

Joseph L. Greenstein, Ph.D.: Whiting School of Engineering at Johns Hopkins University, Baltimore, Maryland.

Raimond L. Winslow, Ph.D.: Whiting School of Engineering at Johns Hopkins University, Baltimore, Maryland.

Robert D. Stevens, M.D.: Johns Hopkins University School of Medicine, Baltimore, Maryland.

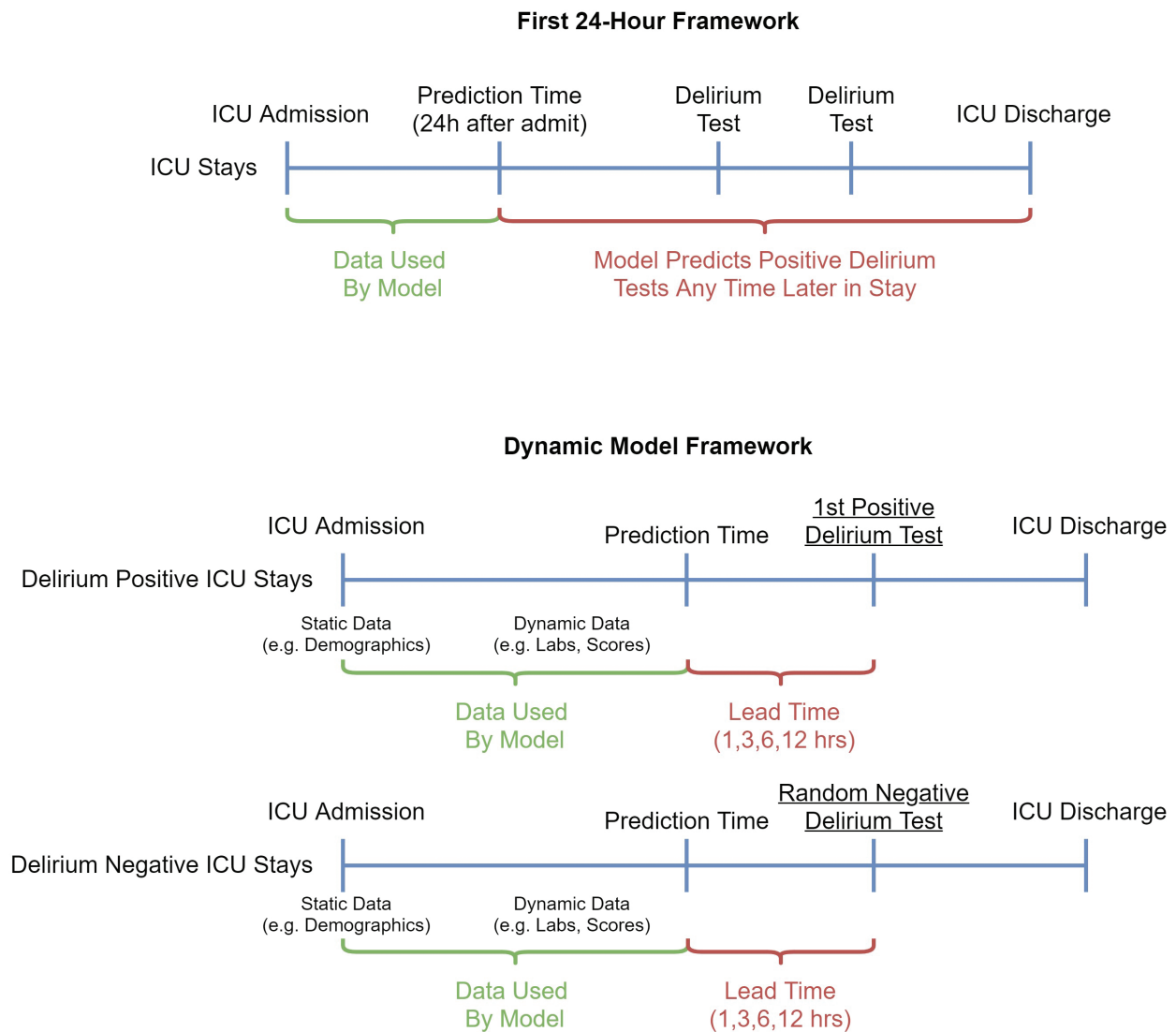


Fig. 1. Model frameworks for the first 24-h and dynamic modeling paradigms. ICU, intensive care unit.

for informed consent was included in the institutional review board approval. Data in the development dataset are also deidentified, and research using the development dataset is exempt from institutional review board approval due to the retrospective design, lack of direct patient intervention, and the security schema, for which the reidentification risk was certified as meeting safe harbor standards by an independent privacy expert (Privacert, Cambridge, Massachusetts; Health Insurance Portability and Accountability Act Certification number 1031219–2).

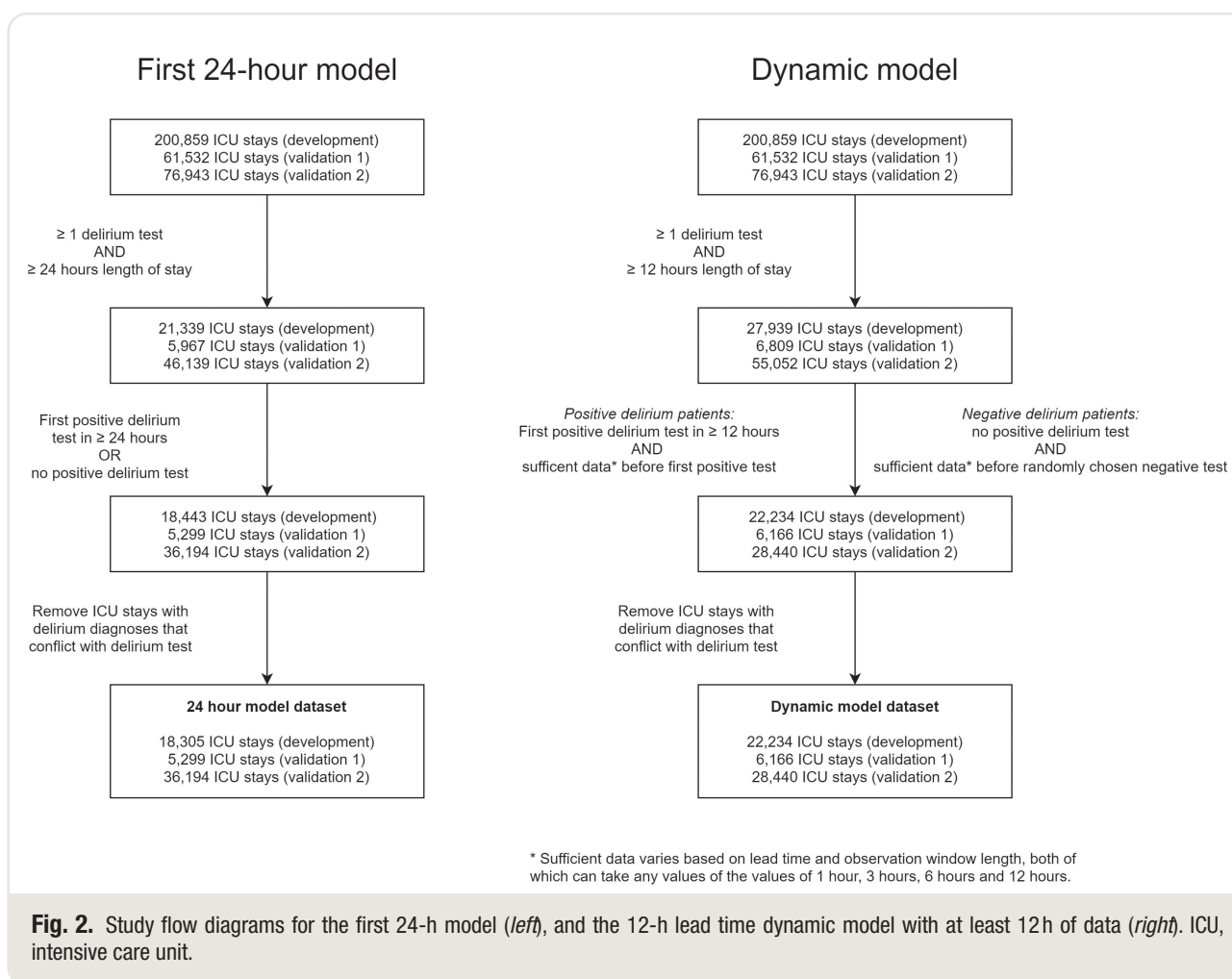
Modeling Paradigms

Two modeling paradigms were created (fig. 1). The first, named the “first 24-hour model,” analyzed data collected

in the 24 h after ICU admission to predict the probability of delirium at any subsequent point during the ICU stay. The second model, designated “dynamic model,” used cumulative data from ICU admission to the prediction time point and computed the probability of delirium onset 0 to 12 h in the future. For ICU stays with delirium, the model was trained on data obtained before the first positive delirium screen. For ICU stays without delirium, the model was trained on data obtained before a randomly selected negative delirium screen.

Case Identification

Flow diagrams illustrating the process for case identification and selection are shown in figure 2. Patient



stays were selected for the first 24-h model if they were admitted to the ICU, remained in the ICU for at least 24h, and were screened for delirium using the Confusion Assessment Method for the Intensive Care Unit¹⁴ or the Intensive Care Delirium Screening Checklist.¹⁵ To limit the possibility that patients had delirium before the time of prediction, we excluded patient stays in which there was a positive delirium test or diagnosis in the first 24 h.

For the dynamic model, we selected ICU stays of patients who were in the ICU for at least 12h and who had at least one delirium screening. To limit the possibility that patients entered the ICU with delirium, we excluded patients in whom there was a positive delirium screen or diagnosis in the first 12h. Delirium-positive cases were identified by finding the first positive Confusion Assessment Method for the ICU or Intensive Care Delirium Screening Checklist screen in a patient stay, defining that time point as delirium onset, and using data preceding onset to make predictions. The median time (and interquartile range) of delirium onset in the 12-h

lead time dynamic development model cohort was 61.3 (38.3 to 109.5) hours after ICU admission. Delirium-negative cases were obtained by finding ICU stays where all delirium screening was negative, randomly selecting one of the screens, and using data from before that delirium test to make predictions. The median time (and interquartile range) of these randomly selected negative delirium screens in the development cohort was 39.7 (30.4 to 59.8) hours after ICU admission. This resulted in the model making predictions across a wide range of times in ICU stays.

Outcome Variable

The primary outcome variable was delirium, defined as a positive Confusion Assessment Method for the ICU screen, a score of 4 or more on the Intensive Care Delirium Screening Checklist, without any contradictions from diagnostic code information. Both Confusion Assessment Method for the ICU and Intensive Care Delirium Screening Checklist scores are documented in the

development dataset, while only the Confusion Assessment Method for the ICU is recorded in both validation databases. Additionally, the development database marks some patients with a free text delirium diagnosis. Patients with this diagnosis alone and no positive delirium screenings were excluded from the study. In the development dataset, the median (interquartile range) interval between delirium tests was 4.0 h (1.0 to 12.0 h), while in validation dataset 1 it was 9.2 h (4.0 to 13.3 h) and in validation dataset 2 it was 9.4 h (4.0 to 12.3 h).

Predictive Variables

Predictive variables to consider in the model were identified through literature review, clinician guidance, and dataset exploration. Variables extracted included patient demographics, medical history and comorbidities, laboratory studies, medications administered, other treatments, nurse documentation, and physiologic time series (both nurse-validated data and automated data from monitors), with all time stamps being recorded at minute-level resolution. All variables used in the model were temporally distinct from data used in assessing outcomes. All analyses up to this point were done using Python, specifically the *numpy*¹⁶ and *pandas*¹⁷ packages, with the exception of the comorbidity features that were created using the R package *comorbidity*.¹⁸

Preprocessing

The distributions of each feature were examined by a fellowship-trained, board-certified intensive care physician, who helped define upper and lower bounds of physiologic plausibility; values deemed implausible were then removed. For each model and lead time, features with more than 20% of samples missing were excluded, which primarily resulted in the removal of less common laboratory tests from the feature space, such as alkaline phosphate measurements or monocyte counts. Missing values were then imputed using mean imputation, based on training data means.

Feature Development and Analysis

Predictive features were created from the processed data. Categorical variables were one-hot encoded into individual features (*i.e.*, translated into binary variables) and sometimes grouped together for simplicity. For numerical variables with multiple values during the patient stay, estimates of central tendency and variance such as means and standard deviations were calculated. For higher frequency variables such as respiratory rate, heart rate, blood pressure, or oxygen saturation data, more complex features such as Fourier transform coefficients or wavelets were computed using the Python *tsfresh* package.¹⁹ A full list of features used in the models is available in table E2 in the Supplemental Digital Content (<http://links.lww.com/ALN/C999>).

Model Development

Model features were analyzed using three machine learning algorithms: logistic regression, random forest,²⁰ and gradient boosting (CatBoost²¹), as well as an ensemble or stacked model using outputs from all three algorithms. All modeling and evaluation, excluding the CatBoost algorithm, was done using Python, specifically the *scikit-learn* package²² and *SciPy* package.²³ Clinically relevant features and their relationships to delirium risk were determined using logistic regression, random forest, or SHapley Additive exPlanations (SHAP or Shapley values).²⁴ Shapley values indicate a quantitative association between a feature and a given model output, with high Shapley values indicating association with high model output, and *vice versa*. Shapley plots are increasingly leveraged to visualize complex relationships captured by machine learning. For each modeling exercise, features were removed if the feature importance as determined internally by each training algorithm was zero, or if they were deemed implausible by a fellowship-trained, board-certified intensive care physician. A nested cross-validation scheme with five inner folds and four outer folds was used to train and evaluate models. In this setup, the complete dataset is split into four different outer training and testing set combinations. Each outer training set is then further split into five different datasets. For a given iteration of the outer loop, hyperparameters are first tuned using 5-fold cross-validation on the training set of the iteration. A model with the optimal hyperparameters is then trained on the outer training set and evaluated on the testing set of the iteration. This process is repeated four times for each different outer training and testing split. To train a final model, hyperparameters are tuned with the outer splits, and then a model with the best hyperparameters is trained on the entire dataset. Hyperparameters were tuned using Bayesian hyperparameter optimization where feasible, or grid search otherwise. For Bayesian hyperparameter optimization, the Tree-structured Parzen Estimator Approach²⁵ was utilized. Final hyperparameters are in table E3 in the Supplemental Digital Content (<http://links.lww.com/ALN/C999>).

A model based on the features from the PREdiction of DELIRium in ICu patients model (often abbreviated as PRE-DELIRIC, and hereafter referred to as the reference model),²⁶ a widely cited reference model in ICU delirium prediction, was created for comparison, with slight adjustments (described in table E4 of the Supplemental Digital Content, <http://links.lww.com/ALN/C999>) to features based on data availability in the development dataset. These reference model-based features were used to train a logistic regression model in the development dataset.

Model Performance Evaluation

Model performances were evaluated by three metrics: area under the receiver operating characteristic curve (AUC), area under the precision recall curve (or mean precision), and

Brier score or calibration curve, while also minimizing computation required for training and making predictions. These metrics indicate the strength of the relationship between the predictive variables and delirium risk. The performances on the outer testing sets are reported. To externally validate the results, the final model trained on the entire development dataset was tested on the validation datasets' extracted features, without using these features in the model training process. For each of these metrics, 95% CIs were also calculated. Detailed performance metrics are reported for the various iterations of the first 24-h model and the dynamic models in table E5, figure E2, and figure E3 in the Supplemental Digital Content (<http://links.lww.com/ALN/C999>). For the primary analysis, we will reject the null hypothesis if AUC is more than 0.5.

Results

Patient Characteristics

Flow diagrams with details of patient inclusion and exclusion are provided in figure 2, and characteristics of the population are in reported in table 1, and online tables E6 and E7 in the Supplemental Digital Content (<http://links.lww.com/ALN/C999>). The cohort for the first 24-h dynamic model consisted of 18,305 total patient stays in the development dataset of which 2,536 (13.9%) were labeled as delirium positive. In validation dataset 1, a total of 5,299 patient stays were identified of which 768 (14.5%) were delirium positive, and in validation dataset 2 a total of 36,194 patient stays were identified, of which 5,955 (11.9%) were delirium positive. Across all datasets, median APACHE IV scores and unadjusted mortality were significantly higher in delirium-positive patients.

For the 12-h lead time dynamic model, the development cohort consisted of 22,234 total patient stays in the development dataset of which 3,791 (17.0%) were labeled as delirium positive and 18,443 (83.0%) were negative. In validation dataset 1, a total of 6,166 patient stays were identified of which 994 (16.1%) were delirium positive and 5,172 (83.9%) were negative, and, in validation dataset 2, a total of 28,440 patient stays were identified, of which 5,955 (20.9%) were delirium positive and 22,485 (79.1%) were delirium negative. Characteristics of admissions analyzed in the development cohort for the first 24-h model are in table 1, and similar characteristics from the validation cohorts are available in table E6 and table E7 in the Supplemental Digital Content (<http://links.lww.com/ALN/C999>).

First 24-h Model Performance

The best-performing algorithm was CatBoost, trained with a pruned feature space of 155 features. All predictive performance metrics are summarized in figure 3. Although AUCs from models that share features do not have a standard statistical test,²⁷ the mean AUC (95% CI) was 0.785 (0.769 to

0.801), which is higher than that of the modified reference model that had a mean AUC of 0.730 (0.704 to 0.757). This model was validated successfully in the validation dataset 1 population (AUC of 0.796) and the validation dataset 2 population (AUC of 0.810). While holding the sensitivity at 0.85, the model achieved a specificity of 0.556 (0.515 of 0.586), negative predictive value of 0.948 (0.943 of 0.950), and positive predictive value of 0.282 (0.264 of 0.296). The mean precision was 0.384 (0.357 to 0.411) in the development dataset, while in validation dataset 1 it was 0.389 and in validation dataset 2 it was 0.475. The mean Brier score was 0.102 (0.097 to 0.108) in the development dataset, 0.105 in validation dataset 1, and 0.110 in validation dataset 2.

Dynamic Model Performance

The dynamic models performed overall better than the first 24-h model, with higher performances noted at short lead times (fig. 4; although the significance of AUC comparisons between models with shared features may not be ascertainable using available statistical methodologies²⁷). The 12-h model had a mean AUC (95% CI) of 0.845 (0.831 to 0.859) and was validated in the validation dataset 1 population (AUC of 0.804) and the validation dataset 2 population (AUC of 0.838). When holding sensitivity at 0.85, the model achieved a specificity of 0.657 (0.623 to 0.691), negative predictive value of 0.955 (0.953 to 0.957), and positive predictive value of 0.337 (0.315 to 0.359). The mean precision was 0.590 (0.566 to 0.613) in the development dataset, while in validation dataset 1 it was 0.449 and in validation dataset 2 it was 0.593. The mean Brier score was 0.111 (0.106 to 0.116) in the development dataset, 0.165 in validation dataset 1, and 0.132 in validation dataset 2. With 6-h lead time, which is greater than the median time between delirium tests in the development dataset, the mean AUC (95% CI) was 0.880 (0.872 to 0.887). External validation performance was variable, with validation dataset 2 results generally within the 95% CI of the development dataset results, and validation dataset 1 performance being slightly worse. However, the maximum absolute difference in AUC between development and validation samples was 0.04. In all instances, the 95% CI of the AUCs excluded 0.5; thus, we reject the null hypothesis that physiologic and clinical variables routinely acquired during intensive care have no relation to the probability of delirium onset.

Feature Importance Analysis

Feature importance was determined using the Shapley values, with relative importance and directionality shown in figure 5 for the dynamic model at 1-h lead time, and for the first 24-h model in figure E7 of the Supplemental Digital Content (<http://links.lww.com/ALN/C999>). Although

Table 1. Characteristics of Cases and Controls from the Development Dataset for the First 24-h Model Cohort

Patient Characteristics	No Delirium	Delirium	Total	P Value
Sex, n (%)				0.916*
Male	8,207 (52.0)	1,409 (55.6)	9,616 (52.5)	
Female	7,559 (47.0)	1,127 (44.4)	8,686 (47.5)	
Median age [interquartile range], yr	65 [53–76]	67 [56–78]	65 [53–76]	< 0.001†
Ethnicity, n (%)				0.989*
Caucasian	11,171 (71.2)	1,858 (73.5)	13,029 (71.5)	
African American	2,912 (18.6)	424 (16.8)	3,336 (18.3)	
Hispanic	677 (4.3)	88 (3.5)	765 (4.2)	
Other/unknown	651 (4.2)	121 (4.8)	772 (4.2)	
Asian	218 (1.4)	30 (1.2)	248 (1.4)	
Native American	56 (0.36)	6 (0.24)	62 (0.34)	
Median first 24 h APACHE IV score [interquartile range]	51.0 [38.0–67.0]	69.0 [52.0–89.0]	53.0 [39.0–70.0]	< 0.001†
Admission source, n (%)				0.931*
Emergency department	7,827 (49.8)	1,203 (47.5)	9,030 (49.5)	
Floor	2,381 (15.1)	447 (17.7)	2,828 (15.5)	
Operating room	1,383 (8.8)	198 (7.8)	1,581 (8.7)	
recovery room	1,093 (7.0)	129 (5.1)	1,222 (6.7)	
Direct admit	927 (5.9)	135 (5.3)	1,062 (5.8)	
Other hospital	533 (3.4)	143 (5.7)	676 (3.7)	
ICU to step-down unit	516 (3.3)	28 (1.1)	544 (3.0)	
Acute care/floor	367 (2.3)	63 (2.5)	430 (2.4)	
Step-down unit	319 (2.0)	88 (3.5)	407 (2.2)	
Other ICU	230 (1.5)	70 (2.8)	300 (1.6)	
ICU	73 (0.5)	11 (0.4)	84 (0.5)	
Postanesthesia care unit	65 (0.4)	14 (0.6)	79 (0.4)	
Chest pain center	13 (0.1)	2 (0.1)	15 (0.1)	
Other	3 (0.0)	0 (0)	3 (0.0)	
Patient history, n (%)				
Dementia				0.029*
No	15,381 (97.5)	2,388 (94.2)	17,769 (97.1)	
Yes	388 (2.5)	148 (5.8)	536 (2.9)	
Alcohol abuse				0.377*
No	13,444 (98.0)	2,263 (96.8)	15,707 (97.8)	
Yes	276 (2.0)	76 (3.3)	352 (2.2)	
Drug abuse				0.851*
No	13,701 (99.9)	2,334 (99.8)	16,035 (99.9)	
Yes	19 (0.1)	5 (0.2)	24 (0.2)	
Treatments in first 24 h, n (%)				
Dialysis				0.584*
No	14,959 (94.9)	2,375 (93.7)	17,334 (94.7)	
Yes	810 (5.1)	161 (6.3)	971 (5.3)	
Mechanical ventilation				< 0.001*
No	11,249 (71.3)	1,188 (46.9)	12,437 (67.9)	
Yes	4,520 (28.7)	1,348 (53.1)	5,868 (32.1)	
Primary diagnostic grouping, n (%)				0.544*
Cardiovascular	6,643 (43.4)	902 (36.0)	7,545 (42.4)	
Respiratory	2,752 (18.0)	592 (23.6)	3,344 (18.8)	
Neurologic	2,139 (14.0)	479 (19.1)	2,618 (14.7)	
Gastrointestinal	1,805 (11.8)	278 (11.1)	2,083 (11.7)	
Metabolic/endocrine	719 (4.7)	48 (1.9)	767 (4.3)	
Genitourinary	449 (2.9)	58 (2.3)	507 (2.9)	
Trauma	411 (2.7)	97 (3.9)	508 (2.9)	
Musculoskeletal/skin	212 (1.4)	25 (1.0)	237 (1.3)	
Hematology	134 (0.9)	17 (0.7)	151 (0.9)	
Transplant	28 (0.2)	12 (0.5)	40 (0.2)	
Outcomes				
Median ICU length of stay [interquartile range], h	52.4 [38.0–86.1]	139.3 [79.2–244.7]	59.1 [39.9–99.0]	< 0.001†
Mortality, n (%)				<0.001*
Alive	15,345 (97.3)	2,307 (91.0)	17,652 (96.4)	
Expired	423 (2.7)	229 (9.0)	652 (3.6)	

*P values derived from chi-square tests for categorical variables. †P values derived from Mann-Whitney U tests for numerical variables.

ICU, intensive care unit

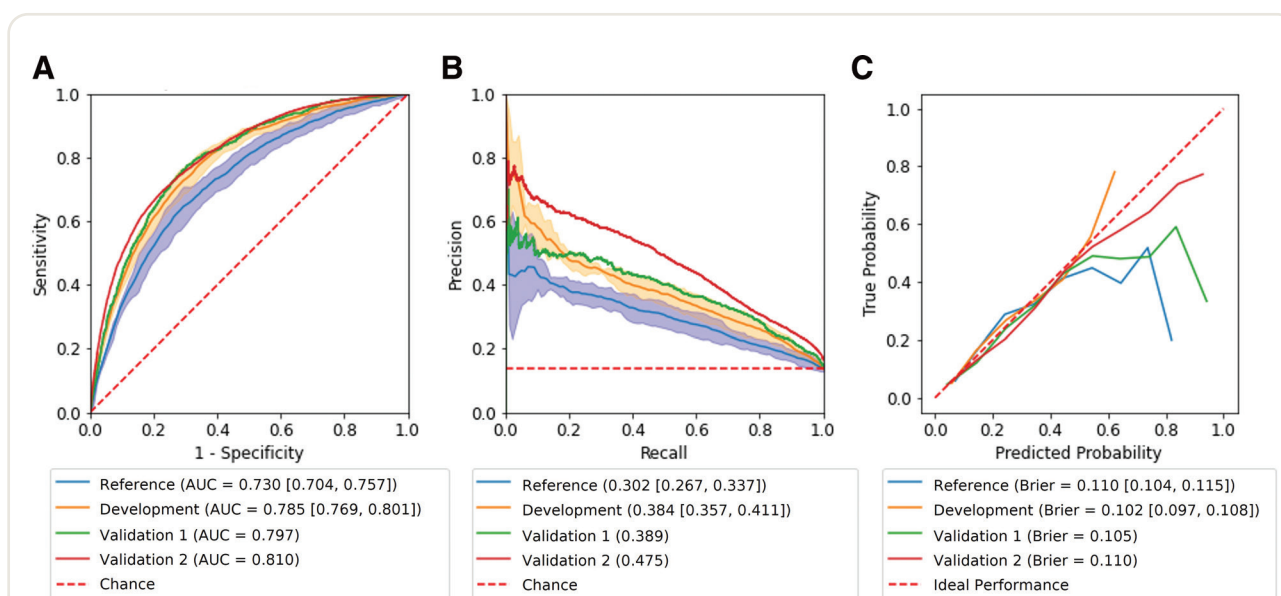


Fig. 3. Model performance metrics for the first 24-h models, including the re-created reference model (Prediction of DELIRium in ICU patients, often abbreviated as PRE-DELIRIC), and our current first 24-h CatBoost model on the development and external validation datasets. (A) Receiver operating characteristic curves with 95% CI shaded. (B) First 24-h model precision-recall curves with average precision and 95% CI shaded. (C) Calibration curves and calculated Brier scores. AUC, area under the receiver operating characteristics curve.

feature importance varied by model, features involving Glasgow Coma Scores, Richmond Agitation Sedation Scale, age, mechanical ventilation, and overall acuity were important in prediction. Length of ICU stay before delirium onset and time of day were important predictors for the dynamic model. Contrary to one of our primary hypotheses, physiologic time series features based on 5-min frequency blood pressure, respiratory rate, heart rate, and oxygen saturation data did not increase either model's performance, as can be seen from performance metrics shown in table E8 in the Supplemental Digital Content (<http://links.lww.com/ALN/C999>).

Discussion

Main Findings

Using large clinical databases, we developed and validated two new models for the prediction of delirium in the ICU. The first 24-h early prediction model performed better than the adapted reference model (fig. 3) and calibrated well in a contemporary dataset (fig. 3). The second dynamic delirium prediction model, which enables estimates of delirium risk that are continually updated over time, had higher discrimination than the modified reference model and similar or better discrimination compared with published delirium prediction models. Both models generally validated well on two external datasets, especially on the more contemporary dataset, although calibration of this model was limited in the validation cohorts, where, at high predicted probability, the observed probability of delirium was considerably lower.

Analysis of Existing Literature

Studies evaluating ICU delirium prediction have varied in patient characteristics, predictive frameworks, and model performance (see table E9 in the Supplemental Digital Content, <http://links.lww.com/ALN/C999>). Many of the most predictive features identified in previous work (e.g., age, mechanical ventilation, severity of illness [APACHE, SOFA], exposure to benzodiazepines) were confirmed in the models presented here. Most previous studies reporting high predictive performance used static models that were unable to predict delirium onset at a specific time point. PREdiction of DELIRium in ICU patients (PRE-DELIRIC)²⁶ is the most studied model of this type, with large variability in performance across different populations internationally, although a meta-analysis estimated an aggregate AUC (95% CI) of 0.844 (0.793 to 0.896).²⁸ Many previous studies had strict patient inclusion criteria, focusing on certain conditions or ICU types, thereby limiting their generalizability.^{29,30} Several reports on higher-performing models lacked external validation and were based on much smaller sample sizes than the ones reported here.^{29,30} The limited number of previous studies that made time-specific predictions of delirium onset evaluated their models on a daily basis,^{29–31} for example, at midnight, and predicted delirium onset in the next 24 h.

Physiologic Time Series

Early in this project we postulated that complex features from physiologic time series data (specifically blood

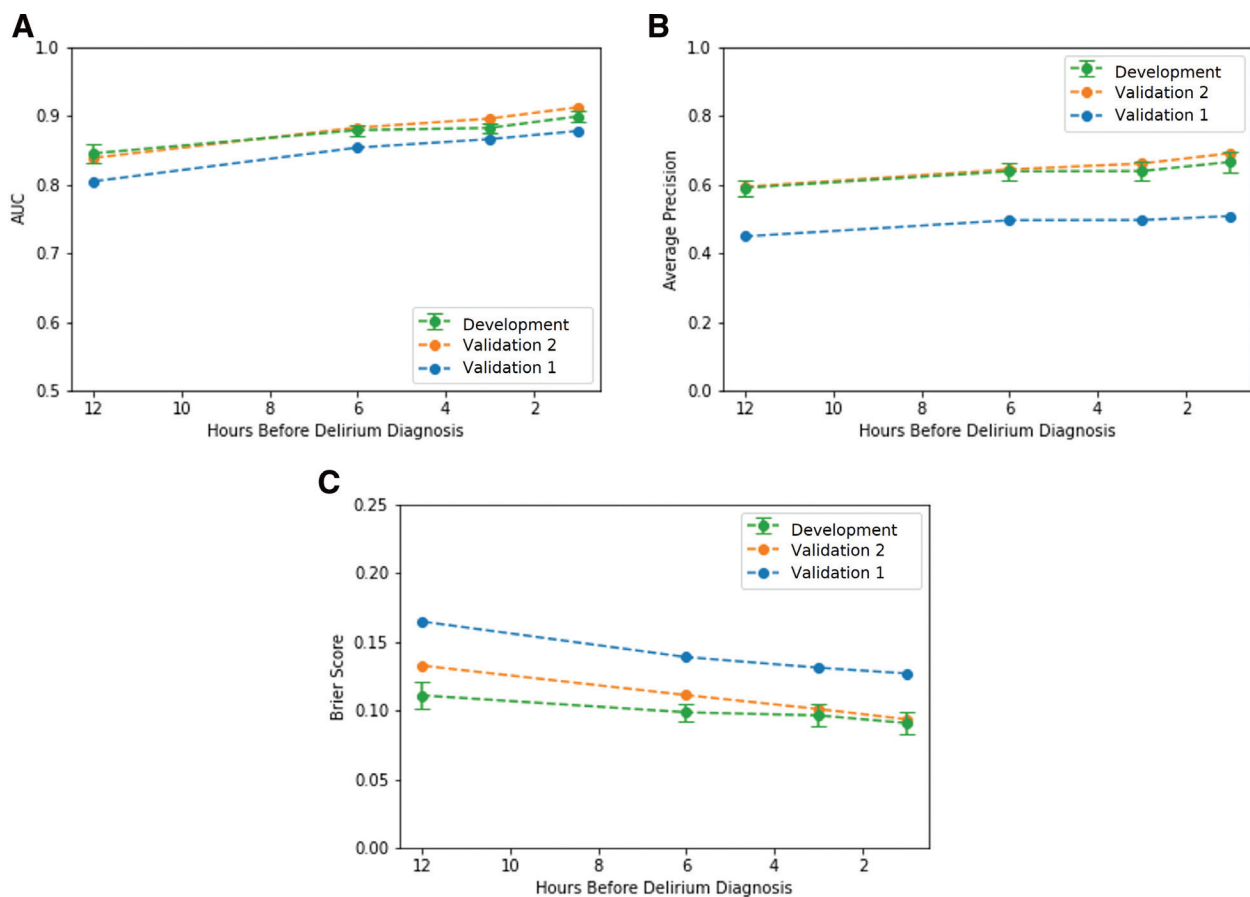


Fig. 4. Time dependence of model discrimination. AUC (A), average precision (B), and Brier scores (C) of the dynamic model at different lead times, with 95% CI indicated by error bars and corresponding external validation performance. AUC, area under the receiver operating characteristics curve.

pressure, respiratory rate, oxygen saturation, and heart rate) could be used to predict the onset of delirium. This hypothesis was not verified in our models. Although such features had some predictive power, they did not improve model performance and were more computationally costly. This counterintuitive result could potentially be due to feature redundancy, or perhaps the lack of hypothesized association.

Strengths

Large and Heterogeneous Datasets

Our study uses data from the Philips eICU Collaborative Research Database, which contains more than 200,000 unique ICU stays from more than 200 hospitals across the United States. This dataset includes data from critical care units in a wide range of different health system sizes, organizational structures, and settings.¹¹ We extracted 22,234 ICU stays from this dataset for training, testing, and validating our dynamic model. This is larger than population

samples used in previous delirium prediction studies, and this population likely has greater heterogeneity than the data used in the original reference model dataset, which trained on data from 1,613 stays in a single hospital in the Netherlands and validated with data from four other hospitals in the same country.²⁶ Model results obtained on diverse populations could be more generalizable, especially in the United States where the data were collected. The publicly available nature of the dataset offers opportunities for other research groups to evaluate our models' reproducibility.

Feature Space

Our models identified several predictive features that were not in the reference model (fig. 5). Low Glasgow Coma Scores, longer length of stay, and the prediction time being late at night were all associated with higher risk of delirium. These new features may explain why our model outperforms the reference model.

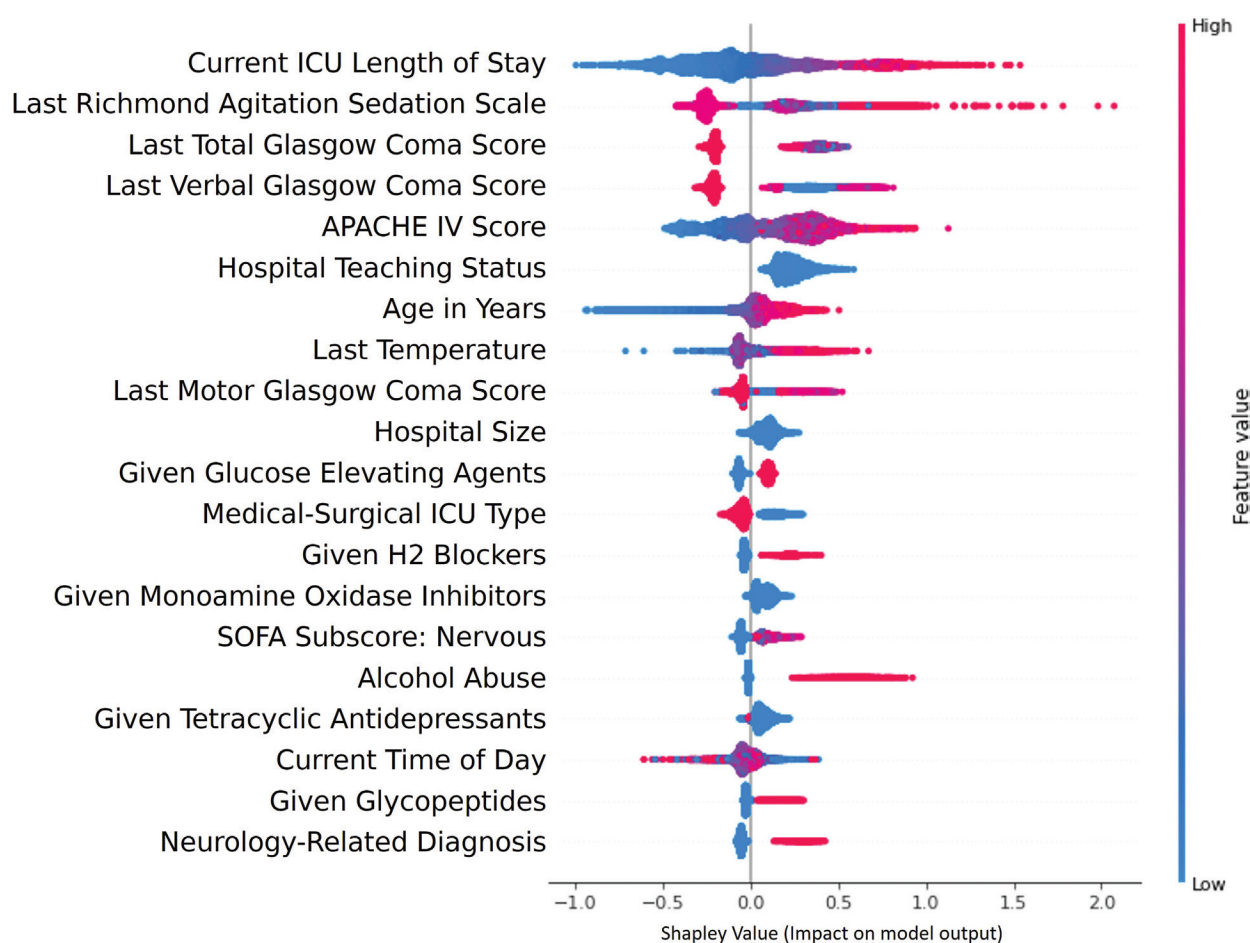


Fig. 5. Feature analysis of the dynamic model. Shapley summary plot of the top 20 features for the dynamic model, at 12-h lead time for prediction of delirium. Each dot represents the Shapley value of one sample for that feature. A feature's Shapley value represents the association of that feature to the risk score, with positive values indicating an association with a higher risk of delirium, and negative values indicating an association with a lower risk of delirium. The location of the dot on the x-axis represents its Shapley value, and its color represents the feature's absolute value. For example, low age is associated with low Shapley values, while high age is associated with high Shapley values, indicating that elderly patients are at higher risk for delirium. ICU, intensive care unit.

Potential Advantages of Dynamic Prediction

The dynamic model presented here is designed to predict delirium at set times up to 12h in the future, potentially a more context-sensitive approach than that of other prediction systems. More time-specific onset predictions could allow targeted implementation of preventive measures in patients with immediate high risk. At shorter lead times (1h or less) this algorithm is identifying delirium close to the present, which could improve the ability to treat ongoing delirium and reduce harm.

External Validation

The delirium prediction models were validated on two large independent external datasets, although validation on the older external dataset was less robust. These results suggest that the models performed well in the development

dataset and may also be applicable to other populations. The vast majority of features were observed in the external validation dataset, suggesting that the features in our model could be generalizable to a range of intensive care settings.

Limitations

Study Design

We have evaluated the relationship between delirium as an outcome and a range of different exposure variables. We feel that this design, which is equivalent to a case-control methodology, is well suited to the modeling task. However, we recognize its limitations, including the inability to determine causality, and potential sources of bias associated with selection and recall, as well as the temporal bias that can occur when there is overemphasis on features that are close in time to the outcome of interest.^{32,33}

Outcome Labels

The frequency of delirium observed in both development and validation samples is lower than that reported in other ICU delirium studies. This may in part be explained by our exclusion of patients who had delirium early in their ICU stay. It is also likely that some patients had been misclassified by clinicians documenting their delirium screens. Hypoactive delirium, in particular, may be overlooked in ICU settings, even when using clinical screens.³⁴ Data based on such documentation may have biased our models, making them more suited for predicting hyperactive delirium.

Another key limitation is the uncertainty regarding the precise timing of delirium onset and resolution, and the impact of this uncertainty on delirium detection and even epidemiology.^{35,36} One of the cardinal features of delirium is its fluctuating nature, challenging precise timing in detection. As in other clinical studies of delirium, we identified cases from documented Confusion Assessment Method for the ICU and Intensive Care Delirium Screening Checklist screening tests; however, the temporal interval between documentation and the clinical state of patients may vary. Similarly, inconsistencies in the frequency of delirium screening represents another limitation. This might reflect clinician workflows in the ICU setting that can directly impact when these tests are conducted and documented.

Feature Data

Another important limitation in this work was the reduced availability or missingness of certain predictive variables in all of the datasets. A number of key variables for delirium prediction (*e.g.*, pre-ICU functional status, detailed histories of cognitive and neurologic conditions, psychologic disorders) were not consistently available, which likely reduced the predictive capabilities of our model. Using routine clinical data means that our predictive features are also susceptible to inconsistency that arises from manual charting.

Model Utility

Although the models presented in this work had overall good performance characteristics, their real-world utility needs to be determined given questions regarding calibration and dynamic prediction. Calibration results were below expectation. Clinical decisions based on a model that overpredicts might lead to unnecessary resource allocation and even harm. Reduced calibration may be due to overfitting, high levels of heterogeneity in the data, use of too many predictive features, and biased sampling.³⁷ Although our training and testing performances do not suggest overfitting, the other cited factors may have influenced our calibration results.

The paradigm of dynamic predictive modeling, while potentially impactful, presents theoretical and implementation challenges. As the temporal offset between the observation and prediction window narrows, the distinction between predicting an event and identifying it becomes

less clear. Regarding implementation of a dynamic prediction system for delirium, one can envision that models with sufficient lead times (*e.g.*, 12h or more) could be leveraged for antidelirium interventions; in contrast the actionable impact of shorter lead times (*e.g.*, 1h or 6h) needs further study.

Singular Prediction per ICU Stay

To maintain independence between samples, our dynamic model was trained by treating each ICU stay as a sample. However, in a realistic clinical setting, a dynamic model would need to make multiple iterative predictions per ICU stay on a regular basis, likely increasing the challenge of accurate and timely prediction. Analysis on one sample's predictive risk over time is shown in figure E8 in the Supplemental Digital Content (<http://links.lww.com/ALN/C999>), and such analyses will be replicated in other samples in future studies.

Comparison with Reference Model

The modified reference model constructed in this work is not identical to the original model, because it includes adjustments (described in table E4, <http://links.lww.com/ALN/C999>). Its performance could have been influenced by the transformation of features.

Conclusion

Leveraging machine learning applied to very large datasets, we have developed and externally validated a novel approach for prediction of delirium in the ICU. After further prospective testing and validation, these models could help support the implementation of delirium-reducing interventions in high-risk individuals.

Acknowledgments

The authors thank Sridevi V. Sarma, Ph.D., Associate Professor, Biomedical Engineering, Whiting School of Engineering, Johns Hopkins University, Baltimore, Maryland, for her invaluable guidance in the early phase of this project, Karol M. Pencina, Ph.D., Chief Biostatistician at Harvard Medical School, Boston, Massachusetts, for his advice on statistical analysis, and Ike Zhang, Student in Biomedical Engineering at the Whiting School of Engineering, Johns Hopkins University, Baltimore, Maryland, for his aid in preparing this manuscript.

Research Support

Support was provided solely from institutional and/or departmental sources at Johns Hopkins University (Baltimore, Maryland).

Competing Interests

The authors declare no competing interests.

Correspondence

Address correspondence to Dr. Stevens: Johns Hopkins University School of Medicine, 600 N. Wolfe Street, Phipps Building, 455A, Baltimore, Maryland 21287. rstevens@jhmi.edu. This article may be accessed for personal use at no charge through the Journal Web site, www.anesthesiology.org.

Supplemental Digital Content

Supplemental Digital Content, <http://links.lww.com/ALN/C999>

References

- Vasilevskis EE, Han JH, Hughes CG, Ely EW: Epidemiology and risk factors for delirium across hospital settings. *Best Pract Res Clin Anaesthesiol* 2012; 26:277–87
- Inouye SK, Westendorp RGJ, Saczynski JS: Delirium in elderly people. *Lancet* 2014; 383:911–22
- Oh ES, Fong TG, Hsieh TT, Inouye K: Delirium in older persons: Advances in diagnosis and treatment. *JAMA* 2018; 318:1161–74
- Hsieh TT, Yue J, Oh E, Puelle M, Dowal S, Trivison T, Inouye SK: Effectiveness of multicomponent nonpharmacological delirium interventions: A meta-analysis. *JAMA Intern Med* 2015; 175:512–20
- Pun BT, Balas MC, Barnes-Daly MA, Thompson JL, Aldrich JM, Barr J, Byrum D, Carson SS, Devlin JW, Engel HJ, Esbrook CL, Hargett KD, Harmon L, Hielsberg C, Jackson JC, Kelly TL, Kumar V, Millner L, Morse A, Perme CS, Posa PJ, Puntillo KA, Schweickert WD, Stollings JL, Tan A, D'Agostino McGowan L, Ely EW: Caring for critically ill patients with the ABCDEF bundle. *Crit Care Med* 2019; 47:3–14
- Burly LD, Cheng W, Williamson DR, Adhikari NK, Egerod I, Kanji S, Martin CM, Hutton B, Rose L: Pharmacological and non-pharmacological interventions to prevent delirium in critically ill patients: a systematic review and network meta-analysis. *Intensive Care Med* 2021; 47:943–60
- Spronk PE, Riekerk B, Hofhuis J, Rommes JH: Occurrence of delirium is severely underestimated in the ICU during daily care. *Intensive Care Med* 2009; 35:1276–80
- Heymann A, Radtke F, Schiemann A, Lütz A, MacGuill M, Wernecke KD, Spies C: Delayed treatment of delirium increases mortality rate in intensive care unit patients. *J Int Med Res* 2010; 38:1584–95
- Collins GS, Reitsma JB, Altman DG, Moons KGM: Transparent reporting of a multivariable prediction model for individual prognosis or diagnosis (TRIPOD): The TRIPOD Statement. *BMC Med* 2015; 13:1–10
- Goldberger AL, Amaral LA, Glass L, Hausdorff JM, Ivanov PC, Mark RG, Mietus JE, Moody GB, Peng CK, Stanley HE: PhysioBank, PhysioToolkit, and PhysioNet: components of a new research resource for complex physiologic signals. *Circulation* 2000; 101:E215–20
- Pollard TJ, Johnson AEW, Raffa JD, Celi LA, Mark RG, Badawi O: The eICU collaborative research database, a freely available multi-center database for critical care research. *Sci Data* 2018; 5:1–13
- Johnson AEW, Pollard TJ, Shen L, Lehman LWH, Feng M, Ghassemi M, Moody B, Szolovits P, Anthony Celi L, Mark RG: MIMIC-III, a freely accessible critical care database. *Sci Data* 2016; 3:1–9
- Johnson AEW, Bulgarelli L, Pollard T, Horng S, Celi LA, Mark R: MIMIC-IV (version 2.0) PhysioNet June 12, 2022. Available at: <https://doi.org/10.13026/7vcr-e114>. Accessed November 20, 2022.
- Ely EW, Margolin R, Francis J, May L, Truman B, Dittus R, Speroff T, Gautam S, Bernard GR, Inouye SK: Evaluation of delirium in critically ill patients: Validation of the Confusion Assessment Method for the intensive care unit (CAM-ICU). *Crit Care Med* 2001; 29:1370–9
- Bergeron N, Dubois MJ, Dumont M, Dial S, Skrobik Y: Intensive care delirium screening checklist: Evaluation of a new screening tool. *Intensive Care Med* 2001; 27:859–64
- Harris CR, Millman KJ, van der Walt SJ, Gommers R, Virtanen P, Cournapeau D, Wieser E, Taylor J, Berg S, Smith NJ, Kern R, Picus M, Hoyer S, van Kerkwijk MH, Brett M, Haldane A, del Río JF, Wiebe M, Peterson P, Gérard-Marchant P, Sheppard K, Reddy T, Weckesser W, Abbasi H, Gohlke C, Oliphant TE: Array programming with NumPy. *Nature* 2020; 585:357–62
- McKinney W: Data structures for statistical computing in Python. In: van der Walt S, Millman J, eds. *Proceedings of the 9th Python in Science Conference*, Austin, Texas, June 28 to July 3, 2010. pp 56–61
- Gasparini A: comorbidity: An R package for computing comorbidity scores. *J Open Source Softw* 2018; 3:648
- Christ M, Braun N, Neuffer J, Kempa-Liehr AW: Time Series Feature Extraction on basis of Scalable Hypothesis tests (tsfresh – A Python package). *Neurocomputing* 2018; 307:72–7
- Breiman L: Random forests. *Mach Learn* 2001; 45:5–32
- Prokhorenkova L, Gusev G, Vorobev A, Dorogush AV, Gulin A: CatBoost: Unbiased boosting with categorical features. *Proceedings of the 32nd International Conference on Neural Information Processing Systems* 2018; 6638–48
- Pedregosa F, Varoquaux G, Gramfort A, Michel V, Thirion B, Grisel O, Blondel M, Prettenhofer P, Weiss

- R, Dubourg V, Vanderplas J, Passos A, Cournapeau D: Scikit-learn: Machine learning in Python. *J Mach Learn Res* 2011; 12:2825–30
23. Virtanen P, Gommers R, Oliphant TE, Haberland M, Reddy T, Cournapeau D, Burovski E, Peterson P, Weckesser W, Bright J, Walt SJ van der, Brett M, Wilson J, Millman KJ, Mayorov N, Nelson ARJ, Jones E, Kern R, Larson E, Carey CJ, Polat I, Feng Y, Moore EW, VanderPlas J, Laxalde D, Perktold J, Cimrman R, Henriksen I, Quintero EA, Harris CR, Archibald AM, Ribeiro AH, Pedregosa F, van Mulbregt P; SciPy 1.0 Contributors: SciPy 1.0: fundamental algorithms for scientific computing in Python. *Nat Methods* 2020; 17:261–72
 24. Lundberg SM, Nair B, Vavilala MS, Horibe M, Eisses MJ, Adams T, Liston DE, Low DKW, Newman SF, Kim J, Lee SI: Explainable machine-learning predictions for the prevention of hypoxaemia during surgery. *Nat Biomed Eng* 2018; 2:749–60
 25. Bergstra J, Bardenet R, Bengio Y, Kégl B: Algorithms for hyper-parameter optimization. 25th Annual Conference on Neural Information Processing Systems. NIPS 2011, December 12 to 17, 2011, Granada, Spain; 2546–54.
 26. Van Den BM, Pickkers P, Slooter AJC, Kuiper MA, Spronk PE, Van Der VP, Van Der HJ, Donders R, Van AT, Schoonhoven L: Development and validation of PRE-DELIRIC (PREdiction of DELIRium in ICu patients) delirium prediction model for intensive care patients: Observational multicentre study. *BMJ* 2012; 344:17
 27. Demler OV, Pencina MJ, D'Agostino RB: Misuse of DeLong test to compare AUCs for nested models. *Stat Med* 2012; 31:2577–87
 28. Chen X, Lao Y, Zhang Y, Qiao L, Zhuang Y: Risk predictive models for delirium in the intensive care unit: A systematic review and meta-analysis. *Ann Palliat Med* 2021; 10:1467
 29. Fan H, Ji M, Huang J, Yue P, Yang X, Wang C, Ying W: Development and validation of a dynamic delirium prediction rule in patients admitted to the Intensive Care Units (DYNAMIC-ICU): A prospective cohort study. *Int J Nurs Stud* 2019; 93:64–73
 30. Marra A, Pandharipande PP, Shotwell MS, Chandrasekhar R, Girard TD, Shintani AK, Peelen LM, Moons KGM, Dittus RS, Ely EW, Vasilevskis EE: Acute brain dysfunction: development and validation of a daily prediction model. *Chest* 2018; 154:293–301
 31. Moon KJ, Jin Y, Jin T, Lee SM: Development and validation of an automated delirium risk assessment system (Auto-DelRAS) implemented in the electronic health record system. *Int J Nurs Stud* 2018; 77:46–53
 32. Breslow NE: Statistics in epidemiology: The case-control study. *J Am Stat Assoc* 1996; 91:14–28
 33. Yuan W, Beaulieu-Jones BK, Yu KH, Lipnick SL, Palmer N, Loscalzo J, Cai T, Kohane IS: Temporal bias in case-control design: preventing reliable predictions of the future. *Nat Commun* 2021; 12:1–10
 34. Cour K, Andersen-Ranberg NC, Weihe S, Poulsen LM, Mortensen CB, Kjer CKW, Collet MO, Estrup S, Mathiesen O: Distribution of delirium motor subtypes in the intensive care unit: a systematic scoping review. *Crit Care* 2022; 26:1–11
 35. Wilson JE, Mart ME, Cunningham C, Shehabi Y, Girard TD, MacLulich AMJ, Slooter AJC, Ely EW: Delirium. *Nat Rev Dis Prim* 2020; 6:1–26
 36. Pandharipande P, Ely EW, Arora RC, Balas MC, Boustani M, La Calle GH, Cunningham C, Devlin JW, Elefante J, Han JH, MacLulich M, Maldonado JR, Morandi A, Needham DM, Page VJ, Rose L, Salluh JIF, Sharshar T, Shehabi Y, Skrobik Y, Slooter AJC, Smith HAB: The intensive care delirium research agenda: A Multinational, interprofessional perspective. *Intensive Care Med* 2017; 43:1329–39
 37. Calster BV, McLernon DJ, Smeden MV, Wynants L, Steyerberg EW: Calibration: The Achilles heel of predictive analytics. *BMC Med* 2019; 17:1–7

ANESTHESIOLOGY

Multidisciplinary Pain Management: A Tale of Two Outcomes

Stephen H. Butler, M.D., John D. Loeser, M.D.

ANESTHESIOLOGY 2023; 138:312–5

The authors of this article were early members of John J. Bonica, M.D.'s Multidisciplinary Pain Clinic at the University of Washington (Seattle, Washington). This program was started in 1960 when Bonica became the founding chairman of the Department of Anesthesiology at the University of Washington. In its original form, this was a diagnostic clinic that brought multiple medical specialists to focus on a single patient. Treatment recommendations were then made and implemented by an individual provider.

The program evolved over the first decade of its existence as more practitioners were enlisted to join the group. Wilbert (Bill) Fordyce, Ph.D., was an important addition in the mid-60s as the group gained faculty members interested in the treatment of pain. Fordyce had a limited practice of behavioral medicine within the Rehabilitation Department at this time. The clinic gained its own space in 1975 with the first expansion of the University Hospital. By 1977, the Anesthesiology Department had six inpatient beds to use in the diagnostic evaluations of pain patients. In 1978, Bonica convinced the University of Washington to establish a Pain Center, which was enriched with two psychologists whose clinical activities were to be in the domain of pain.

In 1982, John Loeser was asked to become the Director of the Pain Center. At this time, an entire ward in the University Hospital was assigned to the Pain Center, and Fordyce and Loeser designed and implemented a 3-week inpatient treatment program for patients with chronic, intractable pain.¹ This was labeled "the structured program" and rapidly became a model for chronic pain treatment both in the United States and throughout the world. It existed at the University of Washington from 1983 until 1997; its demise was mainly due to socioeconomic factors that intruded into health care in the United States.

When Dr. Butler moved from the University of Washington Pain Clinic in Seattle to a new job in Sweden

Economic implications of pain management. By Loeser JD. *Acta Anaesthesiol Scand* 1999; 43:957–95. Reprinted with permission.

Abstract

Multidisciplinary pain management was an invention of John J. Bonica, M.D. He started the Multidisciplinary Pain Clinic at the University of Washington in 1960. This clinical service evolved over the years, and when John Loeser, M.D., became its director in 1982, he collaborated with Bill Fordyce, Ph.D., to create what was known as "the structured program." The program has served as the model for pain treatment programs throughout the world, many of which have fared better than that at the University of Washington. The migration of Stephen Butler, M.D., to Uppsala, Sweden, in 2000 has given us the opportunity to contrast multidisciplinary pain management in the Nordic countries with that in the United States.

(*ANESTHESIOLOGY* 2023; 138:312–5)

in 2000 as acting Chief of the Pain Center at the Academic Hospital of Uppsala, he was surprised to find some familiar programs. The first was a week-long multidisciplinary evaluation on an inpatient basis, very similar to that at the University Hospital in Seattle in the 1970s. A physiatrist, Patrik Uge, had been to Seattle and had brought back Dr. Bonica's concept, which functioned very well. The evaluation week is still in operation.

The second surprise was that an interdisciplinary inpatient pain program had just been transferred to "Akademiska" from a satellite hospital. This had been started several years previously by Basil Finer, M.D., an English anesthesiologist who had moved to Uppsala in the 1960s. Finer had written a few articles on hypnosis for anesthesia and for chronic pain. Bonica had read these and had invited Finer in 1973 to the watershed Issaquah Conference, where the International Association for the Study of Pain was founded. Dr. Finer was inspired and brought the concept of multidisciplinary pain management to Uppsala.

Finer was retiring, but the rest of the team, led by a psychiatrist, was given five hospital beds at "Akademiska" for the multidisciplinary inpatient pain program. Functional improvement was the goal, and various cognitive and behavioral therapies were employed. This version of the Seattle Structured Pain Treatment Program is still thriving in Uppsala.

When Dr. Butler arrived, all interns spent a week on the pain service, and anesthesia residents spent 2 months. There were also continual visitors, mostly anesthesiologists from around Sweden and the world, as well as foreign fellows. It was very easy for Dr. Butler to fit in.

This article is featured in "This Month in Anesthesiology," page A1.

Submitted for publication November 8, 2022. Accepted for publication November 10, 2022. Published online first on January 12, 2023.

Stephen H. Butler, M.D.: Department of Public Health and Caring Sciences, Uppsala Academic University Hospital, Uppsala, Sweden.

John D. Loeser, M.D.: Department of Neurologic Surgery and Anesthesia and Pain Medicine, University of Washington School of Medicine, Seattle, Washington.

Copyright © 2023, the American Society of Anesthesiologists. All Rights Reserved. *Anesthesiology* 2023; 138:312–5. DOI: 10.1097/ALN.0000000000004444



Fig. 1. Dr. Stephen H. Butler presently is Consultant to the Pain Center at the Academic Hospital of Uppsala, Uppsala, Sweden; the Center for Pain and Complex Diseases at St. Olaf's Hospital, Trondheim, Norway; and the Department of Public Health and Caring Sciences at Uppsala University, Uppsala, Sweden. He was a faculty member of the Department of Anesthesiology at the University of Washington from 1970 to 2000. The final 2 yr there, he was Acting Director of the Pain Center. He has been active in research, teaching, and patient care throughout his career. He was a founding member of the International Association for the Study of Pain. He is still active in research in Uppsala and Trondheim and a core teacher in the Scandinavian Society of Anesthesia and Intensive Care Pan-Nordic Course in Chronic Pain, which focuses on multidisciplinary pain management.

The next eye-opener for Dr. Butler came after some discussions with Torsten Gordh, Jr., who had founded the pain service and was the new Chief of Anesthesiology at Akademiska. Gordh was involved with a new project. A Danish anesthesiologist, Jørgen Eriksen, was keen to start a pan-Nordic pain course for anesthesiology specialists who had finished their formal training. He had begun reading pain literature widely and realized that his results from

*The International Association for the Study of Pain definitions distinguish multidisciplinary from interdisciplinary care. The former means a group of caregivers interact with the patient; the latter means that the providers interact with each other and the patient. The latter is the preferred mode of care. Common usage often ignores this distinction, as do we in this article. The Seattle model is interdisciplinary in all respects.



Fig. 2. Dr. John D. Loeser is Professor Emeritus of Neurologic Surgery and Anesthesiology and Pain Medicine at the University of Washington, where he has been a faculty member since 1969. He was the Director of the Multidisciplinary Pain Center at the University of Washington from 1983 to 1997. He has been active in research, teaching, and patient care in the field of pain management for more than 50 yr. He was a founding member and served as President of both the American Pain Society and the International Association for the Study of Pain. He has authored or coauthored more than 250 peer-reviewed articles, 127 book chapters, and 8 books. He is particularly interested in multidisciplinary pain management and the education of healthcare providers about pain.

invasive treatments were disappointing primarily because of patients' psychosocial issues. Eriksen eventually published a landmark article in *Pain* on the epidemiology of chronic pain in the Danish population that proved this point.³

As a result of this research, Eriksen became fascinated with multidisciplinary* pain treatment and education. His course was intended to enlighten interventional anesthesiologists in Denmark, Sweden, Norway, Finland, and Iceland. It was a 3-day program that took place at each nation's capital over a total duration of 2 yr. Little on acute pain, nerve blocks, pumps, and stimulators was on the curriculum. The theme was multi/interdisciplinary pain management with

a focus on the psychosocial problems, not the “bio-.” Dr. Butler became one of the core teachers in this group, which consisted of two anesthesiologists from each country.

Through this course, Dr. Butler has made many friends in the Nordic pain world. It is now midway through its 10th yr. On the first day of each course, he still gives an hour lecture on the history of Bonica, Fordyce, and the Seattle program from the 1970s until the 1990s. The course began with only 20 anesthesiologists in its first year but has now expanded to 45, with half coming from other specialties. By now, well over 200 Nordic physicians have completed the program. The highlight is the last stop in Reykjavik, Iceland, where there is a Jørgen Eriksen Memorial Lecture that was established after Eriksen's untimely death from renal cancer. One of his heroes, Mark Jensen, a Fordyce-trained University of Washington psychologist from Seattle, is the featured lecturer for each Reykjavik course.

Another result of this program is that Dr. Butler has visited pain centers throughout the Nordic countries. His relationship with St. Olav's Hospital in Trondheim has been the longest. A previous professor there, Harald Breivik, M.D., had come to Seattle for a few months in 1975, and Dr. Butler had served as his “mentor”—although it was really a two-way street. As Professor of Anesthesiology in Trondheim, and later in Oslo, Breivik promulgated the multi/interdisciplinary concept, not only in Norway but in all of Scandinavia. He founded the Scandinavian Society for the Study of Pain, an International Association for the Study of Pain chapter, as well as the *Scandinavian Journal of Pain*, serving as its first editor.

After the second Nordic pain course in 2001, Dr. Butler was invited back to Trondheim. St. Olav's had an outpatient multidisciplinary pain clinic that was thriving. The team had become fascinated with the descriptions of the Seattle pain world and wanted him to run a version of the University of Washington Structured Pain Treatment Program as a pilot. After 3 weeks, four of the six patients showed some progress. After discharge to a home program, all of the patients were booked to return 6 weeks later. Three of the six actually returned, and two had made spectacular progress, with one even getting back to work.

That program was a part of the stimulus for a subsequent 5-yr project funded by the regional government at an idyllic site out on the fiord that had been a German fort during World War II. Called “Fortet,” it included a challenging physical reactivation component and various Cognitive and Behavioral Therapy components. After the 5 yr of government funding stopped, Fortet has continued in a modified form under a private group.

Multi/interdisciplinary pain management is alive and well in Norway. Five regional sites have been designated as tertiary pain centers with a common intake evaluation that includes a questionnaire and a structured interview and examination. This expands research potential.

Back to Sweden. Alf Nachemson, M.D., Ph.D., then Professor of Orthopedics at Sahlgrenska University

Hospital in Gothenburg, had gone to Seattle as part of the “Boeing Project,” a team investigating predictors for acute back pain to proceed to a chronic form.⁴ Alf discouraged the surgical approach to chronic back pain and invited Bill Fordyce and others from Seattle to set up a variant of the University of Washington Structured Pain Treatment Program in Sahlgrenska. The program then migrated to Umeå, where it is still active and has a parallel program in a nearby regional hospital.

Iceland also has links to Seattle. An Icelandic physiatrist was an observer of the University of Washington's Structured Pain Treatment Program and set up a very similar program at Reykjalundur.⁵ This program has, in addition, an extended retraining program with a successful back-to-work record. There are two other multidisciplinary pain rehabilitation programs in Iceland as well, impressive for a country with barely more than 300,000 inhabitants.

Finland should not be left out. Eija Kelso, M.D., a Past President of International Association for the Study of Pain, has made several trips to Seattle. She developed and expanded a multi/interdisciplinary pain center with a strong research base at the University of Helsinki. Acute pain and chronic pain programs are alive and well in all the universities in Finland. It should be noted that in addition to Kelso, two other past Presidents of International Association for the Study of Pain have come from the Nordic countries—one from Denmark and one from Sweden.

The political systems of all the Nordic countries are based on social democratic principles. All citizens have comprehensive health insurance under a government agency. In Norway, at least, leading pain specialists have had direct access to federal health ministers—a relationship that has facilitated the growth of pain clinics and pain research. In some Nordic countries, there are also private pain clinics, but they are reimbursed, at least partly, by government agencies. Thus, there is universal access to multidisciplinary care for acute, chronic, and cancer-related pain, although wait lists can be longer than optimal. Expertise varies, but the principle of care for all is the basis of pain management. Clearly, the University of Washington Structured Pain Treatment Program has been the model for a wide network of Scandinavian pain treatment programs.

While pain management was evolving in Nordic countries based on the University of Washington programs, a different set of developments was occurring in the United States. There was no planned governmental approach, save for that which occurred in the Veterans Administration system. Pain programs developed in many institutions, but few survived the economic healthcare chaos in the United States.

The insurance industry played a major role in the destruction of multidisciplinary pain management, for it saw this type of treatment as expensive. Furthermore, there was a bias against funding care that was not provided by an M.D. These payers largely ignored the data on

efficacy and viewed return to work as an irrelevant outcome measure. Providers could earn more money doing procedures and operations—often less effective therapies for chronic pain patients—than participating in a multidisciplinary treatment program. Even continuing medical education programs were biased against multidisciplinary pain programs, as they were commonly funded by their sponsors—drug and device manufacturers. Very few clinical studies reported long-term outcomes or functional status.

Healthcare costs have soared in the United States without any measure of improvement for the general public, and pain treatment has not benefitted from this phenomenon. The intrusion of capitalism into health care has not helped the comprehensive management of chronic pain patients. As we stated in the 1999 article, “To control inappropriate care and escalating costs, we must change concepts of pain and disability and the methods of funding both of these in relation to chronic pain. The outcome of the continuing struggle between the profession of medicine, the state and capitalists will determine how and whether pain management is a part of medical care.”²

Correspondence

Address correspondence to Dr. Loeser: 6247 82nd Avenue SE, Mercer Island, Washington 98040.

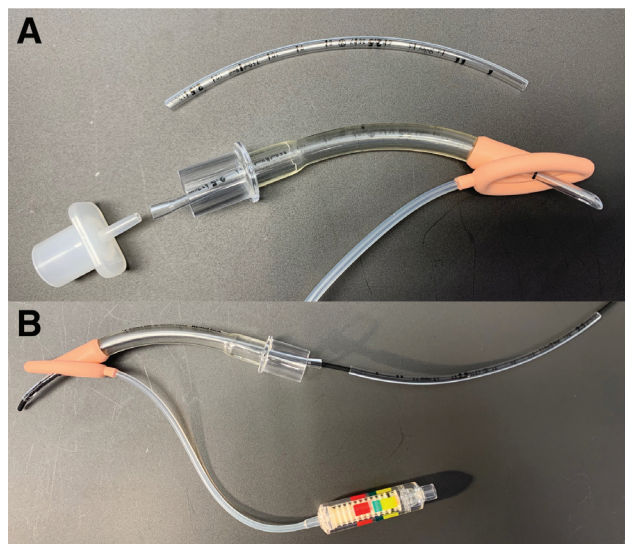
jdloeser@neurosurgery.washington.edu. ANESTHESIOLOGY's articles are made freely accessible to all readers on www.anesthesiology.org, for personal use only, 6 months from the cover date of the issue.

References

1. Loeser JD, Egan K: *Managing the Chronic Pain Patient: Theory and Practice at the University of Washington Pain Clinic*. New York, Raven Press, 1982
2. Loeser JD: Economic implications of pain management. *Acta Anaesthesiol Scand* 1999; 43:957–9
3. Eriksen J, Jensen MK, Sjøgren P, Ekholm O, Rasmussen NK: Epidemiology of chronic non-malignant pain in Denmark. *Pain* 2003; 103:221–8
4. Bigos SJ, Battie MC, Spengler DM, Fisher LD, Fordyce WE, Hansson TH, Nachemson AL, Wortley MD: A prospective study of work perceptions and psychosocial factors affecting the report of back injury. *Spine* 1991; 16:1–6
5. Ólason M, Andrasen RH, Jónsdóttir I, Kristbergisdóttir H, Jensen MP: Cognitive behavioral therapy for depression and anxiety in an interdisciplinary rehabilitation program for chronic pain: A randomized controlled trial with a 3-year follow-up. *Int J Behav Med* 2018; 25:55–66

Difficult Airway Management in Neonates: Fiberoptic Intubation *via* Laryngeal Mask Airway

James Joseph Thomas, M.D., Mahsa Lingruen, C.A.A., M.M.Sc., Abhita Reddy, M.D., Kenny H. Chan, M.D.



The incidence of difficult direct laryngoscopy is higher in patients younger than one *versus* older patients.¹ In neonates with an anticipated or unanticipated difficult airway, a laryngeal mask airway (LMA) is an acceptable temporary airway, because management with an LMA in neonates has been shown to be successful and safe.² After stabilization with an LMA, securing the airway with an endotracheal tube (ETT) becomes paramount.

Although an LMA Unique size 1 (Laryngeal Mask Company Limited, USA) has a limited internal diameter, an uncuffed 2.5-mm or 3-mm ETT will fit inside (fig, panel A). An LMA Unique size 1 is only a few centimeters shorter than an uncuffed 2.5-mm ETT, so advancing the ETT into the trachea through the LMA is impossible without assistance. Devices like the Aintree Intubation Catheter (Cook Critical Care, USA) are too big for this patient population,³ and, although an air-Q LMA would work in this situation, they may not be available in every anesthesia site. Using another 2.5-mm ETT and cutting off both ends creates a “pusher” (not a Food and Drug Administration–approved device) for the intubating ETT, allowing more control in placement.

With the “pusher” placed over a flexible video bronchoscope followed by the intubating ETT, all can be passed through the LMA, taking caution not to advance the ETT too far, which can result in injury or pneumothorax (fig, panel B). Once the flexible video bronchoscope is in the trachea, the intubating ETT can be pushed into place and held there while the LMA and flexible video bronchoscope are removed (Supplemental Digital Content, <http://links.lww.com/ALN/C972>).

Research Support

Support was provided solely from institutional and/or departmental sources.

Competing Interests

The authors declare no competing interests

Correspondence

Address correspondence to Dr. Thomas: james.j.thomas@childrenscolorado.org

Supplemental Digital Content

Supplemental Video, <http://links.lww.com/ALN/C972>

References

1. Heinrich S, Birkholz T, Ihmsen H, Irouschek A, Ackermann A, Schmidt J: Incidence and predictors of difficult laryngoscopy in 11,219 pediatric anesthesia procedures. *Paediatr Anaesth* 2012; 22:729–36
2. Pejovic NJ, Myrnerets Höök S, Byamugisha J, Alfvén T, Lubulwa C, Cavallin F, Nankunda J, Ersdal H, Blennow M, Trevisanuto D, Tyllskär T: A randomized trial of laryngeal mask airway in neonatal resuscitation. *N Engl J Med* 2020; 383:2138–47
3. Wong DT, Yang JJ, Mak HY, Jagannathan N: Use of intubation introducers through a supraglottic airway to facilitate tracheal intubation: a brief review. *Can J Anaesth* 2012; 59:704–15

Supplemental Digital Content is available for this article. Direct URL citations appear in the printed text and are available in both the HTML and PDF versions of this article. Links to the digital files are provided in the HTML text of this article on the Journal's Web site (www.anesthesiology.org).

Published online first on December 2, 2022.

James Joseph Thomas, M.D.: Department of Anesthesiology, University of Colorado, Children's Hospital Colorado, Aurora, Colorado.

Mahsa Lingruen, C.A.A., M.M.Sc.: Department of Anesthesiology, University of Colorado, Children's Hospital Colorado, Aurora, Colorado.

Abhita Reddy, M.D.: Department of Otolaryngology, University of Colorado, Children's Hospital Colorado, Aurora, Colorado.

Kenny H. Chan, M.D.: Department of Otolaryngology, University of Colorado, Children's Hospital Colorado, Aurora, Colorado.

Copyright © 2022, the American Society of Anesthesiologists. All Rights Reserved. *Anesthesiology* 2023; 138:316. DOI: 10.1097/ALN.0000000000004431

ANESTHESIOLOGY

Advanced Point-of-care Bedside Monitoring for Acute Respiratory Failure

Gianmaria Cammarota, M.D., Ph.D., Rachele Simonte, M.D.,
Federico Longhini, M.D., Savino Spadaro, M.D.,
Luigi Vetrugno, M.D., Edoardo De Robertis, M.D., Ph.D.

ANESTHESIOLOGY 2023; 138:317–34

Scan for
CME exam



Acute respiratory failure is one of the leading causes of mechanical ventilation initiation and intensive care unit (ICU) admission.¹ Since the early stages of acute respiratory failure management, in establishing the respiratory support strategy, it is essential to be aware of the potential damage to the lung and respiratory muscles resulting from improper regulation of mechanical ventilation. Injuries to these structures can either happen during spontaneous breathing or be triggered by inadequate ventilator settings.^{2,3} To date, however, despite the identification of specific targets for diaphragm-protective ventilation and the proposal for potential strategies for an integrated protection of the lung and diaphragm,⁴ there are sparse data on the clinical impact of such an approach.

Advanced respiratory monitoring involves several non-invasive or minimally invasive technologies, safely applicable at the bedside, to conduct an in-depth evaluation of the lung and respiratory muscles.⁵ The assessment of the esophageal pressure and electrical activity of the diaphragm, electrical impedance tomography, and ultrasound of the lung and respiratory muscles are potentially useful to support physicians in the daily management of acute respiratory failure, specific to the protection of the lung and respiratory muscles (fig. 1). Despite the information conveyed by

ABSTRACT

Advanced respiratory monitoring involves several mini- or noninvasive tools, applicable at bedside, focused on assessing lung aeration and morphology, lung recruitment and overdistention, ventilation–perfusion distribution, inspiratory effort, respiratory drive, respiratory muscle contraction, and patient–ventilator asynchrony, in dealing with acute respiratory failure. Compared to a conventional approach, advanced respiratory monitoring has the potential to provide more insights into the pathologic modifications of lung aeration induced by the underlying disease, follow the response to therapies, and support clinicians in setting up a respiratory support strategy aimed at protecting the lung and respiratory muscles. Thus, in the clinical management of the acute respiratory failure, advanced respiratory monitoring could play a key role when a therapeutic strategy, relying on individualization of the treatments, is adopted.

(*ANESTHESIOLOGY* 2023; 138:317–34)

advanced respiratory monitoring tools and the technology implementation available in the clinical practice, their clinical use is still limited, probably due to the numerous skills required in their application.

In recent years, several articles providing new insights on the application of these technologies in clinical and research fields have published.^{6–13} Thus, we prepared the current review focused on rendering an updated description of the tools employed at bedside for advanced respiratory monitoring. In particular, we shed light on how these technologies work and what measures they provide, discuss their clinical usefulness, and review the current evidence supporting their application in acute respiratory failure when part of a personalized strategy for lung and respiratory muscles protection.

Esophageal Pressure

Esophageal pressure is used as a surrogate for pleural pressure, and variations in esophageal pressure are indicative of pleural pressure changes on the lung surface.¹⁴ The assessment of esophageal pressure is obtained through a dedicated esophageal catheter equipped with an air-filled or liquid-filled esophageal balloon and connected to a pressure

This article has been selected for the Anesthesiology CME Program (www.asahq.org/JCME2023MAR). Learning objectives and disclosure and ordering information can be found in the CME section at the front of this issue. This article is featured in “This Month in Anesthesiology,” page A1. Supplemental Digital Content is available for this article. Direct URL citations appear in the printed text and are available in both the HTML and PDF versions of this article. Links to the digital files are provided in the HTML text of this article on the Journal’s Web site (www.anesthesiology.org). Jerrold H. Levy, M.D., F.A.H.A., F.C.C.M., served as Handling Editor for this article.

Submitted for publication July 30, 2022. Accepted for publication December 15, 2022.

Gianmaria Cammarota, M.D., Ph.D.: Department of Medicine and Surgery, Università degli Studi di Perugia, Perugia, Italy.

Rachele Simonte, M.D.: Department of Medicine and Surgery, Università degli Studi di Perugia, Perugia, Italy.

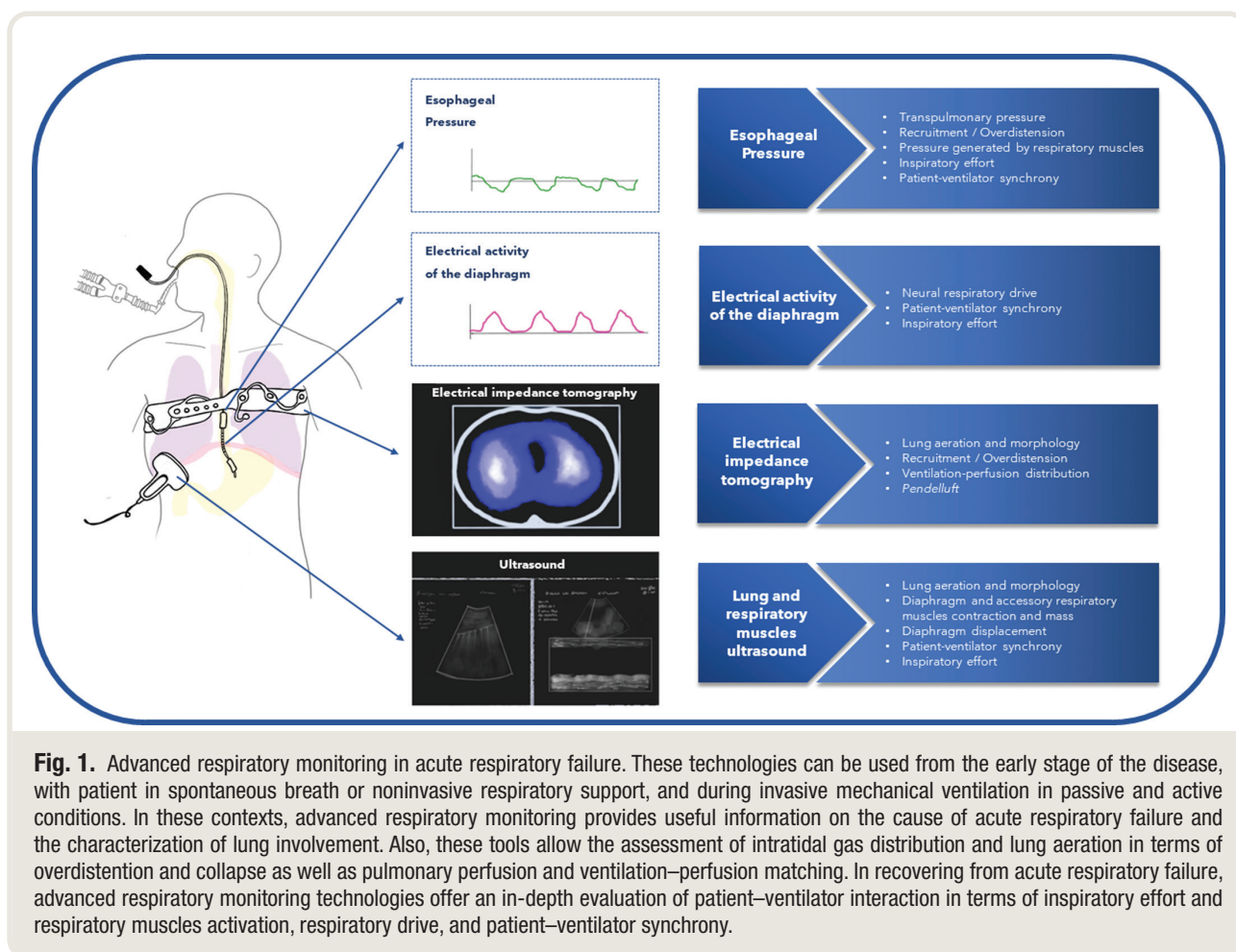
Federico Longhini, M.D.: Department of Medical and Surgical Science, Università della Magna Graecia, Catanzaro, Italy.

Savino Spadaro, M.D.: Department of Translational Medicine for Romagna, Università degli Studi di Ferrara, Ferrara, Italy.

Luigi Vetrugno, M.D.: Department of Anesthesiology and Intensive Care, Ospedale SS Annunziata & Dipartimento di Tecnologie Innovative in Medicina e Odontoiatria, Università di Chieti-Pescara, Chieti, Italy.

Edoardo De Robertis, M.D., Ph.D.: Department of Medicine and Surgery, Università degli Studi di Perugia, Perugia, Italy.

Copyright © 2023, the American Society of Anesthesiologists. All Rights Reserved. *Anesthesiology* 2023; 138:317–34. DOI: 10.1097/ALN.0000000000004480



transducer at its proximal tip.¹⁵ The procedure for catheter placement allows the positioning of the esophageal balloon midway between the apex and the base of the lung, generally at 35 to 45 cm from the nostrils.¹⁵

In clinical and research contexts, the esophageal pressure assessment is used for the partitioning of respiratory mechanics into chest wall component and pulmonary component¹⁶ and the computation of transpulmonary pressure, the real pressure distending the lung. The computation of transpulmonary pressure is obtained through different approaches, the most used of which are the direct method and elastance-derived method.^{17,18} According to the direct method, transpulmonary pressure is obtained by subtracting esophageal pressure from airway pressure,¹¹ while the elastance-derived method accounts for lung stress induced by ventilation.¹⁹ However, the reliability of absolute values of esophageal pressure in reflecting absolute values of pleural pressure is controversial. Indeed, the absolute values of esophageal pressure can be influenced by respiratory system mechanical properties, lung volume, weight of the mediastinum, abdominal pressure, body position, esophageal wall reaction, and the elastic recoil of the esophageal balloon as

well as lung disease distribution and asymmetry.¹⁶ Pleural pressure is not homogeneously distributed in the chest, and esophageal pressure cannot represent the pleural pressure acting on the whole lung surface. Indeed, in the supine position, pleural pressure develops along a vertical gradient from the nondependent to the dependent chest,²⁰ which is magnified in acute respiratory distress syndrome (ARDS) patients.²¹ Accordingly, transpulmonary pressure diminishes from nondependent to dependent lung. In supine position, the esophagus is exposed to mediastinal weight, with a hypothesized increase in esophageal pressure on average of 5 cm H₂O above pleural pressure.²² Also, it has been demonstrated that the two methods for transpulmonary pressure computation yield conflicting results, definitively questioning the accuracy of the esophageal manometry in representing regional pressure across the lung.²³ To correct the artifacts related to esophageal wall contraction in response to balloon inflation and balloon elastic recoil, an *ad hoc* procedure of balloon calibration has been proposed in both invasive controlled mechanical ventilation and assisted breathing.²⁴⁻²⁷ This procedure relies on the identification of the optimal esophageal balloon filling volume

able to optimize the transmission of the esophageal pressure tidal swings, and removal of the artifacts responsible for an incorrect increase in esophageal pressure above the pleural pressure, *i.e.*, esophageal wall and balloon elastance, respectively.^{24–27} By insufflating the esophageal balloon with the optimal filling volume, a validation occlusion test has been demonstrated to be passed *a posteriori* in a higher percentage of cases compared to uncalibrated volume, with which the test was passed in 57% and 52% of the cases in passive and active conditions.²⁶

Recent findings support the validity of esophageal manometry, provided a proper calibration of the esophageal balloon is assured.⁶ In experimental conditions of lung-injured pigs and human cadavers subjected to direct pleural and esophageal pressure monitoring in the supine position,⁶ the vertical gradient of pleural pressure was confirmed. The directly measured transpulmonary pressure reflected the pressure acting on the dependent and midlung adjacent to the esophageal balloon during both inspiration and expiration (fig. 2). The overestimation of pleural pressure due to mediastinal weight on the esophageal balloon was not confirmed, probably due to the suspension of the heart by pericardial ligaments and the wide distribution of atelectasis.

In the same setting,⁶ the end-inspiratory transpulmonary pressure computed through the elastance-derived method matched the end-inspiratory pressure acting on the nondependent lung regions (fig. 2). Indeed, in contrast with mid- and dependent lung regions, transpulmonary pressure was close to 0 at a low positive end-expiratory pressure (PEEP) in nondependent lung zones when lung volume approximated functional residual capacity.

As a clinical implication, in acute respiratory failure patients undergoing invasive mechanical ventilation, transpulmonary pressure assessment is potentially useful to recruit collapsed lung by counterbalancing negative directly measured end-expiratory transpulmonary pressure and avoiding overdistension by reducing end-inspiratory elastance-derived transpulmonary pressure.¹⁹ However, a personalized ventilatory strategy setting PEEP to overcome negative expiratory transpulmonary pressure has been suggested in patients with ARDS with conflicting results.^{28,29} In a randomized trial conducted in intubated ARDS patients,²⁸ PEEP adjusted according to measurements of esophageal pressure was superior to a ventilatory strategy with PEEP set according to low PEEP/fractional inspired oxygen tension table³⁰ in improving oxygenation

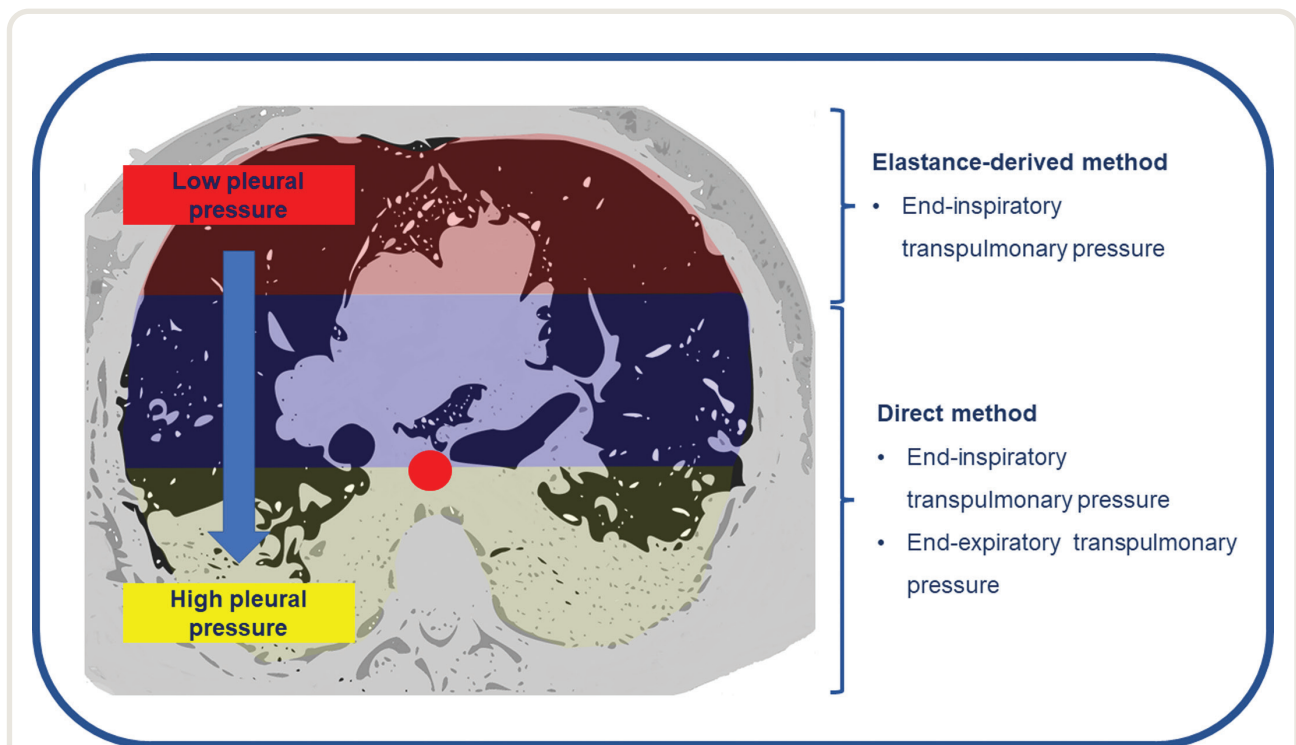


Fig. 2. Transpulmonary pressure. The vertical pleural pressure gradient along with the methods suggested for computation of transpulmonary pressure are represented. In supine patients, pleural pressure varies according to a vertical gradient, lower in nondependent lung and higher in dependent lung. As a consequence, the pressure developed across the lung, namely transpulmonary pressure, is higher in nondependent lung compared to dependent lung. The directly measured transpulmonary pressure reflects the pressure acting on the dependent and midlung adjacent to the esophageal balloon (red solid circle) during both inspiration and expiration. The end-inspiratory transpulmonary pressure computed by the elastance-derived method represents the end-inspiratory pressure acting on the nondependent lung regions.

and mechanics. Conversely, esophageal pressure-guided PEEP provided no benefits in terms of a composite outcome including mortality and ventilator-free days at 28 days compared to an empirically set high PEEP-fraction of inspired oxygen, in a larger and multicenter randomized trial conducted in ARDS patients.²⁹ Despite these findings, the survival of patients subgroup characterized by a less severe multiple organ dysfunction was higher in the arm with an esophageal pressure-guided positive end-expiratory pressure in a secondary analysis of the EPVent-2 trial.³¹ On the other hand, ventilator-induced lung injury is sustained by regional overdistention occurring during tidal ventilation.³² Limiting the elastance-derived inspiratory transpulmonary pressure under 20 to 25 cm H₂O seems a reasonable approach to avoid overdistention in the nondependent lung regions (table 1).¹⁹ Consistent with previous results,³³ a transpulmonary driving pressure 12 cm H₂O or greater, rather than an elastance-derived inspiratory transpulmonary pressure of 24 cm H₂O or more, has been demonstrated to be a risk factor for mortality at 60 days (table 1).

In spontaneously breathing patients and in those subjects undergoing appropriate noninvasive respiratory support or assisted invasive mechanical ventilation for severe acute respiratory failure, vigorous inspiratory efforts may cause an excessive drop in pleural and esophageal pressure as well as an increase in dynamic inspiratory transpulmonary pressure, not homogeneously distributed across the lung.³⁶ In these conditions, the atelectatic dependent lung regions in direct contact with diaphragm are exposed to deeper pleural pressure swings compared to the aerated

nondependent lung regions. This leads to the pendelluft phenomenon, *i.e.*, the movement of alveolar gas from non-dependent to dependent lung at the beginning of inspiration, a well-recognized risk factor for patient self-inflicted lung injury.³⁷ In patients with acute respiratory failure, keeping the esophageal pressure swing in the range of 3 to 15 cm H₂O and dynamic inspiratory transpulmonary pressure below the upper limit of 15 to 20 cm H₂O should help avoid harmful inspiratory efforts during active or assisted breath.³⁴

The main indication for esophageal manometry during acute respiratory failure is assessment of transpulmonary pressure in all those conditions characterized by an increase in chest wall elastance. This has been frequently described in extrapulmonary ARDS as the consequence of an increased intra-abdominal pressure due to abdominal disease or obesity.³⁸ In obese patients with a body mass index 30 kg/m² or more intubated for ARDS, a ventilatory strategy counterbalancing negative expiratory transpulmonary pressure has been associated with an improved survival.³³ Also, a mechanical ventilation driven by transpulmonary pressure rather than airway pressure targets has been useful in improving oxygenation and eliminating the need for extracorporeal membrane oxygenation application in patients intubated for influenza A (H1N1) with an increased chest wall elastance.³⁹

The main pitfall of esophageal manometry can be identified in the assessment of the esophageal pressure in patients who are spontaneously breathing or under noninvasive respiratory support. In these conditions, the calibration procedures previously described are not applicable, and

Table 1. Esophageal Pressure and Derived Parameter Descriptions and Significances with Related Targets for Protective Ventilation

Parameter	Description	Significance	Target
Static condition—passively ventilated patient			
Inspiratory elastance-derived transpulmonary pressure	Inspiratory pressure acting in nondependent lung	Overdistention of nondependent lung	20–25 cm H ₂ O ³³
Inspiratory esophageal-computed transpulmonary pressure	Inspiratory pressure acting in middependent lung	Overdistention of dependent lung	—
Expiratory esophageal-computed transpulmonary pressure	Expiratory pressure acting in middependent lung	Negative value: tendency to atelectasis	≥ 0 cm H ₂ O ^{33*}
Transpulmonary driving pressure	Real distending pressure acting on the lung	Lung stress	< 12 cm H ₂ O ³³
Chest wall driving pressure	Real distending pressure acting on the chest wall	Chest wall stress	—
Dynamic condition—actively breathing patient			
Inspiratory dynamic transdiaphragmatic pressure	Dynamic pressure distending the lung	Dynamic lung stress	< 15–20 cm H ₂ O ³⁴
Inspiratory esophageal pressure swing	Drop of the pressure generated during active inspiration	Inspiratory effort	3–15 cm H ₂ O ³⁴
Pressure generated by respiratory muscles	Inspiratory pressure generated by respiratory muscles	Inspiratory effort	5–10 cm H ₂ O ³⁴
Esophageal pressure-time product	Pressure time integral over inspiration	Inspiratory effort	50–150 cm H ₂ O*s*min ⁻¹
Transdiaphragmatic pressure	Inspiratory pressure generated by diaphragm	Inspiratory diaphragmatic effort	–15 cm H ₂ O ³⁴

Esophageal pressure and derived parameters description and significance are reported along with target to provide protective ventilation, according to current suggestions and evidence, in passive patient—static condition and active patient—dynamic condition.

*The target reported refers to obese patients with body mass index 30 kg/m² or greater.

the esophageal pressure evaluation could lose its validity due to the impossibility of correcting for esophageal wall and balloon reaction.

To date, esophageal pressure monitoring is available at bedside thanks to the implementation of systems for esophageal pressure signal acquisition in some ventilator machines or in dedicated portable devices offering the possibility of an automated *in vivo* calibration procedure.⁴⁰ However, despite this increased availability and the interesting applications of esophageal manometry in the clinical and research fields, this tool is still limited to expert physicians and researchers, due to the numerous technical skills required for its application.

Electrical Activity of the Diaphragm

Electrical activity of the diaphragm is the signal closest to output of the respiratory center, so it may be a sensitive and reliable method to monitor the patient's neural respiratory drive at the bedside.⁴¹ Specifically, electrical activity of the diaphragm monitoring relies on the assumption that sensed activity of the crural diaphragm is representative of the total muscle activity, as demonstrated in patients intubated for acute respiratory failure.⁴² The correct position of the nasogastric catheter is determined by verifying the electrocardiographic aspect of the P and QRS waves and the synchrony of the diaphragm electromyographic signal with the negative deflection of the airway pressure curve during an inspiratory effort against an occluded artificial airway.

Diaphragmatic electrical activity is a useful tool to assess neuromuscular respiratory drive in critically ill patients. Indeed, there is a correlation between the diaphragmatic electrical activity variation over time and the drop in airway pressure 100 ms after the onset of inspiration during an end-expiratory occlusion of the airway (P0.1), the reference method for respiratory drive assessment⁴³ (table 2).

In critically ill patients, wide heterogeneity in electrical activity of the diaphragm has been documented.⁴⁵ Diaphragmatic electrical activity signal varies according to the patient's level of assistance, and its peak values tightly correlate to esophageal pressure and pressure generated by respiratory muscles during inspiration.⁴⁶ This means that diaphragmatic electrical activity evaluation provides quantification of inspiratory effort,⁴⁶ in the presence of a preserved neuro-mechanical coupling.⁴²

Assessing patient-ventilator interactions is crucial to minimize ventilator-induced lung injury and diaphragmatic dysfunction. Growing evidence suggests that the integration of the electrical activity of the diaphragm waveform to the "standard" ventilator curves (flow and airway pressure) improves the ability to detect patient-ventilator asynchronies (table 2)^{47,48} during invasive mechanical ventilation or noninvasive respiratory support, and has been demonstrated to be useful to evaluate the impact of sedation on patient-ventilator interaction in acute respiratory failure patients and a mixed ICU population undergoing assisted breathing.^{49,50} Indeed, oversedation may be the cause of a depressed respiratory drive and a poor patient-ventilator synchrony^{49,50} during invasive mechanical ventilation. The main limitations ascribed to diaphragmatic electrical activity assessment are related to positioning of the dedicated catheter, as in the case of inability to follow the P and QRS waves size reduction criterion.

In summary, diaphragmatic electrical activity assessment provides potentially useful clinical information to guide protective assisted ventilation in patients assisted by invasive mechanical ventilation or noninvasive respiratory support for acute respiratory failure, due to the estimation of patient's neural respiratory drive, inspiratory effort, and patient-ventilator interaction.^{45,51} To date, the patient-ventilator asynchrony assessment is the only application of electrical activity of the diaphragm monitoring supported by some evidence.⁷

Table 2. Electrical Activity of the Diaphragm, Description, Application in Acute Respiratory Failure, and Limitations

Parameter	Description	Application	Advantage Compared to Conventional Monitors	Limitations Compared to Conventional Monitoring	Reference
Peak of electrical activity for the diaphragm	Maximal electric signal of diaphragm	Inspiratory effort during tidal breathing, patient-ventilator synchrony	Signal closest to output of the respiratory center	Minimally invasive, dedicated catheter and ventilator, catheter positioning, wide heterogeneity between patients, integrity of respiratory centers-to-diaphragm pathway, influenced by sedation and ventilator settings	7 μ V, minimally acceptable inspiratory diaphragmatic activity after intubation ⁴⁴
Diaphragmatic electrical activity tidal change	activation during tidal breathing Tidal variation on neural inspiratory time	Neuromuscular respiratory drive, inspiratory effort during tidal breathing			Compared to P0.1, where a threshold of 3.5 cm H ₂ O is associated with a high inspiratory effort, no target has reported for diaphragmatic electrical activity ⁴³
Diaphragmatic electrical activity with description, application in the setting of the acute respiratory failure, and advantages and limitations compared to conventional monitoring are reported.					
P0.1, drop in airway pressure 100 ms after the onset of inspiration during an end-expiratory occlusion of the airway.					

Electrical Impedance Tomography

Electrical impedance tomography is a noninvasive, radiation-free, dynamic, real-time monitoring system that provides data on global and regional changes in lung volumes, ventilation distribution, and lung perfusion. Electrical impedance tomography examination is obtained by placing a silicon belt with 16 to 32 electrodes between the fourth and sixth intercostal space, connected to a dedicated machine.^{52,53}

Pulmonary ventilation monitoring is based on the global and regional functional electrical impedance tomography assessment that also allows for an in-depth spatial and temporal analysis of ventilation distribution⁵⁴ (table 3). The global changes from minimum end-expiratory to maximum end-inspiratory impedance values correlate with global tidal breath. On the other hand, the global changes in end-expiratory impedance reflect the end-expiratory lung volume modifications. Also, the regional impedance variations are correlated with regional air content changes.⁵⁴

In acute respiratory failure, electrical impedance tomography permits the identification of patients at risk of atelectrauma during invasive mechanical ventilation, through the estimation of regional opening and closing pressure (fig. 3) as well as regional hysteresis.^{56,57}

The evaluation of the distribution of the intratidal changes in lung impedance along with end-expiratory lung impedance modifications allows the assessment of overdistended and recruited lung volume in response to PEEP changes during invasive mechanical ventilation.⁵⁸ Several procedures have been proposed to set a protective ventilation achieving the best compromise between lung overdistention and lung collapse. During a decremental PEEP trial after a maximal recruiting maneuver, the “optimal” PEEP value is defined by the intercept point of cumulated collapse and overdistension percentage curves.⁵⁹ Another method consists of choosing the “optimal” PEEP as that value able to stabilize end-expiratory lung impedance after the application of a recruiting maneuver.⁶⁰ If the end-expiratory lung impedance decreases more than 10% within 10 min after recruitment, PEEP needs to be increased by 2 cm H₂O and the recruitment reapplied.⁶⁰ According to this approach, the “optimal” PEEP value is defined as the lowest one avoiding an end-expiratory lung impedance decrease of less than 10%.⁶⁰

The application of the “optimal” PEEP improves the homogeneity of tidal ventilation distribution.⁶¹ Indeed, when a patient is afflicted by acute respiratory failure, the distribution of tidal volume within the lung is inhomogeneous because of the altered mechanical properties and the asymmetry of lung involvement.⁶¹ Based on this assumption, “optimal” PEEP has been demonstrated to correspond to the lowest global inhomogeneity index, indicating the spatial heterogeneity and distribution of the ventilation, during a PEEP trial.⁶¹

In patients intubated for ARDS, PEEP personalized through electrical impedance tomography to achieve a silent space, namely the hypoventilated area, less than or equal to 15% did not correlate with PEEP chosen to positivize end-expiratory transpulmonary pressure.⁶² However, PEEP guided by electrical impedance tomography induced a homogenization of ventilation and an improvement of lung recruitment, whereas PEEP set on transpulmonary pressure was associated with a reduced lung stress.⁶²

Electrical impedance tomography has been employed to assess global and regional lung aeration modifications induced by the prone position⁶³ in awake patients supported by high-flow nasal cannula⁶⁴ and in sedated and paralyzed patients with invasive mechanical ventilation for acute respiratory failure.⁶⁵ Prone position induces a more homogenous distribution of lung aeration as suggested by the uniform improvement in end-expiratory impedance across the lung.^{64,65}

Electrical impedance tomography can also detect the gas distribution and pendelluft phenomenon in patients undergoing assisted mechanical ventilation.⁶⁶ In acute respiratory failure patients, occult pendelluft increasingly occurs with progressive reduction of ventilatory support⁶⁶ and increase of spontaneous breathing effort.⁶⁷ Thus, in the presence of this anomalous alveolar gas distribution detected through electrical impedance tomography at bedside, clinicians are facilitated in the timely application of the corrective measures aimed at abolishing vigorous inspiratory effort and pendelluft and, consequently, at preventing patient self-inflicted lung injury.³⁶

Electrical impedance tomography can also measure the perfusion of the lung. Compared to positron emission tomography as a reference method, electrical impedance tomography underestimates relative pulmonary perfusion in dependent lung region and overestimates relative pulmonary perfusion in nondependent lung regions with small differences (less than 10%) in animal models.⁶⁸ Also, in the same setting,⁶⁸ electrical impedance tomography and positron emission tomography have detected the change of relative lung perfusion in the same direction in 69 to 96% of the measurements.

Perfusion electrical impedance tomography is based on the administration of a 10-ml bolus of hypertonic (5 to 10%) saline during an expiratory hold maneuver.⁹ The injection of hypertonic fluid induces a modification of the lung impedance that is translated into a perfusion image. Perfusion electrical impedance tomography could be an adjunctive bedside tool to identify patients with pulmonary embolism⁶⁹ or to assess the modification of the ventilation/perfusion mismatch after PEEP changes⁸ or prone positioning.⁹ From this perspective, in a small cohort of ARDS patients subjected to invasive mechanical ventilation, the percentage of lung units with an unmatched ventilation-to-perfusion ratio was an independent risk factor for mortality, having been higher in nonsurvivors compared to survivors.⁷⁰

Table 3. Electrical Impedance Tomography

Parameter	Description	Application	Advantage Compared to Conventional Monitors	Limitations Compared to Conventional Monitors	Reference
End-expiratory lung impedance	Global and regional quantification of functional residual capacity	Assessment of lung aeration	Radiation-free, feasibility, applicability at bedside, accuracy	Affected by patient's movements and by presence of pneumothorax or pneumomediastinum or chest skin lesions, availability	—
End-expiratory lung impedance variation	Variation of global and regional quantification of functional residual capacity between two timepoints	Assessment of lung aeration after modifications of ventilator settings (<i>i.e.</i> , positive end-expiratory pressure)	Radiation-free, feasibility, applicability at bedside, accuracy	Affected by patient's movements and by presence of pneumothorax or pneumomediastinum or chest skin lesions, availability, sensitive to modifications of intrathoracic fluid volumes (<i>i.e.</i> , fluid challenge, dialysis)	—
Tidal impedance variation	Global and regional assessment of impedance change generated by inspired gas during a tidal breath	Evaluation of tidal volume distribution within the entire lungs and between different regions of interest	Radiation-free, feasibility, applicability at bedside, accuracy	Affected by patient's movements and by presence of pneumothorax or pneumomediastinum or chest skin lesions, availability	Global tidal impedance variation strictly correlates with the tidal volume of the patient; the distribution among different lung regions depends on the mechanical properties of the lung and the region of interest set by the operator
Inhomogeneity index	Distribution of tidal volume within the lung	Assessment of the homogeneity of distribution of the tidal volume within the lung to set an individualized positive end-expiratory pressure	Radiation-free, feasibility, applicability at bedside, good interpatient comparability	Affected by patient's movements and by presence of pneumothorax or pneumomediastinum or chest skin lesions, availability, offline computation with dedicated software	In a control group (sedated patients with healthy lungs) of the validation study by Zhao <i>et al.</i> , ⁵⁵ the global inhomogeneity index was reported to be 0.40 ± 0.05
Center of ventilation	Ventral-to-dorsal shifts in distribution of lung ventilation	Assessment of the ventral to dorsal distribution of the tidal volume within the lung of the patient induced by different modes of ventilation and amount of inspiratory support	Radiation-free, feasibility, applicability at bedside, good interpatient comparability	Affected by patient's movements and by presence of pneumothorax or pneumomediastinum or chest skin lesions, availability, offline computation with dedicated software	When center of ventilation is expressed as percentage, a value of 50% represents equal distribution between the ventral and dorsal regions; a lower value indicates a shift of ventilation distribution toward the dorsal region; in case of dorsal atelectasis, the center of ventilation shift to the ventral part of the lung and the value increased more than 50%, indicating less ventilation in the dorsal region
Regional ventilation delay	Temporal delay in distribution of inspired air to reach a certain impedance change	Assessment of lung recruitability and individualization of the positive end-expiratory pressure level	Radiation-free, feasibility, applicability at bedside, good interpatient comparability	Affected by patient's movements and by presence of pneumothorax or pneumomediastinum or chest skin lesions, availability, offline computation with dedicated software	A smaller value indicates a more homogeneous distribution; in lung-injured patients, the different lung properties among lung regions increases the regional ventilation delay; when optimal positive end-expiratory pressure is applied to a recruitable lung, regional ventilation delay decreases

Electrical impedance tomography parameters in the setting of the acute respiratory failure along with advantages and limitations of the technology compared to conventional monitoring are reported.

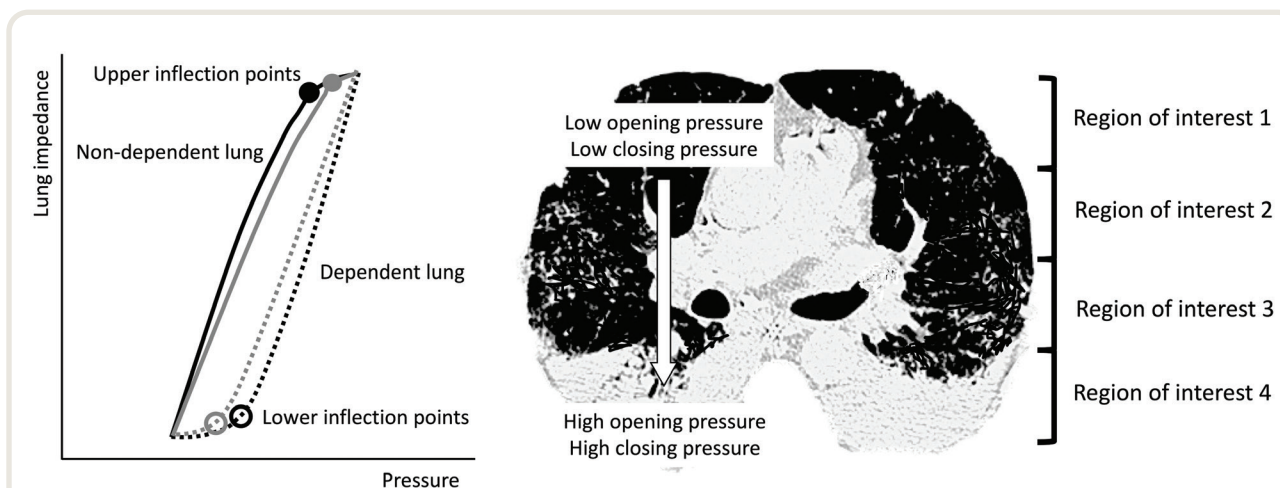


Fig. 3. Lower and upper inflection point distribution. Lower and upper inflection points distribution moving from nondependent (*region of interest 1, black continuous line*) to dependent lung (*region of interest 4, black dotted line*) at electrical impedance tomography examination. At pressure-impedance/volume curve, the lower inflection point of dependent lung (*black hollow circle*) is higher compared to the lower inflection points of the remaining regions of interest, while the upper inflection point of nondependent lung (*black solid circle*) is lower compared to the upper inflection points of the other regions of interest. The opening and closing pressure are lower in nondependent lung compared to the opening and closing pressure in dependent lung. *Black line*, Pressure-impedance/volume curve of region of interest 1; *gray line*, pressure-impedance/volume curve of region of interest 2; *gray dotted line*, pressure-impedance/volume curve of region of interest 3; *black dotted line*, pressure-impedance/volume curve of region of interest 4.

Although it is well known that lung protective ventilation improves clinical outcomes of ARDS patients, robust evidence is currently lacking for or against the use of electrical impedance tomography to individually set the ventilator. Encouraging experimental data have been reported in animals. In 12 Yorkshire swine, electrical impedance tomography-guided ventilation resulted in improved respiratory mechanics and gas exchange and reduced the histopathological findings of ventilator-induced lung injury compared to ARDS network³⁰ indications.⁷¹

A single-center randomized controlled trial has investigated whether setting PEEP with electrical impedance tomography or low PEEP/fractional inspired oxygen tension table from the ARDS network³⁰ improved clinical outcomes in 126 mild-to-severe ARDS patients. The authors reported similar PEEP values set in the two cohorts of patients without any difference in clinical outcomes (28-day mortality, ventilator-free days at day 28, ICU length of stay, successful extubation, and need for tracheostomy).⁷² It should be mentioned that the all-cause mortality was 21% in the electrical impedance tomography group, compared to 27% in the low PEEP/fractional inspired oxygen tension table group. Although not significantly different, the population sample should be considered too small, and 35% of randomized patients were affected by mild ARDS.⁷² Another randomized controlled trial including 87 moderate-to-severe ARDS patients compared PEEP settings guided by electrical impedance tomography or pressure-volume curve.⁷³ Patients randomized to the electrical impedance tomography group had an improved survival (69% vs. 50%).⁷³ Therefore, it seems that electrical impedance tomography-guided PEEP titration may improve the

clinical outcome in more severe ARDS patients, although further investigation is required.

Besides these potential clinical advantages, electrical impedance tomography has some limitations that should be acknowledged. First, this technology suffers from a low resolution compared to other imaging techniques, such as lung ultrasound or computed tomography scan.⁷⁴ However, computer tomography does not assess lung ventilation directly but only the physical density of the lung, namely the static aeration, expressed in Hounsfield units.⁷⁵ Positron emission tomography is a noninvasive technology with a high accuracy in quantifying pulmonary ventilation and volume distribution,⁷⁶ also in response to PEEP and prone position.⁷⁷ In healthy and injured pigs, electrical impedance tomography has allowed accurate measurement of regional lung ventilation and volume in comparison to positron emission tomography,⁷⁸ the accepted standard in quantification of the regional ventilation of the lung.^{76,77}

Electrical impedance tomography cannot be used for monitoring patients with an implanted pacemaker or cardioverter-defibrillator because of possible interference.⁷⁴ Fluid overload or sudden increase in urine output alters measurement of end-expiratory lung impedance, mimicking a reduction or increment in end-expiratory lung volume, respectively.⁷⁹ Finally, perfusion electrical impedance tomography also has the limit of requiring a short time (8s) of apnea during the infusion of the hypertonic solution.⁹ Although the expiratory hold is easily obtained in intubated patients receiving controlled invasive mechanical ventilation or in healthy volunteers, it is not so in the case of dyspneic patients with acute respiratory failure with a spontaneous respiratory activity.⁸⁰

In acute respiratory failure patients, electrical impedance tomography should be exploited as an adjunctive tool to optimize regional distribution of ventilation. Moreover, electrical impedance tomography permits the identification of anomalous gas distribution during active tidal breath, as in the case of the pendelluft phenomenon. Regardless of research interest, the application of perfusion electrical impedance tomography remains limited, and further studies are required to define its clinical application.

Ultrasound for the Evaluation of the Lung and Respiratory Muscles

Lung ultrasound is a versatile, radiation-free tool to assess the real-time lung aeration at the bedside.¹⁰ With this aim, two main approaches to lung ultrasound evaluation are described: a *qualitative* approach, focused on lung morphology assessment, and a *quantitative* approach that is directed to monitoring purpose.^{10,81,82} The *qualitative* approach consists of the formulation of an ultrasound diagnosis by evaluating the pleural line, presence of pleural effusion, lung consolidation, interstitial syndrome, and presence of pneumothorax.⁸¹ The *quantitative* approach relies on the aeration scoring system computation that, in turn, provides a global and/or regional score of lung aeration. Global lung ultrasound scores range from a minimum of 0 (best aeration) to a maximum of 36 (total loss of aeration)¹⁰ (table 4). Regional scores are well correlated to lung density evaluated by quantitative computer tomography scan.⁸⁶

In acute respiratory failure, lung sonography is helpful in assessing the cause and the extent of lung aeration compromise, in following the progression of the disease over time, and in evaluating the response to therapies.^{86,87} First, in the presence of a lung consolidation, lung sonography permits its characterization into inflammatory consolidation (Supplemental Digital Content 1, <http://links.lww.com/ALN/D2>, and bronchogram video, <http://links.lww.com/ALN/D3>) or atelectasis in the presence or absence of dynamic bronchogram, respectively, with a close correlation with computed tomography scan.⁸⁸ In diagnosis and discrimination of noncardiac interstitial syndrome in ICU patients, lung ultrasound has showed a moderate-to-high accuracy (area under the curve = 0.86) with the pleural abnormalities being highly specific (100%) but poorly sensitive (31%), according to recent findings.⁸⁹

Lung ultrasound allows the assessment of intratidal lung recruitment (Supplemental Digital Content 2, <http://links.lww.com/ALN/D4>, and intratidal recruitment video, <http://links.lww.com/ALN/D5>) and lung recruitment after PEEP application (Supplemental Digital Content 3, <http://links.lww.com/ALN/D6>, and PEEP recruitment video, <http://links.lww.com/ALN/D7>)⁸⁶ in real time, at bedside. Due to its characteristics, lung ultrasound is promptly and repeatably applicable whenever clinicians need to evaluate the reaeration, defined as an improvement of the local ultrasound findings in response to a specific maneuver.⁹⁰ However, it is worth considering that in assessing lung recruitment through ultrasound,

global lung ultrasound score involves any improvement in lung aeration irrespective of the initial condition. Indeed, a global reaeration lung ultrasound score is not closely correlated with the reopening of the collapsed areas because a substantial portion of the recruited volume derives from the already, albeit poorly, aerated lung.⁹¹ Conversely, quantitative lung computed tomography scan is unquestionably useful in following the specific reaeration of a previously collapsed zone. From this perspective, the computation of regional lung ultrasound score is potentially more useful than global score in the evaluation of response to the maneuvers executed.

Lung sonography helps in the identification of patients potentially responding to prone positioning according to focal distribution of the disease.⁹² Indeed, patients with a focal distribution of the lung involvement may benefit from prone positioning as a rescue ventilatory therapy. Conversely, when the lung involvement is characterized by a nonfocal distribution, a high PEEP ventilatory strategy should be preferred to enhance lung recruitment.¹⁰ Also in this case, a regional lung ultrasound score, focused on the quantification of the aeration in posterior lung regions, seems more useful in following the response to prone positioning.

Lung ultrasound may also be useful in predicting noninvasive respiratory support outcome. In patients with acute respiratory failure related to COVID-2019, a worsening in global lung ultrasound score is predictive of noninvasive respiratory support failure at 24 h from its commencement.⁹³

Overall, in keeping with recent findings,⁹⁴ lung ultrasound alone or as a part of thoracic ultrasound has a relevant impact on the decision-making process by changing diagnosis and therapy in the emergency department, ICU, and general ward. In critically ill patients undergoing invasive mechanical ventilation, the management was changed in 47% of the cases after lung ultrasound examination, with more than 65% of the modifications adopted involving invasive interventions.⁹⁵

In the ICU, routine use of lung ultrasound for diagnosis and monitoring is effective in reducing the number of ionizing procedures without affecting patient outcome.⁹⁶ However, lung ultrasound and chest x-ray examination should be considered as complementary to each other due to the specific clinical information provided. Thus, in daily clinical practice, lung ultrasound could be employed as a first level examination thanks to its repeatability and the absence of radiation. In the case of clinical uncertainty, chest x-ray examination should be employed. Also, lung sonography does not provide data on the deep lung, for which computed tomography scan is the reference examination.¹⁰ Thus, in acute respiratory failure, computed tomography scan is the standard radiological examination to evaluate lung morphology and to assess the specific aeration changes resulting from PEEP and prone positioning application.⁹⁷ However, the use of radiation and the nonapplicability at bedside, with the consequent necessity to move the patient outside the ICU, definitively limit computed tomography scan execution.

Another important limitation of the lung ultrasound is that it does not allow the evaluation of overdistension

Table 4. Ultrasound for the Lung and Respiratory Muscles

Parameter	Description	Application	Advantage Compared to Conventional Monitors	Limitations Compared to Conventional Monitors	Reference
Ultrasound for the lung Lung ultrasound score	Global and regional quantification of the lung aeration	Assessment of lung aeration	Radiation-free, feasibility, applicability at bedside, repeatability over time, availability, accuracy	Dependency on operator skills, learning curve not defined for quantitative approach, not possible to assess overdistention, not possible to assess deep lung, not possible to assess lung perfusion (compared to computed tomography scan)	Lung ultrasound score varying from 0 (best aeration) to 36 (total loss of aeration). Normal aeration (A-pattern–score 0), characterized by the reverberation of a sliding pleural line at regular intervals (lines A), eventually associated with B-lines < 3; moderate loss of aeration (B1-pattern–score 1) with well-spaced B-lines ≥ 3 at regular interval or coalescent B-lines originating from < 50% of the pleural line; severe aeration loss (B2-pattern–score 2) with multiple coalescent B-lines originating from > 50% of the pleural line; total loss of aeration (C-pattern–score 3) ¹⁰
Ultrasound for the respiratory muscles Diaphragm displacement	Total excursion of a hemi-diaphragm during tidal breathing	Inspiratory diaphragmatic effort only during spontaneous breath, patient–ventilator synchrony	Radiation-free, feasibility, applicability at bedside, repeatability over time, availability, accuracy	Evaluation of a hemi-diaphragm, affected by meteorism and subcutaneous emphysema Under assisted breath, diaphragmatic displacement has demonstrated no modifications at varying inspiratory support as well as no correlation with inspiratory effort, assessed by esophageal pressure time product and transdiaphragmatic pressure time product ⁸³ Affected by parallax error and gain setting, affected by subcutaneous emphysema, need of a cutaneous marker for the ultrasound assessment over time	Quiet breathing $1.6\text{--}1.8 \pm 0.3\text{ cm}$ (right); $1.6\text{--}1.8 \pm 0.4\text{ cm}$ (left) ⁸⁴
Diaphragmatic thickness and inspiratory thickening fraction	Muscle thickness during respiratory cycle and percent change in diaphragm thickness during inspiration	Expiratory diaphragmatic muscle mass Inspiratory diaphragmatic effort Patient–ventilator synchrony	Radiation-free, feasibility, applicability at bedside, repeatability over time, availability, accuracy		Expiratory thickness lower limit: $1.2\text{--}1.3\text{ mm}$ Thickening fraction: 169–204%. Cardenas diaphragmatic ultrasound correlates with inspiratory muscle strength and pulmonary function in healthy subjects Thickening fraction: 3% ⁸⁵
Parasternal intercostal muscle thickness and inspiratory thickening fraction	Muscle thickness during respiratory cycle and percent change in parasternal muscle thickness during inspiration	Inspiratory effort of intercostal muscle	Radiation-free, feasibility, applicability at bedside, repeatability over time, availability, accuracy	Lack of supporting evidence, affected by parallax error and gain setting, affected by subcutaneous emphysema, need of a cutaneous marker for the ultrasound assessment over time	
Ultrasound assessment for expiratory muscles Abdominal wall muscle thickness and expiratory thickening fraction	Thickness of abdominal wall muscles (external oblique, internal oblique, transversus, and rectus abdominis) during respiratory cycle and percent change in muscle thickness during expiration	Expiratory effort during active expiration	Radiation-free, feasibility, applicability at bedside, repeatability over time, availability, accuracy	Lack of supporting evidence, affected by parallax error and gain setting, affected by subcutaneous emphysema, need of a cutaneous marker for the ultrasound assessment over time	Median thickness of the expiratory muscles was $13.1\text{ [}10.2\text{--}16.1\text{ mm]}^{13}$
Ultrasound for the lung and respiratory muscles: parameters, descriptions, applications, advantages and disadvantages compared to conventional monitoring, and reference values are reported.					

during mechanical ventilation,⁹⁷ even if the loss of lung sliding in the nondependent lung zone may be suggestive of hyperinflation, especially if pleural line movements reappear after PEEP reduction.⁹⁸ An integrated approach involving other advanced respiratory monitoring technologies, *i.e.*, electrical impedance tomography, could overcome ultrasound limits.

In summary, lung ultrasound is useful to speed up the diagnosis of acute respiratory failure as well as start the *ad hoc* treatment and follow over time the response to the therapy established since the early stages of the disease. In those patients with a bilateral lung involvement, the characterization of the disease according to its focal and nonfocal distribution allows the personalization of ventilatory strategy with the application of prone position rather than high PEEP. Unfortunately, data are scarce on the role of lung ultrasound in lung protection during mechanical ventilation, mainly because it is impossible to assess overdistention in the ventilated lung.

Ultrasound provides easily accessible information to many of the muscles involved in the respiratory cycle at the bedside (table 4; fig. 4).¹² In acute respiratory

failure, the ultrasound of respiratory muscles may be useful to assess diaphragmatic dysfunction, a condition described in 2.2% of patients admitted to the ICU with acute respiratory failure and responsible for poor prognosis.⁹⁹ In the presence of a diaphragmatic dysfunction, different ultrasonographic patterns can be observed, varying from a paradoxical cranial displacement,¹⁰⁰ namely diaphragmatic paralysis, to diaphragmatic weakness defined as a diaphragmatic excursion less than 10 to 15 mm or thickening fraction less than 20% during inspiration.¹⁰⁰ Conversely, in patients with acute respiratory failure related to COVID-19, an increased thickening fraction of the diaphragm has been observed in those subjects who have failed noninvasive respiratory support.¹¹

Diaphragmatic ultrasound has recently been proposed for the identification of asynchronous events during noninvasive respiratory support at bedside.¹⁰¹ However, although this method has high performance, it has a limitation.¹⁰¹ To obtain asynchronies assessment, it is necessary to import ventilator waveforms in the ultrasound machine while the physician assesses the diaphragm displacement.

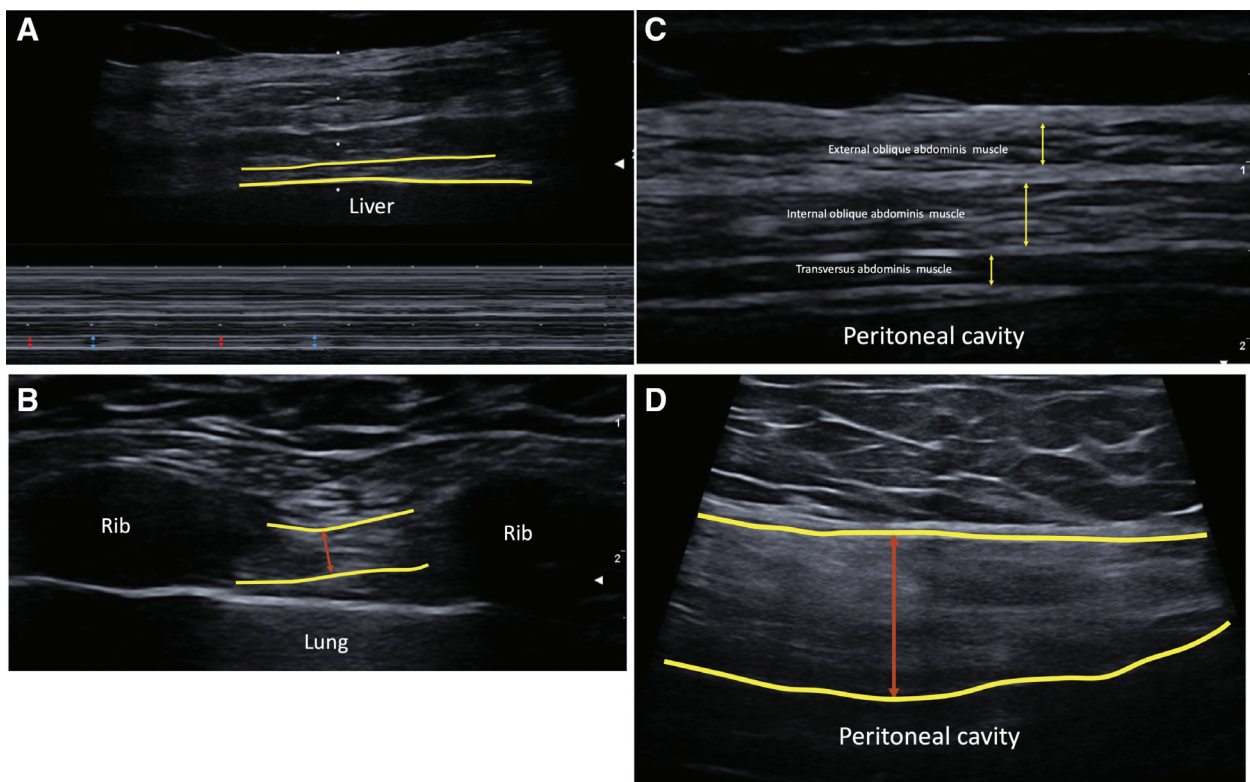


Fig. 4. Respiratory muscles ultrasound. The ultrasound of respiratory muscles is depicted. (A) Diaphragmatic ultrasound for thickness during inspiration (red arrows) and expiration (blue arrows) in M-mode. (B) Intercostal muscles ultrasound. (C) Abdominal wall muscles ultrasound for thickness of external and internal oblique abdominis muscles and transversus abdominis muscle. (D) Rectus abdominis ultrasound for thickness. External and internal boundaries of the muscles are traced in yellow. The orange arrows refer to thickness of the muscles.

In recent years, ultrasound evaluation of accessory respiratory muscles has gained evidence (table 4).¹² Inspiratory accessory muscles comprise the parasternal intercostal muscles, which are easily accessible to ultrasound assessment.¹² In healthy subjects, the thickening fraction of this muscle shows very low values, around 3%.⁸⁵ In patients with documented diaphragmatic dysfunction, the parasternal thickening fraction increases significantly in response to the increased respiratory load imposed.⁸⁵ Ultrasound has also been proposed for the evaluation of appearance and modification of abdominal wall muscles during the respiratory cycle in critically ill patients,¹³ although their role in acute respiratory failure requires further investigation. Of course, an increased expiratory thickening fraction of the abdominal wall muscles suggests an active expiration, that, in some cases, could be a protection against excessive tidal volumes delivered during assisted mechanical ventilation.

Limitations to respiratory muscles ultrasound are mainly related to the acoustic window quality. In particular, left diaphragmatic function is difficult to assess by ultrasound due to the poor quality of the splenic window

affected by gastroenteral content.¹⁰² In performing respiratory muscles ultrasound, it is worth placing the probe as perpendicularly as possible to the chest and abdominal wall surface to reduce parallax error.¹⁰³ Also, it is necessary to exclude the hyperechoic boundaries of the muscular structures in measuring muscular thickness to avoid the artifacts deriving from fascial edema. The application of a cutaneous marker has been demonstrated to enhance intra- and interoperator agreement during diaphragmatic ultrasound.¹⁰²

Ultrasound has proven useful in assessing respiratory muscles during invasive mechanical ventilation and non-invasive respiratory support for acute respiratory failure. However, its impact in management and treatment of acute respiratory failure is still a matter of discussion due to the lack of robust data in support of it.

The main limitation for all the ultrasound examinations is related to the skill of the ultrasound operator. However, according to previous data obtained while assessing the performance of an instrument to evaluate lung ultrasound competence, an interrater agreement of 0.85 among novice and expert operators was observed.¹⁰⁴

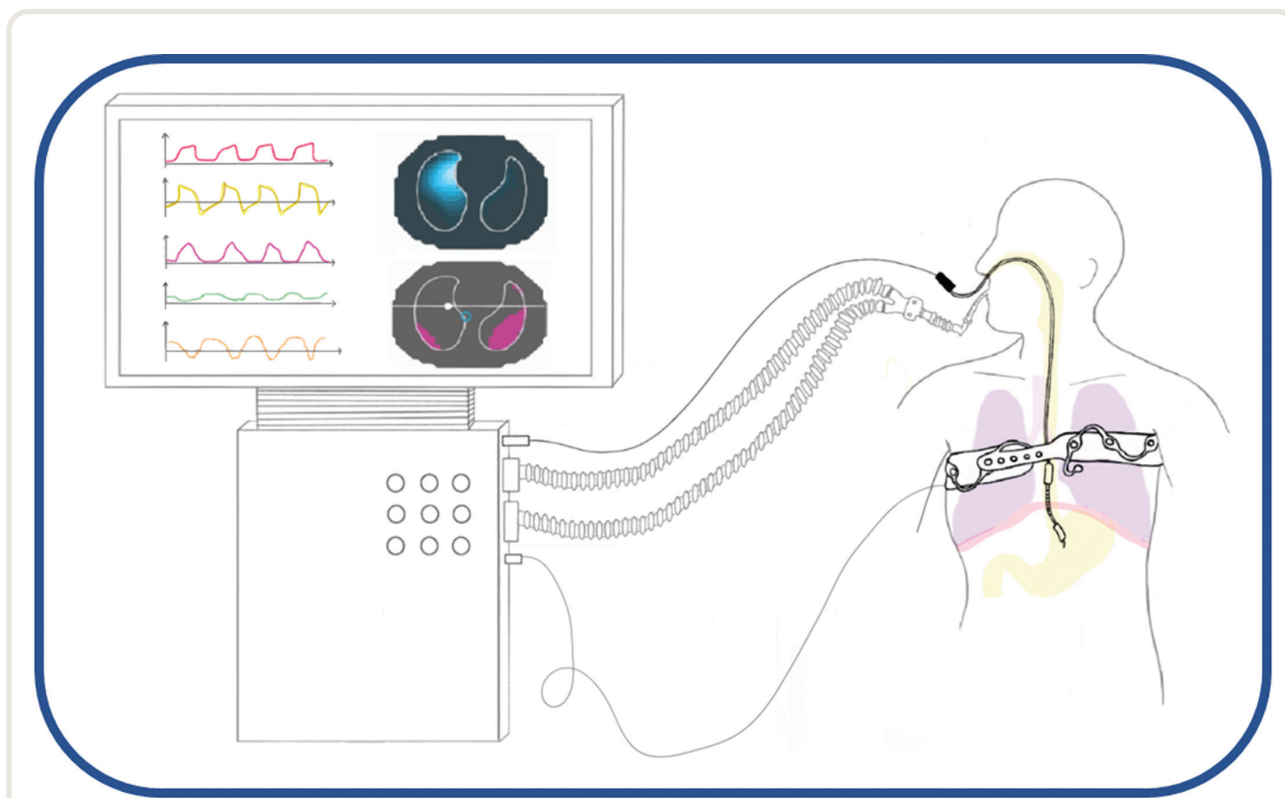


Fig. 5. Implementation of the advanced respiratory monitoring technologies at the bedside. An example of the implementation of some advanced respiratory monitoring technologies on mechanical ventilator at the bedside is depicted. The integration of the signals continuously acquired by ventilator machine is potentially useful in the personalization of the respiratory assistance, also in terms of mechanical ventilation automation. *Red curve*, airway pressure; *yellow curve*, flow; *purple curve*, electrical activity of the diaphragm; *green curve*, transpulmonary pressure; *orange curve*, esophageal pressure; electrical impedance tomography.

Conclusions

In patients with acute respiratory failure, despite the lack of a robust evidence from multicenter trials, advanced respiratory monitoring tools, more or less integrated with each other (fig. 5), have the potential to provide insights on the respiratory system modifications induced by underlying disease as well as to support clinicians in setting up a mechanical ventilation focused on the protection of the lung and respiratory muscles. Hypothetically, an advanced respiratory monitoring assisted approach could be useful to tailor mechanical ventilation on the patient rather than on the disease.

Acknowledgments

The authors thank Francesco Forfori, M.D., Department of Surgical, Medical Pathology, and Critical Care, Università di Pisa, Italy, for his support and data sharing.

Research Support

Support was provided solely from institutional and/or departmental sources.

Competing Interests

Dr. Cammarota and Dr. De Robertis declare speaking honoraria from MSD (Rome, Italy) and Getinge (Gothenburg, Sweden) outside of the current work. Dr. De Robertis received speaking honoraria from Baxter (Deerfield, Illinois) outside of the current investigation. Dr. Longhini contributed to the development of a new device (not discussed in the current study). The patent is in progress (European Patent application No. EP20170199831). He also received speaking fees from Intersurgical (Wokingham, Berkshire), Draeger (Lubeck, Schleswig-Holstein), and Fisher & Paykel (Auckland, New Zealand). The other authors declare no competing interests.

Correspondence

Address correspondence to Dr. Cammarota: Department of Medicine and Surgery, Università Degli Studi di Perugia, Perugia, Italy. gianmaria.cammarota@unipg.it. ANESTHESIOLOGY's articles are made freely accessible to all readers on www.anesthesiology.org, for personal use only, 6 months from the cover date of the issue.

Supplemental Digital Content

Supplementary Material 1. Dynamic bronchogram, <http://links.lww.com/ALN/D2>

Supplementary Material Video. Bronchogram, <http://links.lww.com/ALN/D3>

Supplementary Material 2. Intra-tidal lung recruitment, <http://links.lww.com/ALN/D4>

Supplementary Material Video. Intra-tidal recruitment, <http://links.lww.com/ALN/D5>

Supplementary Material 3. Lung recruitment, <http://links.lww.com/ALN/D6>

Supplementary Material Video. PEEP recruitment, <http://links.lww.com/ALN/D7>

References

1. Bellani G, Laffey JG, Pham T, Fan E, Brochard L, Esteban A, Gattinoni L, Haren FV, Larsson A, McAuley DF, Ranieri M, Rubenfeld G, Thompson BT, Wrigge H, Slutsky AS, Pesenti A: Epidemiology, patterns of care, and mortality for patients with acute respiratory distress syndrome in intensive care units in 50 countries. *JAMA* 2016; 315:788–800
2. Brochard L, Slutsky A, Pesenti A: Mechanical ventilation to minimize progression of lung injury in acute respiratory failure. *Am J Respir Crit Care Med* 2017; 195:438–42
3. Bertoni M, Spadaro S, Goligher EC: Monitoring patient respiratory effort during mechanical ventilation: Lung and diaphragm-protective ventilation. *Crit Care* 2020; 24
4. Goligher EC, Dres M, Patel BK, Sahetya SK, Beitler JR, Telias I, Yoshida T, Vaporidi K, Grieco DL, Schepens T, Grasselli G, Spadaro S, Dianti J, Amato M, Bellani G, Demoule A, Fan E, Ferguson ND, Georgopoulos D, Guérin C, Khemani RG, Laghi F, Mercat A, Mojoli F, Ottenheim CAC, Jaber S, Heunks L, Mancebo J, Mauri T, Pesenti A, Brochard L: Lung- and diaphragm-protective ventilation. *Am J Respir Crit Care Med* 2020; 202:950–61
5. Somhorst P, Gommers D, Endeman H: Advanced respiratory monitoring in mechanically ventilated patients with coronavirus disease 2019-associated acute respiratory distress syndrome. *Curr Opin Crit Care* 2022; 28:66–73
6. Yoshida T, Amato MBP, Grieco DL, Chen L, Lima CAS, Roldan R, Morais CCA, Gomes S, Costa ELV, Cardoso PFG, Charbonney E, Richard J-CM, Brochard L, Kavanagh BP: Esophageal manometry and regional transpulmonary pressure in lung injury. *Am J Respir Crit Care Med* 2018; 15:1018–26
7. Demoule A, Clavel M, Debord CR, Perbet S, Terzi N, Kouatchet A, Wallet F, Roze H: Neurally adjusted ventilatory assist as an alternative to pressure support ventilation in adults: A French multicentre randomized trial. *Intensive Care Med* 2016; 42:1723–32
8. Pavlovsky B, Pesenti A, Spinelli E, Scaramuzzo G, Marongiu I, Tagliabue P, Spadaro S, Grasselli G, Mercat A, Mauri T: Effects of PEEP on regional ventilation-perfusion mismatch in the acute respiratory distress syndrome. *Crit Care* 2022; 1:12
9. Zarantonello F, Sella N, Pettenuzzo T, Andreatta G, Calore A, Dotto D, Cassai AD, Calabrese F, Boscolo A, Navalesi P: Early physiological effects of prone positioning in COVID-19 acute respiratory distress syndrome. *ANESTHESIOLOGY* 2022; 137:327–39
10. Mongodi S, Luca DD, Colombo A, Stella A, Santangelo E, Corradi F, Gargani L, Rovida S, Volpicelli G,

- Bouhemad B, Mojoli F: Quantitative lung ultrasound: Technical aspects and clinical applications. *ANESTHESIOLOGY* 2021; 134:949–65
11. Cammarota G, Rossi E, Vitali L, Simonte R, Sannipoli T, Anniciello F, Vetrugno L, Bignami E, Becattini C, Tesoro S, Azzolina D, Giacomucci A, Navalesi P, De Robertis E: Effect of awake prone position on diaphragmatic thickening fraction in patients assisted by noninvasive ventilation for hypoxemic acute respiratory failure related to novel coronavirus disease. *Crit Care* 2021; 25:1–10
12. Tuinman PR, Jonkman AH, Dres M, Shi ZH, Goligher EC, Goffi A, Korte CD, Demoule A, Heunks L: Respiratory muscle ultrasonography: Methodology, basic and advanced principles and clinical applications in ICU and ED patients — A narrative review. *Intensive Care Med* 2020; 46:594–605
13. Shi Z-H, de Vries H, de Grooth H-J, Jonkman AH, Zhang Y, Haaksma M, van de Ven PM, de Man AAME, Girbes A, Tuinman PR, Zhou J-X, Ottenheijm C, Heunks L: Changes in respiratory muscle thickness during mechanical ventilation: Focus on expiratory muscles. *ANESTHESIOLOGY* 2021; 134:748–59
14. Dornhost AC, Leathart GL: A method of assessing the mechanical properties of lungs and air-passages. *Lancet* 1952; 19:109–11
15. Tobin MJ: Principles and Practice of Intensive Care Monitoring. New York, McGraw-Hill, 1998, pp. 545–52
16. Akoumianaki E, Maggiore SM, Valenza F, Bellani G, Jubran A, Loring SH, Pelosi P, Talmor D, Grasso S, Chiumello D, Gué Rin C, Patroniti N, Ranieri VM, Gattinoni L, Nava S, Terragni PP, Pesenti A, Tobin M, Mancebo J, Brochard L: The application of esophageal pressure measurement in patients with respiratory failure. *Am J Respir Crit Care Med* 2014; 189:520–31
17. Loring SH, O'Donnell CR, Behazin N, Malhotra A, Sarge T, Ritz R, Novack V, Talmor D: Esophageal pressures in acute lung injury: Do they represent artifact or useful information about transpulmonary pressure, chest wall mechanics, and lung stress? *J Appl Physiol* 2010; 108:515–22
18. Chiumello D, Carlesso E, Cadringer P, Caironi P, Valenza F, Polli F, Tallarini F, Cozzi P, Cressoni M, Colombo A, Marini JJ, Gattinoni L: Lung stress and strain during mechanical ventilation for acute respiratory distress syndrome. *Am J Respir Crit Care Med* 2008; 178:346–55
19. Mauri T, Yoshida T, Bellani G, Goligher EC, Carteaux G, Rittayamai N, Mojoli F, Chiumello D, Piquilloud L, Grasso S, Jubran A, Laghi F, Magder S, Pesenti A, Loring S, Gattinoni L, Talmor D, Blanch L, Amato M, Chen L, Brochard L, Mancebo J: Esophageal and transpulmonary pressure in the clinical setting: Meaning, usefulness and perspectives. *Intensive Care Med* 2016; 42:1360–73
20. Agostoni E: Mechanics of the pleural space. *Physiol Rev* 1972; 52:57–128
21. Pelosi P, D'Andrea L, Vitale G, Pesenti A, Gattinoni L: Vertical gradient of regional lung inflation in adult respiratory distress syndrome. *Am J Respir Crit Care Med* 1994; 149:8–13
22. Washko GR, Donnell CRO, Loring SH, George R, Donnell CRO, Loring SH: Volume-related and volume-independent effects of posture on esophageal and transpulmonary pressures in healthy subjects. *J Appl Physiol* 2006; 100:753–8
23. Gulati G, Novero A, Loring SH, Talmor D: Pleural pressure and optimal positive end-expiratory pressure based on esophageal pressure versus chest wall elastance: Incompatible results. *Crit Care Med* 2013; 41:1951–7
24. Mojoli F, Iotti GA, Torriglia F, Pozzi M, Volta CA, Bianzina S, Braschi A, Brochard L: In vivo calibration of esophageal pressure in the mechanically ventilated patient makes measurements reliable. *Crit Care* 2016; 20:98
25. Cammarota G, Santangelo E, Lauro G, Verdina F, Boniolo E, Vita ND, Tarquini R, Spinelli E, Garofalo E, Bruni A, Zanoni M, Messina A, Pesenti A, Della F, Navalesi P, Vaschetto R, Mauri T: Esophageal balloon calibration during Sigh: A physiologic, randomized, cross-over study. *J Crit Care* 2021; 61:125–32
26. Cammarota G, Verdina F, Santangelo E, Lauro G, Boniolo E, Tarquini R, Spinelli E, Zanoni M, Garofalo E, Bruni A, Pesenti A, Della CF, Navalesi P, Vaschetto R, Mauri T: Oesophageal balloon calibration during pressure support ventilation: A proof of concept study. *J Clin Monit Comput* 2020; 34:1223–31
27. Cammarota G, Lauro G, Santangelo E, Sguazzotti I, Perucca R, Verdina F, Boniolo E, Tarquini R, Bignami E, Mongodi S, Orlando A, Della CF, Vaschetto R, Mojoli F: Mechanical ventilation guided by uncalibrated esophageal pressure may be potentially harmful. *ANESTHESIOLOGY* 2020; 133:145–53
28. Talmor D, Sarge T, Malhotra A, O'Donnell CR, Ritz R, Lisbon A, Novack V, Loring SH: Mechanical ventilation guided by esophageal pressure in acute lung injury. *N Engl J Med* 2008; 359:2095–104
29. Beitler JR, Sarge T, Banner-Goodspeed VM, Gong MN, Cook D, Novack V, Loring SH, Talmor D: Effect of titrating positive end-expiratory pressure (PEEP) with an esophageal pressure-guided strategy vs an empirical high PEEP-Fio2 strategy on death and days free from mechanical ventilation among patients with acute respiratory distress syndrome: A randomized clinical trial. *JAMA* 2019; 321:846–57
30. Brower RG, Lanken PN, MacIntyre N, Matthay MA, Morris A, Ancukiewicz M, Schoenfeld D, Thompson BT: Higher versus lower positive end-expiratory pressures in patients with the acute respiratory distress syndrome. *N Engl J Med* 2004; 351:327–36
31. Sarge T, Baedorf-Kassis E, Banner-Goodspeed V, Novack V, Loring SH, Gong MN, Cook D, Talmor D, Beitler JR: Effect of esophageal pressure-guided positive end-expiratory pressure on survival from acute respiratory distress syndrome: A risk-based and mechanistic reanalysis of the EPVent-2 trial. *Am J Respir Crit Care Med* 2021; 204:1153–63

32. Protti A, Maraffi T, Milesi M, Votta E, Santini A, Pugin P, Andreis DT, Nicosia F, Zannin E, Gatti S, Vaira V, Ferrero S, Gattinoni L: Role of strain rate in the pathogenesis of ventilator-induced lung edema*. *Crit Care Med* 2016; 44:838–45
33. Chen L, Grieco DL, Beloncle F, Chen G-Q, Tiribelli N, Madotto F, Fredes S, Lu C, Antonelli M, Mercat A, Slutsky AS, Zhou J-X, Brochard L: Partition of respiratory mechanics in patients with acute respiratory distress syndrome and association with outcome: A multicentre clinical study. *Intensive Care Med* 2022; 48:888–98
34. Goligher EC, Jonkman AH, Dianti J, Vaporidi K, Beitler JR, Patel BK, Yoshida T, Jaber S, Dres M, Mauri T, Bellani G, Demoule A, Brochard L, Heunks L: Clinical strategies for implementing lung and diaphragm-protective ventilation: avoiding insufficient and excessive effort. *Intensive Care Med* 2020; 46:2314–26
35. Mead J, Smith J, Loring S: Volume displacements of the chest wall and their mechanical significance, *The Thorax: Part A*. Edited by Roussos C, Macklem P. New York, Dekker M, 1985, pp 369–92
36. Yoshida T, Uchiyama A, Fujino Y: The role of spontaneous effort during mechanical ventilation: Normal lung versus injured lung. *J Intensive Care* 2015; 3:1–7
37. Yoshida T, Grieco DL, Brochard L, Fujino Y: Patient self-inflicted lung injury and positive end-expiratory pressure for safe spontaneous breathing. *Curr Opin Crit Care* 2020; 26:59–65
38. Gattinoni L, Chiumello D, Carlesso E, Valenza F: Bench-to-bedside review: Chest wall elastance in acute lung injury/acute respiratory distress syndrome patients. *Crit Care* 2004; 8:350–5
39. Grasso S, Terragni P, Birocco A, Urbino R, Sorbo LD, Filippini C, Mascia L, Pesenti A, Zangrillo A, Gattinoni L, Ranieri VM: ECMO criteria for influenza A (H1N1)-associated ARDS: Role of transpulmonary pressure. *Intensive Care Med* 2012; 38:395–403
40. Chiumello D, Caccioppola A, Pozzi T, Lusardi AC, Giorgis V de, Galanti V, Ferrari E, Coppola S: The assessment of esophageal pressure using different devices: A validation study. *Minerva Anestesiol* 2020; 86:1047–56
41. Vaporidi K, Akoumianaki E, Telias I, Goligher EC, Brochard LJ, Georgopoulos D: Respiratory drive in critically ill patients. *Pathophysiology and clinical implications*. *Am J Respir Crit Care Med* 2020; 201:20–32
42. Beck J, Gottfried SB, Navalesi P, Skrobik Y, Comtois N, Rossini M, Sinderby C: Electrical activity of the diaphragm during pressure support ventilation in acute respiratory failure. *Am J Respir Crit Care Med* 2001; 164:419–24
43. Telias I, Junhasavasdikul D, Rittayamai N, Piquilloud L, Chen L, Ferguson ND, Goligher EC, Brochard L: Airway occlusion pressure as an estimate of respiratory drive and inspiratory effort during assisted ventilation. *Am J Respir Crit Care Med* 2020; 201:1086–98
44. Sklar MC, Madotto F, Jonkman A, Rauseo M, Soliman I, Damiani LF, Telias I, Dubo S, Chen L, Rittayamai N, Chen G-Q, Goligher EC, Dres M, Coudroy R, Pham T, Artigas RM, Friedrich JO, Sinderby C, Heunks L, Brochard L: Duration of diaphragmatic inactivity after endotracheal intubation of critically ill patients. *Crit Care* 2021; 25:26
45. Mussi RD, Spadaro S, Volta CA, Bartolomeo N, Trerotoli P, Staffieri F, Pisani L, Iannuzziello R, Dalfino L, Murgolo F, Grasso S: Continuous assessment of neuro-ventilatory drive during 12h of pressure support ventilation in critically ill patients. *Crit Care* 2020; 24:1–11
46. Bellani G, Mauri T, Coppadoro A, Grasselli G, Patroniti N, Spadaro S, Sala V, Foti G, Pesenti A: Estimation of patient's inspiratory effort from the electrical activity of the diaphragm. *Crit Care Med* 2013; 41:1483–91
47. Colombo D, Cammarota G, Alemani M, Carenzo L, Barra FL, Vaschetto R, Slutsky AS, Della Corte F, Navalesi P: Efficacy of ventilator waveforms observation in detecting patient-ventilator asynchrony* 2011; 39:pp 2452–7
48. Longhini F, Colombo D, Pisani L, Idone F, Chun P, Doorduyn J, Ling L, Alemani M, Bruni A, Zhaochen J, Tao Y, Lu W, Garofalo E, Carenzo L, Maggiore SM, Qiu H, Heunks L, Antonelli M, Nava S, Navalesi P: Efficacy of ventilator waveform observation for detection of patient-ventilator asynchrony during NIV: A multicentre study. *ERJ Open Res* 2017; 3:00075–2017
49. Vaschetto R, Cammarota G, Colombo D, Longhini F, Grossi F, Giovanniello A, Della CF, Navalesi P: Effects of propofol on patient-ventilator synchrony and interaction during pressure support ventilation and neurally adjusted ventilatory assist. *Crit Care Med* 2014; 42:74–82
50. Costa R, Navalesi P, Cammarota G, Longhini F, Spinazzola G, Cipriani F, Ferrone G, Festa O, Antonelli M, Conti G: Remifentanyl effects on respiratory drive and timing during pressure support ventilation and neurally adjusted ventilatory assist. *Respir Physiol Neurobiol* 2017; 244:10–6
51. Mussi RD, Spadaro S, Mirabella L, Volta CA, Serio G, Staffieri F, Dambrosio M, Cinnella G, Bruno F, Grasso S: Impact of prolonged assisted ventilation on diaphragmatic efficiency: NAVA versus PSV. *Crit Care* 2016; 20:1–12
52. Bodenstein M, David M, Markstaller K: Principles of electrical impedance tomography and its clinical application. *Crit Care Med* 2009; 37:713–24
53. Cook RD, Saulnier GJ, Gisser DG, Goble JC, Newell J, Isaacson D: ACT3: A high-speed, high-precision electrical impedance tomograph. *IEEE Trans Biomed Eng* 1994; 41:713–22
54. Frerichs I, Dargaville PA, Dudykevych T, Rimensberger PC: Electrical impedance tomography: A method for monitoring regional lung aeration and tidal volume distribution? *Intensive Care Med* 2003; 29:2312–6
55. Zhao Z, Möller K, Steinmann D, Frerichs I, Guttmann J: Evaluation of an electrical impedance tomography-based global inhomogeneity index for pulmonary ventilation distribution. *Intensive Care Med* 2009; 35:1900–6

56. Scaramuzzo G, Spadaro S, Waldmann AD, Böhm SH, Ragazzi R, Marangoni E, Alvisi V, Spinelli E, Mauri T, Volta CA: Heterogeneity of regional inflection points from pressure-volume curves assessed by electrical impedance tomography. *Crit Care* 2019; 23:1–11
57. Scaramuzzo G, Spinelli E, Spadaro S, Santini A, Tortolani D, Dalla Corte F, Pesenti A, Volta CA, Grasselli G, Mauri T: Gravitational distribution of regional opening and closing pressures, hysteresis and atelectrauma in ARDS evaluated by electrical impedance tomography. *Crit Care* 2020; 24:1–8
58. Putensen C, Wrigge H, Zinserling J: Electrical impedance tomography guided ventilation therapy. *Curr Opin Crit Care* 2007; 13:344–50
59. Costa ELV, Borges JB, Melo A, Suarez-Sipmann F, Toufen C, Böhm SH, Amato MBP: Bedside estimation of recruitable alveolar collapse and hyperdistension by electrical impedance tomography. *Intensive Care Med* 2009; 35:1132–7
60. Eronia N, Mauri T, Maffezzini E, Gatti S, Bronco A, Alban L, Binda F, Sasso T, Marengi C, Grasselli G, Foti G, Pesenti A, Bellani G: Bedside selection of positive end-expiratory pressure by electrical impedance tomography in hypoxemic patients: A feasibility study. *Ann Intensive Care* 2017; 7:76
61. Zhao Z, Steinmann D, Frerichs I, Guttman J, Möller K: PEEP titration guided by ventilation homogeneity: A feasibility study using electrical impedance tomography. *Crit Care* 2010; 14:1–8
62. Scaramuzzo G, Spadaro S, Dalla Corte F, Waldmann AD, Böhm SH, Ragazzi R, Marangoni E, Grasselli G, Pesenti A, Volta CA, Mauri T: Personalized positive end-expiratory pressure in acute respiratory distress syndrome: Comparison between optimal distribution of regional ventilation and positive transpulmonary pressure. *Crit Care Med* 2020; 48:1148–56
63. Tomasino S, Sassanelli R, Marescalco C, Meroi F, Vetrugno L, Bove T: Electrical impedance tomography and prone position during ventilation in COVID-19 pneumonia: Case reports and a brief literature review. *Semin Cardiothorac Vasc Anesth* 2020; 24:287–92
64. Riera J, Perez P, Cortes J, Roca O, Masclans JR, Rello J: Effect of high-flow nasal cannula and body position on end-expiratory lung volume: A cohort study using electrical Impedance tomography. *Respir Care* 2013; 58:589–96
65. Dalla Corte F, Mauri T, Spinelli E, Lazzeri M, Turrini C, Albanese M, Abbruzzese C, Lissoni A, Galazzi A, Eronia N, Bronco A, Maffezzini E, Pesenti A, Foti G, Bellani G, Grasselli G: Dynamic bedside assessment of the physiologic effects of prone position in acute respiratory distress syndrome patients by electrical impedance tomography. *Minerva Anestesiol* 2020; 86:1057–64
66. Coppadoro A, Grassi A, Giovannoni C, Rabboni F, Eronia N, Bronco A, Foti G, Fumagalli R, Bellani G: Occurrence of pendelluft under pressure support ventilation in patients who failed a spontaneous breathing trial: An observational study. *Ann Intensive Care* 2020; 10:39
67. Yoshida T, Uchiyama A, Matsuura N, Mashimo T, Fujino Y: The comparison of spontaneous breathing and muscle paralysis in two different severities of experimental lung injury. *Crit Care Med* 2013; 41:536–45
68. Bluth T, Kiss T, Kircher M, Braune A, Bozsak C, Huhle R, Scharffenberg M, Herzog M, Roegner J, Herzog P, Vivona L, Millone M, Dössel O, Andreeff M, Koch T, Kotzerke J, Stender B, Gama de Abreu M: Measurement of relative lung perfusion with electrical impedance and positron emission tomography: An experimental comparative study in pigs. *Br J Anaesth* 2019; 123:246–54
69. Grassi LG, Santiago R, Florio G, Berra L: Bedside evaluation of pulmonary embolism by electrical impedance tomography. *ANESTHESIOLOGY* 2020; 132:896
70. Spinelli E, Kircher M, Stender B, Ottaviani I, Basile MC, Marongiu I, Colussi G, Grasselli G, Pesenti A, Mauri T: Unmatched ventilation and perfusion measured by electrical impedance tomography predicts the outcome of ARDS. *Crit Care* 2021; 25:1–12
71. Wolf GK, Gómez-Laberge C, Rettig JS, Vargas SO, Smallwood CD, Prabhu SP, Vitali SH, Zurakowski D, Arnold JH: Mechanical ventilation guided by electrical impedance tomography in experimental acute lung injury. *Crit Care Med* 2013; 41:1296–304
72. He H, Chi Y, Yang Y, Yuan S, Long Y, Zhao P, Frerichs I, Fu F, Möller K, Zhao Z: Early individualized positive end-expiratory pressure guided by electrical impedance tomography in acute respiratory distress syndrome: a randomized controlled clinical trial. *Crit Care* 2021; 25:1–11
73. Hsu HJ, Chang HT, Zhao Z, Wang PH, Zhang JH, Chen YS, Frerichs I, Möller K, Fu F, Hsu HS, Chuang SP, Hsia HY, Yen DHT: Positive end-expiratory pressure titration with electrical impedance tomography and pressure-volume curve: A randomized trial in moderate to severe ARDS. *Physiol Meas* 2021; 42:014002
74. Spinelli E, Mauri T, Fogagnolo A, Scaramuzzo G, Rundo A, Luca DG, Grasselli G, Volta CA, Spadaro S: Electrical impedance tomography in perioperative medicine: Careful respiratory monitoring for tailored interventions. *BMC Anesthesiol* 2019; 19:140
75. Gattinoni L, Caironi P, Cressoni M, Chiumello D, Ranieri VM, Quintel M, Russo S, Patroniti N, Cornejo R, Bugedo G: Lung recruitment in patients with the acute respiratory distress syndrome. *N Engl J Med* 2006; 354:1775–86
76. Richard JC, Janier M, Lavenne F, Tourvieille C, Bars D Le, Costes N, Gimenez G, Guerin C: Quantitative assessment of regional alveolar ventilation and gas volume using 13N-N2 washout and PET. *J Nucl Med* 2005; 46:1375–83
77. Richard JC, Le BD, Costes N, Bregeon F, Tourvieille C, Lavenne F, Janier M, Gimenez G, Guerin C: Alveolar recruitment assessed by positron emission tomography during experimental acute lung injury. *Intensive Care Med* 2006; 32:1889–94
78. Richard JC, Pouzot C, Gros A, Tourevieille C, Lebars D, Lavenne F, Frerichs I, Guérin C: Electrical impedance

- tomography compared to positron emission tomography for the measurement of regional lung ventilation: An experimental study. *Crit Care* 2009; 13:1–9
79. Kunst PW, Vonk Noordegraaf A, Straver B, Aarts RA, Tesselaar CD, Postmus PE, de Vries PM: Influences of lung parenchyma density and thoracic fluid on ventilatory EIT measurements. *Physiol Meas* 1998; 19:27–34
 80. Wang Y, Zhong M: Bedside evaluation of pulmonary embolism by saline contrast-enhanced electrical impedance tomography: Considerations for future research. *Am J Respir Crit Care Med Conf Am Thorac Soc Int Conf ATS 2017 United States* 2021; 203:394–5
 81. Lichtenstein DA: BLUE-Protocol and FALLS-Protocol: Two applications of lung ultrasound in the critically ill. *Chest* 2015; 147:1659–70
 82. Mojoli F, Bouhemad B, Mongodi S, Lichtenstein D: Lung ultrasound for critically ill patients authors. *Am J Respir Crit Care Med* 2019; 199:701–14
 83. Umbrello M, Formenti P, Longhi D, Galimberti A, Piva I, Pezzi A, Mistraletti G, Marini JJ, Iapichino G: Diaphragm ultrasound as indicator of respiratory effort in critically ill patients undergoing assisted mechanical ventilation: A pilot clinical study. *Crit Care* 2015; 19:1–10
 84. Boussuges A, Gole Y, Blanc P: Diaphragmatic motion studied by M-mode ultrasonography. *Chest* 2009; 135:391–400
 85. Dres M, Dubé BP, Goligher E, Vorona S, Demiri S, Morawiec E, Mayaux J, Brochard L, Similowski T, Demoule A: Usefulness of parasternal intercostal muscle ultrasound during weaning from mechanical ventilation. *ANESTHESIOLOGY* 2020; 132:1114–25
 86. Chiumello D, Mongodi S, Algieri I, Vergani GL, Orlando A, Via G, Crimella F, Cressoni M, Mojoli F: Assessment of lung aeration and recruitment by CT scan and ultrasound in acute respiratory distress syndrome patients. *Crit Care Med* 2018; 46:1761–8
 87. Caltabeloti FP, Monsel A, Arbelot C, Brisson H, Lu Q, Gu WJ, Zhou GJ, Auler JOC, Rouby JJ: Early fluid loading in acute respiratory distress syndrome with septic shock deteriorates lung aeration without impairing arterial oxygenation: A lung ultrasound observational study. *Crit Care* 2014; 18:R91
 88. Lichtenstein DA, Lascols N, Mezière G, Gepner A: Ultrasound diagnosis of alveolar consolidation in the critically ill. *Intensive Care Med* 2004; 30:276–81
 89. Heldeweg MLA, Smit MR, Kramer-Elliott SR, Haaksma ME, Smit JM, Hagens LA, Heijnen NFL, Jonkman AH, Paulus F, Schultz MJ, Girbes ARJ, Heunks LMA, Bos LDJ, Tuinman PR: Lung ultrasound signs to diagnose and discriminate interstitial syndromes in ICU patients. *Crit Care Med* 2022; 50:1607–17
 90. Tusman G, Acosta CM, Costantini M: Ultrasonography for the assessment of lung recruitment maneuvers. *Crit Ultrasound J* 2016; 8:8
 91. Mayo PH, Copetti R, Feller-Kopman D, Mathis G, Maury E, Mongodi S, Mojoli F, Volpicelli G, Zanoibetti M: Thoracic ultrasonography: A narrative review. *Intensive Care Med* 2019; 45:1200–11
 92. Haddam M, Zieleskiewicz L, Perbet S, Baldovini A, Guervilly C, Arbelot C, Noel A, Vigne C, Hammad E, Antonini F, Lehingue S, Peytel E, Lu Q, Bouhemad B, Golmard JL, Langeron O, Martin C, Muller L, Rouby JJ, Constantin JM, Papazian L, Leone M; CAR'Echo Collaborative Network, AzuRea Collaborative Network: Lung ultrasonography for assessment of oxygenation response to prone position ventilation in ARDS. *Intensive Care Med* 2016; 42:1546–56
 93. de Alencar JCG, Marchini JFM, Marino LO, da Costa Ribeiro SC, Bueno CG, da Cunha VP, Lazar Neto F, Brandão Neto RA, Souza HP, the COVID USP: Registry Team: Lung ultrasound score predicts outcomes in COVID-19 patients admitted to the emergency department. *Ann Intensive Care* 2021; 11:6
 94. Heldeweg MLA, Vermue L, Kant M, Brouwer M, Girbes ARJ, Haaksma ME, Heunks LMA, Mousa A, Smit JM, Smits TW, Paulus F, Ket JCF, Schultz MJ, Tuinman PR: The impact of lung ultrasound on clinical-decision making across departments: A systematic review. *Ultrasound J* 2022; 14:5
 95. Xirouchaki N, Kondili E, Prinianakis G, Malliotakis P, Georgopoulos D: Impact of lung ultrasound on clinical decision making in critically ill patients. *Intensive Care Med* 2014; 40:57–65
 96. Brogi E, Bignami E, Sidoti A, Shawar M, Gargani L, Vetrugno L, Volpicelli G, Forfori F: Could the use of bedside lung ultrasound reduce the number of chest x-rays in the intensive care unit? *Cardiovasc Ultrasound* 2017; 15:1–5
 97. Bitker L, Talmor D, Richard JC: Imaging the acute respiratory distress syndrome: Past, present and future. *Intensive Care Med* 2022; 48:995–1008
 98. Pesenti A, Musch G, Lichtenstein D, Mojoli F, Amato MBP, Cinnella G, Gattinoni L, Quintel M: Imaging in acute respiratory distress syndrome. *Intensive Care Med* 2016; 42:686–98
 99. Valette X, Seguin A, Daubin C, Brunet J, Sauneuf B, Terzi N, du Cheyron D: Diaphragmatic dysfunction at admission in intensive care unit: The value of diaphragmatic ultrasonography. *Intensive Care Med* 2015; 41:557–9
 100. Santana PV, Cardenas LZ, de Albuquerque ALP, de Carvalho CRR, Caruso P: Diaphragmatic ultrasound: A review of its methodological aspects and clinical uses. *J Bras Pneumol* 2020; 46:1–17
 101. Vivier E, Haudebourg AF, Le Corvoisier P, Mekontso Dessap A, Carteaux G: Diagnostic accuracy of diaphragm ultrasound in detecting and characterizing patient-ventilator asynchronies during noninvasive ventilation. *ANESTHESIOLOGY* 2020; 132:1494–502
 102. Cammarota G, Sguazzotti I, Zanoni M, Messina A, Colombo D, Vignazia GL, Vetrugno L, Garofalo E, Bruni A, Navalesi P, Avanzi GC, Della CF, Volpicelli G, Vaschetto R: Diaphragmatic ultrasound assessment in subjects with acute hypercapnic respiratory failure admitted to the emergency department. *Respir Care* 2019; 64:1469–77

103. Goligher EC, Laghi F, Detsky ME, Farias P, Murray A, Brace D, Brochard LJ, Sebastien-Bolz S, Rubinfeld GD, Kavanagh BP, Ferguson ND: Measuring diaphragm thickness with ultrasound in mechanically ventilated patients: Feasibility, reproducibility and validity. *Intensive Care Med* 2015; 41:642–9
104. Skaarup SH, Laursen CB, Bjerrum AS, Hilberg O: Objective and structured assessment of lung ultrasound competence: A multispecialty Delphi consensus and construct validity study. *Ann Am Thorac Soc* 2017; 14:555–60

ANESTHESIOLOGY REFLECTIONS FROM THE WOOD LIBRARY-MUSEUM

Advertising McNeil's Pain Exterminator: A General for the Specific?



McNeil's Pain Exterminator was a 19th-century pharmaceutical "specific" or remedy touted to allay pain, cough, and diarrhea. Before the creation of the Federal Drug Administration (1906), pervasive patent medications had promised fantastical cures while delivering questionable results. Like most patent medications, the Exterminator's ingredients were guarded, but this specific likely included ether, alcohol, and opium. Developed by Thomas S. McNeil (1814 to 1874, *right*), the cure-all enticed both Union and Confederate troops to ingest purifying pills or apply a miracle ointment. Advertisements attempting to legitimize the ubiquitous concoction featured, posthumously, the revered Union General and 18th president of the United States, Ulysses S. Grant (1822 to 1885, *left*). More talented militarily than politically, the cigar-smoking icon had succumbed to aggressive and painful squamous epithelioma cancer in 1885. After agonizing throat cancer had overwhelmed the "exterminating" capacity of McNeil's or other specifics, the General had resorted to cocaine-laced throat sprays for terminal pain relief. (Copyright © the American Society of Anesthesiologists' Wood Library-Museum of Anesthesiology. www.woodlibrarymuseum.org)

Melissa L. Coleman, M.D., Associate Professor, Department of Anesthesiology and Perioperative Medicine, Penn State College of Medicine, Hershey, Pennsylvania, and George S. Bause, M.D., M.P.H., Wood Library-Museum Curator Emeritus.

Hypotension and Cardiac Surgical Outcomes: Comment

To the Editor:

We read with interest the study by de la Hoz *et al.*,¹ focusing on the association between intraoperative hypotension and postoperative complications in the field of cardiac surgery. We strongly agree with the importance of perfusion pressure during cardiac surgery with cardiopulmonary bypass. However, considering hemodynamic concepts and recent literature, we believe that the definition of hypotension used could be discussed. The authors used a mean arterial pressure (MAP) value of 65 mmHg as the hypotension threshold for all patients. Although this value is used as a threshold for organ perfusion in clinical situations such as septic shock² or the perioperative period,³ randomized data showed that a higher threshold should be obtained in hypertensive patients to avoid acute kidney injury in specific settings.⁴ In the described cohort of cardiac surgery patients, hypertensive patients represent 79% of the population. The trend of individualizing the arterial pressure goal to the reference baseline of each patient is inspired by the pathophysiologic rightward shift of the perfusion autoregulation curve in hypertensive patients.⁵ In cardiac surgery, few randomized data using individualized MAP as a target exist, but a recent trial showed that adapting the MAP to the autoregulation curve of the patient, determined by cerebral Doppler monitoring, improved neurologic outcome.⁶ Given these elements, we are intrigued by the use of an absolute hypotension threshold definition of 65 mmHg in the specific setting of cardiac surgery. More randomized trials are needed to further address the optimal MAP during cardiac surgery, such as the Perioperative Individualized Optimization of Mean Arterial Pressure in Cardiac Surgery trial (ClinicalTrials.gov Identifier: NCT05403697).

Competing Interests

The authors declare no competing interests.

Richard Descamps, M.D., Alina Denisenko, M.D.,
Marc-Olivier Fischer, M.D., Ph.D. Caen University Hospital,
Caen, France (R.D.). descamps-r@chu-caen.fr

DOI: 10.1097/ALN.0000000000004416

References

1. de la Hoz MA, Rangasamy V, Bastos AB, Xu X, Novack V, Saugel B, Subramaniam B: Intraoperative hypotension and acute kidney injury, stroke, and mortality during and outside cardiopulmonary bypass: A retrospective observational cohort study. *ANESTHESIOLOGY*. 2022; 136:927–39
2. Evans L, Rhodes A, Alhazzani W, Antonelli M, Coopersmith CM, French C, Machado FR, Mcintyre L, Ostermann M, Prescott HC, Schorr C, Simpson S, Wiersinga WJ, Alshamsi F, Angus DC, Arabi Y, Azevedo L, Beale R, Beilman G, Belley-Cote E, Burry L, Cecconi M, Centofanti J, Coz Yataco A, De Waele J, Dellinger RP, Doi K, Du B, Estenssoro E, Ferrer R, Gomersall C, Hodgson C, Hylander Møller M, Iwashyna T, Jacob S, Kleinpell R, Klompas M, Koh Y, Kumar A, Kwizera A, Lobo S, Masur H, McGloughlin S, Mehta S, Mehta Y, Mer M, Nunnally M, Oczkowski S, Osborn T, Papathanassoglou E, Perner A, Puskarich M, Roberts J, Schweickert W, Seckel M, Sevransky J, Sprung CL, Welte T, Zimmerman J, Levy M: Surviving sepsis campaign: International guidelines for management of sepsis and septic shock 2021. *Crit Care Med*. 2021; 49:e1063–143
3. Mathis MR, Naik BI, Freundlich RE, Shanks AM, Heung M, Kim M, Burns ML, Colquhoun DA, Rangrass G, Janda A, Engoren MC, Saager L, Tremper KK, Kheterpal S, Aziz MF, Coffman T, Durieux ME, Levy WJ, Schonberger RB, Soto R, Wilczak J, Berman MF, Berris J, Biggs DA, Coles P, Craft RM, Cummings KC, Ellis TA 2nd, Fleishut PM, Helsten DL, Jameson LC, van Klei WA, Kooij F, LaGorio J, Lins S, Miller SA, Molina S, Nair B, Paganelli WC, Peterson W, Tom S, Wanderer JP, Wedeven C; Multicenter Perioperative Outcomes Group Investigators: Preoperative risk and the association between hypotension and postoperative acute kidney injury. *ANESTHESIOLOGY* 2020; 132:461–75
4. Asfar P, Meziani F, Hamel JF, Grelon F, Megarbane B, Anguel N, Mira JP, Dequin PF, Gergaud S, Weiss N, Legay F, Le Tulzo Y, Conrad M, Robert R, Gonzalez F, Guitton C, Tamion F, Tonnelier JM, Guezennec P, Van Der Linden T, Vieillard-Baron A, Mariotte E, Pradel G, Lesieur O, Ricard JD, Hervé F, du Cheyron D, Guerin C, Mercat A, Teboul JL, Radermacher P; SEPSISPAM Investigators: High versus low blood-pressure target in patients with septic shock. *N Engl J Med* 2014; 370:1583–93
5. Paulson OB, Strandgaard S, Edvinsson L: Cerebral autoregulation. *Cerebrovasc Brain Metab Rev* 1990; 2:161–92

6. Brown CH 4th, Neufeld KJ, Tian J, Probert J, LaFlam A, Max L, Hori D, Nomura Y, Mandal K, Brady K, Hogue CW, Shah A, Zehr K, Cameron D, Conte J, Bienvenu OJ, Gottesman R, Yamaguchi A, Kraut M; Cerebral Autoregulation Study Group: Effect of targeting mean arterial pressure during cardiopulmonary bypass by monitoring cerebral autoregulation on post-surgical delirium among older patients: a nested randomized clinical trial. *JAMA Surg* 2019; 154:819–26

(Accepted for publication October 12, 2022. Published online first on January 18, 2023.)

Hypotension and Cardiac Surgical Outcomes: Reply

In Reply:

We read with interest the correspondence by Descamps *et al.*¹ They discuss several well-known studies concerning the need for a higher perioperative blood pressure threshold in hypertensive patients to prevent acute kidney injury. The primary outcome of our study was not a single adverse event, rather a composite of three (acute kidney injury, stroke, and mortality).² As previously reported from retrospective observational studies, blood pressure harm thresholds for different organs could differ.^{3,4} Descamps *et al.* mention that individualizing blood pressure threshold from a patient's baseline could improve outcomes. First, there is no clear consensus regarding a blood pressure threshold that could prevent adverse outcomes. Although some randomized studies in cardiac surgery did show that complications are lower in groups with high mean arterial pressure (MAP) compared with low-MAP groups,^{5,6} other studies could not find any difference in adverse outcomes attributed to different MAP thresholds.^{7–9} Descamps *et al.* also state that they are intrigued with the blood pressure threshold of MAP less than 65 mmHg. MAP less than 65 mmHg is frequently used to define intraoperative hypotension in both research and clinical practice. Moreover, this threshold has been found to be a population-based lower limit that could be associated with adverse outcomes.¹⁰ In a retrospective observational study that included a large number of noncardiac surgical patients, associations with relative blood pressure thresholds from baseline (greater than 20% reduction) were no stronger than absolute thresholds (MAP less than 65 mmHg).⁴ In our previous retrospective observational study, we found no associations between baseline pulse pressure and adverse outcomes.¹¹ Our point is, at this time, that the randomized

data are limited. We need more prospective clinical trials to define clinically meaningful blood pressure thresholds and whether interventions to maintain blood pressure above these thresholds will affect clinical outcomes.

Research Support

Dr. Subramaniam is supported by the National Institute of Health (Bethesda, Maryland), Research Project Grant GM 098406 and R01AG065554.

Competing Interests

The authors declare no competing interests.

Valluvan Rangasamy, M.D., D.N.B., D.E.S.A.,
Miguel Armengol de la Hoz, M.S.,
Balachundhar Subramaniam, M.D., M.P.H., F.A.S.A. Beth Israel
Deaconess Medical Center, Harvard Medical School, Boston,
Massachusetts (B.S.). bsubrama@bidmc.harvard.edu

DOI: 10.1097/ALN.0000000000004417

References

1. Descamps R, Denisenko A, Fischer M-O: Hypotension and cardiac surgical outcomes: Comment. *ANESTHESIOLOGY* 2023; 138:335–6
2. de la Hoz MA, Rangasamy V, Bastos AB, Xu X, Novack V, Saugel B, Subramaniam B: Intraoperative hypotension and acute kidney injury, stroke, and mortality during and outside cardiopulmonary bypass: A retrospective observational cohort study. *ANESTHESIOLOGY* 2022; 136:927–39
3. Mascha EJ, Yang D, Weiss S, Sessler DI: Intraoperative mean arterial pressure variability and 30-day mortality in patients having noncardiac surgery. *ANESTHESIOLOGY* 2015; 123:79–91
4. Salmasi V, Maheshwari K, Yang D, Mascha EJ, Singh A, Sessler DI, Kurz A: Relationship between intraoperative hypotension, defined by either reduction from baseline or absolute thresholds, and acute kidney and myocardial injury after noncardiac surgery: A retrospective cohort analysis. *ANESTHESIOLOGY* 2017; 126:47–65
5. Gold JP, Charlson ME, Williams-Russo P, Szatrowski TP, Peterson JC, Pirraglia PA, Hartman GS, Yao FS, Hollenberg JP, Barbut D: Improvement of outcomes after coronary artery bypass. A randomized trial comparing intraoperative high versus low mean arterial pressure. *J Thorac Cardiovasc Surg* 1995; 110:1302–11; discussion 1311
6. Siepe M, Pfeiffer T, Gieringer A, Zemmann S, Benk C, Schlensak C, Beyersdorf F: Increased systemic perfusion pressure during cardiopulmonary bypass is associated with less early postoperative cognitive dysfunction and delirium. *Eur J Cardiothorac Surg* 2011; 40:200–7
7. Azau A, Markowicz P, Corbeau JJ, Cottineau C, Moreau X, Baufreton C, Beydon L: Increasing mean

arterial pressure during cardiac surgery does not reduce the rate of postoperative acute kidney injury. *Perfusion* 2014; 29:496–504

8. Charlson ME, Peterson JC, Krieger KH, Hartman GS, Hollenberg JP, Briggs WM, Segal AZ, Parikh M, Thomas SJ, Donahue RG, Purcell MH, Pirraglia PA, Isom OW: Improvement of outcomes after coronary artery bypass II: a randomized trial comparing intraoperative high versus customized mean arterial pressure. *J Card Surg* 2007; 22:465–72
9. Vedel AG, Holmgaard F, Rasmussen LS, Langkilde A, Paulson OB, Lange T, Thomsen C, Olsen PS, Ravn HB, Nilsson JC: High-target versus low-target blood pressure management during cardiopulmonary bypass to prevent cerebral injury in cardiac surgery patients: a randomized controlled trial. *Circulation* 2018; 137:1770–80
10. Saugel B, Sessler DI: Perioperative blood pressure management. *ANESTHESIOLOGY* 2021; 134:250–61
11. Asopa A, Jidge S, Schermerhorn ML, Hess PE, Matyal R, Subramaniam B: Preoperative pulse pressure and major perioperative adverse cardiovascular outcomes after lower extremity vascular bypass surgery. *Anesth Analg* 2012; 114:1177–81

(Accepted for publication October 12, 2022. Published online first on

January 18, 2023.)

Alternative Sleep Apnea Treatment: Comment

To the Editor:

The analysis, by Sakaguchi *et al.*, of the role of high-flow nasal oxygen administered postoperatively in those diagnosed with obstructive sleep apnea (OSA) in lieu of conventional continuous positive airway pressure therapy is interesting.¹ We would welcome further commentary from the authors on a few points, however.

First, although we agree that high-flow nasal oxygen improves sleep time and oxygenation compared with simple oxygen therapy and overcomes upper airway obstruction in OSA *via* a continuous positive airway pressure–like effect, the institution of 30-degree head-of-bed elevation can also increase pulmonary functional residual capacity and reduce pharyngeal critical closing pressure. These are known to improve oxygenation and relieve upper airway obstruction postoperatively.^{2,3} Surprisingly, this was not observed here. Conversely, oxygenation in the 30-degree head-of-bed elevation group was inferior to that in the supine position (table 2¹). Curiously, although

the combination of high-flow nasal oxygen and 30-degree head-of-bed elevation showed additive or even synergistic effects, neither alone showed much impact on the apnea-hypopnea index. This seems hard to understand, and we would welcome the authors' thoughts on the point.

Second, most patients in this study were not particularly obese, and none were morbidly so. In severe obesity, airway obstruction is a major problem. Although a greater number of patients in the second group had moderate OSA, more in the first group had higher apnea-hypopnea indices and more desaturation. This seems surprising. Most patients with OSA have associated chronic obstructive pulmonary disease. Thus, it seems counterintuitive to initiate postoperative delivery of 40% oxygen in the high-flow nasal oxygen group, itself a cause of hypopnea and apnea as is evident table 2. We wonder why the oxygen therapy was not titrated to peripheral oxygen saturation or arterial blood gas analysis?

We thank the authors for their insightful study on combined high-flow nasal oxygen and 30-degree head-of-bed elevation in OSA. However, we would invite further comment on the points mentioned earlier.

Competing Interests

The authors declare no competing interests.

Amrita Roy, M.D., Mohanchandra Mandal, M.D., Pradipta Bhakta, M.D., M.N.A.M.S., F.C.A.I., E.D.R.A., E.D.I.C., Brian O'Brien, F.C.A.R.C.S.I., F.J.F.I.C.M.I., F.C.I.C.M. (ANZ), Antonio M. Esquinas, M.D., Ph.D., F.C.C.P., F.N.I.V., F.A.A.R.C. Seth Sukhlal Karnani Memorial Hospital, Kolkata, West Bengal, India (M.M.). drmcmandal@gmail.com

DOI: 10.1097/ALN.0000000000004433

References

1. Sakaguchi Y, Nozaki-Taguchi N, Hasegawa M, Ishibashi K, Sato Y, Isono S: Combination therapy of high-flow nasal cannula and upper-body elevation for postoperative sleep-disordered breathing: Randomized crossover trial. *ANESTHESIOLOGY* 2022; 137:15–27
2. Souza FJFB, Genta PR, de Souza Filho AJ, Wellman A, Lorenzi-Filho G: The influence of head-of-bed elevation in patients with obstructive sleep apnea. *Sleep Breath* 2017; 21:815–20
3. Souza FJ, Evangelista AR, Silva JV, Périco GV, Madeira K: Cervical computed tomography in patients with obstructive sleep apnea: Influence of head elevation on the assessment of upper airway volume. *J Bras Pneumol* 2016; 42:55–60

(Accepted for publication November 1, 2022. Published online first on December 6, 2022.)

Alternative Sleep Apnea Treatment: Reply

In Reply:

We thank Roy *et al.*¹ for their relevant comments on our article.² As Roy *et al.* correctly pointed out, head-of-bed elevation by 30 degrees did not significantly improve oxygenation variables such as mean nadir oxygen saturation measured by pulse oximetry (SpO₂), lowest SpO₂, and percent time SpO₂ < 90% in our study although, Souza's previous study demonstrated improvement of both apnea hypopnea index (15.7 to 10.7 events/h) and lowest SpO₂ (83.5 to 87%) in symptomatic obstructive sleep apnea (OSA) patients with only 7.5-degree head-of-bed elevation.³ It would be easy to comment that different patient populations and study design are the cause of the difference. However, we consider that Roy's question has an important pathophysiologic background calling the readers' attention. First, Souza's patients are more obese than ours (body mass index: 29.6 ± 4.8 *vs.* 26.3 ± 4.5 kg/m²), and, therefore, head-of-bed elevation is expected to increase functional residual capacity and improve oxygenation more effectively in such obese patients. Furthermore, head-of-bed elevation improves pharyngeal airway collapsibility as many previous studies have reported. Our research group demonstrated approximately 6 cm H₂O improvement of pharyngeal closing pressure by 60-degree sitting position in anesthetized and paralyzed patients with OSA.⁴ Notably, the improvement of pharyngeal closing pressure was indirectly associated with the severity of OSA. Accordingly, apnea hypopnea index is expected to decrease more effectively in Souza's patients with less severe OSA (15.7 *vs.* 59.6 events/h), and, in fact, application of only 7.5-degree head-of-bed elevation did achieve successful improvement. Considering both Souza's and our findings, head-of-bed elevation does provide better nocturnal oxygenation and breathing pattern, but the optimal degree of head-of-bed elevation may depend on the severity of obesity and OSA.

Second, Roy *et al.* raised optimal oxygen therapy for patients with the overlap syndrome, in which two diseases, chronic obstructive pulmonary disease and OSA, coexist in a single patient. In our study, four participants had both diseases. Two of them did not improve apnea hypopnea index with the combination therapy of head-of-bed elevation and high-flow nasal cannula with 40% oxygen concentration. Currently, the overlap syndrome receives special attention in the fields of pulmonology and sleep medicine because of its greater degrees of nocturnal oxygen desaturation and

cardiovascular consequences than those with either condition in isolation.⁵ Although this is not the original scope of our study, the overlap syndrome also needs to be paid more attention by anesthesiologists because of the possible development of severe sustained and episodic hypoxemia after surgery, leading to poor postoperative outcome. To date, we do not know whether continuous or bilevel positive airway pressure therapy is effective and what level of oxygen concentration is appropriate for postoperative respiratory management in patients with the overlap syndrome. Optimal continuous positive pressure for OSA may negate the auto-positive end-expiratory pressure in the overlap syndrome patients with emphysema phenotype. In contrast, bilevel positive pressure ventilation may be advantageous in emphysema-predominant patients because continuous positive pressure may exacerbate mechanical disadvantage of the flattened diaphragm contraction leading to severe hypoventilation during sleep. We would like to close our comments by sharing the most recent clinical study demonstrating the effectiveness of high-flow nasal oxygen therapy (30 to 60 l/min with oxygen concentration titrated to increase awake SpO₂ by 3 to 4%) for treatment of the overlap syndrome.⁶ Yes, all issues raised by Roy *et al.* are clinically relevant and to be fully answered in the near future.

Competing Interests

The authors declare no competing interests.

Yuichi Sakaguchi, M.D., Natsuko Nozaki-Taguchi, M.D.,
Shiroh Isono, M.D.
Chiba University Graduate School of Medicine, Chiba,
Japan (S.I.).
shirohisono@yahoo.co.jp

DOI: 10.1097/ALN.0000000000004434

References

1. Roy A, Mandal M, Bhakta P, O'Brien B, Esquinas AM: Alternative sleep apnea treatment: Comment. *ANESTHESIOLOGY* 2023; 138:337
2. Sakaguchi Y, Nozaki-Taguchi N, Hasegawa M, Ishibashi K, Sato Y, Isono S: Combination therapy of high-flow nasal cannula and upper-body elevation for postoperative sleep-disordered breathing: Randomized crossover trial. *ANESTHESIOLOGY* 2022; 137:15–27
3. Souza FJFB, Genta PR, de Souza Filho AJ, Wellman A, Lorenzi-Filho G: The influence of head-of-bed elevation in patients with obstructive sleep apnea. *Sleep Breath* 2017; 21:815–20
4. Tagaito Y, Isono S, Tanaka A, Ishikawa T, Nishino T: Sitting posture decreases collapsibility of the passive pharynx in anesthetized paralyzed patients with obstructive sleep apnea. *ANESTHESIOLOGY* 2010; 113:812–8

5. Suri TM, Suri JC: A review of therapies for the overlap syndrome of obstructive sleep apnea and chronic obstructive pulmonary disease. *FASEB Bioadv* 2021; 3:683–93
6. Spicuzza L, Sambataro G, Schisano M, Ielo G, Mancuso S, Vancheri C: Nocturnal nasal high-flow oxygen therapy in elderly patients with concomitant chronic obstructive pulmonary disease and obstructive

sleep apnea. *Sleep Breath* [Epub ahead of print 2022 September 3]

(Accepted for publication November 1, 2022. Published online first on December 6, 2022.)

We Are All Perfectly Fine: A Memoir of Love, Medicine and Healing

By Jillian Horton, M.D. Toronto, HarperCollins Publisher Ltd., 2021. Pages: 290. Price: \$18.99 (softcover); \$15.99 (ebook).

Burnout is such a hot topic that one wonders whether physicians have become burned out hearing about burnout. The syndrome is hardly new; the psychologist Herbert Freudenberger coined the term “burnout” in the 1970s to describe the plight of child mental health workers in free clinics in New York City.¹ (Interestingly, a wide range of professions that are intensely involved with people—including medicine, nursing, and education—appear to be particularly vulnerable to burnout.) Resulting from work-related stress, the phenomenon is characterized by emotional exhaustion, feelings of cynicism and detachment from patients (depersonalization), and a low sense of personal accomplishment. These dimensions can coexist in different degrees, rendering burnout a continuous, heterogeneous construct rather than a dichotomous one. Burnout differs from depression in that burnout exclusively involves a person’s relationship to his or her work, whereas depression is a more global experience, affecting virtually every aspect of an individual’s life. The high prevalence of physicians with symptoms of burnout (typically cited at approximately 60%), which increased during the pandemic, is extremely concerning because burnout can erode professionalism, contribute to medical errors, lead to attrition, trigger suicidal ideation, and be a contributing factor to substance abuse and relationship difficulties.

When Christina Maslach, Ph.D., published the Maslach Burnout Inventory in 1981,² initial efforts to mitigate burnout focused mainly on the individual practitioner rather than the healthcare system. Although educating physicians about stress management, resiliency, and mindful meditation has an important mollifying role, if these are the exclusive approaches to remediating the issue, we risk sending the message that “you are the problem and you need to toughen up.”

We Are All Perfectly Fine: A Memoir of Love, Medicine and Healing chronicles the experiences of Dr. Jillian Horton, a 40-something-yr-old Canadian internist and medical educator who struggled with burnout. Dr. Horton, the recipient of the 2020 Association of Faculties of Medicine of Canada Gold Humanism Award, is currently associate chair of the Department of Internal Medicine at the University of Manitoba Max Rady College of Medicine in Winnipeg. Hers is a compelling story. An accomplished clinician, musician, and writer, she decided at a young age to become a physician largely because medical mistakes and callousness

destroyed the lives of her older sister, who developed debilitating postoperative meningitis after resection of a brain tumor, and her brother, who died of undetermined cause(s) in a psychiatric hospital during the COVID-19 pandemic. Dr. Horton became resolute that she would not be one of *those doctors* and developed into a caring, compassionate, and highly competent medical leader. Nonetheless, she was on the verge of personal and professional collapse a few years ago, struggling with an amorphous discontent that has become medicine’s not-so-secret ailment, when she attended a 5-day retreat for burned-out physicians at Chapin Mill, a Zen center in upstate New York.

During the Chapin Mill retreat, she bonded with similarly afflicted colleagues who shared stories about secret guilt and grief. Many of them harbored a deep-rooted sense of culpability about some of their patients who had poor outcomes despite excellent care. They described feelings of marginalization and isolation, being overwhelmed by work compression, and experiencing a lack of respect and an enervating sense of lack of control over their lives. The attendees were especially troubled by administrative burdens, often exacerbated by the cumbersome and much-criticized electronic health record, and by not being allowed to work at the top of their license, functioning as cogs in a wheel rather than as valued professionals. Others grappled with a sense of moral injury when they were unable to deliver optimal care to their patients owing to a lack of critical resources, such as adequate staffing or necessary equipment.

Realizing that she was not alone, that she was one of many physicians who love their profession but have been brought to their knees by it, Dr. Horton had an epiphany that she wanted to live differently and reconfigure the parts of her psyche that were causing unnecessary pain. She began to appreciate the life-altering benefits of simple restorative practices such as mindfulness and deep breathing. She further realized, however, that mindfulness alone—although it can help us see things more clearly—is insufficient to fix the systemic and organizational problems that are driving medicine’s burnout crisis. She and her colleagues at Chapin Mill spoke often about the “toxic” culture of medicine, about the fact that their training was “an apprenticeship in the art of self-immolation,” and that physicians have the highest suicide rate of any white-collar profession.

Although Dr. Horton successfully delivers a full-hearted and powerfully intimate account of the overdetermined

phenomenon of burnout, I suspect many readers would have welcomed, in addition, a deeper and more comprehensive exploration of potential *solutions* to the systemic and organizational root causes of this critical problem. Dr. Tait Shanafelt^{3,4} and others, for example, have argued that workload expectations should be realistically established, and physician well-being should be measured, tracked, and benchmarked as a strategic imperative necessary to the provision of high-quality care. Rather than being victims in a broken system, physicians should be valued partners working with institutional leadership to change the clinical environment for the better. Restoring meaning to physicians' time commitment, facilitating supportive social interactions, and promoting the separation of work and home life may be challenging but could pay dividends in terms of physician well-being.

If burnout is not adequately addressed, the already serious shortage of physicians will become devastating. Consider that while the number of U.S. medical schools has increased dramatically during the past few decades, graduate medical education slots have not expanded commensurately. Moreover, the recent "great resignation" in our profession saw 4 yr worth of retirements in 1 yr!⁵ Owing to workplace disruption caused by the COVID-19 pandemic, approximately 38 million healthcare workers quit their jobs, and retirements among baby boomers doubled. Before the pandemic, the physician shortage in the United States was projected to reach 90,000 by 2025. Current predictions suggest a deficit of 122,000 physicians by 2032.

Ponder the adage that culture will eat strategy for breakfast, lunch, and dinner and realize that potential solutions must be anchored in a nurturing work culture. Moreover, the new generation of physicians will likely want to work differently than baby boomers, and this will affect the supply of fulltime equivalents. Hence, one of the healthcare system's many challenges will be to offer scheduling patterns that align with younger physicians' cultural imperatives.

In summary, burnout is a critical contemporary problem that has serious consequences for physicians, the healthcare

system, and patients. Recently, there has been a welcome paradigm shift from viewing burnout as a sign of weakness in individual physicians to an indication of a flawed healthcare system, rooted in issues related to the clinical learning environment and organizational culture. Such a shift is necessary if we are to effectively remediate this ongoing public health crisis.

Competing Interests

Dr. McGoldrick received no funding for this article. During the past 36 months, she received money from the Accreditation Council for Graduate Medical Education, *Current Reviews in Clinical Anesthesia*, and *UpToDate*. These financial relationships, however, are not relevant to this book review, and she does not consider them competing interests.

Kathryn Elizabeth McGoldrick, M.D., F.C.A.I. (Hon.).

New York Medical College, Valhalla, New York.

kathryn_mcgoldrick@nymc.edu

References

1. Freudenberger HJ: Staff burn-out. *J Soc Issues* 1975; 30:159–65
2. Maslach C, Jackson SE: The measurement of experienced burnout. *J Occup Behav* 1981; 2:99–113
3. Dyrbye LN, Shanafelt TD: Physician burnout: A potential threat to successful health care reform. *JAMA* 2011; 305:2009–10
4. West CP, Dyrbye LN, Erwin PJ, Shanafelt TD: Interventions to prevent and reduce physician burnout: A systematic review and meta-analysis. *Lancet* 2016; 388:2272–81
5. Peterson MD: Anesthesia workforce: Help! I need help. *ASA Monitor* 2022;20,22

(Accepted for publication November 30, 2022. Published online first on January 6, 2023.)

Ketamine Psychedelic and Antinociceptive Effects Are Connected: Erratum

In the Materials and Methods section under Data Collection (page 793), the sentence: “Data were collected before and during racemic ketamine infusion[.]” should be changed to: “Data were collected before and during both the racemic ketamine and S-ketamine infusions.”

The authors regret this error. The online version and PDF of the article have been corrected.

DOI: 10.1097/ALN.0000000000004281

Reference

Olofsen E, Kamp J, Henthorn TK, van Velzen M, Niesters M, Sarton E, Dahan A: Ketamine psychedelic and antinociceptive effects are connected. *ANESTHESIOLOGY* 2022; 136:792–801

Preoperative Plasmapheresis in Patients Undergoing Cardiac Surgery Procedures: Retraction

The article by Boldt *et al.*, entitled “Preoperative plasmapheresis in patients undergoing cardiac surgery procedures” by J Boldt, B von Bormann, D Kling, M Jacobi, R Moosdorf, G Hempelmann, published in *ANESTHESIOLOGY* 1990; 72:282–8, has been retracted in its entirety by the Journal Editor-in-Chief, Evan Kharasch, M.D., Ph.D.

This article is being retracted following an investigation at Justus Liebig University, Giessen, Germany concerning allegations that Dr. Boldt manipulated and falsified data in several published articles, and which “recommends that journal editors retract all papers where Dr. Boldt is the responsible author even if there is no obvious indication of falsification.”¹

DOI: 10.1097/ALN.0000000000004373

Reference

1. JLU letter can be found in: Supplementary Multimedia 3 from <https://doi.org/10.1016/j.bja.2020.02.024> in *BJA*



Wolters Kluwer

Essential Titles in **ANESTHESIOLOGY**



Search articles, register for eAlerts,
view abstracts at **journals.lww.com**
SUBSCRIBE at **shop.lww.com**.

Careers & Events

Marketing solutions for Career, Education
and Events advertisers.



Wolters Kluwer | Lippincott
Health Williams & Wilkins

LWW's All Access Recruitment bundle offers advertisers access to the strongest portfolio of print journals, and online advertising in medical media. Build and deploy a powerful and targeted campaign to raise awareness and drive results anytime, anywhere and across all platforms. Contact an LWW Sales Specialist to learn more.

For rates and dealines, visit:

advertising.lww.com

Contact

Dave Wiegand

847-361-6128

dave.wiegand@wolterskluwer.com



UVA Health

University of Virginia School of Medicine, Department of Anesthesiology

Vice-Chair of Education in Anesthesiology

Division Chief of Regional Anesthesiology

Open Rank Faculty Position in Anesthesiology

Come join our team in the heart of the Blue Ridge Mountains! We are rapidly expanding our services with the addition of several new operating rooms on our main UVA Health campus, a community surgery center, and the opening of the new Orthopedic Center at Ivy Road. The Department of Anesthesiology at the University Of Virginia School Of Medicine seeks multiple American Board of Anesthesiology certified or Board-eligible candidates. Duties include clinical care; medical supervision of residents and Certified Registered Nurse Anesthetists (CRNA); teaching fellows, residents, and medical students; and research (if interested). The department offers competitive compensation, excellent benefits, and a generous retirement plan. Administrative time is available for academic, research, and/or administrative projects.

SPECIFICALLY RECRUITING NOW FOR:

- ❖ Adult Multi-Specialists ❖ Critical Care Medicine ❖ Neuro Anesthesia
- ❖ Pediatric Anesthesiology ❖ Regional Anesthesia

For additional information about the positions

or questions: anesthesia-apply@virginia.edu.

To Apply: <https://uva.wd1.myworkdayjobs.com/UVAJobs> POSTING # R0027663

UVA DEPARTMENT of ANESTHESIOLOGY | PO Box 800710 | Charlottesville, VA 22908
434.924.2283 | Fax 434.982.0019



Department of Anesthesiology

UNIVERSITY OF WISCONSIN
SCHOOL OF MEDICINE AND PUBLIC HEALTH

WE'RE GROWING. JOIN OUR TEAM.



63
RESIDENTS/
INTERNS



80
CRNAs/CAAs



100+ FACULTY
AND FELLOWS



1ST U.S.
ACADEMIC DEPT.
OF
ANESTHESIOLOGY



GLOBAL
PROGRAM

LEADERSHIP OPPORTUNITIES

- Vice Chair of Education
- Vice Chair of Quality and Safety
- Associate Vice Chair of Clinical Affairs

ABOUT THE ROLES: These leadership positions report to the Chair and collaborate with other leaders to oversee the Department's current programs. The incumbents will be in charge of program development as well as providing managerial assistance to a large team. Clinical candidates who are chosen will care for patients while also teaching residents, fellows, medical students, and other learners. Candidates should be Associate Professors or higher in status and have prior program experience.



WWW.ANESTHESIA.WISC.EDU/CAREERS

Dual appointment with
UW Madison and UW Medical
Foundation.

REQUIRED:

Active Wisconsin medical license
(or eligibility)

American Board of Anesthesiology
Board Certification (or eligibility).

EXCELLENCE IN CLINICAL PRACTICE, EDUCATION, AND RESEARCH

CLINICAL SPECIALTIES

ADULT CARDIOTHORACIC AND VASCULAR | AMBULATORY
CHRONIC PAIN AND PAIN MANAGEMENT | CRITICAL CARE
MULTISPECIALTY | NEUROANESTHESIA | PEDIATRIC
REGIONAL AND ACUTE PAIN | TRANSPLANT

★★★★★
QUATERNARY
ACADEMIC
MEDICAL
CENTER

UW-MADISON IS AN EO/AA EMPLOYER,
WOMEN AND MINORITIES ARE ENCOURAGED TO APPLY.

WOOD LIBRARY-MUSEUM OF ANESTHESIOLOGY

RESEARCH • VISIT OUR
WEBSITE • DONATE



KEEPING ANESTHESIA HISTORY ALIVE

www.woodlibrarymuseum.org



HAVE SOMETHING
IMPORTANT
TO SAY?

Deliver your message in
**THE SOURCES
PHYSICIANS TRUST**

Visit for more information advertising.lww.com



Wolters Kluwer

Lippincott Williams & Wilkins

PhysiciansJobsPlus

The Health Career Authority
www.physiciansjobsplus.com

ANESTHESIOLOGY
The Journal of the American Society of Anesthesiologists, Inc. • anesthesiology.org

Volume 138, Number 3, March 2023

Advertiser Index

Edwards Lifesciences C2

Careers & Events A19-A21

For more information about advertising and the next
available issue, contact your sales manager:

Careers & Events Advertising Sales Manager
Dave Wiegand, 847-361-6128

Downloaded from /anesthesiology/issue/138/3 by guest on 19 April 2024



PhysiciansJobsPlus

PhysiciansJobsPlus.com Connect to the Best Talent Pool in Healthcare

Be top of mind with physicians who are actively engaged in reading and researching valued clinical content. From basic job listings to sophisticated recruitment programs, PhysiciansJobsPlus offers a range of budget-friendly solutions that place your positions at the fingertips of the right candidates at the right time.

- Reach professionals in virtually every medical specialty
- Gain exposure across our network of 250+ journal websites
- Quickly measure results with reporting and management tools
- Enhance your listings with Visibility Enhancement Upgrades and Posting Packages



Wolters Kluwer

Getting Published is a Process.

We're Here to Help.



Get started today!

authors.lww.com



Wolters Kluwer

Global Research – Open for All



Wolters Kluwer's publishing program offers peer-reviewed, open access options to meet the needs of authors and maximize article visibility.



wkopenhealth.com



Wolters Kluwer



Visit

www.LWW.com/journals/renew

*and Renew Your Subscription
Online Today!*

Save Time...

with the ease and speed of online
subscription renewal.

Save Money...

by subscribing for up to 3 years
at the current rates!

Are you a Society member?

If your journal subscription is a member benefit,
contact your society to renew membership.



Wolters Kluwer
Health

Lippincott
Williams & Wilkins

AAR356CF

CALL FOR NOMINATIONS

ASA Award for Excellence in Research

Recognizing an individual for outstanding achievement in research that has or is likely to have an important impact on the practice of anesthesiology.



DEADLINE: March 31, 2023

James E. Cottrell, MD, Presidential Scholar Award

Recognizing colleagues who dedicate their formative careers to research.



DEADLINE: March 31, 2023

Learn more about these awards and qualifications for nominating candidates at pubs.asahq.org/anesthesiology/pages/call_for_nominations



Please submit nominations or any questions regarding these awards to Managing Editor, *Anesthesiology*, at managing-editor@anesthesiology.org.

EDITORIALS

- 115 Centre for Perioperative Care anaemia guideline: implications for anaesthesia
T. Hawkins, S. Agarwal and C. R. Evans
- 119 Assessment of haemostatic function in paediatric surgical patients: 'if you prick us, do we not bleed?'
K. Tanaka and A. J. de Armendi

CARDIOVASCULAR

- 122 Physiological relationship between cardiorespiratory fitness and fitness for surgery: a narrative review
B. H. Roxburgh, J. D. Cotter, H. A. Campbell, U. Reymann, L. C. Wilson, D. Gwynne-Jones, A. M. van Rij and K. N. Thomas

CLINICAL PRACTICE

- 133 Comparison of the effects of sugammadex versus neostigmine for reversal of neuromuscular block on hospital costs of care
L. J. Wachtendorf, T. M. Tartler, E. Ahrens, A. S. Witt, O. Azimaraghi, P. Fassbender, A. Suleiman, F. C. Linhardt, M. Blank, S. Y. Nabel, J. Y. Chao, P. Goriacko, P. Mirhaji, T. T. Houle, M. S. Schaefer and M. Eikermann
- 142 Dexmedetomidine provides type-specific tumour suppression without tumour-enhancing effects in syngeneic murine models
W. Chen, Z. Qi, P. Fan, N. Zhang, L. Qian, C. Chen, Y. Huang and S. Jin

NEUROSCIENCE AND NEUROANAESTHESIA

- 154 Sex-specific hypnotic effects of the neuroactive steroid (3 β ,5 β ,17 β)-3-hydroxyandrostane-17-carbonitrile are mediated by peripheral metabolism into an active hypnotic steroid
F. M. Manzella, O. H. Cabrera, D. Wilkey, B. Fine-Raquet, J. Klawitter, K. Krishnan, D. F. Covey, V. Jevtovic-Todorovic and S. M. Todorovic

OBSTETRIC ANAESTHESIA

- 165 Thromboelastometry-guided treatment algorithm in postpartum haemorrhage: a randomised, controlled pilot trial
S. Jokinen, A. Kuitunen, J. Uotila and A. Yli-Hankala

PAEDIATRIC ANAESTHESIA

- 175 Factor XIII levels, clot strength, and impact of fibrinogen concentrate in infants undergoing cardiopulmonary bypass: a mechanistic sub-study of the FIBCON trial
K. Siemens, B. J. Hunt, K. Parmar, D. Taylor, C. Salih and S. M. Tibby
- 183 Determination of reference ranges for the ClotPro® thromboelastometry device in paediatric patients
K. Laukova, V. Petrikova, L. Poloniová, L. Babulicova, L. Wsolova and T. Haas
- 191 Repeated early-life exposure to anaesthesia and surgery causes subsequent anxiety-like behaviour and gut microbiota dysbiosis in juvenile rats
X. Zhou, X. Xu, D. Lu, K. Chen, Y. Wu, X. Yang, W. Xiong, X. Chen, L. Lan, W. Li, S. Shen, W. He and X. Feng

PAIN

- 202 Effect of intrathecal *NIS-IncRNA* antisense oligonucleotides on neuropathic pain caused by nerve trauma, chemotherapy, or diabetes mellitus
C.-H. Wen, T. Berkman, X. Li, S. Du, G. Govindarajulu, H. Zhang, A. Bekker, S. Davidson and Y.-X. Tao

REGIONAL ANAESTHESIA

- 217 Assistive artificial intelligence for ultrasound image interpretation in regional anaesthesia: an external validation study
J. S. Bowness, D. Burckett-St Laurent, N. Hernandez, P. A. Keane, C. Lobo, S. Margetts, E. Moka, A. Pawa, M. Rosenblatt, N. Sleep, A. Taylor, G. Woodworth, A. Vasalauskaitė, J. A. Noble and H. Higham
- 226 Evaluation of the impact of assistive artificial intelligence on ultrasound scanning for regional anaesthesia
J. S. Bowness, A. J. R. Macfarlane, D. Burckett-St Laurent, C. Harris, S. Margetts, M. Morecroft, D. Phillips, T. Rees, N. Sleep, A. Vasalauskaitė, S. West, J. A. Noble and H. Higham
- 234 Effectiveness of oral versus intravenous tranexamic acid in primary total hip and knee arthroplasty: a randomised, non-inferiority trial
C. J. DeFrancesco, J. F. Reichel, E. Gbaje, M. Popovic, C. Freeman, M. Wong, D. DeMeo, J. Liu, A. Gonzalez Della Valle, A. Ranawat, M. Cross, P. K. Sculco, S. Haskins, D. Kim, D. Maalouf, M. Kirksey, K. Jules-Elysee, E. M. Soffin, K. Kumar, J. Beathe, M. Figgie, A. Inglis Jr., S. Garvin, M. Alexiades, K. DelPizzo, L. A. Russell, A. Sideris, J. Saleh, H. Zhong and S. G. Memtsoudis

CORRESPONDENCE

See full Table of Contents for Correspondence

BOOK REVIEW

- 242 *Managing Long COVID Syndrome*, T. Vasu
A. Bhatia, J. Chen and J. Huang

MEMORY AND AWARENESS IN ANAESTHESIA

Edited by Lis Evered

Editorials

See full Table of Contents for Editorials

Consciousness

See full Table of Contents for Consciousness

Delirium

See full Table of Contents for Delirium

Monitoring

See full Table of Contents for Monitoring

Neuroscience

See full Table of Contents for Neuroscience

Paediatric neuroanaesthesia

See full Table of Contents for Paediatric Neuroanaesthesia

Abstracts

See full Table of Contents for Abstracts